



nano bio & med 2018

nov. 20-22, barcelona (Spain)

www.nanobiomedconf.com



abstracts book



Organisers



Institute for Bioengineering of Catalonia



Universität für Bodenkultur Wien
University of Natural Resources
and Applied Life Sciences, Vienna





Index

Foreword **2**

Organising Committee **3**

Media Partners **3**

Sponsors **3**

Exhibitors **3**

Speakers / Orals / Posters list **4**

Abstracts **8**

On behalf of the Organizing Committee, we take great pleasure in welcoming you to Barcelona (Spain) for the NanoBio&Med2018 International Conference.

This event, after successful editions organized within ImagineNano in Bilbao 2011 & 2013, and in Barcelona in 2014, 2015, 2016 & 2017, is going to present the most recent international developments in the field of Nanobiotechnology and Nanomedicine and will provide a platform for multidisciplinary communication, new cooperations and projects to participants from both science and industry. Emerging and future trends of the converging fields of Nanotechnology, Biotechnology and Medicine will be discussed among industry, academia, governmental and non-governmental institutions. NanoBio&Med2018 will be the perfect place to get a complete overview into the state of the art in those fields and also to learn about the research carried out and the latest results. The discussion in recent advances, difficulties and breakthroughs will be at his higher level.

As in previous editions, an industrial forum will be organized to promote constructive dialogue between business and public leaders and put specific emphasis on the technologies and applications in the nanoBioMed sector.

We are indebted to the following Companies, Scientific Institutions and Government Agencies for their support: Institute for Bioengineering of Catalonia (IBEC), Bicosome, ThermoFisher Scientific, NANOMED Spain, PerkinElmer and ICEX Spain Trade and Investment.

We would also like to thank the following companies for their participation: Promethean Particles, ONI and MDPI.

In addition, thanks must be given to the staff of all the organising institutions whose hard work has helped planning this conference.

Organising committee

- Antonio CORREIA
President of the Phantoms Foundation (Spain)
- Dietmar PUM
Deputy Head of the Biophysics Institute – BOKU (Austria)
- Josep SAMITIER
Director of the Institute for Bioengineering of Catalonia – IBEC
Coordinator of the Spanish Nanomedicine Platform - NanomedSpain (Spain)



Media Partners



Sponsors



exhibitors



Speakers/Orals/Posters list: Alphabetical order

Authors	Session	Page
Oscar Ahumada (Mecwins, Spain) <i>Detection of protein biomarkers at femtogram per milliliter levels using Mecwins technology</i>	Invited	9
Irene Anton Sales (Institute of Materials Science of Barcelona, Spain) <i>Bacterial nanocellulose as a cell culture platform</i>	Oral Plenary	43
Irene Anton Sales (Institute of Materials Science of Barcelona, Spain) <i>Bacterial nanocellulose as a cell culture platform</i>	Poster	75
Xavier Arqué (IBEC, Spain) <i>Effect of enzyme type, quantity and distribution on the motion behavior of microswimmers</i>	Oral Plenary	44
Xavier Arqué (IBEC, Spain) <i>Effect of enzyme type, quantity and distribution on the motion behavior of microswimmers</i>	Poster	76
Thomas Bakkum (Leiden University, The Netherlands) <i>Ultrastructural Imaging of Salmonella–Host Interactions Using Super-resolution Correlative Light-Electron Microscopy of Bioorthogonal Pathogens</i>	Poster	77
Sandra Ballesteros (Universitat Autònoma de Barcelona, Spain) <i>MicroRNAs expression changes associated to long term nanomaterials exposure</i>	Poster	78
Ricardo Baltà Foix (Institut de Recerca i Tecnologia Agroalimentàries, Spain) <i>Formation of protein-based nanoparticles in Lactobacillus plantarum as a new source for the isolation of functional protein.</i>	Poster	80
Aurélien Bancaud (LAAS, France) <i>DNA concentration, purification and identification with μLAS microreactor: (i) identification of DNA biomarkers in the blood, and (ii) Cas9- targeted sequencing</i>	Keynote	10
Larysa Baraban (TU Dresden, Germany) <i>Nanoscale sensor devices: from molecules to a whole cell detection</i>	Keynote	11
Giuseppe Battaglia (University College London, UK) <i>Multivalency and cooperativity in nanoparticle blood brain barrier crossing</i>	Keynote	12
Roy Beck (Tel Aviv University, Israel) <i>Physics, biology and multiple sclerosis</i>	Keynote	13
Angela Bejarano Villafuerte (Promethean Particles Ltd, UK) <i>Development of a novel multifunctional bioglass-based coating for the next generation of prostheses</i>	Oral Plenary	45
Ofra Benny (The Hebrew University of Jerusalem, Israel) <i>Tight control of polymeric nanoparticles fabrication for optimized interaction with cells and tissues</i>	Keynote	14
Taisiia Berestok (Catalonia Institute for Energy Research, Spain) <i>Nanocrystal-based magnetic aerogels for hyperthermia and environmental remediation</i>	Poster	81
Gustavo Bodelón (Universidad de Vigo, Spain) <i>Surface-enhanced Raman scattering (SERS) imaging of bioactive metabolites in mixed bacterial populations</i>	Oral Plenary	46
Roger Bresolí-Obach (Institut Químic de Sarrià, Universitat Ramon Llull, Spain) <i>Small particles, big improvement: Fluorescent nanoprobos for singlet oxygen and other reactive oxygen species detection in biological systems</i>	Poster	82
Marta Bustos (MICITT/Universidad de Barcelona, Spain) <i>Validation of a titration method to determine chondroitin sulfate loaded to solid lipid nanoparticles in an experimental factorial design.</i>	Poster	83

Authors	Session	Page
Inmaculada Conejos-Sanchez (Centro de investigacion Principe Felipe, Spain) <i>Polymer Therapeutics for treating neurodegenerative disorders: exploring the intranasal route to bypass the BBB</i>	Poster	85
Constanza Cortes Crignola (Universitat Autònoma de Barcelona, Spain) <i>Effects of differently shaped TiO₂NPs (nanospheres, nanorods and nanowires) on the in vitro model (Caco-2/HT29) of the intestinal barrier</i>	Poster	86
Nikolas Daskalakis (Centre for Process Innovation, UK) <i>Development of a Microfluidic-Based Pilot Line for the Production of Novel Nanomedicines</i>	Oral Plenary	47
Cecile Delacour (Institut Néel - CNRS, France) <i>Graphene Neuroelectronics</i>	Invited	15
Josefa Domenech (Universitat Autònoma de Barcelona, Spain) <i>Effects of GO and GNPs on the in vitro model of the intestinal barrier (Caco2/HT29)</i>	Poster	88
Fernando Dominguez (CIMUS, Universidad de Santiago de Compostela, Spain) <i>Silver Atomic Quantum Clusters for Cancer Therapy: Targeting Chromatin</i>	Oral Plenary	48
Cigdem Dönmez güngünes (Hitit University, Turkey) <i>Cytotoxic Effects of Magnetite Nanoparticles on Human Periodontoal Ligament Fibroblast Cells</i>	Oral Plenary	49
Jordi Esquena (IQAC-CSIC, Spain) <i>Contact lenses functionalized with antimicrobial peptides for the prevention of corneal infections</i>	Oral Plenary	50
Federico Fenaroli (University of Oslo, Norway) <i>Long circulating nanoparticles passively accumulate in tuberculosis granulomas in zebrafish and mouse models</i>	Oral Plenary	51
Juan Fernandez (VLC Photonics S.L., Spain) <i>Silicon Nitride Photonic Integrated Circuits for Biophotonics and medical applications</i>	Oral Plenary	52
Carlos Fito-López (ITENE, Spain) <i>Occupational exposure to nanobiomaterials in the medical sector</i>	Invited	16
Helena Florindo (University of Lisbon, Portugal) <i>Polymeric nano-vaccines improved immune checkpoint anti-tumor efficacy against breast cancer</i>	Oral Plenary	54
Thibaut Fourniols (Université Catholique de Louvain, Belgium) <i>Impairment of colorectal tumor microenvironment with lipid nanocapsules</i>	Poster	90
Giancarlo Franzese (Universitat de Barcelona, Spain) <i>Hydrated Biomembranes and Nanomaterials: Perspectives for Blood-Brain-Barrier Crossing of Nanoparticles.</i>	Oral Plenary	55
Ana Gallego Lleyda (Universidad de Zaragoza, Spain) <i>Optimized lipid nanoparticles decorated with TRAIL exhibit enhanced cytotoxicity against cancer cells</i>	Poster	91
Jose García-Guirado (ICFO, Spain) <i>Enantio-Selective Sensing Using Plasmonic Racemic Arrays</i>	Oral Plenary	56
Jose García-Guirado (ICFO, Spain) <i>Enantio-Selective Sensing Using Plasmonic Racemic Arrays</i>	Poster	93
Diana Gaspar (Instituto de Medicina Molecular, Portugal) <i>Challenging breast cancer brain metastases formation with the plant defensin PvD1</i>	Poster	95
Gerardo F. Goya (UNIZAR-INA, Spain) <i>New developments in the field of Drug Release instrumentation</i>	Invited	18
Pablo Guardia (Catalonia Institute for Energy Research - IREC, Spain) <i>Nanostructuring and assembling magnetic nanoparticles for biomedical applications</i>	Oral Plenary	58
Rita Guedes (University of Lisbon, Portugal) <i>Small-molecule immune system modulators: A step forward in cancer immunotherapy</i>	Oral Plenary	59
Hakan Gungunes (Hitit Universty, Turkey) <i>AC susceptibility and Mössbauer analysis of Mn -Y substituted Sr_{1-x}MnxFe_{12-y}Y₀₋₁₉ (0.0 ≤ x=y ≤ 0.5) nanohexaferrites</i>	Oral Plenary	60
Silvia Hernández Ainsa (University of Zaragoza/ INA, Spain) <i>Engineered DNA nanostructures for photoacoustics bioimaging</i>	Oral Plenary	61

Authors	Session	Page
Frank Koppens (ICFO, Spain) <i>Next Generation Wearable Wellness Trackers with Graphene-based Flexible Photodetectors</i>	Keynote	19
Anna Lagunas (IBEC, Spain) <i>Long distance electron transfer between redox partner proteins through the aqueous solution</i>	Invited	20
Meytal Landau (Technion, Israel) <i>Functional Protein Fibrils</i>	Keynote	21
Jiahui Li (The Forest Next S.L., Spain) <i>Controlled drug release of PLA/PLGA microspheres</i>	Oral Plenary	62
María José Limeres (University of Barcelona, Spain) <i>Characterization and stability of chitosan-based nanoparticles as efficient non-viral gene delivery system</i>	Poster	96
Ana Candida Lopes Hortelao (IBEC, Spain) <i>Enzyme-Powered Nanomotors for Biomedical Applications</i>	Poster	98
Jesus M de la Fuente (ICMA, CSIC/ UNIZAR / CIBER-BBN, Spain) <i>New Biotechnological Challenges for Magnetic Hyperthermia</i>	Keynote	22
Xing Ma (Harbin Institute of Technology (Shenzhen), China) <i>Fabrication and Multifunctional Applications of Micro/Nano-Motors</i>	Invited	23
Veronika Magdanz (TU Dresden, Germany) <i>Teaming up sperm cells with micro- & nanostructures for novel diagnostic tools in reproductive biology</i>	Invited	24
Shlomo Magdassi (The Hebrew University of Jerusalem, Israel) <i>Nanomaterials in 2D, 3D, 4D printing</i>	Keynote	25
Lluis F. Marsal (Universitat Rovira i Virgili, Spain) <i>Nanoporous anodic alumina optical biosensors and biomedical applications</i>	Keynote	26
Cécilia Ménard-Moyon (CNRS, France) <i>Multifunctionalized carbon nanotubes towards targeted anticancer radiotherapy</i>	Keynote	28
Ernest Mendoza (Astrea Materials / UPC, Spain) <i>From the laboratory to the market. Our history of commercialising a nanotechnology discovery</i>	Invited	-
Rafael Mestre (IBEC, Spain) <i>Training and force adaptability of 3D-bioprinted biological actuators based on skeletal muscle tissue</i>	Oral Plenary	63
Idoia Mikelez Alonso (CIC biomaGUNE and BioCruces, Spain) <i>IL15 vehiculized Iron Oxide nanoparticles as a tool to enhance NK cell mediated-activity</i>	Poster	99
Xavier Milà Niubó (PERKINELMER, Spain) <i>Single Cell ICP-MS: The Advantages of Quantifying Metals and Nanoparticulate Number Content in Individual Cells</i>	Oral Plenary	64
Marta Monge Azemar (IQAC-CSIC, Spain) <i>Monitoring cancer cell treatment by Nanoparticle-assisted lab-on-a-chip (LoC)</i>	Poster	100
Yaiza Montes-Cebrián (University of Barcelona, Spain) <i>A Portable System for Measuring the Tactile Temporal Discrimination Threshold in Cervical Dystonia</i>	Poster	102
Livia Neves Borgheti Cardoso (IBEC, Spain) <i>Purification, characterization and drug loading of extracellular vesicles derived from Plasmodium-infected and non-infected red blood cells</i>	Poster	104
Samuel Ojosnegros Martos (IBEC, Spain) <i>Imaging receptor-ligand response to nanopatterns of surface-bound ligands</i>	Keynote	29
Felipe Olate-Moya (Universidad de Chile, Chile) <i>Poly(pseudorotaxane) / Graphene Oxide supramolecular hydrogels for controlled drug release</i>	Poster	106
Salvador Pané i Vidal (ETH Zurich, Switzerland) <i>Magnetoelectric Small-Scale Machines for Biomedical Applications</i>	Keynote	30
Danny Porath (The Hebrew University of Jerusalem, Israel) <i>Novel DNA-Based Molecules and Their Charge Transport Properties</i>	Keynote	31
Maruthi Prasanna (CIMUS, University of Santiago de Compostela, Spain) <i>Antigen-loaded chitosan nanoparticles and their interaction with immune cells</i>	Poster	108

Authors	Session	Page
Beatriz Prieto Simón (Universitat Rovira i Virgili, Spain) <i>Nanostructured electrochemical biosensors as fit-for-purpose analytical devices</i>	Oral Plenary	65
Silvia Pujals (IBEC, Spain) <i>Super resolution microscopy for nanomedicine: visualizing nanomaterials in action</i>	Invited	33
Fabiana Quaglia (University of Napoli Federico II, Italy) <i>Enhancing anticancer activity of chemotherapeutics with antiangiogenic biodegradable nanoparticles</i>	Oral Plenary	66
Loris Rizzello (University College London, UK) <i>Designing principles of nanotherapies</i>	Invited	34
Miguel Roncales (AlphaSip, Spain) <i>TBD</i>	Invited	-
Silvia Ruiz Rincón (Instituto de Nanociencia de Aragón - INA, Spain) <i>Reversible monolayer-bilayer transition in supported phospholipid Langmuir-Blodgett films: morphological and nanomechanical behavior</i>	Oral Plenary	68
Silvia Ruiz Rincón (Instituto de Nanociencia de Aragón - INA, Spain) <i>Reversible monolayer-bilayer transition in supported phospholipid Langmuir-Blodgett films: morphological and nanomechanical behavior</i>	Poster	110
Virginia Saez-Martinez (i+Med S. Coop. / R&D, Spain) <i>I+Med S. Coop. an innovative company in the field of controlled delivery</i>	Oral Plenary	69
Samuel Sánchez (IBEC, Spain) <i>Bioengineering hybrid machines for nanomedicine and soft robotics</i>	Keynote	36
Ronit Satchi-Fainaro (Tel Aviv University, Israel) <i>Reverting cancer 's poor prognosis using precision polymeric nanomedicines based on molecular fingerprints of long-term survivors</i>	Keynote	37
Avi Schroeder (Technion, Israel) <i>Personalized Cancer Nanomedicines</i>	Keynote	38
Anna Scomparin (Tel Aviv University, Israel) <i>Multicellular spheroids as novel tools for the evaluation of melanoma nano-vaccines and BRAF-MEK-targeted nanomedicines</i>	Oral Plenary	71
Salvatore Sortino (University of Catania, Italy) <i>Engineered Combinations of Nitric Oxide Photoreleasers with Doxorubicin as Innovative Strategy to Overcome Multidrug Resistance</i>	Oral Plenary	72
Vojislav Spasojevic (Institute of Nuclear Sciences "Vinca", Serbia) <i>Multifunctional (Mg,Fe)₃O₄ nanoparticles: Test for possible magnetic hyperthermia and radionuclide carriers applications</i>	Poster	111
Masanori Tachikawa (Yokohama City University, Japan) <i>Molecular dynamics study on substituent and solvent effects for nanocube formed with gear-shaped amphiphile molecules</i>	Poster	112
Giuseppina Tatulli (Università del Salento/Istituto Italiano di Tecnologia, Italy) <i>Colorimetric tests for food safety and genetic traceability based on DNA-functionalized gold nanoparticles</i>	Poster	113
Ernesto Tinajero Diaz (Universitat Politècnica de Catalunya, Spain) <i>Novel nanoparticles made of polyester-peptide copolymers</i>	Poster	114
Philip Tinnefeld (LMU München, Germany) <i>DNA Origami Tools for NanoBioTec</i>	Keynote	39
Dumitru Ulieru (SITEX 45 SRL, Romania) <i>Development of a non-invasive breath test for early diagnosis of tropical diseases "TROPSENSE"</i>	Oral Plenary	73
Reinaldo Vallejo Vicente (Universidad de Valladolid, Spain) <i>Encapsulation of docetaxel with Elastin Like Recombinamers by supercritical CO₂ for advanced anticancer applications in biomedicine</i>	Poster	116
Thomas Velten (Fraunhofer IBMT, Germany) <i>Biosensors based on roll-to-roll printed graphene electrodes</i>	Keynote	40
María J. Vicent (Príncipe Felipe Research Center, Spain) <i>Targeting Tumor Microenvironment with Rationally Designed Polypeptide-based Conjugates</i>	Keynote	41
Diana Vilela (IBEC, Spain) <i>Medical Imaging for the Tracking of Micromotors</i>	Poster	118



Keynote & Invited

Detection of protein biomarkers at femtogram per milliliter levels using Mecwins' technology

O. Ahumada¹,

V. Cebrián¹, A. Diaz¹, V. Pini¹, A. Salvador-Matar C. Rodríguez, A. Thon¹

¹Mecwins S.A., Plaza de la Encina 10-11, Tres Cantos, Spain

oahumada@mecwins.com

Mecwins offers an ultrasensitive and multiplexed protein biomarker detection technology. This innovative technology has been developed under a technique based on plasmonic emission in a sandwich immunoassay format, providing a solution for those diagnostic situations where ultra-sensitive detection is needed. The technology is also suitable for the development of a POC system. Our technology has applications across Life Science Research, Diagnostics and Precision Health & Screening Markets. The adoption of ultra-sensitive detection technology will open the realm to infinite possibilities, detecting and quantifying biomarkers where traditional technologies are blind.

The technology consists in a lecture platform and a sensor to be read for biomarker detection. Mecwins' sensor is based on a silicon wafer coated with antibodies specific to the biomarker of interest. Once the sample has been incubated, gold nanoparticles (GNPs) are added. The surface of the GNPs is covered with a second specific antibody which binds to a free region of the captured antigen, establishing a "sandwich" structure (figure 1). This structure can be detected and quantified with Mecwins' platform due to the distinct optical properties of the GNPs.

Our proprietary detection technology is one million more sensitive than ELISA technology, which has been the standard for protein detection for over forty years. Researchers and clinicians rely on protein biomarkers for use in research and clinical decisions. However, current standard clinical tools cannot detect low levels of many proteins. To achieve such ultrasensitivity we rely on a couple of strengths:

1) The reading technology key parameters:

- Amplification of the scattered light
- Single particle counting and positioning
- Spectral information of every particle found
- Multiplexing Capabilities

2) Our own immunoassay fabrication process

- High density of capture antibodies on the surface
- Antibody activity improved by orientation
- Good blocking to avoid unspecific binding

An example of the extraordinary capabilities of the technology is shown in Figure 2.

The Human Immunodeficiency Virus (HIV) is the etiologic agent of acquired immunodeficiency syndrome. The gag protein p24 (~24 kDa) is the structural protein of the HIV capsid, with approximately 2000 p24 molecules per HIV particle. During acute HIV infection, the virus replicates exponentially, and p24 becomes detectable in blood. Mecwins has developed a p24 immunoassay which exhibits a high-sensitivity for detection of p24 in human serum samples.

Figures

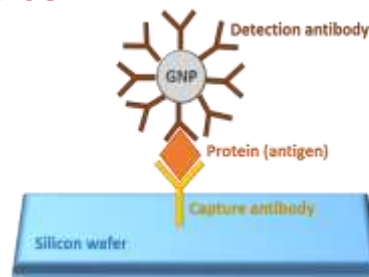


Figure 1. Schematic representation of the sandwich assay on the surface of a silicon wafer.

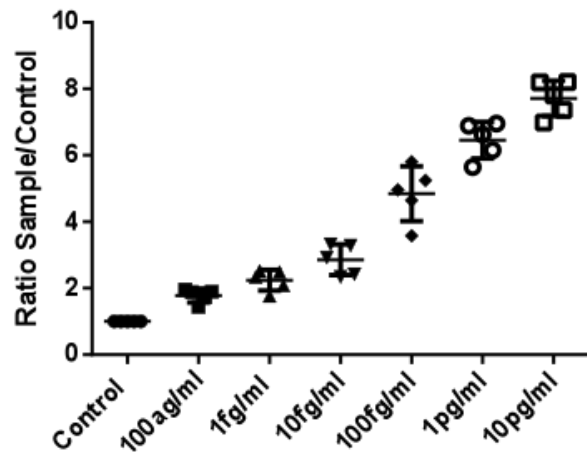


Figure 2. Calibration curve for Mecwins' p24 immunoassay in human diluted serum. The data are represented as ratio sample/control.

DNA concentration, purification and identification with μ LAS microreactor: (i) identification of DNA biomarkers in the blood, and (ii) Cas9- targeted sequencing

Aurélien BANCAUD¹,

B. Chami¹, N. Milon¹, J. Teillet¹, I. Tijunelyte¹

¹LAAS-CNRS, Université de Toulouse, F-31400 Toulouse, France

abancaud@laas.fr

Abstract

We recently developed the μ LAS technology for nucleic acids processing. μ LAS is based on the fine control of DNA transport in a viscoelastic liquid under the combined action of hydrodynamic and electrophoretic forces (1). Size separation and concentration can be simultaneously performed in a micro-reactor (Figure 1), which consists of a funnel-shape geometry (2). This technology has been patented and transferred to the SME Picometrics Technologies, which has for instance established the conditions to analyze residual DNA with a sensitivity of 5 fg/ μ L. In our talk, we will present the technology and exploit its performances for sizing cell-free DNA (cfDNA) circulating in the blood (3). We will notably demonstrate that cfDNA profiling is a promising biomarker for the follow-up of cancer patients. We will then present the principle of a DNA size-selective valve for the purification of genomic regions targeted with the Cas9 endonuclease. We will reach high quality sequencing compatible with accurate *de novo* sequencing of 30 kb fragments excised from plant genomes.

References

- [1] Ranchon et al., Lab Chip (2016)
- [2] Chami et al., Soft Matter (2018)
- [3] Andriamanampisoa et al., Anal Chem (2018)

Figures

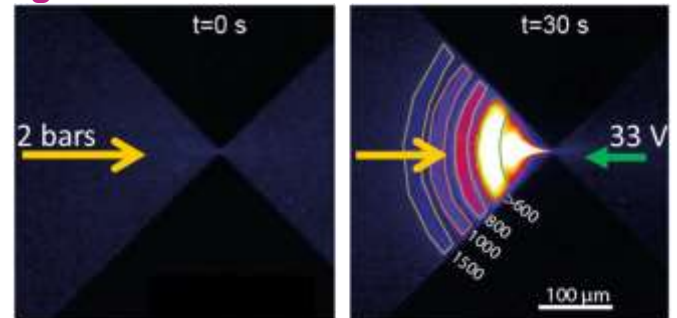


Figure 1. Operation of μ LAS technology for DNA separation and concentration. The technology involves the combined action of hydrodynamic and electrophoretic forces acting in opposite direction.

Nanoscale sensor devices: from molecules to a whole cell detection

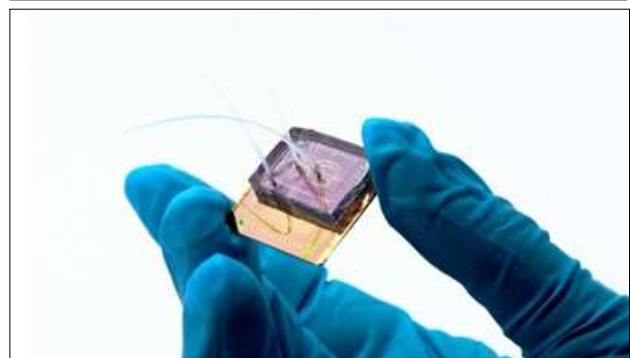
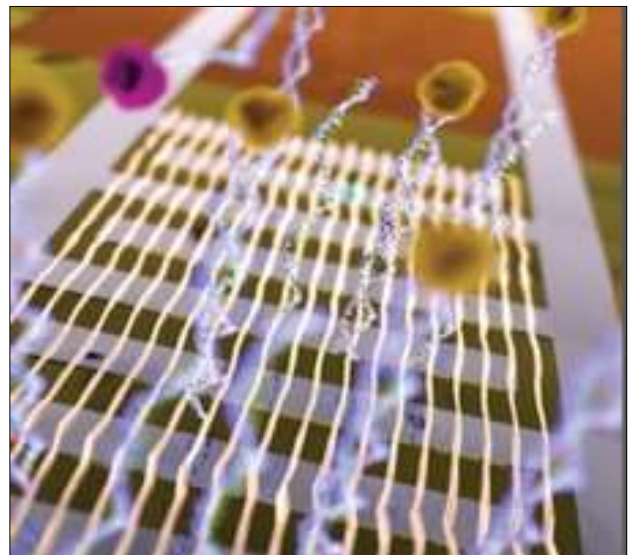
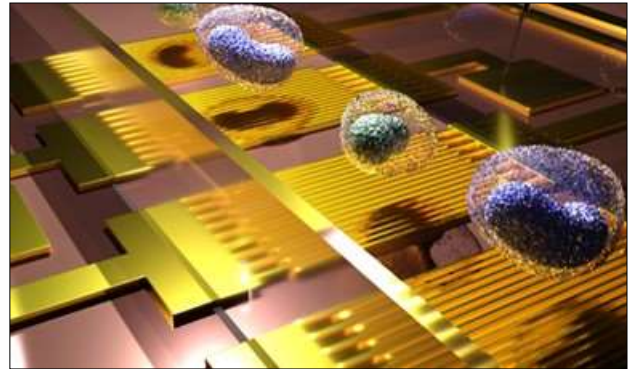
Larysa Baraban
Gianaurelio Cuniberti

TU Dresden (Germany)

larysa.baraban@nano.tu-dresden.de

Personalized diseases diagnostics and ubiquitous environmental monitoring are only two possible applications, which could address a number of societal challenges ahead related to human life in a strongly globalized world. Nanoparticles, nanowires, 2D materials are dominated by quantum effects and employing them as active elements in transducers for novel devices opens up enormous perspectives for innovative sensor systems. Such devices bear the potential to not only outperform conventional sensor technology with respect to speed, sensitivity, long time stability and signal reliability, but even to define completely new application fields in platforms that are cost efficient, flexible and portable. After an introduction of the fundamental sensing mechanisms of nanomaterials-based devices, I will present the innovative design and fabrication strategies for our sensor elements. The close interaction of simulation and experiment allows us to elaborate tailored, but also transferable, technological functionalization strategies for different analytes to cover a wide range of application scenarios. In a strongly interdisciplinary approach, we face the need for sophisticated integration and packaging solutions of the sensors into versatile lab-on-a-chip systems. Integrating the latter in microfluidic setups to provide large numbers of different assays just-in-time directs our technology in direction of highly automatized analytic procedures. The results of our research prove the vast potential of our sensing approach but also show the enormous space for further fundamental developments to boost the concept of nanomaterials-based sensor technology to a powerful and smart analytic tool capable of multiplexed studies, providing and evaluating rich and robust statistical output data. Recent results on artificial neuron behavior in our sensor devices will help shedding new light on the role of nanoarchitectures for a true neuromorphic computing.

Figures



Multivalency and cooperativity in nanoparticle blood brain barrier crossing

Giuseppe Battaglia^{1,2,3}

¹Department of Chemistry, University College London, UK.

²Institute for the Physics of Living Systems, University College London, UK.

³Department of Chemical Engineering, University College London, University College London, UK

g.battaglia@ucl.ac.uk

Abstract (Arial 10)

The interface between the circulatory system and the brain tissues, appropriately named the blood-brain barrier (BBB), is the largest brain barrier by surface area, and allows short diffusion distances (<25µm) between blood and neural tissue. The BBB plays an important physiological role by tightly gating the passage of ions and molecules, delivering nutrients according to the demanding neuronal needs and, at the same time, protecting the brain from toxins and pathogens.¹ The BBB is formed by specialised brain endothelial cells (BEC) whose phenotypic functions are conditioned by associated brain cells together forming a so called 'neurovascular unit'. BECs differ from other endothelial cells; they lack fenestrations, show low expression of immune cell adhesion molecules, and express extremely tight 'tight junctions' leading to severe restriction of paracellular transport.

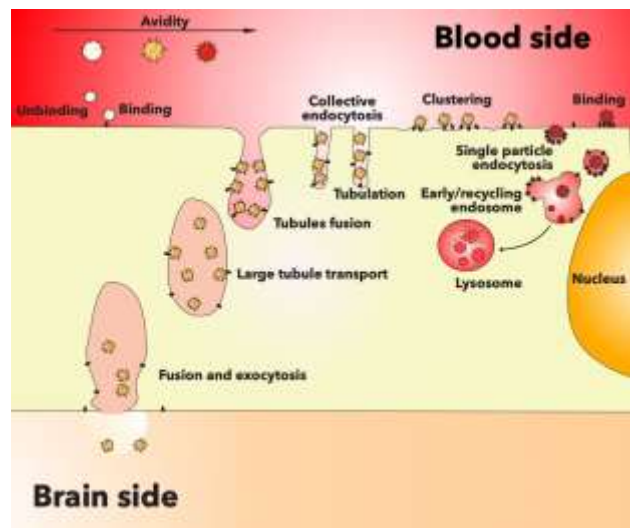
In the last 10 years we have focussed our attention on a technology that combines together two of the most clinically successful nanomedicines: liposomes and polymer nanoparticles. Polymersomes, like liposomes, are vesicles that allow the simultaneous encapsulation of hydrophilic and hydrophobic actives, however instead of using low molecular weight lipids, polymersomes are made by amphiphilic copolymers. The polymersome macromolecular nature allows multi-valency and enhances protein-fouling resistance. We have adapted polymersomes to cross the blood brain barrier and deliver within the CNS decorating them with Low density lipoprotein receptor-related protein 1 (LRP1) peptide Angiopep2 (LA). We have showed that careful conjugation of ligands on the polymersomes surface creates the required balance of selectivity and affinity to cross the blood brain barrier.^{2,3} We have set up an in vitro 3D models for BBB to study both the details of crossing and its cellular mechanisms.⁴ I will discuss here how multivalency allows for high selectivity and triggers a specific arrangement of membrane deformation that leads to controlled tabulation and fast crossing. We demonstrate that transcytosis of polymersomes occurs independently of the canonical endosomal trafficking pathway. Transcytosis is inhibited by small molecule inhibitors to the SNARE complex or dynamin, and also through depletion of cholesterol

at the basolateral membrane, indicating an interdependency between these structures for endocytosis and exocytosis of LA-psomes. These studies give new insight into transcytosis of macromolecules at the BBB, reinforcing the highly specialised phenotype of brain endothelial cells.

This is why shedding light on the mechanism that regulate BBB transport is critical to both understanding its physiology as well as to inform the bioengineering of solutions to delivery to the central nervous system (CNS).

References

1. Fullstone et al *Int. Rev Neurobiol.* 2016, 130, 41
2. Tian et al *Sci. Rep.* 2015, 5, 11990;
3. Joseph et al *Science. Adv.* 2017,3, e1700362
4. Tian et al *Sci. Rep.* 2017, 7, 39676;



Figures

Figure 1. Mechanism of multivalent BBB transcytosis.

Physics, biology and multiple sclerosis

Roy Beck¹

¹Tel-Aviv University, School of Physics and Astronomy,
Tel Aviv, Israel

roy@tauex.tau.ac.il

Key hurdle in modelling biological systems originates from complex interaction between multiple components. Physical models and experiments often reduce the number of components aiming to address the fundamental mechanisms. Nevertheless, in most cases, the inherent heterogeneity is an essential ingredient in the biological context. Here, I will present our recent efforts to model and understand the development of multiple sclerosis (MS) from a biophysical perspective [1,2].

Myelin sheath is a multilamellar complex of various lipids and proteins that surround axons and acts as an insulating layer for proper nerve conduction. In MS, the myelin structure is disrupted impairing its function. Previous studies showed that MS is correlated with small lipid composition variation and reduction in the adhesive myelin basic protein (MBP).

We find such alterations result in structural instabilities and pathological phase transition from a lamellar to inverted hexagonal that involve enhanced local curvature (Figure 1). Similar curvatures are also found in vivo in diseased myelin sheaths. Moreover, alteration in local environmental conditions, such as salinity and temperature, similarly induce the inverted hexagonal phase pathological structures.

Since the etiology and recovery pathways of MS are currently unclear, these findings delineate novel functional roles to dominant constituents in cytoplasmic myelin sheaths. It further shed new light on mechanisms disrupting lipid-protein complexes, and suggest new courses for diagnosis and treatment for MS.

References

- [1] R. Shaharabani, M. Ram-On, R. Avinery, R. Aharoni, R. Arnon, Y. Talmon, R. Beck, *Journal of the American Chemical Society*, 138 (2016) 12159–12165
- [2] R. Shaharabani, M. Ram-On, Y. Talmon, R. Beck, *Proceedings of the National Academy of Sciences USA*, in-press (2018)

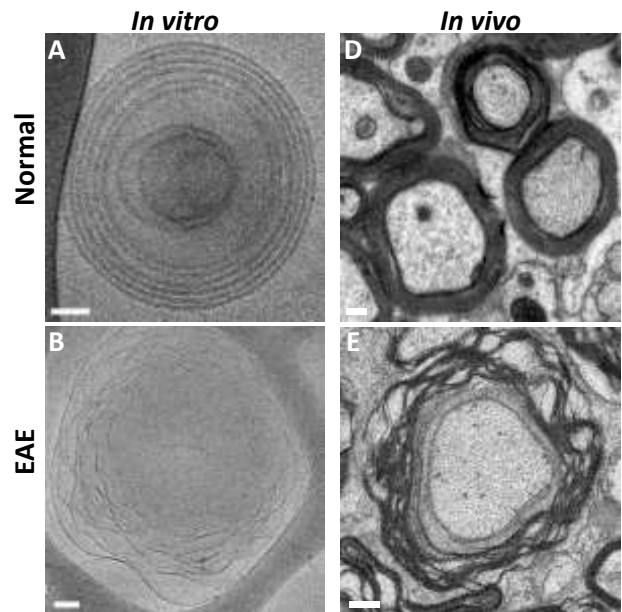


Figure 1. In-vivo and in-vitro nano-scale pathology of myelin membranes in healthy and diseased state. Taken from Shaharabani et al. [1].

Tight control of polymeric nanoparticles fabrication for optimized interaction with cells and tissues

Amoyav. B, Orehov N., Benny O.

¹ Institute for Drug Research, School of Pharmacy, Faculty of Medicine, The Hebrew University, Jerusalem, Israel

ofrab@ekmd.huji.ac.il

Abstract

Drug delivery is a central challenge in cancer therapy. The ability to cross biological barriers is a critical parameter for success of treatment. Nanoparticles are being extensively studied as drug carriers which potentially can improve efficacy and selectivity of anti-cancer treatments. Polymer nanoparticles may vary in size and rigidity thus presenting different cell interaction and drug performance accordingly (2). Using new methodology we show that tight control over particle preparation can assist to optimize interactions with cells and tissues. Microfluidics technology enables the manipulation of fluid flow at the microscopic scale. The capability to use small volumes of samples flowing through special designed micro-channels embedded into a chip, provides a new and improved platform for fabricating of drug delivery systems. Here we introduce the development of a highly tunable and controlled encapsulation technique for particles ranging from microns to nano-size using the same microfluidic chip design. Poly(lactic-co-glycolic acid) (PLGA 50:50)/Polyethylene glycol (PEG) polymeric particles were prepared with focused-flow chip-design, yielding of monodisperse particle batches. We show that by varying flow rates, solvents and polymers type we are able to optimize the size and decrease polydispersity index, using simple chip designs with no further related adjustments or costs. The performance of different types of particles in penetrating tumor cells and tissues was evaluated in ex-vivo 3D cellular models of patient derived cells (3). Using the novel microfluidic based platform with the ex-vivo "tissue-like" model may offer the tight tuning of particle properties which could potentially pave the way for a better precision nanomedicine.

References

- [1] Abramov E, Cassiola F, Schwob O, Karsh-Bluman A, Shapero M, Ellis J, Luyindula D, Adini I, D'Amato RJ, Benny O. *Nanomedicine*. 2015 Nov;11(8):1993-2002
- [2] Stern T, Kaner I, Laser Zer N, Shoval H, Dror D, Manevitch Z, Chai L, Brill-Karniely Y, Benny O. *J Control Release*. 2017 Jul 10;257:40-50.

- [3] Shoval H, Karsch-Bluman A, Brill-Karniely Y, Stern T, Zamir G, Hubert A, Benny O. *Sci Rep*. 2017 Sep 5;7(1):10428.
- [4] Amoyav B, Benny O. *Applied Nanoscience* 2018, Volume 8, Issue 4, pp 905–914

Figures

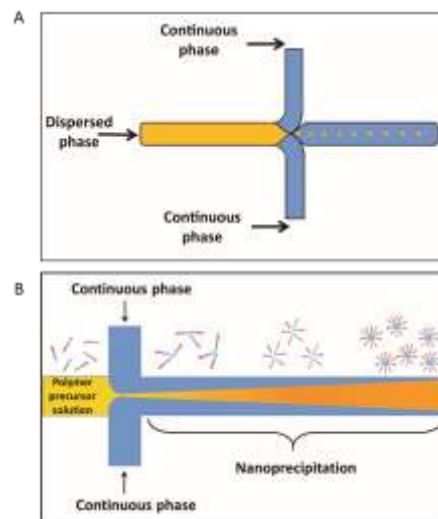


Figure 1. Focused-flow geometry chip design for droplet generation production. Schematic illustration of enlarged junction, controlled break-up droplet at the orifice. The flow through the orifice enables a controlled droplets break-up which is required for yielding monodisperse micro-emulsions.

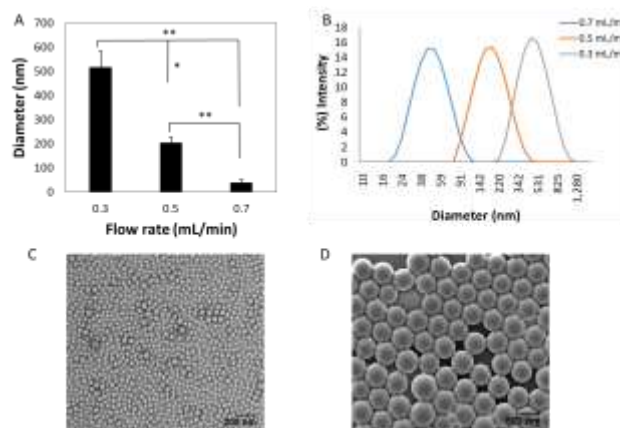


Figure 2. Diameter of PEG-PLGA nanoparticles can be controlled by gently varying continuous phase flow rates. Images of PEG-PLGA 1% solution particles fabricated at focused flow chip design. Continuous rates of 0.3 mL/min, 0.5 mL/min and 0.7 mL/min with constant dispersed flow rate of 0.005 mL/min. (A) Nanoparticles homogeneity summarized graph obtained in varying flow rates by rapid mixing solvent displacement method of 1% PEG-PLGA solution, (B) size measurement obtained by Dynamic Light Scattering (DLS). (C), (D) TEM and SEM images of PEG-PLGA particles respectively. *P<0.05; **P<0.01.

Graphene Neuroelectronics

Cécile Delacour,

Farida Veliev, Antoine Bourrier, Vincent Bouchiat

Institut Néel, F-38000 Grenoble, FRANCE

cecile.delacour@gmail.com

New methods and new technology are currently required to interrogate neuronal cells by many means and at multi-scale, in-vivo and within model neural networks in-vitro. In particular, to understand how neural circuits operate, we need access to activity of large numbers of neurons at the same time, and record their activity at the single cell level and at the nanoscale regarding the lot of information which relies at the level of synapses and ion channels. In that race, Graphene offers an ideal platform for recording and culturing neural networks, regarding its exceptional neuronal affinity and the presence of readily accessible surface charges which give the unprecedented possibility to realize a direct coupling with cells. Here, we report the cytocompatibility study of pristine monolayer graphene, and its significant advantage for neuroprostheses and fundamental research compared with the current electrodes materials of neuronal interfaces. We have shown that CVD-grown graphene monolayers [1] actively promotes neurites outgrowth without any surface functionalization with cell-adhesive coating (for instance poly-L-lysine). Our investigation with Raman spectroscopy show the impact of graphene crystallinity on the neurons adhesion and further growth, the monolayer becoming cell-repulsive with increasing amount of defect [2]. The ability to control the neuronal affinity of the graphene-coated substrate opens the way to a variety of applications for patterning long-lasting (in-vitro) neural networks (Fig.1) and for in-vivo implants with reduced inflammatory response and glial scars [3]. Moreover, the nano-structuration of those large (mm²) graphene monolayers allows the fabrication of dense arrays of highly sensitive field effect transistors [4]. The graphene liquid-gated transistors (G-FETs, fig.1b) show reproducible electrical properties (mobility and sensitivity being around 6000 cm².V⁻¹.s⁻¹ and 3-4 mS/V) and allow a rapid detection of very small (75 μV) potential spikes comparable with neuronal signaling. As graphene could be transferred on a wide range of substrate, it could be combined with multiple addressing and manipulation ports to record neurons electrical activity (Fig.1c), from single spike to nanoscale events such as ion channel currents [5].

References

1] Z. Han, A. Kimoche, D. Kalita, A. Allain, H. Arjmandi-Tash, A. Reserbat-Plantey, L. Marty, S.

Pairis, N. Bendiab, J. Coraux, V. Bouchiat, Adv. Func. Mat., 24 (2014) 964-970.

[2] Veliev, F., Briançon-Marjollet, A., Bouchiat, V., Delacour, C. Biomaterials, 86 (2016). 33-41.

[3] Salatino, J. W., Ludwig, K. A., Kozai, T. D., and Purcell, E. K. (2017). Nature Biomed. Eng. 1(11), 862.

[4] Veliev, F., Han, Z., Briançon-Marjollet, A., Bouchiat, V., Delacour, C. (2017). Front. in Neurosc., 11, 466.

[5] Veliev, F., Kalita, D., Bourrier, A., Belloir, T., Bouchiat, V., Delacour, C. (2018) 2D materials, 5(4), 045020

Figures

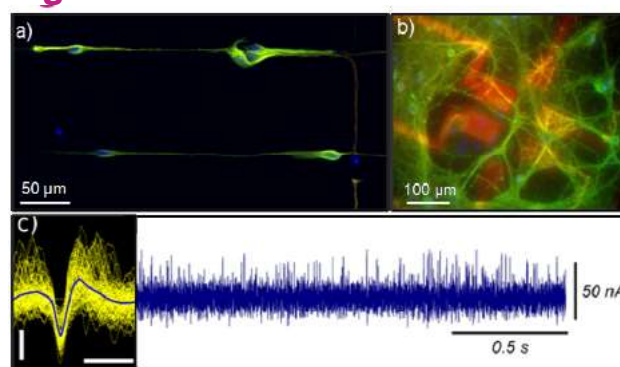


Figure 1. (a) Enhanced growth and confinement of primary hippocampal neurons (DIV2) on graphene micro-patterns. IF staining: the nuclei (bleu), the neurites (green) and the axons (red). (b) Neurons cultured 21 days on graphene FETs array. (c) Surimposed extracellular spikes (scale bar 2ms and 200μV) detected with the G-FETs(left), obtained from the drain-source current ISD time-traces (right).

Occupational exposure to nanobiomaterials in the medical sector

Carlos Fito-López¹,
Arantxa Ballester¹

¹ITENE, Albert Einstein 1. 46980 Paterna, Spain

cfito@itene.com

Abstract

In terms of occupational exposure, there is a variety of pathways through which nanobiomaterials can enter the human body that may pose an occupational health hazard, being inhalation the most common route of exposure in the workplace (Murashov, V., 2009).

In the medical sector, the workers who are most likely exposed to nanomaterials are those who prepare or administer nano-based pharmaceuticals “nanodrugs” or who work in areas where these nanobiomaterials are used, including pharmacy and nursing personnel, physicians, environmental service workers, shipping and receiving personnel, amongst others.

Other exposure situations may occur during handling of nanomaterial-contaminated items, cleaning and maintenance of areas where nanodrugs are handled. Exposure can also occur during handling of contaminated items, consuming food and beverages, which came in contact with drugs, and during cleaning and maintenance (Polovich M, 2003).

Possible exposure situations can be found in dental and surgical procedures involving the milling, drilling, grinding and polishing of applied medical devices containing nanomaterials, where there is a risk of nanoparticles becoming airborne and being inhaled by both the patient and healthcare personnel.

Table 1 shows a non-exhaustive list of possible exposure situations that can be found during ATMP/MD manufacturing and use.

As it can be observed in the table, occupational exposure to NBMs may occur during very different life cycle stages. The most studied ones are the production phase (e.g. recovering from reactor, packing...) and their use in the manufacture of nano-enabled products (e.g. prosthesis, bandages...), where the potential exposure mainly affects workers.

Table 1. . Possible exposure situations to NBMs in medical applications (H2020 BIORIMA project*)

Activities	Tasks	Exposure route	Target
ATMP			
Routine laboratory task with NBMs in R&D facilities	Weighing operations	Inhalation	Laboratory employees
	Mixing operations	Dermal	
	Functionalization		
	Purification		
	Collection and sorting		
	Packing / Re-packing		
Manufacturing	<i>In vitro & In vivo</i> testing		
	Weighing operations	Inhalation	Company employees
	Dissolution preparation	Dermal	
	Sampling		
	Discharge / Transfer		
	Packing / Re-packing		
Cleaning and maintenance			
Applications in health care settings			
Therapy preparation: Cancer treatment using intratumoral injections)	Flask filling and mixing operation	Inhalation Dermal	Health care workers
	Syringe filling (1 – 60 mL)	Dermal	
	NBM Delivery	Inhalation	
Handling of contaminated items	Handling patient excreta	Dermal	Health care workers
	Spills treatments	Dermal	Health care workers and cleaning staff
Maintenance operations	Maintenance of drug preparation devices	Dermal	Health care workers and maintenance staff
Medical devices			
Manufacturing			
Manufacturing of prosthesis	NBMs dosage during manufacturing	Inhalation Dermal	Company employees
	Injecting molding	Inhalation	
	Machining & abrasion		
Neural Prosthetics Devices	Mixing operations	Inhalation Dermal	
	Film coatings	Inhalation	
Surgical procedures			
Treatment of tooth cavities using high-speed tools	Drilling	Inhalation	Health care workers
	Polishing & Sanding	Inhalation	
Burns treatment: Wound dressings to protect patients (NanoAg based)	Dermal contact	Dermal	

The widely use of NBMs in medical sector leads to an increased potential for occupational exposure to these materials, warranting a need for prevention and effective measures to control their exposure.

Figure 1 summarize the most relevant parameters for inhalation of nanobiomaterials

Figures

Figure 1. Parameters relevant for inhalation of nanobiomaterials

Physico-chem. Properties	Activity patters
Nanobiomaterials Size, agglomeration / agregation state, moisture level	Work related Inhalation rates Body location Chemical co-exposures Lung diseases
Medical devices Concentration in articles Surface to volumen ratio Nano-scale material state (coatings, liquids, encapsulated particles)	Activity emission Potential for alteration of nanobiomaterial properties Frequency of exposure Duration of exposure Energy applied to the process Applied amount of NBMs
Advanced therapy medicinal products (ATMPs) Concentration in mixture Viscosity, Vapour pressure Nano-scale material state (coatings, liquids, encapsulated particles)	

References

- [1] Murashov V, Howard J. (2009). Essential features for proactive risk management. Nature Nanotechnology 4, 467-470.
- [2] Polovich, M. (September 30, 2004). "Safe Handling of Hazardous Drugs". Online Journal of Issues in Nursing. Vol. 9 No. 3,

*The research leading to these results has received funding from the European Union's Horizon 2020 research and innovation programme under grant agreement No 760928

New developments in the field of Drug Release instrumentation.

Gerardo F. Goya¹,

B. Sanz², I. Bruvera¹, A. Toro-Córdova¹

¹ Departamento de Física de la Materia Condensada - Instituto de Nanociencia, University of Zaragoza

²nB Nanoscale Biomagnetics S.L.

goya@unizar.es

A large number of nanotechnology-based drug delivery systems (DDS) are reported every year in the scientific literature. However, only a tiny fraction of these innovative approaches reaches pre-clinical or clinical phase studies. Different nanocarriers and release methods have shown good therapeutic efficiency at *in vitro* and *in vivo* levels, and some of those have proven positive therapeutic results in humans. From silica-based porous nanoparticles to liposomes or polymeric nanoparticles, new products commercially available already include nanovectors as drug carriers, and these new systems need to be characterized accordingly.

Non-invasive strategies for remotely triggering drug release have been proposed mainly for liposomal-based nanovectors. [1] These strategies can be based on different triggering stimuli, including (but not restricted to) enzymatic [2], temperature [3], light [4], magnetic fields [5] and ultrasound. [6] Of special clinical interest is the control of drug release profiles *on demand* by a remote alternating magnetic field of low frequency (i.e., at the low part of the RF spectrum, 100 – 800 kHz), because of the deep penetration of these waves without noticeable interaction with biological tissues.

In a collaborative effort between the Magnetic Hyperthermia Group and nB Nanoscale Biomagnetics S.L., we developed a new device (see Figure 1) capable of remote triggering and *in situ* quantification of therapeutic drugs, whenever a magnetically-responsive material need to be tested. Some examples are hydrogels (made of alginates, PNIPAAm, etc.) or functionalized MNPs as drug carriers. The heating efficiency of these materials can be measured by their specific power absorption (SPA) values, concurrently with the kinetics profiles of drug release.

The rates of drug release of any thermo-responsive material can be further controlled through application of AC magnetic field, using a time-modulated set of pulses to release the desired amount of drug. After several tests of standard thermoresponsive materials loaded with B12 vitamin as a concept drug, the outcome has shown good control of the kinetics profiles by time and field exposure. For example, using calibration methods before experiments, a time-pulse programming was applied to ferrogels samples to control the kinetic release

profiles. Under these conditions, the device was able to detect amounts of drug released as tiny as 5-12(1) ng, demonstrating its potential for high-precision real-time quantitative control of drug release.

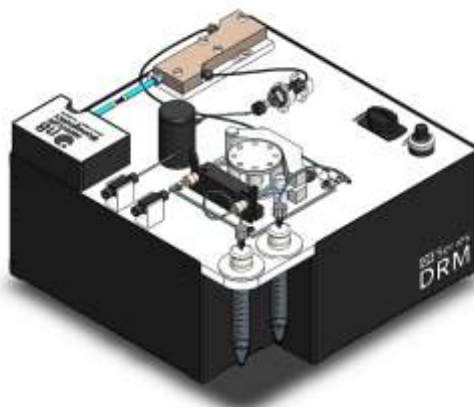


Figure 1. Schematic view of the device for real-time spectrophotometric sensing of drug release in magnetically-triggered thermosensitive materials.

References

- [1] Wang Y, Kohane DS. External triggering and triggered targeting strategies for drug delivery. *Nature Reviews Materials*. 2017;2:17020.
- [2] Meers P. Enzyme-activated targeting of liposomes. *Advanced drug delivery reviews*. 2001;53:265-72.
- [3] Burke C, Dreher MR, Negussie AH, Mikhail AS, Yarmolenko P, Patel A, et al. Drug release kinetics of temperature sensitive liposomes measured at high-temporal resolution with a millifluidic device. *International Journal of Hyperthermia*. 2018;34:786-94.
- [4] Vankayala R, Hwang KC. Near-Infrared-Light-Activatable Nanomaterial-Mediated Phototheranostic Nanomedicines: An Emerging Paradigm for Cancer Treatment. *Advanced Materials*. 2018;30:1706320.
- [5] Hoare T, Timko BP, Santamaria J, Goya GF, Irusta S, Lau S, et al. Magnetically triggered nanocomposite membranes: a versatile platform for triggered drug release. *Nano letters*. 2011;11:1395-400.
- [6] Salkho N, Turki R, Guessoum O, Martins A, Vitor R, Hussein G. Liposomes as a Promising Ultrasound-Triggered Drug Delivery System in Cancer Treatment. *Current molecular medicine*. 2017;17:668-88.

Next Generation Wearable Wellness Trackers with Graphene-based Flexible Photodetectors

Frank Koppens, Emre Polat, Stijn Goossens, Gabriel Mercier, Turgut Durduran, Gerasimos Konstantatos^{1,2},

¹The Institute of Photonic Sciences (ICFO), Castelldefels (Barcelona), Spain

²ICREA, Barcelona, Spain

Frank.koppens@icfo.eu

Sensors for ubiquitous sensing purposes should be low-cost, invisible and seamlessly integrable with many different surfaces such as bendable plastic, textiles and glass. Graphene based light sensors [1,2] are inherently flexible and transparent and can be integrated with low-cost CMOS technology [3], hence providing a disruptive platform for future wearables and vision devices.

We will show a prototype non-invasive wellness monitor based on graphene- colloidal quantum dot hybrid photo detectors (sensitive for wavelength range 300-2000 nm, <1ms time response). We leveraged graphene's flexible and transparent properties to create a wearable device that is conformal to the human body so that it can reliably extract vital signs such as heart rate, breathing rate and oxygen saturation (figure 1a). Furthermore, we present a graphene based UV-sensing patch. It records harmful UV-exposure on the skin. The patch does not need a battery as a smartphone provides energy via wireless power transfer (figure 1b).

The graphene-based sensing platform enables reliable monitoring of different vital signs and ambient conditions (figure 2). This provides the user a complete picture of his/her current wellbeing, which will be very valuable in preventive healthcare.

References

- [1] G. Konstantatos, et al., Nature Nanotechnol., 7 (June 2012)
- [2] Nikitskiy et al., Nat. Commun., 7 (June 2016)
- [3] Goossens et al., Nat. Phot. 11 (June 2017)

Figures



Figure 1. (a) Graphene based flexible and transparent wellness sensing platform.(b) Battery-less UV monitor powered via NFC communication.



Figure 2. Artist impression of graphene and 2D material based patch for monitoring personal wellbeing.

Long distance electron transfer between redox partner proteins through the aqueous solution

Anna Lagunas^{1,2},

Alejandra Guerra-Castellano³, Alba Nin-Hill⁴, Irene Díaz-Moreno³, Miguel A. De la Rosa³, Josep Samitier^{2,1,5}, Carme Rovira^{4,6}, Pau Gorostiza^{2,1,6,*}

¹Networking Biomedical Research Center (CIBER), Madrid 28029 Spain.

²Institute for Bioengineering of Catalonia (IBEC), The Barcelona Institute of Science and Technology (BIST), Barcelona 08028 Spain.

³Institute of Chemical Research (IIQ) – Centre of Scientific Research *Isla de la Cartuja* (icCartuja), University of Sevilla - CSIC, Sevilla 41092 Spain.

⁴Inorganic and Organic Chemistry Department & Institute of Theoretical and Computational Chemistry (IQTCUB), University of Barcelona (UB), Barcelona 08028 Spain.

⁵Department of Electronics and Biomedical Engineering, University of Barcelona (UB), Barcelona 08028 Spain.

⁶Catalan Institution for Research and Advanced Studies (ICREA), Barcelona 08010 Spain.

alagunas@ibecbarcelona.eu

Electrons flow through biological membranes yet they are not passively transported. Instead, they are carried individually by redox proteins. The demands on the ET capabilities of these proteins are conflicting: Their binding must be tight to keep ET rates high, but binding should be sufficiently weak to allow a high turnover rate and overall ET efficiency. As the distance between redox partners is reduced, an initial encounter complex is formed that leads to a final active complex. The structure of some active complexes between redox protein partners has been revealed by X-ray crystallography [1]. However, substantial differences can be observed in the distance between the active sites of several redox protein partner complexes, which raises the question of whether ET between proteins already occurs while the protein is approaching its partner site [1]. Despite the importance of electron transfer (ET) in biological processes such as photosynthesis and respiration, the inter-protein ET rate between redox partner proteins has never been dynamically measured as a function of their separation in aqueous solution.

Here we use electrochemical tunneling spectroscopy (ECTS) [2,3] under bipotentiostatic control to measure the current between two ET partner proteins and its dependence with their separation in an aqueous electrolyte. We chose the ET process between cytochrome *c* (Cc) and complex III (CIII or cytochrome *bc*1) as a well-known and representative step of the mitochondrial respiratory chain [4,5] We observe that current decays along more than 10 nm in the solution. Molecular dynamics simulations reveal a reduced ionic density and extended electric field in the volume confined between the proteins. The distance decay factor and the calculated local

barrier for ET are regulated by the electrochemical potential applied to the proteins, which highlights the physiological relevance of the results. We conclude that redox partner proteins could use electrochemically gated, long distance ET through the solution to conciliate high specificity with weak binding, thus keeping high turnover rates in the crowded environment of cells.

References

- [1] Solmaz, S. R. N. & Hunte, C. *J. Biol. Chem.* 283 (2008) 17542.
- [2] Halbritter, J., Repphun, G., Vinzelberg, S., Staikov, G. & Lorenz, W. *J. Electrochimica Acta* 40 (1995) 1385.
- [3] Díez-Pérez, I., Güell, A. G., Sanz, F. & Gorostiza, P. *Anal. Chem.* 78 (2006) 7325.
- [4] Nyola, A. & Hunte, C. *Biochem. Soc. Trans.* 36 (2008) 981.
- [5] Kokhan, O., Wraight, C. A. & Tajkhorshid, E. *Biophys. J.* 99 (2010) 2647.

Figures

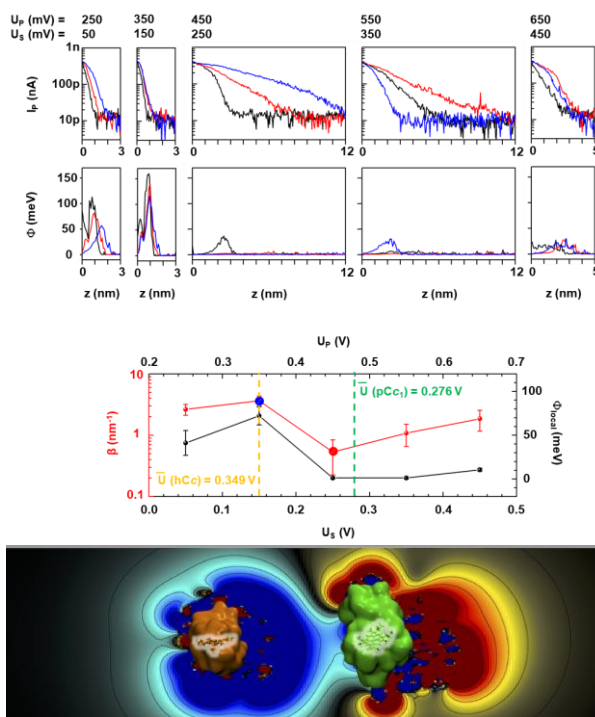


Figure 1. Semilogarithmic retrace current-distance plots at 200 mV constant bias for pCc₁-hCc at the indicated probe (U_p) and sample (U_s) potentials and the corresponding Φ dependence with distance. Below, plot of the averaged β (red) and Φ_{local} (black) values, obtained from individual I - z curves, as a function of U_s and U_p potentials showing minima reached in both cases near the redox midpoint potentials of hCc and pCc₁ (dashed lines). In the image below, side view of the equipotential lines from -1.1 kT/e (red) to 1.1 kT/e (blue) calculated by Poisson-Boltzmann equation (APBS). hCc (orange) and pCc₁ (green) proteins are superimposed for visualization purposes.

Functional Protein Fibrils

Meytal Landau¹,

Einav Tayeb-Fligelman¹, Nir Salinas¹, Sergei Perov¹,
Ofir Lidor¹, Itzik Engelberg¹, Nimrod Golan¹

¹ Department of Biology, Technion – Israel Institute of
Technology, Haifa, Israel

mllandau@technion.ac.il

The mechanisms of amyloid protein assembly into fibrous structures have been studied for decades, particularly since amyloids are associated with neurodegenerative and systemic human diseases. In contrast, functional amyloids that participate in dedicated physiological activities in all kingdoms of life were poorly characterized and their importance to human health is only starting to emerge. Functional amyloids were discovered mostly in microbes, serving as key virulence factors and thus present novel targets for antimicrobial agents. The structural hallmarks of functional amyloids – if any – and how they can be distinguished from disease-associated amyloids remain unclear. We investigated the structure-function-fibrillation relationships of microbial functional amyloids, their interactions with host amyloids and receptors and explore routes to modulate their activities. By leveraging unique methodologies of X-ray microcrystallography, we were the first to obtain atomic structures of bacterial functional amyloids. We discovered unique amyloid-like structures, including, to our surprise, a structure of a full-length bacterial cross-alpha amyloid-like fibril revealing surprising departure from pathological amyloids in which beta-rich structures are central. The fibrils, of the PSM α 3 peptide secreted by the pathogenic bacterium *Staphylococcus aureus*, are toxic to human cells, clarifying their involvement in pathogenicity. In contrast, amyloidogenic peptides involved in biofilm structuring share similar atomic structures with pathological amyloids, forming ultra stable cross-beta structures that stabilize the biofilm matrix. Surprisingly, three fibrillating antibacterial peptides secreted by different organisms (bacteria, amphibian and human) exposed extremely polymorphic fibrous architectures, all markedly different from the cross-beta fibril. Given our results we predict that the structural and functional repertoire of functional amyloids is far more diverse than previously anticipated, providing a rich source of targets for antimicrobial drug discovery.

Figure

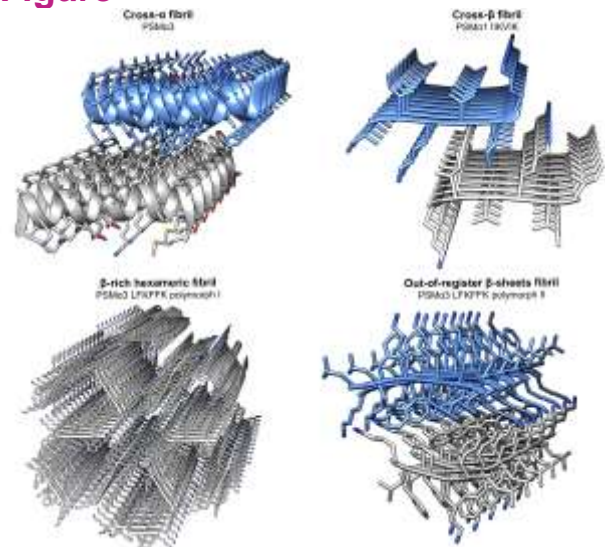


Figure 1. Highly polymorphic amyloid fibril structures of *S. aureus* PSM α peptides.

References

- [1] Tayeb-Fligelman, O. Tabachnikov, A. Moshe, O. Goldshmidt-Tran, M.R. Sawaya, N. Coquelle, J-P. Colletier, and M. Landau, *Science* 355:6327 (2017) 831-833
- [2] R. Malishev, E. Tayeb-Fligelman, S. David S, M. Meijler, M. Landau, and R. Jelinek, *J. Mol. Biol.* 430:10 (2018) 1431-1441
- [3] N. Salinas, A. Moshe, J-P. Colletier, and M. Landau. *Nat. Commun.* 9:1 (2018) 3512
- [4] M. Landau, *Nat. Chem. Biol.* 14:9 (2018) 833-834

New Biotechnological Challenges for Magnetic Hyperthermia

Prof. Jesús M. De la Fuente¹,

¹Aragon Material Science Institute, ICMA, CSIC-University of Zaragoza & CIBER-BBN

jmfuente@unizar.es

The use of nanoscale structures has been used by Nature for billions of years. Two properties that make them very interesting for use in biomedical applications are (i) they have a typical size similar to biological components and (ii) the possibility of manipulating and designing materials with almost à la carte properties controlling the size, composition and shape. The research of our group is mainly focused on the use of magnetic nanoparticles and their ability to generate heat applying an alternating magnetic field. For that, different iron oxides nanoparticles has been prepared by different methodologies and with different size and organic or inorganic coatings. The potential of using the generated heat by applying alternating magnetic fields in the microenvironment of magnetic nanoparticles to activate multienzymatic industrial bioprocesses has been explored. This feature will be also used for the treatment of cancer by magnetic hyperthermia or targeted enzyme therapy. Our research is divided into two distinct but clearly related fields through a common nexus: the type of material used to generate heat by applying an alternating magnetic field (magnetic nanoparticles).

1) **Magnetic Hyperthermia for Biocatalysis:**

We report here how the properties of magnetic nanoparticles (NPs) and of thermophilic enzymes can be combined to obtain NP-enzyme systems capable to be activated in a wireless fashion. Conjugation of α -amylase and L-aspartate oxidase to the surface of magnetic nanoparticles and using different strategies obtaining different orientations of the enzymes respect to NP surface. This allowed us to create effective biocatalysts with different activities (ranging from 17 to 87 % of the initial activity). Furthermore, spectroscopic studies showed that the conjugation of the enzyme to the NP modifies its 3D structure and that different conjugation strategies lead to different stretching of the protein. Results clearly demonstrate that the application of an AMF activates the nano-systems, without a significant increasing in the reaction media temperature. Furthermore, we successfully reused the nano-systems for at least three consecutive cycles of AMF activation with the loss of only the 40% of the initial activity.

2) **Magnetic Hyperthermia and 3D cell culture models:** Understanding the mechanisms involved in the cellular damage generated by

magnetic hyperthermia is crucial for its successful application. In order to evaluate the treatment efficacy, two different 3D cell culture models were prepared using a collagen matrix, which is one of the major component of the tumour extracellular matrix. A strong effect of the hyperthermia treatment was observed on the location of the particles within the 3D cell culture for one of the models. The treatment facilitated the migration of the particles from the outer areas of the 3D structure, achieving a faster homogeneous distribution throughout the whole structure and providing access to the particles to the inner cells. Moreover, although in both models cells were exposed to the same amount of nanoparticles, as a consequence of the 3D model generation, the cell death mechanism activated by the magnetic hyperthermia treatment was different in both models.

Fabrication and Multifunctional Applications of Micro/Nano-Motors

Xing Ma¹,

Yong Wang^{1,2}, Dandan Xu^{1,2}, Chunyan Liang^{1,2}

¹State Key Laboratory of Advanced Welding and Joining (Shenzhen), Harbin Institute of Technology (Shenzhen), Shenzhen 518055, China

²Flexible Printed Electronic Technology Center, School of Materials Science and Engineering, Harbin Institute of Technology (Shenzhen), Shenzhen 518055, China
maxing@hit.edu.cn

Abstract: Self-propelled micro/nano-motors (MNM) are active matters that can convert energy from their surroundings into kinetic force to propel themselves. MNM have been proven as powerful tools that can accomplish a variety of on-demand tasks at small scales, leading to revolutionary solutions to traditional strategies. For instance, MNM have exhibited great potential in biomedical and environmental applications, such as active targeted drug delivery, pollutant removal by controllable MNM or active sensing. However, regarding the fabrication techniques, different applications requires varied functional materials for the construction of MNM. MNM for biomedical purpose such active drug delivery system should be biocompatible in terms of fabrication materials, as well as fuel providing the energy to power their self-propulsion. Meanwhile, integration of multiple functions into a single motor is highly demanded. Novel nanomaterials such as mesoporous silica have been proved wide applications in virtue of unique structure and specific functions at small scale. [1] Hereby, by integration between novel nanomaterials, we successfully fabricated a series of MNM capable of self-propulsion by consuming non-toxic fuel or by fuel free propulsion, and realizing multiple functionalities.[1-5] We also achieved reversible velocity control on the motors by manipulating the enzymatic activity with inhibitors/re-activation molecules.[3] Magnetic guidance was utilized to control the motors' movement direction, towards target locations.[3-4] In addition to magnetic and enzymatic control, we also utilized external field such as light to propel and control the motion of the MNM by photocatalytic reactions. The nanopores of the mesoporous silica with internal pore diameter about 2-3 nm can be utilized for drug loading or pollutant adsorption in large quantity, indicates great potential of using them for active target drug delivery in future biomedical applications,[1] as well as pollutant sample collection at small scale.[4] By combining with surface enhanced Raman spectroscopy, we realized active and intelligent biochemical sensing with self-propelled motors as well, giving new solution to the intelligent Raman analysis.[5]

References

- [1] Xing Ma, Kersten Hahn, Samuel Sanchez. *J. Am. Chem. Soc.* **2015**, 137, 4976–4979.
 [2] Xing Ma, Anita Jannasch, Urban-Raphael Albrecht, Kersten Hahn, Albert Miguel López, Erik Schäffer and Samuel Sanchez. *Nano Lett.* **2015**, 15, 7043–7050.
 [3] Xing Ma, Xu Wang, Kersten Hahn, Samuel Sanchez. *ACS Nano.* **2016**, 10, 3597–3605.
 [4] Chunyan Liang, Chen Zhan, Fanyu Zeng, Dandan Xu, Yong Wang, Weiwei Zhao, Jiaheng Zhang, Jinhong Guo,* Huanhuan Feng* and Xing Ma*. *ACS Appl. Mater. Interfaces* 2018
 DOI: 10.1021/acsami.8b10921
 [5] Yong Wang, Chao Zhou, Wei Wang, Dandan Xu, Fanyu Zeng, Chen Zhan, Jiahui Gu, Mingyu Li, Weiwei Zhao, Jiaheng Zhang, Jinhong Guo,* Huanhuan Feng,* Xing Ma*. *Angew. Chem. Int. Ed.* 2018, 130, 1-5.

Figures

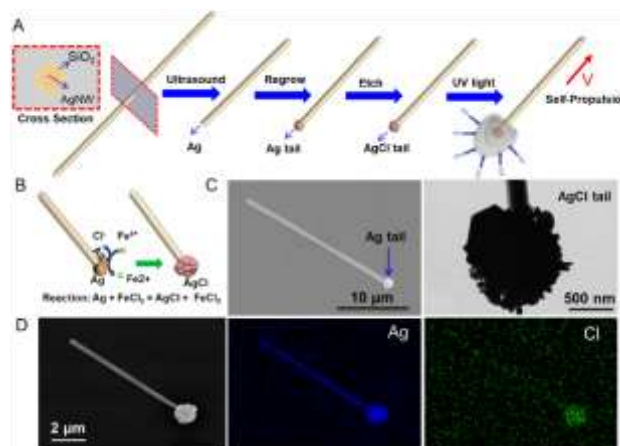


Figure 1. Fabrication and characterization of the Photocatalytically Powered “Match-Like” Nano-Motor for Light-Guided Active SERS Sensing.[5]

Teaming up sperm cells with micro- & nanostructures for novel diagnostic tools in reproductive biology

Veronika Magdanz¹

Johannes Gebauer¹

Juliane Simmchen²

¹Applied Zoology, TU Dresden, Germany

²Physical Chemistry, TU Dresden, Germany

veronika.magdanz@tu-dresden.de

The development of autonomous microdevices which are motile, display smart functionalities and can be remotely controlled is a fascinating and quickly emerging field that combines expertise from nano- and biotechnology as well as chemistry, biology and physics. Biohybrid microrobots have been developed by integrating motile sperm cells into microstructures, in which the spermatozoa serve as propulsion source. [1] This talk will give an overview of the prospects of teaming up spermatozoa with micro- and nanostructures in terms of actuation, imaging, sensing and cell manipulation tasks.

The interaction between micro- and nanoparticles and spermatozoa depending on their surface charge is investigated and gives promising applications in cell surface charge mapping, actuation and sperm conditioning. The lecture will point out the possibilities of this approach to investigate sperm migration in vitro and in vivo as well as novel tools for reproductive biology and medicine that evaluate sperm quality.

References

- [1] V. Magdanz, S. Sanchez, O.G. Schmidt, *Advanced Materials* 25, 45 (2013)

Figures

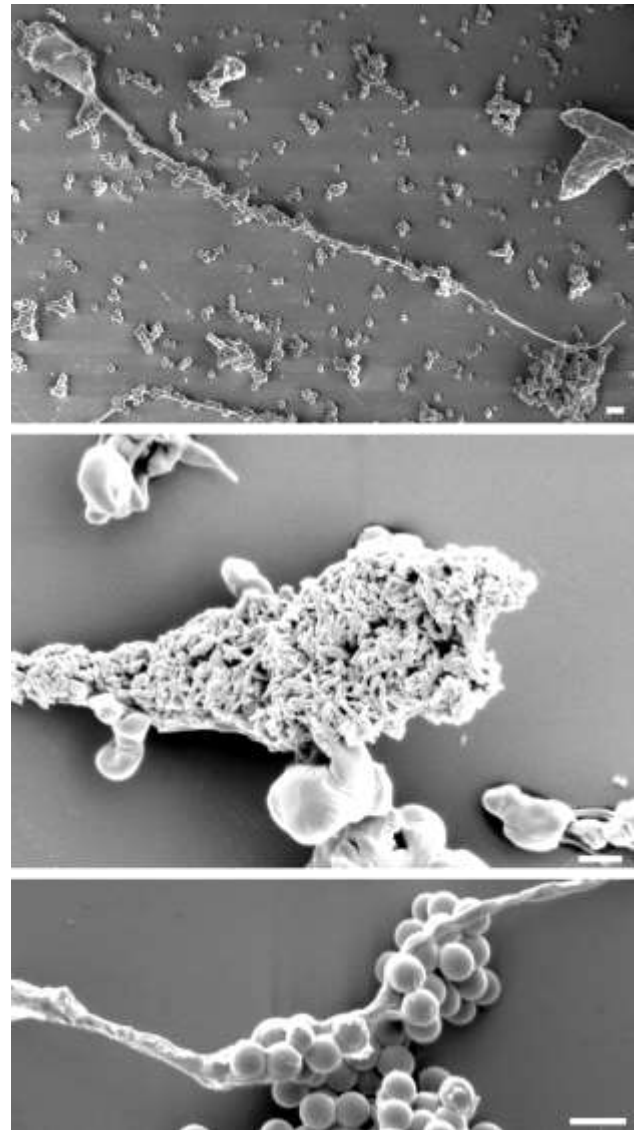


Figure 1. Micro-/nanoparticles binding to bovine sperm cells. Top: silica-particles binding on head and tail of the sperm cell. Middle: elongated silica-coated magnetite particles binding on sperm head. Bottom: magnetite particles binding on sperm flagellum. Scale bars 2 μ m.

Nanomaterials in 2D, 3D, 4D printing

Shlomo Magdassi,

The Hebrew University of Jerusalem
Institute of Chemistry, Jerusalem, Israel

magdassi@mail.huji.ac.il

Functional printing brings additional performance of printed patterns, beyond graphic output. Additive manufacturing enables fabrication of objects and devices through printing processes. Our research is focused on synthesis and formulations of nanoparticles and inks, and their utilization for manufacturing devices and 3D objects for various fields. New findings on printed biosensors will be presented, as well as printing 3D objects. 3D printing is considered as the next industrial revolution, which is based on layer by layer digital deposition of materials. Nowadays, 3D objects can be fabricated by a variety of processes, including laser melting, binder jetting and stereolithography. The later is based on localized photopolymerization, which is initiated by exposure to light. It is mostly used to print polymeric objects while starting with inks composed of monomers, oligomers and photoinitiators. Biological applications such as 3D scaffolds for implants requires water compatibility of the objects, such as in a form of hydrogels. However, most of the available photoinitiators are water insoluble, and therefore there is an unmet need for materials that enable 3D printing in water. Various water-based printing approaches will be presented, including fabrication of responsive objects, which opens the way to biological applications and 4D printing.

References

- [1] Amol A. Pawar, Saada, G., Cooperstein, I., Larush, L., Jackman, J.A., Tabaei, S.R., Cho, N.J., Magdassi, S., Science Advances, (2016), 2: e1501381.
- [2] A. Pawar, S. Halivni, N. Waiskopf, Y. Ben-Shahar, M. Soreni Harari, S. Bergbreiter, U. Banin, S. Magdassi, Nano Lett. (2017) , 17 , 4497-4501.
- [3] L. Larush, I. Kaner, A. Fluksman , A. Tamsut, A. A. Pawar , P. Lesnovski , O. benny S. Magdassi, J. 3D Print. Med. (2017) 219-229

Nanoporous anodic alumina optical biosensors and biomedical applications

Lluís F. Marsal

Laura K. Acosta, Elisabet Xifre-Perez,
Josep Ferre-Borrull, Pilar Formentin

Universitat Rovira i Virgili, Department of Electronic Engineering, Avda Paisos Catalans 26, 43007 Tarragona, Spain

lluis.marsal@urv.cat

Nanoporous anodic alumina (NAA) is a versatile and low-cost material which can be used to develop optical biosensing platforms and other innovative biomedical applications such as selective molecular separation, chemical and biological sensing, cell culture, tissue engineering and drug delivery [1-2]. NAA presents a versatile nanoporous geometry and its surface chemistry can be engineered to tune its optical and chemical properties. The geometric characteristics of NAA (pore diameter, interpore distance, and thickness) can be modified by different anodization strategies and by post-anodization treatments (etching and annealing). Under specific anodization conditions (type of electrolyte, anodization potential or current and temperature), hexagonal straight cylindrical nanopore arrays with pore diameters between 10 nm and 400 nm and interpore distances until 900 nm can be obtained [3-4]. Figures 1 and 2 show the pore distribution of NAA obtained under different fabrication conditions. Chemical resistance, biocompatibility, thermal stability, and intrinsic photoluminescence are some of the outstanding properties of NAA [5]. Its highly effective surface area (hundreds of m^2/cm^3) makes of NAA an interesting platform for sensing and loading-releasing of active agents.

The application of periodic variations of current or voltage during the anodization is transferred to the material as the periodic variation of the pore diameter with depth and consequently, to the periodic variation of the effective refractive index. In this way, we can design one-dimensional photonic crystals with stop bands tunable within the UV-VIS-NIR range.

In this work, we present the use of NAA for developing advanced drug delivery systems and complex gated materials for biosensing applications [6]. In these systems, the NAA nanopores are utilized for the storage of drugs or molecules that are released in a controlled way under selective external conditions. The pore geometry has been tuned to control the diffusion of molecules. Recently, stimuli-responsive release drug delivery systems based on stimuli such as temperature, pH, temperature, magnetism, sound, and light have been reported with NAA platforms.

We have also engineered NAA to produce one-dimensional photonic crystals (1D-PC) with an enhanced optical response. We demonstrate that it is possible to tune the photonic bands of simple and complex NAA 1D-PC in the UV-Vis-NIR spectra. We deeply study the fabrication technological parameters that determine the properties of the optical response. Furthermore, low-cost NAA 1D-PC biosensors are presented for the detection of substances of interest for the health and the environment like fungus, bacteria, proteins or drugs. NAA membranes have already been used for developing cell culture scaffold substrates with enhanced adhesion and proliferation of cells. We have demonstrated the suitability of NAA structures for reproducing 3D cellular microenvironments. Here, we present the results of our investigations about the effect of the geometry and functionalization of NAA on the adhesion and morphology of human aortic endothelial cells. This work has allowed the understanding of the complex cellular interactions and behaviors.

Finally, micro and nanoparticles of NAA are proposed for biological applications. We have fabricated, characterized, and functionalized NAA micro and nanoparticles with different shapes. Figure 3 shows nanoparticles with a tubular shape [7]. We have successfully linked a protein/antibody to the NAA particles with a simplified process. The analysis of cell viability and cytotoxicity of the particles have shown their biocompatibility and demonstrated their interesting potential use for localized treatments.

Acknowledgements:

The Spanish Ministry of Economy and Competitiveness TEC2015-71324-R, the Catalan authority AGAUR 2017SGR1527, and the ICREA Academia Award.

References

- [1] A. Santos, P. Formentín, J. Ferré-Borrull, J. Pallarès, L.F. Marsal, *Mater. Lett.* 67 (2012) 296
- [2] J. Ferré-Borrull, J. Pallarès, G. Macías, L.F. Marsal, *Materials* 7 (2014) 5225
- [3] L. F. Marsal, L. Vojkuvka, P. Formentin, J. Pallarès, J. Ferré-Borrull, *Optical Mater.* 31 (2009) 860.
- [4] Y. Ma, Y. Wen, J. Li, Y. Li, Z. Zhang, C. Feng, R. Sun, *Scientific Reports* 6, (2016) 39165.
- [5] E.Xifre-Perez, J. Ferré-Borrull, J. Pallarès, L.F. Marsal, *Microporous Mesoporous Mater.* 239 (2017) 363
- [6] A. Ribes, E. Xifre-Pérez, E. Aznar, F. Sancenón, T. Pardo, L.F. Marsal, R. Martínez-Mañez, *Sci. Rep.* 6 (2016) 38649.
- [7] E. Xifre-Perez, S. Guaita-Esteruelas, M. Baranowska, J. Pallares, L. Masana, L.F. Marsal, *ACS Appl. Mater. Interfaces*, 7(2015) 18600.

Figures

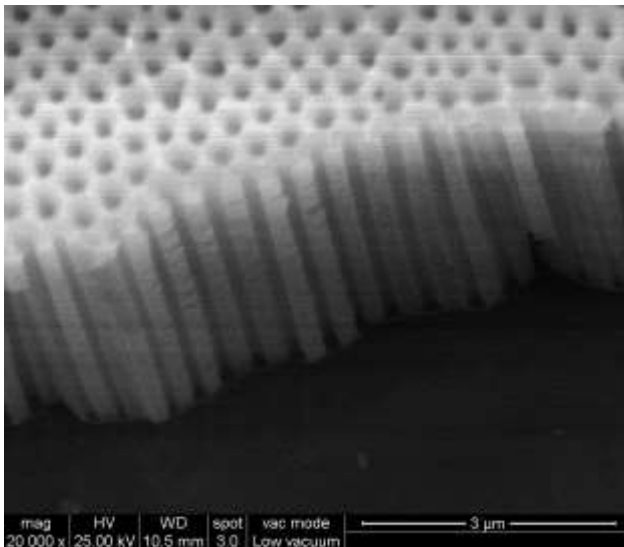


Figure 1. SEM image (transversal view) of a NAA layer.

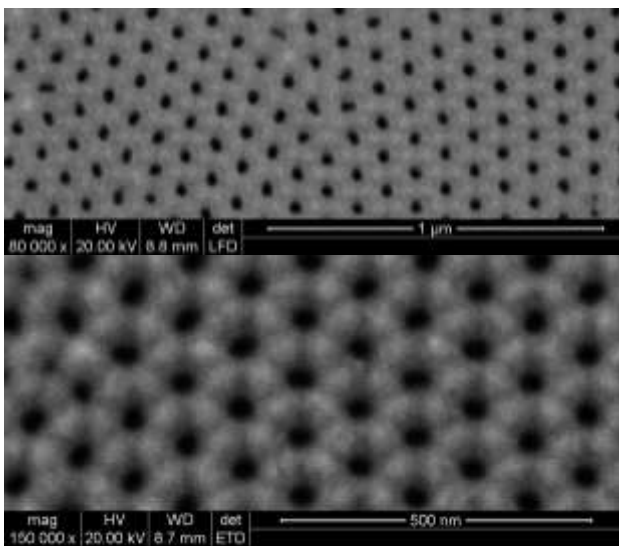


Figure 2. SEM image (top view) of NAA obtained with oxalic acid (top) and phosphoric acid (bottom).

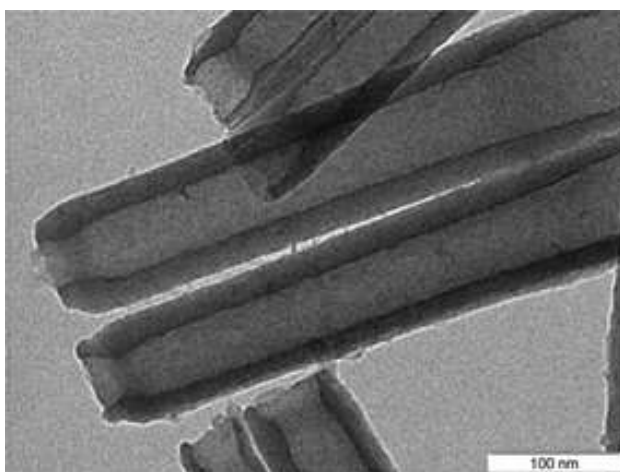


Figure 3. TEM image of nanoparticles of NAA with a tubular shape.

Multifunctionalized carbon nanotubes towards targeted anticancer radiotherapy

Cécilia Ménard-Moyon

University of Strasbourg, CNRS, Immunology, Immunopathology and Therapeutic Chemistry, UPR 3572, 67000 Strasbourg, France

c.menard@ibmc-cnrs.unistra.fr

Due to their outstanding physicochemical properties, the application of carbon nanotubes (CNTs) has been extensively explored in nanomedicine.[1] Thanks to their high aspect ratio, they have the capability to easily cross biological barriers and to be internalized into cells. Functionalization is a fundamental step to increase their dispersibility and biocompatibility, conjugate bioactive molecules, and impart multimodality.[2] Up to date, only few studies have explored CNTs as carriers of radionuclides for imaging and/or therapy. In this context, we have synthesized a CNT carrier for the targeted delivery of radioactivity through a combination of endohedral and exohedral functionalization. CNTs filled with metal halides as radioactive analogues confined in the inner cavity, have been functionalized on their surface with a monoclonal antibody targeting the epidermal growth factor receptor (EGFR) overexpressed by several cancer cells.[3] We have proved that the filled and functionalized carbon nanotubes can target cancer cells overexpressing the EGFR by flow cytometry, confocal microscopy, and elemental analyses. We have evaluated the immunological profile of the conjugates *in vitro* and *in vivo*. [4] We have also performed *in vivo* experiments in lung-tumor bearing mice to evaluate the biodistribution and therapeutic effect of the conjugates.[5] Overall, this work demonstrates that the encapsulation of radioisotopes within CNTs and subsequent surface functionalization with targeting ligands is promising for the selective delivery of radioactivity at ultrasensitive doses for therapy and/or diagnosis. We hope that our results will inspire the development of novel nanomaterials for biomedical applications in the areas of cancer diagnosis and therapy.

References

- [1] Kumar S., Rani R., Dilbaghi N., Tankeshwar K., Kim K.H., Chem. Soc. Rev., 46 (2017) 158.
- [2] Battigelli A., Ménard-Moyon C., Da Ros T., Prato M., Bianco A., Adv. Drug. Deliv. Rev., 65 (2013) 1899.
- [3] Spinato C., Perez Ruiz de Garibay A., Kierkowicz M., Pach E., Martincic M., Klippstein R., Bourgognon M., Wang J.T.,

- Ménard-Moyon C., Al-Jamal K.T., Ballesteros B., Tobias G., Bianco A., Nanoscale, 8 (2016) 12626.
 - [4] Perez Ruiz de Garibay A., Spinato C., Klippstein R., Bourgognon M., Martincic M., Pach E., Ballesteros B., Ménard-Moyon C., Al-Jamal K.T., Tobias G., Bianco A., Sci. Rep., 7 (2017) 42605.
 - [5] Manuscripts in preparation.
-

Imaging receptor-ligand response to nanopatterns of surface-bound ligands

Samuel Ojosnegros¹,
Verónica Hortigüela¹,
Enara Larrañaga¹,
Anna Seriola¹,
Francesco Cutrale²,
Anna Lagunas^{1,4},
María García-Díaz¹,
Jordi Andilla³,
Pablo Loza³,
Josep Samitier^{1,4,5},
Elena Martínez^{1,4,5}.

Institute for Bioengineering of Catalonia (IBEC),
The Barcelona Institute of Science and Technology
(BIST), Barcelona, Spain¹
University of Southern California, Translational
Imaging Center, Los Angeles, CA, USA²
ICFO-Institut de Ciències Fotoniques, Castelldefels,
Spain³
Centro de Investigación Biomédica en Red
(CIBER), Madrid, Spain⁴
Dep. of Electronics and Biomedical Engineering,
University of Barcelona (UB), Barcelona, Spain⁵

sojosnegros@ibecbarcelona.eu

Cell membrane receptors, including the outstanding family of Receptor tyrosine kinases (RTK), are key to crucial cellular processes, such as division, migration or positioning. Membrane receptors bind to specific ligands which often induce receptor clustering, fostering transactivation of the receptors and transduction of ligand cues into the cell. Despite the broad interest in designing nanostructured materials to modulate receptor activation, solving the kinetics of receptor clustering in diffusive membranes demands live-imaging operating at the nanoscale, which is beyond the capabilities offered by conventional methods. Here, we overcome these limitations by delivering ligands to cells on nanopatterned surfaces¹ combined with a novel fluorescence fluctuation analysis termed enhanced Number and Brightness (eN&B)². We study the activation of the EphB2 receptor by using a nanostructured platform to deliver ligands in patterns of regular nanosized (< 30 nm) clusters. We based our platform in self-assembled diblock copolymers composed of poly(styrene) (PS) and poly(methyl methacrylate) (PMMA) that tend to segregate into nanodomains. We then use eN&B to discriminate, with molecular sensitivity, the oligomeric state of the receptor during real time

activation. Our substrates accelerated the dynamics of receptor oligomerization process when compared to antibody-induced ligand clustering. Such an efficiency was induced even when ligand surface coverage was 9-fold lower in the nanopatterned presentation. Therefore, our ligand presenting platform is thought to induce multivalent ligand-receptor interactions, and might be a useful strategy to precisely tune and potentiate receptor responses. This feature can benefit applications such as the design of new bioactive materials and drug-delivery systems.

References

- [1] Hortigüela, V. *et al.* Nanopatterns of Surface-Bound EphrinB1 Produce Multivalent Ligand-Receptor Interactions That Tune EphB2 Receptor Clustering. *Nano letters* **18**, 629-637, doi:10.1021/acs.nanolett.7b04904 (2018).
- [2] Ojosnegros, S. *et al.* Eph-ephrin signaling modulated by polymerization and condensation of receptors. *Proceedings of the National Academy of Sciences of the United States of America* **114**, 13188-13193, doi:10.1073/pnas.1713564114 (2017).

Figures

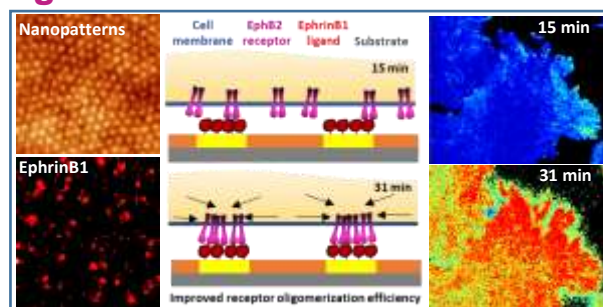


Figure 1. Nanopatterned ephrinB1 in diblock copolymers induces oligomerization efficiently. Enhanced Number and Brightness allows imaging receptor dynamics at the nanoscale.

Magnetolectric Small-Scale Machines for Biomedical Applications

Salvador Pané

Multi-Scale Robotics Lab
 Institute of Robotics and Intelligent Systems
 ETH Zurich, 8092 Zurich (Switzerland)

vidalp@ethz.ch

Over the past two decades researchers have been working to create synthetic small-scale machines ranging from molecular entities or miniaturized structures, to more complex assemblies of micro- and nanomaterials. These machines are able to navigate in complex environments by harvesting fuel from the surrounding media or from external power sources. One of the most sought-after applications for these miniaturized machines is to perform minimally invasive interventions, in which these devices will ultimately reduce risk, cost, and discomfort compared to conventional interventions. This has driven researchers to produce a myriad of small-scale robots loaded with therapeutic cargo.

One of the main aspects investigated has been the fabrication and optimization of the motility component of these small agents, and one of the most promising approaches is to use electromagnetic systems to wirelessly control and actuate magnetic micro and nanostructures. While many efforts have been dedicated to locomotion, there are many other challenges in small-scale robotics, for instance, the development of miniaturized mobile platforms capable of integrating multiple functionalities. We present here magnetolectric-composite small-scale machines that, under the same source of energy, are able to perform two different functionalities depending on how magnetic fields are applied. The magnetostrictive component enables this machine to propel, while the magnetolectric composite can be used to generate wirelessly a piezoelectric field [1]. The first part of this talk will focus on the concept of magnetically induced piezochemical potential, which can be exploited, for instance, to induce chemical processes such as electrodeposition [2] (Figure 1). In the second part of this talk, we will focus on the potential biomedical applications of these magnetolectric small-scale robots. As an example, we will show how core-shell

magnetolectric nanowires are able to release *in vitro* anti-cancer drugs on-demand using the magnetolectric approach [3].

References

- [1] J. Ma et al., Adv. Funct. Mater. 23 (2011), 1062
- [2] Chen et al., Mater. Horiz. 3 (2016), 199.
- [3] Chen et al., Adv. Mater. 29 (2017), 1605458.

Figures

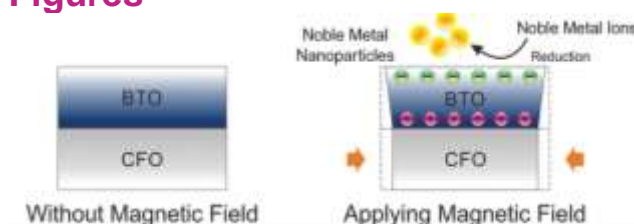


Figure 1. Schematic illustration of the magneto-electrochemical reduction of noble metal ions.

Novel DNA-Based Molecules and Their Charge Transport Properties

Danny Porath ¹,

¹ Institute of Chemistry and Center for Nanoscience and Nanotechnology, The Hebrew University of Jerusalem, 91904 Israel

danny.porath@mail.huji.ac.il

Abstract (Arial 10)

Charge transport through molecular structures is interesting both scientifically and technologically. To date, DNA is the only type of polymer that transports significant currents over distances of more than a few nanometers in individual molecules.

Nevertheless and in spite of large efforts to elucidate the charge transport mechanism through DNA a satisfying characterization and mechanistic description has not been provided yet. For molecular electronics, DNA derivatives are by far more promising than native DNA due to their improved charge-transport properties.

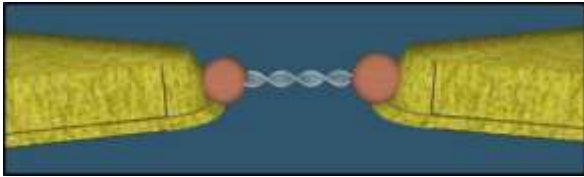
In recent years we have invested great efforts to address the above issues. Measuring the charge transport in DNA was elusive due to great technical difficulties leading to curious results. We were recently able to devise an experiment in which double-stranded DNA is well positioned between metal electrodes. Electrical measurements give surprisingly high currents over 100 base-pairs (~30 nm) elevated from the surface. The temperature dependence indicates backbone-related band-like transport.

In collaboration with the Kotlyar group, We were also able to synthesize and measure long (hundreds of nanometers) DNA-based derivatives that transport significant currents when deposited on hard substrates. Among the molecules metal containing DNA which is true metal-organic hybrid, a smooth and thin metal coated DNA and G-quadruplex DNA. Step by step we improve the synthesized constructs and the measurement methods of single DNA-based molecules. I will present new and surprising results on dsDNA molecules. I will present new DNA-based molecules and report on our measurements of their properties.

References

- [1] "Direct measurement of electrical transport through DNA molecules", Danny Porath, Alexey Bezryadin, Simon de Vries and Cees Dekker, **Nature** **403**, 635 (2000).
- [2] "Charge Transport in DNA-based Devices", Danny Porath, Rosa Di Felice and Gianarelio Cuniberti, Topics in Current Chemistry Vol. **237**, pp. 183-228 Ed. Gary Shuster. Springer Verlag, 2004.
- [3] "Direct Measurement of Electrical Transport Through Single DNA Molecules of Complex Sequence", Hezy Cohen, Claude Nogues, Ron Naaman and Danny Porath, **PNAS** **102**, 11589 (2005).
- [4] "Long Monomolecular G4-DNA Nanowires", Alexander Kotlyar, Nataly Borovok, Tatiana Molotsky, Hezy Cohen, Errez Shapir and Danny Porath, **Advanced Materials** **17**, 1901 (2005).
- [5] "Electrical characterization of self-assembled single- and double-stranded DNA monolayers using conductive AFM", Hezy Cohen et al., **Faraday Discussions** **131**, 367 (2006).
- [6] "High-Resolution STM Imaging of Novel Poly(G)-Poly(C)DNA Molecules", Errez Shapir, Hezy Cohen, Natalia Borovok, Alexander B. Kotlyar and Danny Porath, **J. Phys. Chem. B** **110**, 4430 (2006).
- [7] "Polarizability of G4-DNA Observed by Electrostatic Force Microscopy Measurements", Hezy Cohen et al., **Nano Letters** **7(4)**, 981 (2007).
- [8] "Electronic structure of single DNA molecules resolved by transverse scanning tunneling spectroscopy", Errez Shapir et al., **Nature Materials** **7**, 68 (2008).
- [9] "A DNA sequence scanned", Danny Porath, **Nature Nanotechnology** **4**, 476 (2009).
- [10] "The Electronic Structure of G4-DNA by Scanning Tunneling Spectroscopy", Errez Shapir, et.al., **J. Phys. Chem. C** **114**, 22079 (2010).
- [11] "Energy gap reduction in DNA by complexation with metal ions", Errez Shapir, G. Brancolini, Tatiana Molotsky, Alexander B. Kotlyar, Rosa Di Felice, and Danny Porath, **Advanced Materials** **23**, 4290 (2011).
- [12] "Quasi 3D imaging of DNA-gold nanoparticle tetrahedral structures", Avigail Stern, Dvir Rotem, Inna Popov and Danny Porath, **J. Phys. Cond. Mat.** **24**, 164203 (2012).
- [13] "Comparative electrostatic force microscopy of tetra- and intra-molecular G4-DNA", Gideon I. Livshits, Jamal Ghabboun, Natalia Borovok, Alexander B. Kotlyar, Danny Porath, **Advanced materials** **26**, 4981 (2014).
- [14] "Long-range charge transport in single G4-DNA molecules", Gideon I. Livshits et. al., **Nature Nanotechnology** **9**, 1040 (2014).
- [15] "Synthesis and Properties of Novel Silver containing DNA molecules", Gennady Eidelshstein et. al., **Advanced Materials** **28**, 4839 (2016).
- [16] "Highly conductive thin uniform gold-coated DNA nanowires", Avigail Stern et. al., **Advanced Materials** **30**, 1800433 (2018).
- [17] "Advances in Synthesis and Measurement of Charge Transport in DNA-Based Derivatives", Roman Zhuravel Avigail Stern Natalie Fardian-Melamed Gennady Eidelshstein Liat Katrivas Dvir Rotem Alexander B. Kotlyar and Danny Porath, **Advanced Materials Online** (2018).

Figures



Super resolution microscopy for nanomedicine: visualizing nanomaterials in action

Silvia Pujals¹,
Lorenzo Albertazzi^{1,2}

¹ Nanoscopy for Nanomedicine group, Institute of Bioengineering of Catalonia (IBEC), the Barcelona Institute of Science and Technology (BIST), C\ Baldiri Reixac 15-21, Helix Building 08028 Barcelona, Spain

² Department of Biomedical Engineering, Institute for Complex Molecular Systems (ICMS), Eindhoven University of Technology 5612AZ Eindhoven, The Netherlands

spujals@ibecbarcelona.eu

Our group uses advanced microscopy techniques to visualize and track in living cells and tissues self-assembled nanomaterials with therapeutic potential. The understanding of materials-cell interactions is the key towards the development of novel nanotechnology-based therapies for treatment of cancer and infectious diseases.

Many biological structures are made of multiple components that self-organize into complex architectures. Here we want to mimic this phenomenon to develop novel bioactive materials such as nanoparticles or nanofibers able to build themselves (1D or 3D self-assembled nanomaterials). Having the self-assembly motif decorated with different functionalities allows a modular and tunable approach that eases sample preparation.[1]

To study the behavior of such complex nanomaterials in action we make use of a variety of optical microscopy techniques, in particular super resolution microscopy (SRM). SRM can achieve a resolution down to 20 nm and represents an ideal tool to visualize nanosized objects in the biological environment. In particular we demonstrate how STORM (Stochastic Optical Reconstruction Microscopy) can be used to image a wide range of nanomaterials beyond the diffraction limit: nanoparticles[2], BTA fibers[3], peptidic nanostructures [4], etc.

Remarkably, STORM allows this observation in the biological environment, thus we are able to follow the journey of nanomaterials inside the body: from protein corona formation[5] to extravasation, targeting and tracking nanomaterials inside the cell.[6,7] Moreover, we were able to achieve correlative SRM and TEM, thus having key information on the cellular ultrastructure.[8]

Combining the powerful information obtained by STORM and the unique self-assembled materials we aim to create efficient platforms for targeted drug delivery and immunotherapy.

References

- [1] Casellas, N.M., Pujals, S., Bochicchio, D., Pavan, G.M., Torres, T., Albertazzi, L., García-Iglesias, M. *Chem. Comm.*, 54(33) (2018) 4112-4115.
- [2] Delcanale P, Miret-Ontiveros B, Arista-Romero M, Pujals S, Albertazzi L. *ACS Nano.*, 12(8) (2018) 7629-7637.
- [3] Albertazzi L, van der Zwaag D, Leenders CM, Fitzner R, van der Hofstad RW, Meijer EW. *Science* 344(6183), (2014) 491-5.
- [4] Pujals, S., Tao, K., Terradellas, A., Gazit E., Albertazzi L. *Chem Commun (Camb)*. 53(53), (2017) 7294-7297.
- [5] Feiner-Gracia, N., Beck, M., Pujals, S., Tosi, S., Mandal, T., Buske, C., Linden, M., Albertazzi, L. *Small*, 13(41) (2017) 1701631.
- [6] Feiner-Gracia, N., Buzhor, M., Fuentes, E., Pujals, S., Amir, R.J., Albertazzi, L. *J. Am. Chem. Soc.*, 22;139(46) (2017) 16677-16687.
- [7] Liu, Y., Pujals, S., Stals, P. J. M., Paulöhr, T., Presolski, S.I., Meijer, E.W., Albertazzi, L., Palmans, A. R. A. *J. Am. Chem. Soc.* 140(9) (2018) 3423-3433.
- [8] van Elsland, D., Pujals, S., Bakkum, T., Bos, E., Oikonomias-Koppas, N., Berlin, I., Neeffjes, J., Meijer, A.H., Koster, A.J., Albertazzi, L., van Kasteren, S.I. *Chembiochem* 19 (2018) 1766-1770.

Designing principles of nanotherapies

Loris Rizzello^{1,2},
Giuseppe Battaglia²

¹Institute for Bioengineering of Catalonia (IBEC), C/ Baldiri Reixac, 15-21 · 08028 Barcelona (Spain)

²University College London, Department of Chemistry, 20 Gordon Street, WC1H 0AJ London (UK)

irizzello@ibecbarcelona.eu

Section 1

How nanoparticles shapes tunes cell behaviours

Understanding how the physicochemical properties of nano-sized delivery systems affect cellular behaviour is a crucial topic that still lacks of analytical investigation. We are now able to generate an enormous set of nano-sized structures with defined physicochemical properties¹. However, it is important to remember that the nanoscopic nature of these structures can interfere with the physiological processes taking place within the cells at the mesoscopic level². Therefore, it is paramount to explore, and even categorise, the boundless field of interactions between nanoparticles, cellular components and molecular targets according to the physicochemical properties of the nanoparticles investigated.³⁻⁵ In addition, there is a general lack of characterisation criteria, in terms of both nanomaterials physicochemical properties and final biological effects. Consequently, despite more than a decade of research works, unanimously accepted theories regarding the role of nanoparticle shape in inducing specific molecular outcomes in cells are yet far from being proposed.

In this work, we explore the biomolecular effects induced by polymeric nanoparticles with different shapes (sphere and tubular vesicles) on cancer and non-cancer cell lines. We used the pH-responsive amphiphilic diblock copolymer poly(2-(methacryloyloxy)ethyl phosphorylcholine)-poly(2-(diisopropylamino)ethyl methacrylate) (PMPC-PDPA),⁶ which can form vesicles (known as polymersomes) or tubes, under specific conditions.

First, we isolated discrete geometrical structures (spheres and tubes) from a heterogeneous sample using specific purification techniques. Then, we characterised the cellular internalisation and the kinetics of uptake of both types of polymersomes in either tumour or non-tumour cells. We also investigated the cellular metabolic response as a function of the shape of the structures internalised, and demonstrated that tubular vesicles induce a significant decrease in the replication activity of tumour cells. We related this effect to the significant up-regulation of the tumour suppressor genes *p21* and *p53* with a concomitant activation of caspase 3/7. Moreover, we observed that primary (non-tumour) cells were completely unaffected by

nanoparticle shape, both in terms of cell division and genes expression. Finally, we demonstrated that combining the intrinsic shape-dependent effects of tubes with the delivery of doxorubicin we could significantly increase the cytotoxicity of the system. Our results illustrate how geometrical conformation of nanoparticles could impact on cell behaviour and how this could be tuned to create novel drug delivery systems tailored to specific biomedical application. All these data shed light first on the importance of using homogeneous samples of nanoparticles (in this case the shape) for a given biological application. Furthermore, it is evident that cells are able to “sense” different geometries, which involves molecular and genetical activations. Finally, tumour cells were demonstrated to sense and respond differently to shape compared to non-tumour cells, thus providing new suggestions for the development of novel nanoparticle-based anticancer therapies.

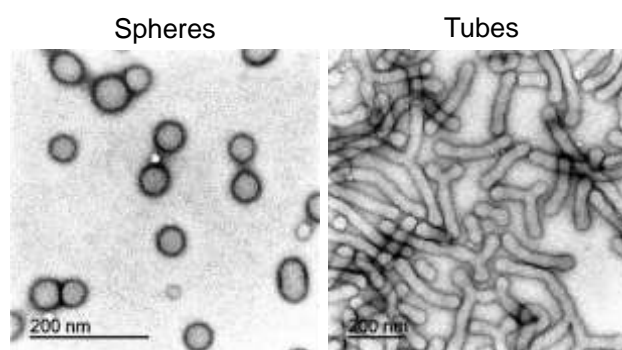


Figure 1. Polymeric spheres (left) and tubes (right) to study how shape affect cell behavior.

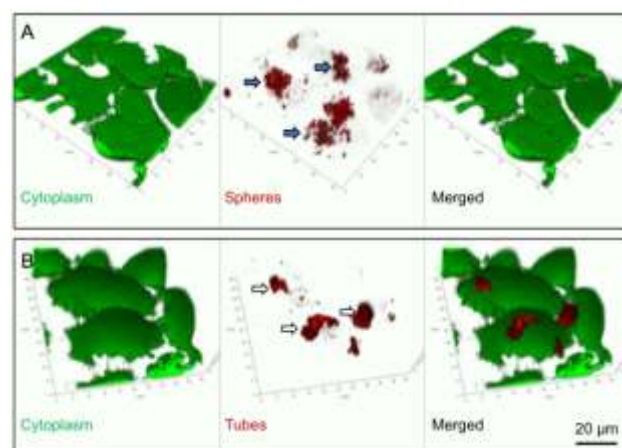


Figure 2. Uptake of spherical (top) and tubular (bottom) polymersomes.

Section 2

Nano-therapies for intracellular pathogens

The human innate immune system - our frontline defence against potential pathogens - includes a range of effector cells. Examples are professional phagocytes, such as granulocytes (*i.e.*, basophils, eosinophils and neutrophils) and mononuclear phagocytes (macrophages, dendritic cells, and

monocytes).⁷ Phagocytes are responsible for the clearance of bacterial pathogens from the host, and have attracted much interest in the context of focused antimicrobial drug delivery. In parallel, some of the deadliest pathogens have acquired the ability to evade the phagocytes's unique panel of molecular defences. As a consequence, while such phagocytes have evolved to eradicate invading pathogens, certain bacteria have simultaneously developed strategies to exploit macrophages as their preferential niche in which to evade host killing. This is known as the 'macrophage paradox' and it is the product of millions of years of co-evolution.⁸ Pathogens may inhabit different compartments in the macrophage; *L. monocytogenes*, *S. flexneri* and the *R. rickettsii* proliferate within the macrophage cytosol, *Listeria pneumophila* colonises the ER-like vacuoles, and *Salmonella enterica* exploits the late endosomal compartments. More recently, a similar strategy has been reported for *S. aureus*, suggesting that these bacteria are capable of hiding within professional phagocytes. *M. tuberculosis*, survives within macrophages phagosomes, considered the most detrimental environment for pathogens. Yet, *M. tuberculosis* has evolved proteins that hinder phagosome maturation, and prevent its fusion with lysosomes.⁹ The optimal design of drug delivery systems should incorporate targeting specificity for the host cells type, the presence of the pathogen, and the pathogen sub-cellular location. Hence, there is a need for novel antibacterial compounds that combine potent antibacterial activity with the ability to cross biological barriers and finally reach the intracellular niche where the microorganisms hide - even more critical today with the emergence of drug resistant strains. Here we propose the use of synthetic vesicles - known as polymersomes - that are able to target infected phagocytes, to reach intracellular pathogens in their sub-cellular compartment, and locally release their antibacterial cargo. These polymersomes are formed through the self-assembly of amphiphilic copolymers in aqueous media, and combine the advantages of long-term stability with the potential to encapsulate a broad range of cargoes.⁶ We have previously demonstrated that the pH sensitive block copolymer poly(2-(methacryloyloxy) ethyl-phosphorylcholine)-co-poly(2-(diisopropylamino)ethyl methacrylate) (PMPC-PDPA) can combine specific cellular targeting efficiency (through the PMPC block and its affinity toward the scavenger receptor B1),⁶ with effective endosomal escape and cytosolic delivery following internalisation (by the pH sensitive PDPA). In this study, we describe the half-life and bio-distribution of the PMPC-PDPA polymersomes *in vivo*, showing the dynamics of accumulation within different tissues. We then show the bio-molecular mechanism of cellular uptake and intracellular trafficking (namely, the polymersomes localisation in specific sub-cellular organelles). Finally, we demonstrate the potential of this strategy to revolutionise the treatment of several intracellular pathogens both *in vitro* and *in vivo*, namely *S.*

aureus, *M. bovis*-attenuated Bacillus Calmette-Guérin (BCG), *M. tuberculosis*, and *M. marinum*. We demonstrate *in vitro* that PMPC-PDPA polymersomes loaded with antimicrobials (gentamicin, lysostaphin, vancomycin, rifampicin, and isoniazid) are able to decrease, and potentially even eradicate, these intracellular pathogens. Using embryos of the zebrafish (*Danio rerio*) as a model, we further demonstrate that encapsulated antimicrobials can effectively reduce the bacterial burden in disseminated infections *in vivo*.

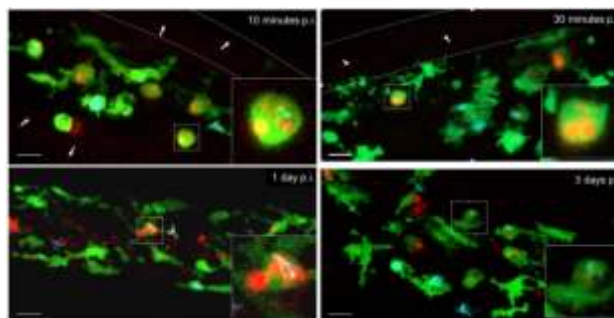


Figure 3. *In vivo* circulation (*D. rerio*) of polymersomes, and macrophages (in green) targeting

References

- [1] Toy, R.; Peiris, P. M.; Ghaghada, K. B.; Karathanasis, E. *Nanomedicine* 9 (2014) 121-134.
- [2] Mann, S. *Angewandte Chemie - International Edition* 47 (2008) 5306-5320
- [3] Park, K. H.; Chhowalla, M.; Iqbal, Z.; Sesti, F. *J. Biol. Chem.* 278 (2003) 50212-50216.
- [4] Andón, F. T.; Fadeel, B. *Acc. Chem. Res.* 19 (2012) 733-742.
- [5] Leifert, A.; Pan, Y.; Kinkeldey, A.; Schiefer, F.; Setzler, J.; Scheel, O.; Lichtenbeld, H.; Schmid, G.; Wenzel, W.; Jahnen-Dechent, W.; et al. *Proc. Natl. Acad. Sci.* 14 (2013) 8004-8009.
- [6] Ruiz-Perez, L.; Messenger, L.; Gaitzsch, J.; Joseph, A.; Sutto, L.; Gervasio, F. L.; Battaglia, G. *Sci. Adv.* 2 (2016) e1500948-e1500948.
- [7] Florent Ginhoux and Steffen Jung. Monocytes and macrophages: developmental pathways and tissue homeostasis. *Nature Rev. Immunol.*, 14:392-404, June 2014.
- [8] Price JV, and Vance RE. *Immunity* 41 (2014) 685-693.
- [9] Ferrari G, Langen H, Naito M, and Pieters J. *Cell* 97 (1999) 435-447.

Bioengineering hybrid machines for Nanomedicine and soft robotics

Samuel Sánchez,

¹Institute for Bioengineering of Catalonia, Barcelona, Spain)

²Catalan Institute for Research and Advanced Studies, Barcelona, Spain

ssanchez@ibebarcelona.eu

The combination of biological components and artificial ones that emerges into “living machines” is a research field that spans from active matter at the nanoscale to soft robotics.

In this talk, I will summarize or recent advances in this field of hybrid machines from the nano-bots to 3D Bioprinted actuators. Nano-bots are made of nanoparticles which act as chassis and enzymes as engines that convert bio-available fuels into products creating chemical gradients around the particles. In the presence of their substrates, enzyme catalysts generate a propulsion force for the nanoparticles to overcome Brownian forces that dominate at the nanoscale. In addition to the two main components, nanobots can transport drugs into their pores, active as smart drug delivery systems. Although nanobots have been mainly tested in vitro, and some initial reports claim their use in in vivo settings, they may be eventually used in vivo for transporting drugs to target locations in a controlled and directed manner. However, fundamental understanding on motion mechanism, materials considerations, in vitro assessment of drug delivery, toxicity, and their shape and size dependence on those parameters is needed. We have explored the role of catalysis, the number and distribution of enzymes on the particles, as well as their capabilities as drug vehicles in different viscous and physiological media.

Nanobots can sense the environment where they swim, and be imaged by molecular and medical imaging techniques such as STORM or PET-CT.

At a larger scale, hybrid micro-robots combine microparticles with motile cells for efficient delivery, and biofilm penetration.

On a larger scale, we use 3D bioprinting techniques to fabricate cm-scaled hybrid BioRobots based on the combination of hydrogels and cells that contract in synchrony upon external stimuli, and exercise training, alike artificial muscles.

References

[1] R Mestre, T Patiño, X Barceló, S Sanchez Conference on Biomimetic and Biohybrid Systems, 2018, 316-320

[2] T. Patiño, X. Arqué, R. Mestre, L. Palacios, and S. Sánchez *Acc. Chem. Res.* 2018. ASAP. DOI: 10.1021/acs.accounts.8b00288

[3] T. Patiño, et al. *Am. Chem. Soc.*, 2018, 140 (25), pp 7896–7903

[4] J Katuri, X Ma, MM Stanton, S Sánchez *Acc. Chem.Res.* 2018, 50 (1), 2-11

Figures



Figure 1. Cover images from reference 3 and reference 4.

Reverting cancer's poor prognosis using precision polymeric nanomedicines based on molecular fingerprints of long-term survivors

Prof. Ronit Satchi-Fainaro, Ph.D.

Head, Cancer angiogenesis and Nanomedicine Laboratory; Chair, Department of Physiology and Pharmacology, Sackler Faculty of Medicine, Tel Aviv University, Tel Aviv 69978, Israel

ronitsf@post.tau.ac.il

Abstract

Tumor progression is dependent on a number of sequential steps, including initial tumor-vascular interactions and recruitment of blood vessels, as well as established interactions of tumor cells with their surrounding microenvironment and its different immune, endothelial and connective cellular and extra-cellular components. Failure of a microscopic tumor, either primary, recurrent or metastatic, to complete one or more of these early stages may lead to delayed clinical manifestation of the cancer. Micrometastasis, dormant tumors, and minimal residual disease, contribute to the occurrence of relapse, and constitute fundamental clinical manifestations of tumor dormancy that are responsible for the majority of cancer deaths. However, although the tumor dormancy phenomenon has critical implications for early detection and treatment of cancer, it is one of the most neglected areas in cancer research and its biological mechanisms are mostly unknown.

To that end, we created several models of patient-derived cancer models mimicking pairs of dormant *versus* fast-growing, primary *versus* metastatic and drug-sensitive *versus* drug-resistant cancers using cutting-edge techniques of patient-derived xenografts, 3D printing and genetically-modified mouse models. We investigated the molecular changes in tumor-host interactions that govern the escape from dormancy and contribute to tumor progression. Those led to the discovery of novel targets and provided important tools for the design of novel cancer nano-sized theranostics (**therapeutics** and **diagnostics**) (1-3). Our libraries of precision nanomedicines are synthesized as highly controlled micellar, nanogels, coiled or globular particulated supramolecular structures consisting of linear, hyperbranched or dendritic polymers based on polyglutamic acid (PGA), polyethyleneglycol (PEG), poly(N-(2-hydroxypropyl)methacrylamide) (HPMA) copolymer, polyglycerol (PG), poly(lactic-glycolic acid) (PLGA) and hybrid systems (4-9).

We hypothesize that the acquired knowledge from this multidisciplinary research strategy will revolutionize the way we diagnose and treat cancer (Figure 1).

References

- [1] Tiram G, *et al.* ACS Nano, 10, 2028-2045 (2016).
- [2] Ferber S*, Tiram G*, *et al.* eLife, 6. pii: e25281 (2017).
- [3] Gibori H, *et al.*, Nature Communications, 9(1):16 (2018).
- [4] Baabur-Cohen H, *et al.* J Control Release, 257,118-131 (2017).
- [5] Ofek P, *et al.* Nanomedicine, 12, 2201-2214 (2016).
- [6] Polyak D*, Krivitsky A*, Scomparin A*, *et al.* J Control Release, 257:132-143 (2017).
- [7] Scomparin A, *et al.* J Control Release, 208, 106-120 (2015).
- [8] Shatsberg Z, *et al.* J Control Release, 239, 159-168 (2016).
- [9] Markovsky E, *et al.* Mol Cancer Therapeutics, 16(11):2462-2472 (2017).

Figures

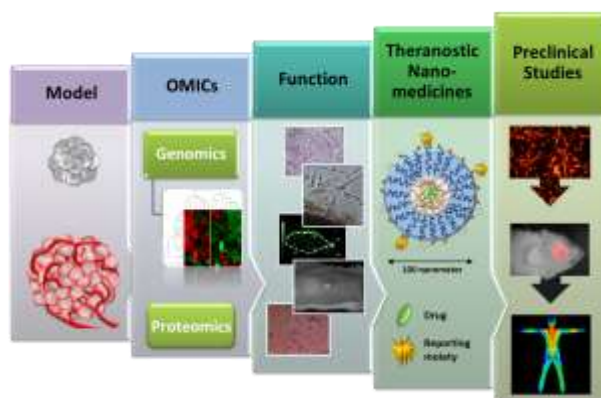


Figure 1. A comprehensive approach to address tumor dormancy- from bed-site to bench and back.

Personalized Cancer Nanomedicines

Avi Schroeder¹,

¹Dept. of Chemical Engineering, Technion – Israel Institute of Technology, Haifa 32000, Israel

avids@technion.ac.il

Medicine is taking its first steps towards patient-specific precision care. Nanoparticles have many potential benefits for treating cancer, including the ability to transport complex molecular cargoes including siRNA and protein, as well as targeting specific cell populations and metastasis.

The lecture will discuss 'barcoded nanoparticles' that target sites of cancer where they perform a programmed therapeutic task. Specifically, particles that inform the physician regarding patient-specific drug potency against the primary tumor and metastasis.

The evolution of drug delivery systems into *synthetic cells*, programmed nanoparticles that have an autonomous capacity to synthesize diagnostic and therapeutic proteins inside the body, and their promise for treating cancer and immunotherapy, will be discussed.

References

- [1] Theranostic barcoded nanoparticles for personalized cancer medicine, Yaari et al. *Nature Communications*, 2016, 7, 13325
- [2] Synthetic Cells Synthesize Therapeutic Proteins inside Tumors, Krinsky et al., *Advanced Healthcare Materials*, 2017
- [3] Proteolytic nanoparticles replace a surgical blade by controllably remodeling the oral connective tissue, Zinger et al., *ACS Nano*, 2018

Figures

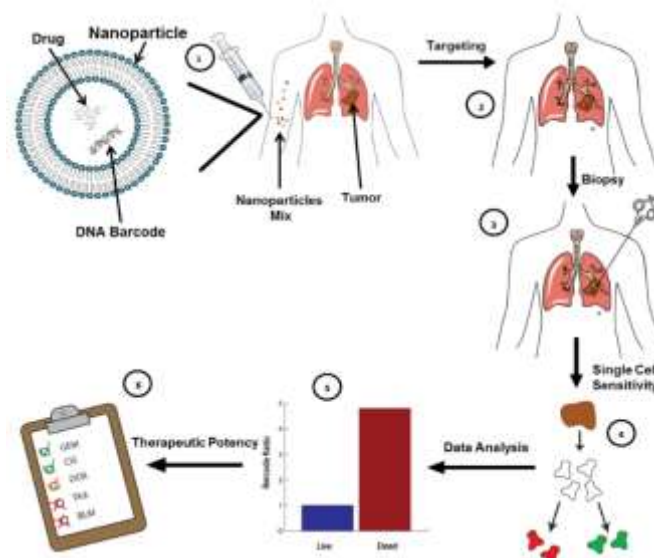


Figure 1. Barcoded nanoparticles performing a diagnostic assay directly inside the patient's primary tumor and metastasis, indicating which medicine is best for the specific patient.

DNA Origami Tools for NanoBioTec

Philip Tinnefeld¹,

Viktorija Glembocskytė, Lennart Grabenhorst, Ija Jusuk, Sarah Ochmann, Mario Raab, Tim Schröder, Florian Selbach, Florian Steiner, Johan Bohlen, Kristina Hübner, Jan Vogelsang, Andres Vera, Kateryna Trofymchuk¹

¹Department of Chemistry and Center for NanoScience, Ludwig-Maximilians-Universität München, 80539 München, Germany

Philip.tinnefeld@lmu.de

Abstract

In recent years, DNA nanotechnology has matured to enable robust production of complex nanostructures and hybrid materials. We have combined DNA nanotechnology with sensitive optical detection to create functional single-molecule devices that enable new applications in single-molecule biophysics. Starting with superresolution nanorulers [1], a single-molecule mirage [2] and energy transfer switches [3] we developed DNA origami nano-adapters for targeted placement of single molecules in zeromode waveguides used for DNA sequencing [4].

Furthermore, a plasmonic fluorescence amplifier [5] is used for sensitive biosensing and single-molecule detection on low-tec detection devices such as a smartphone. The optical antennas assembled by DNA origami are further developed to improve fluorescence detection in molecular diagnostics. Finally, we present a molecular force spectroscopy employing DNA origami force clamps that work autonomously without any physical connection to the macroscopic world [6]. We used the conformer switching of a Holliday junction as a benchmark and studied the interaction of DNA binding proteins with DNA when the DNA is under 0-15 pN tension.

References

- [1] Schmied, J.J. et al. DNA origami-based standards for quantitative fluorescence microscopy. *Nature protocols* 9, 1367-1391 (2014).
 [2] Raab, M., Vietz, C., Stefani, F.D., Acuna, G.P. & Tinnefeld, P. Shifting molecular localization by plasmonic coupling in a singlemolecule mirage. *Nature communications* 8, 13966 (2017).
 [3] Stein, I.H., Steinhauer, C. & Tinnefeld, P. Single-Molecule Four-Color FRET Visualizes Energy-Transfer Paths on DNA Origami. *J Am Chem Soc* 133, 4193-4195 (2011).
 [4] Pibiri, E., Holzmeister, P., Lalkens, B., Acuna, G.P. & Tinnefeld, P. Single-molecule positioning in zeromode waveguides by DNA origami nanoadapters. *Nano letters* 14, 3499-3503 (2014).

[5] Acuna, G.P. et al. Fluorescence enhancement at docking sites of DNA-directed self-assembled nanoantennas. *Science* 338, 506-510 (2012).

[6] Nickels, P.C. et al. Molecular force spectroscopy with a DNA origami-based nanoscopic force clamp. *Science* 354, 305-307 (2016)

Figures

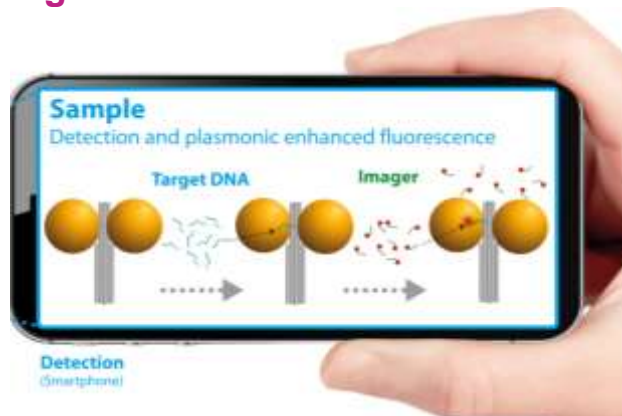


Figure 1. Sketch of a biomolecular sandwich assay of pathogenic DNA using signal amplification by a self-assembled DNA origami optical antenna.

Biosensors based on roll-to-roll printed graphene electrodes

Thomas Velten,

Thorsten Knoll, Axel Brenner, Anke Schultz, Herbert Schuck

¹ Fraunhofer-Institut für Biomedizinische Technik IBMT
Joseph-von-Fraunhofer-Weg 1, 66280 Sulzbach,
Germany

thomas.velten@ibmt.fraunhofer.de

Graphene is a relatively new material that, in addition to many other interesting properties, has a high electrical conductivity and is considered biocompatible [1]. Due to these properties, graphene is interesting for the production of biocompatible sensors in the field of cell-based assays. Cells play a central role in these assays and the sensor signal is a measure of the effect that certain parameters have on the behaviour of the cells.

We report on sensors that can be used to test the efficacy of antiviral substances. To this end, so-called indicator cell lines are used which produce a confluent cell monolayer on interdigital electrodes of the sensor and isolate them electrically. Added viruses lead to a morphological change of the cells or to a detachment of the cells from the cell monolayer, the so-called cytopathic effect (CPE).

The addition of antiviral substances inhibits cell infection or viral replication in the cells and thus the cytopathic effect. This circumstance can be used to infer the inhibition of the cytopathic effect and thus the efficacy of the antiviral substances from the changes in the measured impedance values.

The sensors are manufactured by printing of two substances. The interdigital structures are produced from conductive ink with graphene platelets. For improved adhesion of the confluent cell monolayer, an additional protein layer is applied. Printing was done by a roll-to-roll gravure printing machine at a speed of 40 m/min [2]. Corona activation immediately before printing was necessary in order to increase the wetting of the film substrate. The achieved thickness of the printed graphene electrodes was around 5 µm. Inline drying of such thick layers was challenging but could be performed with near-infrared dryers.

Thin films comprising the printed sensor structures in multiwell plate format were bonded to bottomless well plates. The connection of the printed sensor contact pads to a board was realized using ZIF (Zero Insertion Force) connectors (see Figure 1).

First tests showed that the impedance value increases when cells (here: TZM-bl) grow in a well up to confluency. After addition of SDS (sodium dodecyl sulfate), the cells dissolved and the measured impedance abruptly decreased by about 100 Ω. Next, it was examined whether the virus-induced cytopathic effect on the cell culture and its

inhibition by the antiviral substance Efavirenz (non-nucleoside reverse transcriptase inhibitor) is reflected in the time course of measured impedance values (Figure 2). The TZM-bl / HIV-1 pseudovirus system, well established at IBMT, was used. 1×10^4 cells (TZM-bl) were used per well. Virus stock (HIV-1 pseudovirus PVO.4 in a concentration usually used in neutralisation assays) or virus stock plus 1 µM Efavirenz were added 24 h after cell addition. It could be shown that online monitoring of the viral effect on cell culture and inhibition of the virus-induced cytopathic effect by antiviral substances is possible with the help of the developed sensors.

References

- [1] Sahni, D.; Jea, A.; Mata, J. A.; Marcano, D. C.; Sivaganesan, A.; Berlin, J. M.; Kent, T. A.: Biocompatibility of pristine graphene for neuronal interface. *Journal of Neurosurgery: Pediatrics* 11 (2013) No. 5, pp. 575–583.
- [2] Knoll et al., Zweifarben-Druckanlage für die Sensorherstellung, wt-online 11/12-2017, pp. 827-833.

Figures



Figure 1. The sensor in well plate format is connected to a circuit board. The ribbon cables lead to the measuring device. On the left an enlarged picture of one well with an interdigital structure is shown.

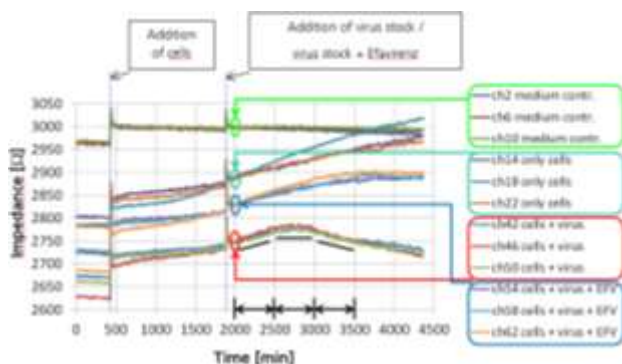


Figure 2. Impedance curves of 12 wells. The legend indicates whether medium or cells were in the respective wells and whether only HIV-1 pseudo virus stock PVO.4 or PVO.4 plus Efavirenz was added. By means of an offset shift of the measured curves, all curves of a group are combined. Addition of viruses changes the slope of the impedance curve (time 2000 - 3500 min). Efavirenz in the used concentration inhibits this effect.

Targeting Tumor Microenvironment with Rationally Designed Polypeptide-based Conjugates

María J. Vicent

Polymer Therapeutics Lab. Centro Investigación Príncipe Felipe. Av. Eduardo Primo Yúfera 3, 46012, Valencia, Spain

mjvicent@cipf.es

The intrinsic characteristics of the tumor microenvironment (TME), including acidic pH and overexpression of hydrolytic enzymes, offer an exciting opportunity for the rational design of TME-drug delivery systems (DDS).

The physico-chemical parameters of a polypeptide-conjugate, and hence its biological performance, are defined by an intricate interplay of multiple structural factors. This highlights the need for detailed structure-activity relationship studies to develop the hierarchical strategies of polypeptide conjugate design. However, structural complexity also represents a unique opportunity, since small changes at the structural level might endow therapeutics with outstanding and unexpected biological performance [1,2].

In our group, we have overcome the main classical limitations for the synthesis of defined polypeptides using precise controlled reactions followed by an adequate characterization yielding to well-defined polypeptidic architectures (including stars, graft and block-copolymers) by NCA polymerization techniques [3]. In addition, post-polymerization techniques allow us the introduction of a variety of functionalities yielding a set of orthogonal reactive attachment sides [4]. Using these techniques and following a bottom-up strategy we have been able to obtain star-based polypeptide architectures with the capacity to self-assemble yielding supramolecular nanostructures with interesting properties [5]. This strategy enabled *in vitro* and *in vivo* evaluation, revealing a lack of toxicity, an enhanced *in vitro* cell internalization rate and significantly greater terminal and accumulation half-life *in vivo* together with a significant lymph node accumulation [5].

In order to target TME with the developed carriers, we synthesized and characterized pH-responsive biodegradable poly-L-glutamic acid (PGA)-based combination conjugates with the aim of optimizing anticancer effects. Different hydrazone pH sensitive linkers that can promote the specific release of the drug from the polymeric backbone within the TME have been implemented, together with a range of drug loading in order to achieve optimal effects on primary tumor growth, lung metastasis (~90% reduction), and toxicological profile in a preclinical metastatic triple-negative breast cancer (TNBC)

murine model. The use of transcriptomic analysis helped us to identify the molecular mechanisms responsible for such results including a differential immunomodulation and cell death pathways among the conjugates. This data highlights the advantages of targeting the TME, the therapeutic value of polymer-based combination approaches, and the utility of -omics-based analysis to accelerate anticancer DDS [6].

References

- [1] Duro-Castano A., Conejos-Sánchez I., Vicent M.J. *Polymers* 2014, 6, 515-551.
- [2] Zagorodko O., Arroyo-Crespo, J.J., Nebot, V.J., and Vicent, M.J. *Macromolecular Bioscience* 2017, 17, 1600316-n/a.
- [3] a) Duro-Castano A., England, R.M., Razola, D., Romero, E., Oteo-Vives, M., Morcillo, M.A., and Vicent, M.J. *Molecular Pharmaceutics* 2015, 12, 3639-3649; b) Conejos-Sánchez I. Duro-Castano, A., Birke, A., Barz, M., and Vicent, M.J. *Polymer chemistry* 2013, 4, 3182-3186.
- [4] Barz M., Duro-Castano A., Vicent M.J. *Polymer Chemistry* 2013, 4, 2989-2994
- [5] Duro-Casaño Nebot, V. J., Niño-Pariente, A., Armiñán, A., Arroyo-Crespo, J. J., Paul, A., Feiner-Gracia, N., Albertazzi, L. and Vicent, M. J. *Advanced Materials* 2017, doi. 10.1002/adma.201702888
- [6] Arroyo-Crespo, J.J, Armiñán A., Charbonnier D., Balzano-Nogueira L., Huertas-López F., Martí C., Tarazona S., Forteza J., Conesa A., Vicent M.J. *Biomaterials* 2018, 186, 8-21.

Acknowledgements

Spanish Ministry of Economy and Competitiveness (SAF2016-80427-R) and the European Research Council (Grant ERC-CoG-2014-648831 MyNano) for financial support. Part of the equipment employed in this work has been funded by Generalitat Valenciana and co-financed with FEDER funds (PO FEDER of Comunitat Valenciana 2014-2020).



Orals

Bacterial nanocellulose as a cell culture platform

Irene Anton-Sales

Soledad Roig-Sánchez, Anna Laromaine, Anna Roig

¹Institute of Materials Science of Barcelona
Campus de la UAB, Bellaterra, Spain

Contact: ianton@icmab.es

Nanocelluloses are cellulosic products with at least one dimension in the nanoscale. Nanocellulose can be extracted from natural sources like wood, cotton or algae but it can also be directly produced by microorganisms [1].

Bacterial nanocellulose (BNC) is a biopolymer naturally synthesized and secreted by *Komagataeibacter xylinus* that forms a 3D-network of pure cellulose nanofibres (Image 1) resembling the structure of collagen. BNC exhibits attractive properties for biomedical applications such as high liquid holding capacity, high tensile strength, flexibility and porosity [2]. On the other hand, there are still a limited number of natural biomaterials that meet all the requirements to fit in the regenerative medicine settings. Thus, our goal is to develop versatile and portable supports based on BNC for cell-manipulation, envisioning regenerative medicine applications.

The BNC pellicles were obtained after 3-day static cultures of *Komagataeibacter xylinus*. The BNC films were then thoroughly washed and autoclaved (Image 2b) before being used for culturing human dermal fibroblasts. When appropriate, BNC was functionalized with TiO₂ nanoparticles by a microwave-assisted method [3]. Attachment, morphology, distribution and growth kinetics of cells cultured on these BNC-based supports were studied by cell viability assays and confocal microscope imaging.

Firstly, structural characterization of BNC and BNC functionalized with TiO₂ nanoparticles (BNC/TiO₂) will be presented. Then, we will show in detail that both BNC and BNC/TiO₂ films support the attachment and proliferation of human dermal fibroblasts (Image 2c). Growth kinetics on BNC substrates is very similar to that on culture plates with the advantage of representing a transportable platform for adherent cells. Moreover, cell morphology studies showing that fibroblasts exhibit their expected phenotype on BNC and BNC/TiO₂ substrates (Image 2a) will be presented. Altogether, our data point out that BNC is a promising and versatile biomaterial to be used i.e. as a cell carrier in cell transplantation therapies and that BNC

functionalization with model functional nanoparticles (TiO₂) does not alter its properties.

References

- [1] Klemm D, Cranston ED, Fischer D, Gama M, Kedzior SA, Kralisch D, et al., *Mater Today*, 7 (2018) 720-748
- [2] De Oliveira Barud HG, da Silva RR, da Silva Barud H, Tercjak A, Gutierrez J, Lustrri WR, et al., *Carbohydr Polym*, 153 (2016) 153:406–20
- [3] Zeng M, Laromaine A, Feng WQ, Levkin PA, Roig A., *J Mater Chem C*, 31 (2015) 6312-8

Figures

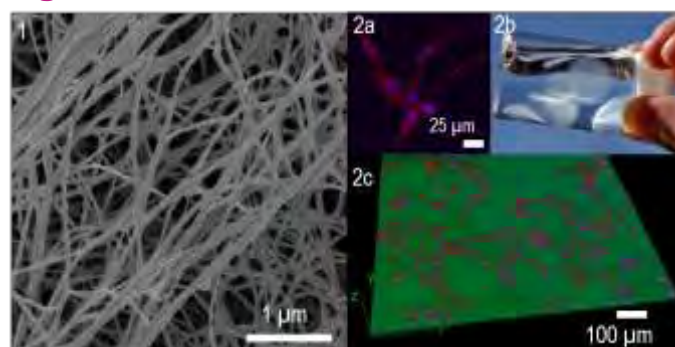


Figure: Image 1 shows a scanning microscope image of the bacterial nanocellulose fibres. Image 2a and 2c depict human dermal fibroblast growing on top of bacterial nanocellulose substrates at different magnifications under confocal microscope. 2b corresponds to a digital picture of the bacterial nanocellulose hydrogels used in our research.

Effect of enzyme type, quantity and distribution on the motion behavior of microswimmers

Xavier Arqué¹,

Tania Patiño¹, Natalia Feiner¹,
Lorenzo Albertazzi^{1,4}, Samuel Sánchez^{1,3}

¹ Insitut de Bioenginyeria de Catalunya (IBEC), Baldiri i Reixac 10-12, Barcelona, Spain

² Department of Biomedical Engineering, Institute for Complex Molecular Systems (ICMS), Eindhoven University of Technology, Eindhoven, The Netherlands

³ Institució Catalana de Recerca i Estudis Avançats (ICREA), Pg. Lluís Companys 23, Barcelona, Spain

xarque@ibecbarcelona.eu
tpatino@ibecbarcelona.eu
ssanchez@ibecbarcelona.eu

Biocatalytic micro- and nanoswimmers are able to navigate due to the enzymatic conversion of substrates into products.¹ Biocatalysis offers a unique combination of properties, such as biocompatibility, bioavailability and versatility, making it greatly appealing for certain biomedical applications.² However, to make these implementations feasible, a deeper understanding on the fundamental aspects that rule self-propulsion is still required. We have focused our research on the role of the enzyme type, quantity and distribution.

In order to achieve active motion, asymmetry has been claimed to be crucial³, yet an enhanced Brownian diffusion (self-propulsion) has been reported for non-Janus nanoparticles.⁴ In this project, the effect of enzyme quantity and distribution was investigated with stochastically optical reconstruction microscopy (STORM) to detect single enzymes on polystyrene microswimmers with and without an outer silica surface.⁵ The binding efficiency was observed to be significantly higher on the rough silica, although both present a non-homogeneous enzyme distribution. This was correlated with the propulsive force measured using optical tweezers and the speeds produced by these forces, which were obtained through optical tracking.

We also tested the capacity of different enzymes to study the versatility of such systems. Acetylcholinesterase (AChE), glucose oxidase (GOx) and aldolase (ALS) were used to propel hollow silica microcapsules and the motion behavior was compared with microswimmers powered by urease (UR). The motion behavior appeared to be strongly dependent on the enzyme type and its intrinsic properties. The different enzymes are studied to elucidate what are the relevant enzymatic parameters ruling self-propulsion. Among these properties, the catalytic rate appeared to be a key factor for the generation of active motion, which was

further confirmed by exposing urease microswimmers to a competitive reversible inhibitor. These results provide new insights on the underlying mechanism of active motion and on the intelligent design of enzymatic micro- and nanoswimmers.

References

- [1] (1) Ma, X.; Hortelão, A. C.; Patiño, T.; Sánchez, S. Enzyme Catalysis To Power Micro/Nanomachines. *ACS Nano* 10 (2016) 9111–9122.
- [2] (2) Hortelão, A. C.; Patiño, T.; Perez-Jiménez, A.; Blanco, À.; Sánchez, S. Enzyme-Powered Nanobots Enhance Anticancer Drug Delivery. *Adv. Funct. Mater.* 28 (2018) 1705086.
- [3] (3) Golestanian, R.; Liverpool, T. B.; Ajdari, A. Propulsion of a Molecular Machine by Asymmetric Distribution of Reaction Products. *Phys. Rev. Lett.* 94 (2005) 1–4.
- [4] (4) Dey, K. K.; Zhao, X.; Tansi, B. M.; Méndez-Ortiz, W. J.; Córdova-Figueroa, U. M.; Golestanian, R.; Sen, A. Micromotors Powered by Enzyme Catalysis. *Nano Lett.* 15 (2015) 8311–8315.
- [5] (5) Patiño, T.; Feiner-Gracia, N.; Arqué, X.; Miguel-López, A.; Jannasch, A.; Stumpp, T.; Schäffer, E.; Albertazzi, L.; Sánchez, S. Influence of Enzyme Quantity and Distribution on the Self-Propulsion of Non-Janus Urease-Powered Micromotors. *J. Am. Chem. Soc.* 140 (2018) 7896–7903.

Figures

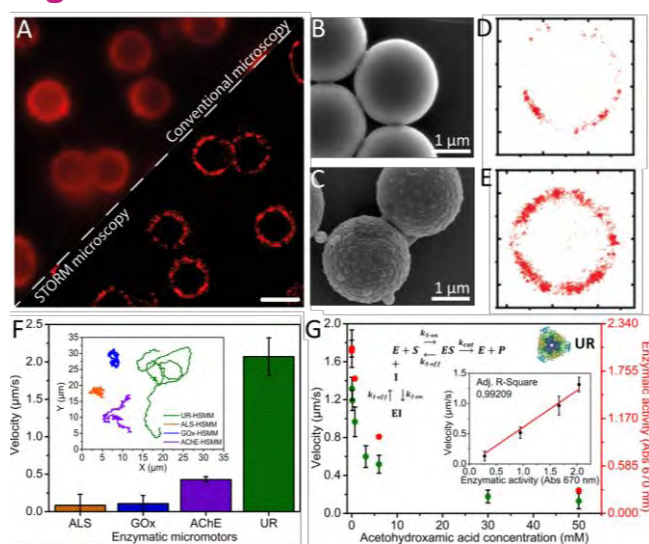


Figure 1. A) Comparison between the conventional fluorescence and STORM images. SEM micrographs of B) PS- and C) PS@SiO₂-microswimmers. STORM single-molecule detection of urease on the D) PS- and E) PS@SiO₂-microswimmers' surface. F) Average velocities of different enzymatic microswimmers. Inset: Representative tracking trajectories of the microswimmers. G) Average velocity of urease microswimmers, extracted from the MSD analysis, for different inhibitor concentrations with substrate (urea) present in excess (500 mM). Inset: Correlation of velocity with enzymatic activity depending on inhibition.

Development of a novel multifunctional bioglass-based coating for the next generation of prostheses

Angela Bejarano-Villafuerte¹,

Selina Ambrose¹, William McDonnell², Rebecca Yuan³, Robert Allaker³

¹ Promethean Particles, 1 Genesis Park, Midland Way, Nottingham, NG7 3EF Organization, Address, City,

² Johnson Matthey Technology Centre, Blounts Court Road, Sonning Common, Reading, RG4 9NH

³ Queen Mary University London, Blizzard Building, 4 Newark Street, Whitechapel, London, E1 2AT

angela.bejarano@proparticles.co.uk

Promethean Particles is a UK-based SME that designs and develops inorganic nanomaterials in liquid dispersions. The company's technology is based on a patented reactor design that allows truly continuous hydrothermal (or solvothermal) synthesis of inorganic nanoparticles [1]. Promethean use small scale reactor systems for rapid prototyping to tune the optimum product for each application and backs this up with pilot-scale production facilities, as well as a multi-ton scale nanoparticle manufacturing plant (capacity more than 1000 tons per year), see figure 1.a. Our unique production process allows us to tailor the nanoparticles to get the best functionality for an end use application.

Innovation is a large focus of our business, as a direct outcome of our R&D activities. We are currently active partners in three Innovate UK-funded projects and four EU-funded Horizon 2020 projects. One of our Innovate UK projects aims to develop a novel multifunctional bioglass-based coating for the next generation of prostheses. The cost of implant failure can be massive, both financially for medical services (€ 800 m/year in Europe alone in 2010 for dental implants) and personally to the patient where amputations can be life altering. Bioglass-based coatings can help bone integration of the implant and reduce these costly infections from occurring.

Due to the versatility of our lab-scale technology, we are able to tailor bioglass-based materials using different components and with dopants such as ZnO and Cu. We have achieved excellent control over the ratio of components, the particle size within an amorphous matrix (see figure 1.b-c) and the solid phase. Further tests have been performed by our partners Johnson Matthey (JM) and Queen's Mary University London (QMUL). Our bioglass-based materials are used by JM to coat substrates which are then tested by QMUL to investigate their biocompatibility and antimicrobial properties. Within this project, Bioglass-based materials are demonstrating promising antimicrobial activities.

References

- [1] Edward Lester, Paul Blood, Joanne Denyer, Donald Giddings, Barry Azzopardi, Martyn Poliakov. The Journal of Supercritical Fluids, Issue 2 (2006), Volume 37, 209-214.

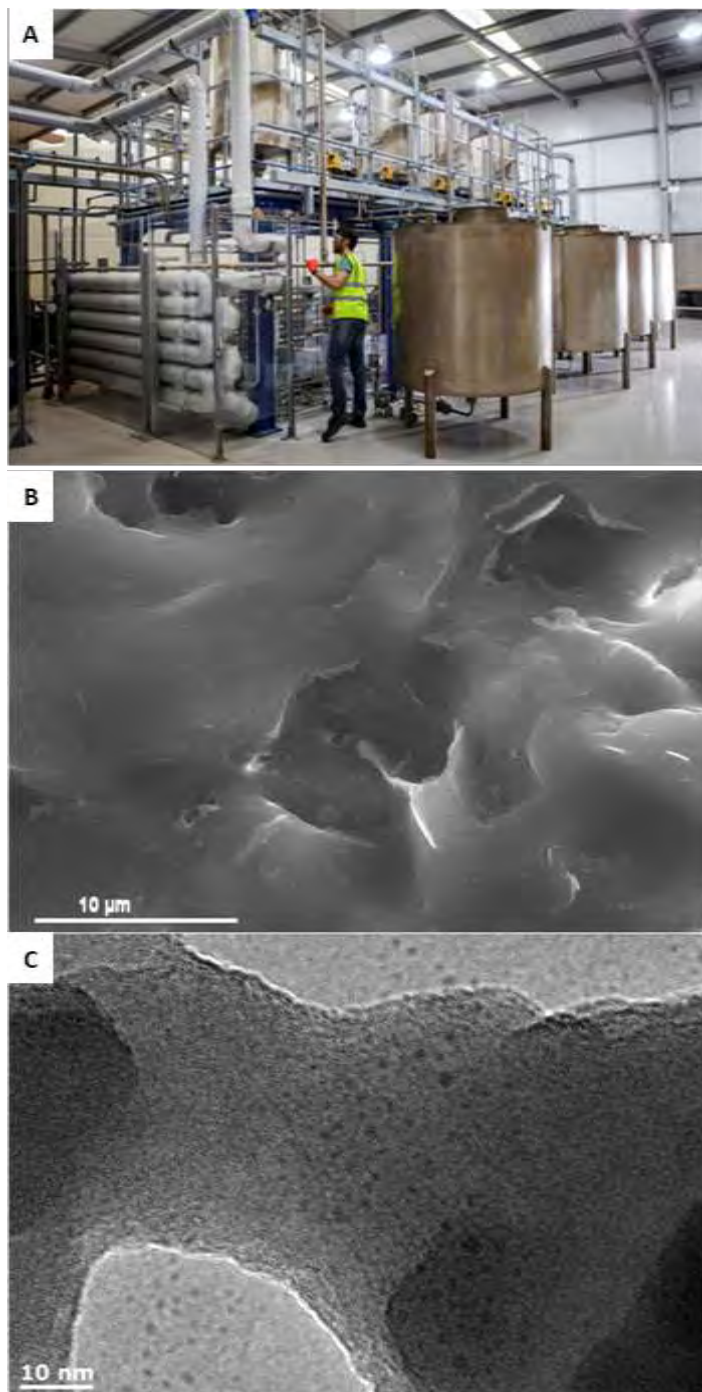


Figure 1. (A) Promethean's multi-ton scale nanoparticle manufacturing plant (capacity more than 1000 tons per year). (B) SEM image of a bioglass-based material. (C) TEM image of a bioglass-based material.

Surface-enhanced Raman scattering (SERS) imaging of bioactive metabolites in mixed bacterial populations

Gustavo Bodelón¹, Sarah De Marchi Lourenço¹, Lorena Vázquez-Iglesias¹, Luis M. Liz-Marzán^{1,2,3,4}, Jorge Pérez-Juste¹, and Isabel Pastoriza-Santos¹

¹Department of Chemistry-Physics and Biomedical Research Centre (CINBIO), Universidade de Vigo, 36310 Vigo, Spain

²Bionanoplasmonics Laboratory, CIC biomaGUNE, Paseo de Miramón 182, 20014 Donostia-San Sebastián, Spain

³Ikerbasque, Basque Foundation for Science, 48013 Bilbao, Spain

⁴Biomedical Research Networking Center in Bioengineering, Biomaterials, and Nanomedicine (CIBER-BBN), 20014 Donostia-San Sebastián, Spain

gbodelon@uvigo.es

In nature bacteria live in mixed microbial communities shaped by the action of bioactive metabolites secreted by the residing microorganisms. The identification and tracking of such chemical exchange processes is fundamental for understanding how they modulate microbial community and function. In this framework, most chemical imaging approaches have focused on the analysis of metabolic interactions taking place between microbial populations co-cultured separately. With the aim to mimic the complexity of natural microbial communities, herein we applied surface enhanced Raman scattering (SERS) as an imaging tool^{1,2} for the non-invasive detection and visualization of bioactive metabolites secreted by *Escherichia coli* and *Pseudomonas aeruginosa* bacteria cultured as mixed populations. As shown in this study, SERS enabled the simultaneous detection and visualization of indole and pyocyanin *in situ*, and revealed the down-regulation of pyocyanin expression due to indole signaling. The SERS-based sensing strategy described not only provides a complementary tool to investigate the chemistry underpinning multispecies microbial communities, but it can also be implemented for the detection and monitoring of microbial metabolites with potential medical, pharmacological, or biotechnological interest.

References

- [1] Bodelón et al., Nat. Mater. 15, (2016), 1203
 [2] Bodelón et al., ACS Nano 11, (2017), 4631

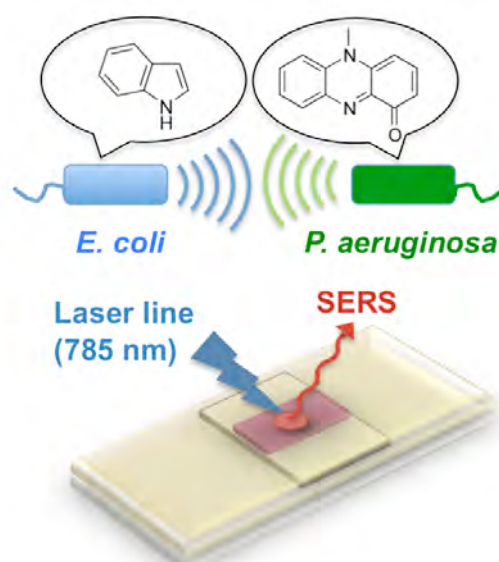


Figure 1. *In situ* SERS detection of secreted bioactive metabolites produced by mixed *E. coli* and *P. aeruginosa* bacterial populations

Development of a Microfluidic-Based Pilot Line for the Production of Novel Nanomedicines

Nikolas N. Daskalakis¹

Centre for Process Innovation, National Formulation
Centre, The Coxon Building, John Walker Road,
Sedgefield, County Durham, TS21 3FE, UK¹

Nikolas.Daskalakis@uk-cpi.com

Nanomedicines unique features have great potential for therapeutic applications. However, product development at scale with precisely controlled attributes for optimal clinical performance is a major challenge. The lack of robust manufacturing methods for nanoformulations is a barrier for the introduction of innovative products to the market. Novel microfluidic technology allows design flexibility and control over nanoparticle formation parameters that are critical for product quality and performance. A microfluidic pilot line is being developed at the Centre for Process Innovation (CPI) to accelerate nanomedicine development by allowing rapid, controlled and reproducible nanoformulations production. A modified NanoAssemblr™ Blaze™ from Precision Nanosystems is utilised to scale up nanoformulations production up to 80 mL/min. Microfluidic technology will be used for the production of liposomes, lipid nanoparticles and polymer nanoparticles entrapping hydrophilic and hydrophobic Active Pharmaceutical Ingredients (APIs). At-line particle size analysis and in-line formulation purification will be integrated to optimise product quality and process efficiency. This facility will provide the test bed to demonstrate scalability and process robustness to prospective manufacturers.

Silver Atomic Quantum Clusters for Cancer Therapy: Targeting Chromatin

F. Domínguez¹,

V. Porto¹, E. Borrajo¹, S. González¹, D. Buceta², C. Carneiro¹, S. Huseyinova², B. Domínguez², K. J. E. Borgman³, M. Lakadamyali⁴, M. F. Garcia-Parajo³, J. Neissa¹, T. García-Caballero⁵, G. Barone⁶, M. C. Blanco², N. Busto⁷, B. García⁷, J. M. Leal⁷, J. Blanco⁸, J. Rivas⁸, M. A. Lopez-Quintela²

1) Department of Physiology and Centro de Investigaciones en Medicina Molecular y Enfermedades Crónicas (CIMUS) IDIS, Universidade de Santiago de Compostela, Spain

2) Departments of Physical Chemistry and Applied Physics, Nanomag Laboratory, Universidade de Santiago de Compostela, Spain

3) ICFO-Institut de Ciències Fotoniques. The Barcelona Institute of Science and Technology Castelldefels (Barcelona), Spain

4) Department of Physiology, Perelman School of Medicine. University of Pennsylvania, Philadelphia, USA

5) Department of Morphological Sciences, School of Medicine-University Clinical Hospital, Universidade de Santiago de Compostela, Santiago de Compostela, Spain

6) Department of Biological Chemical and Pharmaceutical Sciences and Technologies, University of Palermo, Palermo, Italy

7) Department of Chemistry, University of Burgos, Burgos, Spain

8) International Iberian Nanotechnology Laboratory (INL), Braga, Portugal

fernando.dominguez@usc.es

Nanomaterials with very low atomicity deserve consideration as potential pharmacological agents owing to their very small size and to their properties that can be precisely tuned with minor modifications to their size [1]. Here, it is shown that silver clusters of three atoms (Ag₃-AQC)s—developed by an ad hoc method—augment chromatin accessibility. Targeting of DNA has been proven to cause relatively potent and selective destruction of tumor cells. However, resistance mechanisms hamper their effectiveness; for instance, a sufficient amount of cisplatin (CDDP) may fail to reach the DNA. Ag₃-AQC increases DNA accessibility. The coadministration of CDDP with Ag₃-AQC increases not only the amount of CDDP bound to DNA but also CDDP cytotoxicity. Given the differential effect that Ag₃-AQC presents between the tumor and healthy tissue, coadministration of Ag₃-AQC increases the therapeutic index of chemotherapy. This effect only occurs during DNA replication. Coadministration of Ag₃-AQC increases the cytotoxic effect of DNA-acting drugs on human lung carcinoma cells. In mice with orthotopic lung tumors, the coadministration of Ag₃-AQC increases the amount of cisplatin (CDDP) bound to the tumor DNA by fivefold without modifying CDDP levels in normal tissues. As a result, CDDP coadministered with Ag₃-AQC more strongly reduces the tumor burden. Evidence of the

significance of targeting chromatin compaction to increase the therapeutic index of chemotherapy is now provided. Our results thus underscore the importance of targeting chromatin compaction to increase the efficacy of chemotherapeutic drugs. Together, our findings establish the groundwork for exploring the potential therapeutic properties of clusters, a goal that mainly depends on the development of efficient synthetic procedures capable of providing precise size control at the lowest scale of nanomaterials.

References

- [1] Porto V, Borrajo E, Buceta D, Carneiro C, Huseyinova S, Domínguez B, Borgman KJE, Lakadamyali M, Garcia-Parajo MF, Neissa J, García-Caballero T, Barone G, Blanco MC, Busto N, García B, Leal JM, Blanco J, Rivas J, López-Quintela MA, Domínguez F. *Adv Mater.* 2018 Jul 3:e1801317. doi: 10.1002/adma.201801317.

Cytotoxic Effects of Magnetite Nanoparticles on Human Periodontoal Ligament Fibroblast Cells

Çiğdem DÖNMEZ GÜNGÜNEŞ^{1,2}

Şükran ŞEKER¹, Hakan GÜNGÜNEŞ³, Ayşe ESER ELÇİN¹, and Yaşar Murat ELÇİN¹

¹ Tissue Engineering, Biomaterials and Nanobiotechnology Laboratory, Ankara University Faculty of Science, Ankara University Stem Cell Institute, Ankara, Turkey

² Faculty of Arts and Sciences, Chemistry Department, Hitit University, Corum, Turkey

³ Faculty of Arts and Sciences, Physics Department, Hitit University, Corum, Turkey

cigdemdonmez@hitit.edu.tr

The cytotoxicity and cellular uptake of the magnetite nanoparticles were examined by characterization and cell response studies. Magnetite NPs were characterized by using transmission electron microscopy, X-ray diffraction, Brunauer–Emmett–Teller surface area analysis, dynamic light scattering and zeta sizer analyses. The Mössbauer spectroscopy was used in order to magnetically characterize the NPs. hPDLF cells were exposed to different concentrations of magnetite NPs and tested for viability, membrane leakage and generation of intracellular reactive oxygen species. Additionally, cell response was determined in real time using an impedance based biosensor system. The data obtained showed that the toxic cell response of hPDLF cells to magnetite nanoparticles is dose and time dependent.

References

- [1] Kong, L. X., Peng, Z., Li, S. D., & Bartold, P. M. (2006). Nanotechnology and its role in the management of periodontal diseases. *Periodontology 2000*, 40(1), 184-196.
- [2] Ramesh, V., Ravichandran, P., Copeland, C. L., Gopikrishnan, R., Biradar, S., Goornavar, V., ... & Hall, J. C. (2012). Magnetite induces oxidative stress and apoptosis in lung epithelial cells. *Molecular and cellular biochemistry*, 363(1-2), 225-234.
- [3] Xiao, W., Liu, X., Hong, X., Yang, Y., Lv, Y., Fang, J., & Ding, J. (2015). Magnetic-field-assisted synthesis of magnetite nanoparticles via thermal decomposition and their hyperthermia properties. *CrystEngComm*, 17(19), 3652-3658.

Figures

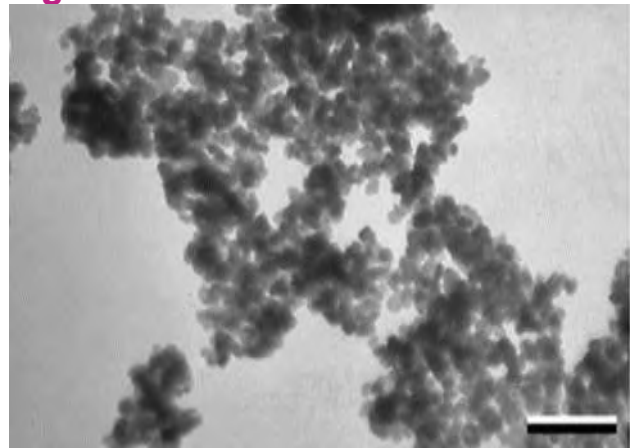


Figure 1. TEM micrograph of Fe₃O₄. Scale bar: 100 nm.

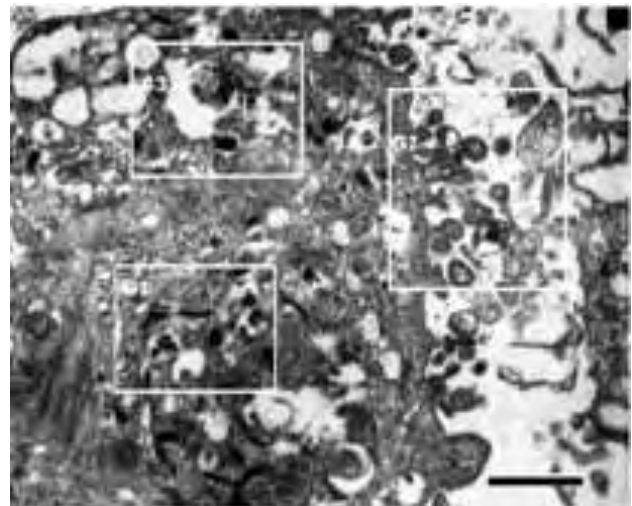


Figure 2. TEM micrograph showing the morphology of Fe₃O₄-treated hPDLF cells. Scale Bar: 1 μ m.

CONTACT LENSES FUNCTIONALIZED WITH ANTIMICROBIAL PEPTIDES FOR THE PREVENTION OF CORNEAL INFECTIONS

Emiliano Salvagni¹, Clara García¹, Àngels Manresa², Carlos Rodríguez-Abreu¹, Maria José Garcia-Celma², Claudia Müller-Sánchez³, Manuel Reina³, **Jordi Esquena¹**.

¹ Institute for Advanced Chemistry of Catalonia, Spanish National Research Council (IQAC-CSIC) and Networking Research Center on Bioengineering, Biomaterials and Nanomedicine (CIBER-BBN), Barcelona, Spain

² Faculty of Pharmacy and Food Sciences, University of Barcelona, Spain

³ Celltec-UB, Faculty of Biology, University of Barcelona, Spain

jordi.esquena@iqac.csic.es

One of the most common problems related to contact lenses is the risk of eye microbial infection, which is a significant health issue given the large population of contact lenses wearers worldwide [1]. Soft contact lenses are made of hydrogel materials, and are commonly used because of its comfort and superior properties, in comparison to rigid contact lenses. However, the high water content of soft contact lenses makes them prone to bacterial growth, and thus, good hygiene practices are required for wearing such contact lenses [2]. Previous studies have demonstrated that bacteria and fungi can cause corneal infections with serious consequences. *Pseudomonas aeruginosa* and *Klebsiella pneumoniae* have been identified as common pathogen agents in corneal infections [3].

Antimicrobial Peptides (AMPs), effective against these bacteria, have been anchored on commercial contact lenses, with the objective of imparting bactericidal activity on those materials. The hydrogel chemical modification was performed under mild conditions (room temperature, pH=7.4) Covalent anchoring was achieved by using appropriate linkers, capable of binding the lens surface at one side and the AMP at the other side. Examples of surface-modified contact lenses are shown in Fig. 1.

Contact lenses, surface-functionalized with AMPs, were characterized by analytical techniques that included wettability, Raman confocal microscopy and fluorescence studies. The results demonstrated that chemical binding of AMPs, on the surface of contact lenses, was quantitative and irreversible in normal conditions. Stability studies, with a fluorescently tagged peptide, showed that covalently bound AMPs were stable on the surface of contact lenses, in PBS solutions, for long storage periods.

Microbiology studies were performed to evaluate the efficacy of contact lenses, surface-modified with AMPs, in inhibiting the formation of biofilms. The

bacteria strains studied were *P. aeruginosa*, *K. pneumoniae*, and *S. aureus*. The results showed that AMP-modified contact lenses greatly decreased the amount of bacteria adhered on their surface. Moreover, the possible cytotoxicity of AMP-modified contact lenses was evaluated using human retinal pigment epithelial cells and immortalized human corneal epithelial cells. These cells were cultured in contact with AMP-modified contact lenses. The results demonstrated that AMP-modified contact lenses were not cytotoxic against the above cells. In these cytotoxicity experiments, results were compared to those of both positive and negative controls, using sodium dodecyl sulfate as a model cytotoxic agent. All these results demonstrated that AMP-modified contact lenses offer the potential to minimize corneal bacterial infection and represent a suitable platform for future ophthalmic devices.

Acknowledgements

We would like to acknowledge Generalitat de Catalunya (TecnioSpring programme) for funding (TECSPR14-2-0044 project).

References

- [1] S.A. Collier, M.P. Gronostaj, A.K. MacGurn, J.R. Cope, K.L. Awsumb, J.S. Yoder, M.J. Beach. *Morbidity and Mortality Weekly Report*. 2014,63(45) 1027-1030
- [2] C. Alvarez-Lorenzo, H. Hiratani, A. Concheiro. *AmJ Drug Deliv* 2006;4:131–51.
- [3] P. Preechawat, U. Ratananikom, R. Lerdivitayasakul, S. Kunavisarut. *J Med Assoc Thai* 2007; 90 (4): 737-43

Figures

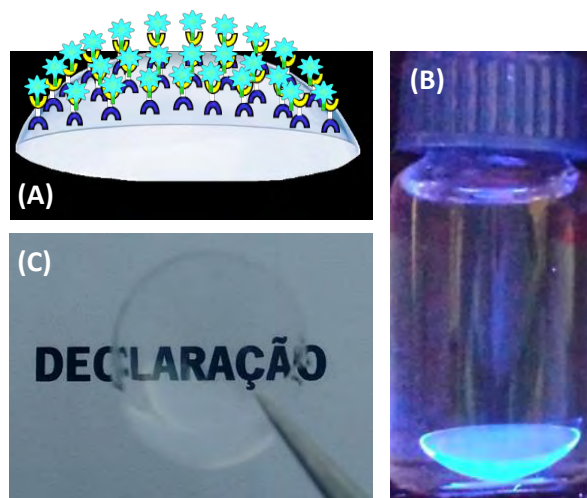


Figure 1. (A) Scheme of a contact lens with an active agent anchored to its surface by covalent binding through a linker; (B) Example of contact lenses surface-functionalized with a fluorescent dye; (C) AMP-modified contact lens, showing its transparency.

Long circulating nanoparticles passively accumulate in tuberculosis granulomas in zebrafish and mouse models

Federico Fenaroli¹,
Gareth Griffiths¹

¹University of Oslo, Blindernveien 31, Oslo, Norway
federico.fenaroli@ibv.uio.no

The enhanced permeability and retention (EPR) effect is the only described mechanism enabling nanoparticles (NP) flowing in blood to reach tumours by a non-active targeting mechanism. Using the transparent zebrafish model infected with *Mycobacterium marinum* we show that an EPR-like process also occurs allowing different NP to extravasate from the vasculature to reach granulomas that assemble during tuberculosis (TB) infection¹. PEGylated liposomes and other NP types cross endothelial barriers near infection sites within minutes after injection and accumulate close to granulomas (figure 1). We show that NP can concentrate strongly in distinct foci on the abluminal side of the endothelium. EM analysis suggests that NP cross the endothelium via the paracellular route. PEGylated NP also accumulated efficiently in granulomas in a mouse model of TB infection with *Mycobacterium tuberculosis*, arguing that the zebrafish embryo model can be used to predict NP behaviour in mammalian hosts. In earlier studies we and others showed that uptake of NP by macrophages that are attracted to infection foci is one pathway for NP to reach TB granulomas. This study reveals that when NP are designed to avoid macrophage uptake they can also efficiently target granulomas via a mechanism that shares some features with EPR.

References

1 Fenaroli, F.; Repnik, U; Xu, Y.; Johann, K.; Van Herck, S.; Dey, P.; Skjeldal, F. M.; Frei, D. M.; Bagherifam, S.; Kocere, A.; Haag, R.; De Geest, B. G.; Barz, M.; Russell, D. G.; Griffiths, G. ACS Nano, 8 (2018), 8646-8661.

Figures

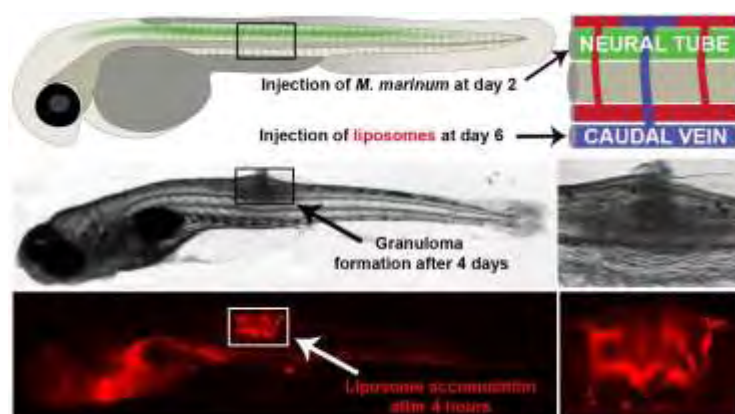


Figure 1. Accumulation of intravenously injected PEGylated liposomes in a zebrafish *M. marinum* granuloma.

Silicon Nitride Photonic Integrated Circuits for Biophotonics and medical applications

Juan Fernandez¹, Marco A. G. Porcel¹,
Hilde Jans², Douwe Geuzebroek³, Sara Mas⁴,
Patrick Leisching⁵, Jeremy Witzens⁶

¹Photonics S.L, Camino de vera s/n, UPV, Ed. 9B-D2,
46022, Valencia, Spain.

²imec, Kapeldreef 75, 3001 Heverlee, Belgium.

³LioniX International, Hengelosestraat 500, 7521 AN
Enschede, The Netherlands.

⁴MedLumics Plaza de la Encina, 10-11 Núcleo 3 -2º A,
28760 Tres Cantos (Madrid), Spain

⁵TOPTICA Photonics AG, Lochhamer Schlag 19, 82166
Graefelfing (Munich), Germany

⁶Institute of Integrated Photonics, RWTH Aachen
University, Sommerfeldstraße 18/24, 52074 Aachen,
Germany

*juan.fernandez@vlcphotonics.com

Here, we present the characteristics of the photonic integrated circuits technology developed for the European pilot line PIX4life. In addition, the details of two different silicon nitride fabrication platforms are summarized.

Photonic Integrated Circuits (PICs): Many high accuracy, high sensitivity biophotonic measurement systems are based on expensive, bulky free space optics built with complex lens arrangements, being difficult to stabilize in a robust way, miniaturize and scale up for production. Examples of these are fluorescent, absorption and hyperspectral microscopes, OCT scanners (see Fig. 1) and sources for cytometers (see Fig. 2) [1, 2, 3, 4, 5].

Silicon nitride photonic integrated circuits: Silicon nitride has gained a lot of interest in the last 10 year. Its chemical, mechanical and optical properties make it a suitable material for integrating optical systems into PICs. Furthermore, the availability of fabrication facilities and the compatibility with CMOS integration, make it the perfect platform for low loss, visible range applications. SiN-based life-science applications are explored widely e.g., for the development of biochemical and medical sensing applications as well as light sources for the newest microscopy and spectroscopy techniques [3, 5, 6, 7, 8].

The PIX4life pilot line (<https://pix4life.eu>) is composed of a consortium having both companies and research institutes. It started in 2016 providing an end-to-end and scalable framework and supply chain for the development of silicon nitride (SiN)

photonic integrated circuits (PIC), mainly focusing on life science applications working at visible wavelengths (400-1100 nm). The capabilities of PIX4life span from design and test services, to packaged PICs ready to use in a larger module or system. These services are mostly aimed for life-science users not familiar with photonic integration technology, and towards support, alignment and extension of the current European know-how in design tools, hybrid integration and micro-fluidic assembly.

The core of PIX4life are the two SiN waveguide platforms, BioPIX and TriPleX™, offered respectively by imec (Belgium) and LioniX International (Netherlands). The most important characteristic of these SiN PIC platforms is their low propagation loss at visible and short near-infrared wavelengths, at which silicon PICs are opaque.

Both foundries organize periodic Multi-Project Wafer (MPW) runs, where multiple users can place their PIC designs for low-cost prototyping by sharing wafer space. During 2018 and 2019, PIX4life is operating in early Open-Access mode. Since the services is subsidized by the EU, the pilot line reviews all incoming requests for development of SiN PICs. Priority is given to European customers developing life science applications.

BioPIX: Manufactured by the Belgian research institute imec, the BioPIX technology comprises two different flavours: one for short-visible wavelengths (from 400 to 700 nm); BioPIX150, and a second one for long visible to short near-infrared wavelengths (from 700 to 1000 nm), BIOPIX300. The waveguide thickness of the two flavours is 150 and 300 nm respectively. To maintain CMOS compatibility, the waveguides are deposited on top of a 2.3 to 3.3 µm silicon dioxide layer via PECVD technique [9,10].

TriPleX™ Vis: Manufactured by the Dutch company LioniX International, TriPleX™ is the branding name of their thin LPCVD SiN waveguide embedded in silicon dioxide (thermal oxide below and TEOS above). Originally designed for ultra-low propagation loss in the C-Band, their performance in the visible range has been improved for four different wavelengths: 405, 488, 532, and 640 nm [11, 12].

The [PIX4life project](#) is funded by the European Community as part of the Horizon 2020 research and innovation program (grant agreement n° 688519).

References

- [1] F. Aparicio et al., J. Phys. Appl. Phys. 47, 40 (2014), 405401.

- [2] M. Fukuta et al., *Sci. Rep.* 5, 1 (2015), 16068.
- [3] R. Diekmann et al., *Nature Photon.* 11, 5 (2017), 322–328.
- [4] A. Nitkowski et al., *NSTI-Nanotech*, 2 (2014), 435–438.
- [5] S. Romero-García et al., *Proc. SPIE*, 10108 (2017) 101080Z.
- [6] B. I. Akca et al., *Opt. Express*, 21, 14 (2013), 16648.
- [7] M. S. Luchansky and R. C. Bailey, *Anal. Chem.* 84, 2 (2013), 793–821.
- [8] J. T. Kindt and R. C. Bailey, *Curr Opin Chem Biol.* 17, 5 (2013), 818–826.
- [9] M. Mahmud-UI-Hasan et al., *ACS Photonics*, 4, 3 (2017), 495–500.
- [10] P. Muellner et al., *Procedia Eng.* 120 (2015), 578–581.
- [11] K. Wörhoff et al., *AOT*, 4, 2 (2015), 189-207.
- [12] R. Heideman, M. Hoekman and E. Schreuder, *IEEE J. Sel. Top. Quantum Electron.* 18, 5 (2012), 1583–1596.
- [13] D. Herranz, et al., *The Journal of Innovations in Cardiac Rhythm Management*, 6 (2015), 2086-2091

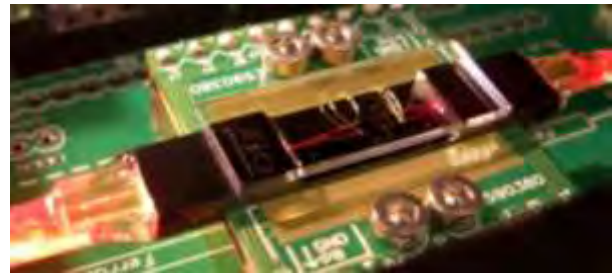


Figure 3. Example of sensing chip from LioniX International



Figure 4. Pilot line logo

Figures

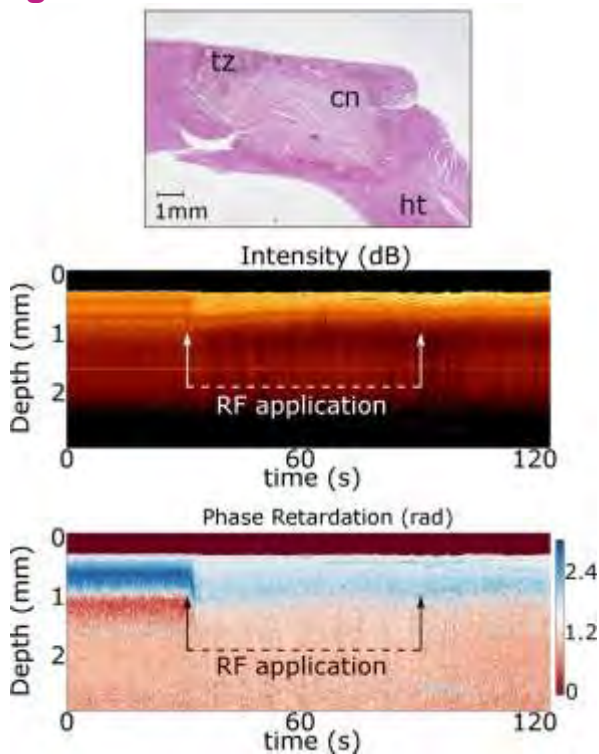


Figure 1. Example of OCT application from MedLumics S.L.[13]



Figure 2. Example of laser light combiner from TOPTICA Photonics AG & Chair of integrated photonics, RWTH Aachen University

Polymeric nano-vaccines improved immune checkpoint anti-tumor efficacy against breast cancer

Helena F. Florindo¹,

C. Peres¹, A.I. Matos¹, L. Moura¹, J. Conniot¹, A. Scomparin², E. Yeini², L. Graça³, V. Prêat⁴, Ronit Satchi-Fainaro²

¹Research Institute for Medicines (iMed.Ulisboa), Faculty of Pharmacy, Universidade de Lisboa, Lisbon, Portugal.

²Department of Physiology and Pharmacology, Sackler Faculty of Medicine, Tel Aviv University, Tel Aviv, Israel

³Instituto de Medicina Molecular, Faculty of Medicine, University of Lisbon, Portugal

⁴LDRI – Louvain Drug Research Institute, Faculté de Pharmacie, Université Catholique de Louvain, Brussels, Belgium;

hflorindo@ff.ulisboa.pt

Cancer vaccines are promising alternatives for cancer treatment. However, limited effects on tumor regression have been obtained due to multiple tumor immune evasion mechanisms [1]. OX40 is an immune checkpoint co-stimulator expressed by activated cytotoxic T cells and regulatory T cells. It triggers the expansion and trafficking of effector T cells, while overcoming the suppression of CD4+ T cells by inhibiting foxp3, TGF- β and IL-10 expression. However, limited outcomes have been obtained with anti-OX40 agonists at clinical settings [2]. This study characterized the immune-mediated antitumor responses induced by a multifunctional nano-vaccine combined with anti-OX40 in a triple negative breast cancer mouse model.

Poly(lactide acid) (PLA) nanoparticles (NP) were synthesized by the double emulsion solvent evaporation method to incorporate alpha-lactalbumin, as breast cancer antigen, and the toll-like receptor ligands (TLRI) CpG and Poly (I:C). To potentiate the delivery of these TLRI to tumor microenvironment, NP surface was modified by hyaluronic acid to target CD44 overexpressed on 4T1 mouse breast cancer cells [3]. NP size, surface charge (ZP) and morphology were analyzed by Dynamic Light Scattering, Laser Doppler Electrophoresis and Atomic Force Microscopy, respectively. Antigen and adjuvants entrapment efficiencies (EE) were quantified by HPLC and Oligreen reagent, respectively. Cell viability was assessed by Alamar Blue assay. NP internalization and DC activation profile were evaluated in vivo by flow cytometry. The immunotherapeutic potential of our multifunctional nano-vaccines was assessed, isolated and in combination with anti-OX40 monoclonal antibody, in 4T1 mammary carcinoma.

NP presented a mean diameter close to 200 nm with low polydispersity index (Pdl) values (lower than 0.16), surface charge close to neutrality, and EE superior to 85%. NP showed no negative effects on the viability of DC after 72 h of incubation, even at

high NP concentrations (up to 1 mg/mL). Targeted PLA NP, labeled with rhodamine, were extensively taken up by DC, but also by 4T1 breast cancer cells. Nano-vaccines induced the DC activation and maturation, significantly increasing the expression of CD80, CD86 and MHC-I surface markers.

A noteworthy tumor remission was observed in 4T1 tumor-bearing animals treated with the multifunctional nano-vaccine combined with anti-OX40. These animals presented a long-term survival, with a tumor volume 4-fold lower than that obtained in OX40-treated mice (Figure 1). Of note, the combinatorial schedule did not induce any signs of toxicity in treated animals. The analysis of the different subpopulations of cells within the tumor microenvironment evidenced a marked infiltration of effector immune cells, namely cytotoxic T lymphocytes specific for the entrapped breast cancer antigen, thus evidencing the role of the nano-vaccine in the overall immune-mediated anti-tumor response observed in animals treated with this combination immunotherapy.

This study reveals the synergy between a multi-targeting nano-vaccine and anti-OX40 in triple-negative breast cancer, providing important insights for the establishment of novel combination regimens against this poorly immunogenic tumor.

References

- [1] Brent A. Hanks, *Discov Med*, 21 (2016) 135–142.
- [2] Melero, I. et al., *Clin Cancer Res*, 19 (2013) 997–1008.
- [3] Yan Y, Zuo X, Wei D, *Stem Cells Transl Med*, 4 (2015) 1033–1043.

Figures

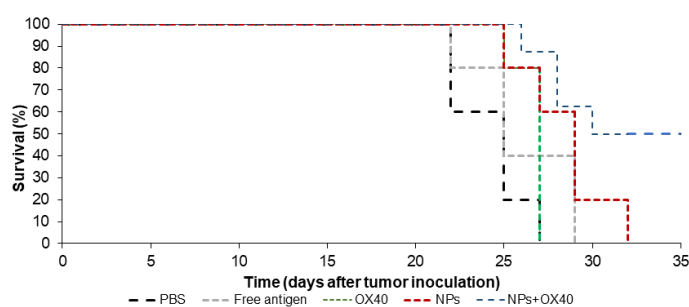


Figure 1. Combination of polymeric nano-vaccine with anti-OX40 monoclonal antibodies prolongs triple negative breast carcinoma mice survival

Hydrated Biomembranes and Nanomaterials: Perspectives for Blood-Brain-Barrier Crossing of Nanoparticles.

Giancarlo Franzese^{1,2}

¹Interdisciplinary and Statistical Physics Section-
Condensed Matter Physics Department, Universitat de
Barcelona

²Institute of Nanoscience and Nanotechnology (IN2UB)

gfranzese@ub.edu

The Blood-Brain-Barrier (BBB) is the tight membrane that protects our brain and represents the major hindrance to the use of chemotherapeutic agents for brain tumors.

Recently it has been showed by *in vitro* and *in vivo* studies that the adsorption of apolipoprotein E4 (ApoE4) on lipid nanoparticles (NPs) produces a protein corona that enhances the BBB-crossing, improving brain NP accumulation 3-fold compared to undecorated particles [1-2]. Therefore, it is possible to increase the ability to cross the BBB for engineered NPs carrying a loose layer of proteins. Nevertheless, the NP-protein corona composition—and, as a consequence, the cellular biological response to the NP—change over time as a consequence of the competition among the plasma proteins once the NP is in the blood stream, as we showed [3].

In collaboration with experimental groups, we develop a multiscale approach for the study of bio-membranes, proteins, NPs and nanomaterials in aqueous solution oriented to applications to the BBB crossing for oncological treatments. We model the kinetics of NP interaction with proteins [3-5], of proteins with water [6-10], and of water with membranes and nanomaterials [11-14], with the aim of finding how to optimize the NP-protein corona formation to cross the BBB.

In particular, here, we will focus on our recent results by all-atom simulations showing that the water-membrane interface has a structural effect at ambient conditions that propagates further than the often-invoked 1 nm length scale and that the translational and rotational dynamics of water molecules is strongly determined by their local distance to the membrane so that we can identify the existence of an interface between the first hydration shell, partially made of hydration water bound to the membrane, and the next shells entirely made of unbound hydration water. These results could drastically affect the kinetics of the protein-corona, determining the fate of NPs during the BBB crossing.

References

- [1] P. Blasi, et al., Adv. Drug. Deliver. Rev. 59, 454 (2007).
- [2] R. Dal Magro, et al., (with Blasi) Nanomedicine: NBM 14, 429 (2018).
- [3] O. Vilanova, J. J. Mittag, P. M. Kelly, S. Milani, K. A. Dawson, J. O. Rädler, G. Franzese, ACS Nano 10, 10842–10850 (2016).
- [4] P. Vilaseca, K. A. Dawson, G. Franzese, Soft Matter 9, 6978–6985 (2013).
- [5] O. Vilanova, V. Bianco, G. Franzese, Multi-scale approach for self-assembly and protein folding, in "Design of self-assembling materials", ed. I. Coluzza (Springer Publishing, New York), 2017.
- [6] V. Bianco, S. Iskov, and G. Franzese J. Biol. Phys. 38, 27 (2012).
- [7] V. Bianco and G. Franzese, Sci. Rep. 4, 4440 (2014).
- [8] V. Bianco and G. Franzese, Phys. Rev. Lett. 115, 108101 (2015).
- [9] V. Bianco, N. Pagès, I. Coluzza, G. Franzese, J. Mol. Liq. 245, 129 (2017).
- [10] V. Bianco, G. Franzese, C. Dellago, I. Coluzza, Phys. Rev. X 7, 021047 (2017).
- [11] C. Calero, E. H. Stanley, and G. Franzese, Materials 9, 319 (2016).
- [12] J. Martí, C. Calero, G. Franzese, Entropy 19, 135 (2017).
- [13] F. Martelli, H.Y. Ko, C. Calero, and G. Franzese Front. Phys. 13, 136801 (2018).
- [14] C. Calero, and G. Franzese, "Membranes with different hydration levels: the interface between bound and unbound hydration water" J. Mol. Liq. accepted (2018).

Figures

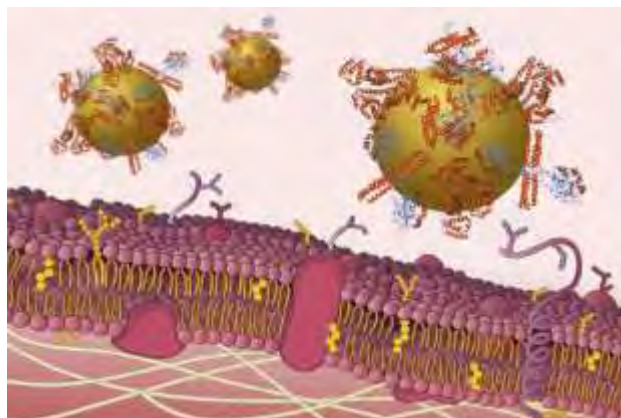


Figure 1. Cartoon of NP-Protein corona complexes near a cellular membrane [3].

Enantio-Selective Sensing Using Plasmonic Racemic Arrays

Jose García-Guirado¹,
Mikael Svedendahl^{1,2}, Joaquim Puigdollers³,
Romain Quidant^{1,4}

¹ICFO Institut de Ciències Fotòniques, The Barcelona Institute of Science and Technology, 08860 Castelldefels (Barcelona), Spain

²KTH Royal Institute of Technology, Roslagstullsbacken 21, 10691 Stockholm, Sweden

³UPC Universitat Politècnica de Catalunya, Departament d'Enginyeria Electrònica, 08034 Barcelona, Spain

⁴ICREA Institució Catalana de Recerca i Estudis Avançats, 08010 Barcelona, Spain

romain.quidant@icfo.eu

Abstract

Building blocks of life show well-defined chiral symmetry which has a direct influence on their biochemical properties and role in Nature. Chirality, geometrically understood as the lack of symmetry under specular reflection, is typically exhibited by bio-molecules with a single configuration, i.e. left or right handed. Such molecules are involved in physiological processes like odor, taste, metabolism, neural transmission etc. However, when they are artificially synthesized both enantiomers, the mirrored images, occur. In general, the asymmetric specie does not follow the natural pathways and in the worse scenario one enantiomer acts as a medicine while the other has detrimental effects. Therefore, it is of mayor importance for the pharmaceutical industry to properly synthesize and characterize the artificial chiral compounds [1-3].

On the side of characterizing chiral molecules, several techniques have been developed over the years to differentiate enantiomers. Such techniques include circular dichroism (CD), optical rotatory dispersion (ORD) or Raman optical activity (ROA), where CD is the most widely used. However, the weak chiro-optical activity of the molecules and low sensitivity of the technique makes high concentration and sample volumes a requirement. Additionally, the location of the molecular resonances in the ultraviolet (UV) spectral range makes CD equipment expensive [4,5].

Recent developments in nanotechnologies and photonic sensors come with promising properties that can boost sensitivity in bio-sensing applications [6,7]. In the field of chirality, plasmonic structures have been specially designed to mimic the properties of chiral molecules as well to generate optical fields that better interact with such molecules. These structures can be used as sensors as their optical responses are modified under molecular

interaction. This approach allows translating the CD measurements from the UV to the visible (VIS) spectral range and enables better sensitivity and lower sample volumes than the classical CD technique [8]. However, the best implementation remains unknown and controvert due to low reproducibility of the results presented in the literature over the last years. One of the major drawbacks is to find the optimal sensor, which provides the optimal near and far fields while keeping the experimental implementation feasible. It has been a matter of discussion if sensors producing near-optimal near field configurations and simultaneously high CD signals are the most appropriate for sensing, as their large CD might over-shadow the molecular signatures. At the same time, the theoretical optimization of these parameters has often led unrealizable nanostructures due to nanofabrication limitations. The other major drawback is the reproducibility of the methods and the standards for comparing results. On this side, discussions about the molecular coating of the sensors, solvent compatibility or the significance of the molecular model have been raised [9,10].

In this contribution [11] we present a novel plasmonic sensor configuration that allows the discrimination of chiral molecules. The sensor consists of handed gold nanostructures of gammadion shape, distributed in a racemic (50/50 mixture) matrix with C_4 symmetry. Its optical response enhances the electric field as well as the optical chirality in the near field. Thus, the interaction with molecules is enhanced, while the bare sensors exhibit a flat CD signal, providing background-free CD measurements for molecular detection (Fig. 1a-b). We have used a complete chiral molecular model based on L-, D-, and the racemic mixture of phenylalanine, which allows us to evaluate the opposite chiral effects while having a reference system. Additionally, we have used molecular thermal evaporation (MTE) technique to deposit a dense molecular layer on top of the sensors in a controllable and reproducible way (Fig. 1c-d). Our results show the discrimination of phenylalanine enantiomers through positive or negative peaks while the racemic mixture shows a flat signal (Fig. 2).

As an outlook, we therefore present preliminary results that show that this approach is also suitable for microfluidics systems with much lower density of chiral molecules [12].

References

- [1] Brandt, J. R.; Salerno, F.; Fuchter, M. J.; Nat. Rev. Chem. 2017, 1 (6), 0045.
- [2] Chhabra, N.; Aseri, M.; Padmanabhan, D. A.; Int. J. Appl. Basic Med. Res. 2013, 3 (1), 16.

- [3] Maugh, T. H.; Science (80). 1983, 221 (4608), 351–354.
- [4] Berova, N.; Nakanishi, K.; Woody, R.; John Wiley & Sons, 2000.
- [5] Berova, N.; Polavarapu, P. L.; Nakanishi, K.; Woody, R. W.; Wiley, 2012.
- [6] Aćimović, S. S.; Ortega, M. a.; Sanz, V.; Berthelot, J.; Garcia-Cordero, J. L.; Renger, J.; Maerkl, S. J.; Kreuzer, M. P.; Quidant, R.; Nano Lett. 2014, 14 (5), 2636–2641.
- [7] Yavas, O.; Svedendahl, M.; Dobosz, P.; Sanz, V.; Quidant, R.; Nano Lett. 2017, 17 (7), 4421–4426.
- [8] Hentschel, M.; Schäferling, M.; Duan, X.; Giessen, H.; Liu, N.; Sci. Adv. 2017, 3 (5), e1602735.
- [9] Hendry, E.; Carpy, T.; Johnston, J.; Popland, M.; Mikhaylovskiy, R. V.; Laphorn, a J.; Kelly, S. M.; Barron, L. D.; Gadegaard, N.; Kadodwala, M.; Nat. Nanotech. 2010, 5 (11), 783–787.
- [10] Maoz, B. M.; Chaikin, Y.; Tesler, A. B.; Bar Elli, O.; Fan, Z.; Govorov, A. O.; Markovich, G.; Nano Lett. 2013, 13 (3), 1203–1209.
- [11] García-Guirado, J.; Svedendahl, M.; Puigdollers, J.; Quidant, R.; Nano Lett. 2018, acs.nanolett.8b02433.
- [12] Guirado, J. G.; Quidant, R.; UPC Universitat Politecnica de Catalunya, 2018.

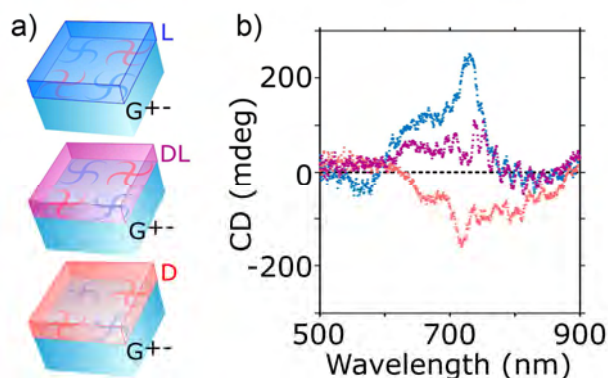


Figure 2. Enantiomer detection in the visible spectral range using racemic gammadian arrays. (a) The molecules were deposited on different sensor arrays, showing the corresponding (b) CD spectrum.

Figures

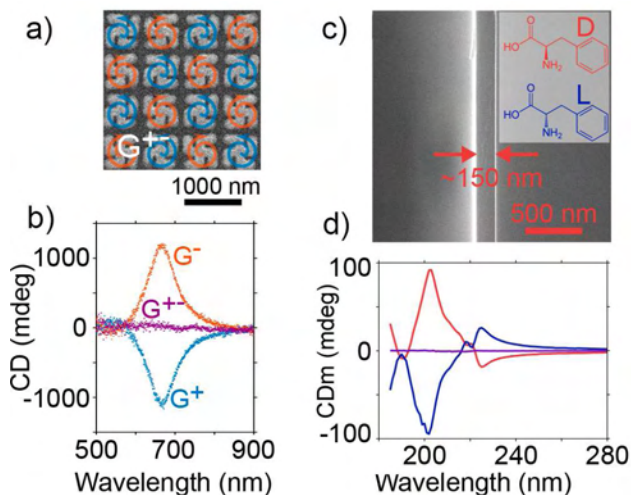


Figure 1. Optical characterization of handed and racemic gammadian arrays and phenylalanine coatings. (a) SEM images of the racemic G⁺ array. (b) CD spectra of the fabricated nanostructures. (c) SEM image of a 150 nm thin layer of DL phenylalanine. (d) CD spectra of the molecular coatings, named CD_m to be distinguished from sensors CD.

Nanostructuring and assembling magnetic nanoparticles for biomedical applications

Pablo Guardia^{1,2}, Taisiia Berestok¹, Maria Materia², Susana Carregla-Romero³, Wolfgang J. Parak³, Teresa Pellegrino² and Andreu Cabot^{1,3}

¹ Catalonia Institute for Energy Research—IREC, 08930 Sant Adrià de Besòs, Barcelona, Spain

² Italian Institute of Technology, via Morego 30, 16163, Genova, Italy

³ Fachbereich Physik, Philipps Universität Marburg, Marburg, Germany

⁴ ICREA, Pg. Lluís Companys 23, 08010 Barcelona, Spain

pguardia@irec.cat

Iron oxide nanoparticles (IONPs) and specially nanocubes (IONCs) represent one of the most promising iron-based NPs for biomedical applications. Nevertheless, once reached control over the size and crystallinity of the NP at the nanoscale, the performance limit of the material is reached. Structuration of NPs into dimers or its controlled aggregation into micron to centimeter scale structures are smart strategies to: on one hand, improve some of the performances beyond the material's one; on the other hand, implement nanoscale properties into a macroscopic structure. Here, we show four different approaches to exploit IONPs and IONCs as building blocks for more complex structures, and increase their performances beyond the material's limit. IONPs can be produced as dimers combining a gold domain which provides synergetic effects for magnetic mediated hyperthermia. Controlled aggregation of IONCs into magnetic nanobeads or microcapsules within a polymeric shell provide structures with excellent performances for MRI imaging and drug release respectively. Finally, gelation process of IONPs allow producing macroscopic gels showing a superparamagnetic behavior.

References

- [1] Guardia, P.; Nitti, S.; Materia, M. E.; Pugliese, G.; Yaacoub, N.; Greneche, J. M.; Lefevre, C.; Manna, L.; Pellegrino, T., *Journal of Materials Chemistry B* 2017, 5 (24), 4587-4594.
- [2] Berestok, T.; Guardia, P.; Du, R.; Portals, J. B.; Colombo, M.; Estradé, S.; Peiró, F.; Brock, S. L.; Cabot, A., *Metal Oxide ACS Applied Materials & Interfaces* 2018, 10 (18), 16041-16048
- [3] Materia, M. E.; Guardia, P.; Sathya, A.; Pernia Leal, M.; Marotta, R.; Di Corato, R.; Pellegrino, T., *Langmuir* 2015, 31 (2), 808-816.
- [4] Carregal-Romero, S.; Guardia, P.; Yu, X.; Hartmann, R.; Pellegrino, T.; Parak, W. J., *Magnetically triggered release of molecular cargo*

from iron oxide nanoparticle loaded microcapsules. *Nanoscale* 2015, 7 (2), 570-576.

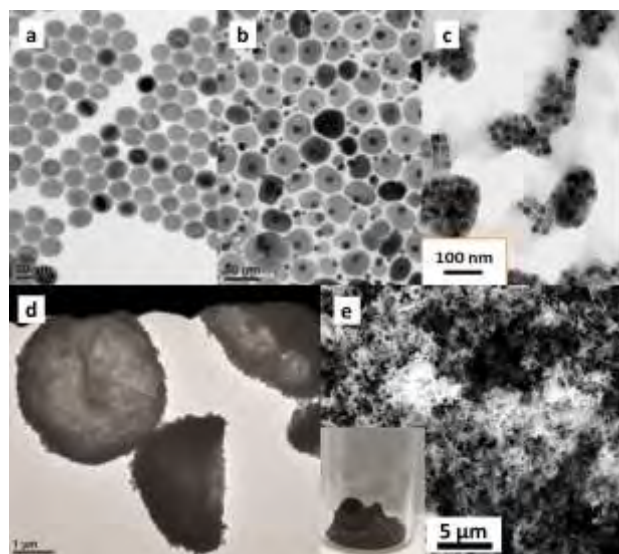


Figure 1. TEM images of the evolution from simple IONPs (a) to iron oxide-gold dimers (b), IONC nanobeads (c), IONC microcapsules (d) and IONP-gels and aerogels (e) by exploiting different structuring and assembly strategies.

Small-molecule immune system modulators: A step forward in cancer immunotherapy

Rita C. Guedes¹,

R. Acúrcio¹, A. Scomparin², R. Satchi-Fainaro², H. F. Florindo¹

¹Research Institute for Medicines (iMed.Ulisboa), Faculty of Pharmacy, Universidade de Lisboa, Lisbon, Portugal.

²Department of Physiology and Pharmacology, Sackler Faculty of Medicine, Tel Aviv University, Tel Aviv, Israel

rguedes@ff.ulisboa.pt

Immunotherapy is nowadays a powerful strategy in cancer therapy with very exciting outcomes. In particular, modulation of immune checkpoint receptors have gain special attention. These immune regulators limit activation and proliferation of T cells and other immune cells enrolled in these signaling pathways. Under normal conditions, they are essential in modulating immune responses; however, they are also one of the major mechanisms used by tumors to evade immune system recognition and destruction. To date, several immune checkpoint receptors have been identified and used as therapeutics in oncology, as programmed cell death protein 1 (PD-1). When engaged by one of its ligands (PD ligand 1 (PD-L1) and PD ligand 2) PD-1 limits autoimmunity. PD-1 ligands are upregulated in many human cancers and their blockade could lead to activation of T cells and therefore enforce tumor recognition. In fact, PD-1/PD-L1 pathway is one of the most successful pathways in the context of clinical cancer immunotherapy with several approved drugs. The most successful therapies relay on the use of antibodies. However, despite their outstanding success, they still have numerous disadvantages as severe immune-related adverse [1, 2].

Recently, the hypothesis of small-molecule modulators as safer therapeutic alternatives has been raised. However, limited efforts have been directed toward immune checkpoint receptors. Our study is focused on the discovery of small molecules targeting PD-L1 that can block PD-1/PD-L1 interaction in order to overcome antibody therapy disadvantages. The limited structural information concerning PD-L1 led us to a detailed structural characterization based on in silico studies in order to assess structural flexibility, gating or binding pockets. Following a computer assisted drug discovery approach to achieve PD-L1 inhibitors, we accomplished a de novo design campaign based on the (2-methyl-3-biphenyl)methanol derivatives generating several scaffolds. Potential PD-L1 inhibitors were selected using several parameters. The binding affinity and functionality of selected PD-L1 inhibitors were assessed on different human and

mice cancer cell lines by ELISA and Flow Cytometry.

References

- [1] Pardoll D. et al., *Cancer Cell*, 27 (2015) 451.
- [2] Sharma P. et al., *Cell*, 161 (2015) 205.

Figures

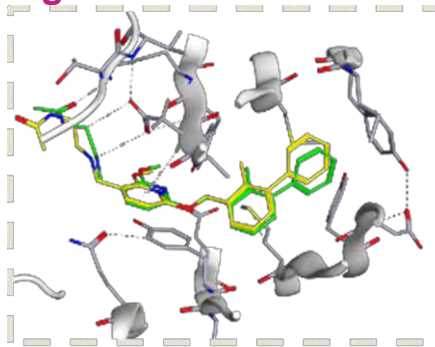


Figure 1. The crystallographic inhibitor docked and superimposed on the 5J89 structure.

AC susceptibility and Mössbauer analysis of Mn – Y substituted $\text{Sr}_{1-x}\text{Mn}_x\text{Fe}_{12-y}\text{Y}_y\text{O}_{19}$ ($0.0 \leq x=y \leq 0.5$) nanohexaferrites

H. Gungunes¹

M.A. Almessiere^{2,3}

Y. Slimani⁴,

A. Baykal³

¹Department of Physics, Hitit University, 19030 Corum, Turkey

²Department of Physics, College of Science, Imam Abdulrahman Bin Faisal University, 31441 Dammam, Saudi Arabia

³Department of Nano-Medicine Research

⁴Department of Physics, Institute for Research & Medical Consultations (IRMC), Imam Abdulrahman Bin Faisal University, 31441 Dammam, Saudi Arabia

hgungunes@gmail.com

$\text{Sr}_{1-x}\text{Mn}_x\text{Fe}_{12-y}\text{Y}_y\text{O}_{19}$ ($0.0 \leq x=y \leq 0.5$) nanohexaferrites were synthesized through citrate sol-gel auto combustion method. Structure, microstructure and magnetic properties have been investigated with respect to Mn and Y content using XRD, FE-SEM, Mossbauer spectroscopy and VSM techniques. The magnetic properties of $\text{Sr}_{1-x}\text{Mn}_x\text{Fe}_{12-y}\text{Y}_y\text{O}_{19}$ ($0.0 \leq x=y \leq 0.5$) were examined. The blocking temperature (T_B) shifts to lower temperatures with rising Mn^{2+} and Y^{3+} contents. This is attributed to the decrease of particles size with Mn^{2+} and Y^{3+} substitutions. The AC susceptibility experiments confirmed that the magnetic interactions are weakened in substituted nanohexaferrites. This is derived from the replacement of both Sr^{2+} and Fe^{3+} ions by respectively Mn^{2+} and Y^{3+} ions. From ^{57}Fe Mössbauer spectroscopy data, the variation in line width, isomer shift, quadrupole splitting and hyperfine magnetic field values on Mn and Y substitutions have been determined.

References

- [1] S. Katlakunta, S. Katlakunta, S.S. Meena, S. Srinath, M. Bououdina, R. Sandhya, K. Praveena, Mater. Res. Bull. 63 (2015) 58–66.
- [2] S Md. Amir, A. Baykal, H. Gungunes, S. Asiri, I. Ercan, S.E. Shirsath, J. Inorg. Organomet. Polym. 28 (2018) 212–222.
- [3] S. Asiri, M. Sertkol, S. Guner, H. Gungunes, K.M. Batoo, T.A. Saleh, H. Sozeri, M.A. Almessiere, A. Manikandan, A. Baykal, Cer. Inter. 44 (2018) 5751–5759.
- [4] A. Baykal, Y. Slimani, A. Manikandan, J. Magn. Mater. 458 (2018) 204-212.

Figures

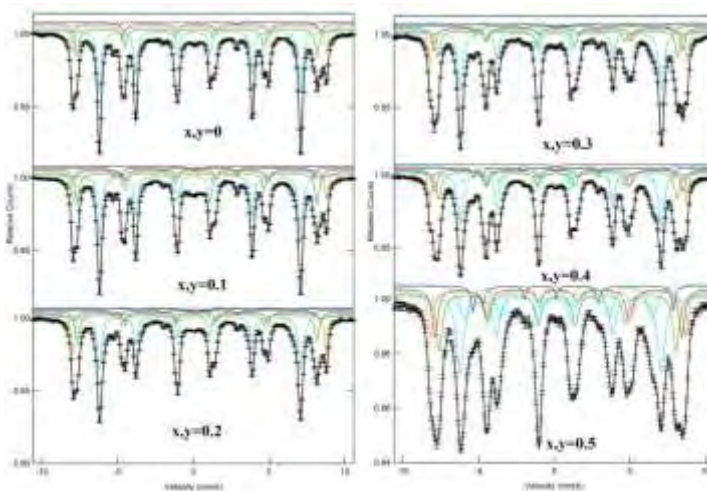


Figure 1. Room Temperature Mössbauer spectra of $\text{Sr}_{1-x}\text{Mn}_x\text{Y}_y\text{Fe}_{8-y}\text{O}_{19}$ samples

Engineered DNA nanostructures for photoacoustics bioimaging

Silvia Hernández-Ainsa,^{1,2}

James Joseph,^{3,4} Kevin N. Baumann,³

Alexandra C. Fux,³ Philipp Koehler,³ Judith Weber,³

Sarah E. Bohndiek^{3,4}

¹Instituto de Nanociencia de Aragón (INA), University of Zaragoza, Campus Río Ebro, Edificio I+D, 50018 Zaragoza, Spain

²ARAID Foundation, Government of Aragón, Zaragoza 50018, Spain

³Department of Physics, University of Cambridge, 19 JJ Thomson Avenue, CB3 0HE, Cambridge, UK

⁴Cancer Research UK Cambridge Institute, University of Cambridge, Robinson Way, CB2 0RE, Cambridge, UK

silviamh83@unizar.es

DNA nanotechnology is a unique assembly tool to engineer structures with accurate control in the location of any introduced functionality.[1]

In this regard, fluorophores can be arranged at controlled distances into DNA nanostructures to investigate molecular processes that occur on the nanometer scale based on the Förster resonance energy transfer (FRET) mechanism.[2] However, the use of this fluorescent pairs in biological samples is limited to shallow imaging depths due to the light scattering. Photoacoustic tomography (PAT)- a recently emerged high resolution modality for *in vivo* imaging that that combines optical excitation with ultrasound detection- represents an interesting approach to study such processes at centimeter depths.[3]

In this respect, we have shown the possibility to produce controlled distance dependent photoacoustics (PA) signal using several DNA helices containing Near Infrared (NIR) fluorophore-quencher pairs located over a range of different controlled distances (Figure 1). Indeed, we have demonstrated their potential use to reveal deep FRET processes within tissue mimicking phantoms.[4]

We have also proved that PA signal of NIR fluorophores can be enhanced by precise positioning into DNA nanostructures.[4] This property together with their biocompatibility make DNA nanostructures very promising as contrast agents nanocarriers (NCs) for cancer imaging using PAT. Namely, some of our investigated DNA NCs bearing NIR fluorophores present superior PA signal generation capabilities and tumor accumulation when compared to the free fluorophore.

Finally, we have shown that DNA nanostructures can be tailored to act as nanoprobe for photoacoustics pH imaging using a ratiometric approach (Figure 2). Interestingly, these nanoprobe work in a pH range relevant for tumour microenvironment.[5]

These reported achievements evidence the multiple applications that DNA nanotechnology can offer to PA bioimaging.

References

- [1] F. Zhang, J. Nangreave, Y. Liu and H. Yan, *J. Am. Chem. Soc.* 2014, 136, 11198
- [2] I. H. Stein, V. Schüller, P. Böhm, P. Tinnefeld, T. Liedl, *Chem. Phys. Chem.* 2011, 12, 689
- [3] L. V. Wang, S. Hu, *Science* 2012, 335, 1458
- [4] J. Joseph, K. N. Baumann, P. Koehler, T. J. Zuehlsdorff, D. Cole, J. Weber, S. E. Bohndiek, S. Hernández-Ainsa, *Nanoscale* 2017, 9, 16193
- [5] K. N. Baumann, A. Fux, J. Joseph, S. E. Bohndiek, S. Hernández-Ainsa, *Chem. Commun.* 2018, 58, 10176

Figures

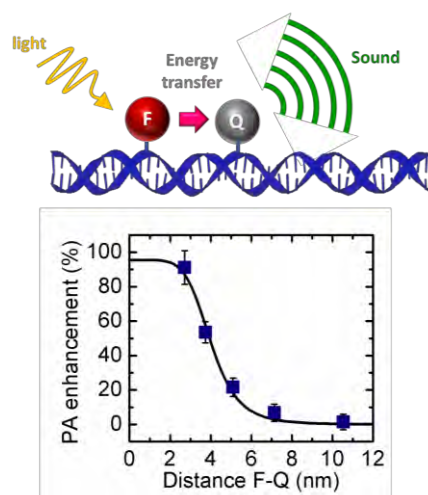


Figure 1. Scheme and graph showing the enhancement of PA signal as the distance between fluorophore and quencher attached to a DNA helix is reduced.

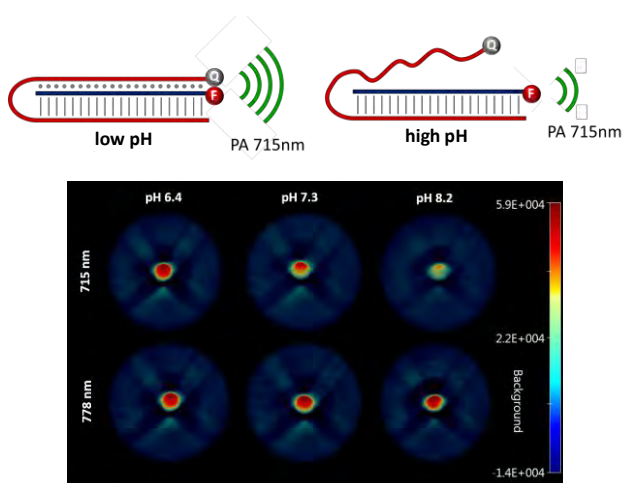


Figure 2. Scheme of the pH responsive DNA-based nanoprobe and images of samples held in phantoms showing the PA signal dependence with pH.

Controlled drug release of PLA/PLGA microspheres

Jiahui Li¹,

Gemma Sanjuan Gómez¹, Manuel Jose Lis Arias²,
Vanessa Martínez Rodríguez¹, Paul Florín Coldea¹,
Cristian López de Prada¹, Jorge Fernández Vela¹,
Guido Ruffini¹

¹The Forest Next S.L., Avinguda Compositor Bizet 2,
Rubí, Spain

²ESEIAAT-UPC, Colom 1, Terrassa, Spain

qli@theforestnext.com

Drug release of ibuprofen encapsulated biodegradable polymer microspheres have been studied in many works [1,2,3]. In the present study, ibuprofen release profile from microspheres based on blend of poly(lactic acid) (PLA) and poly(lactic-co-glycolic acid) (PLGA) with poly(vinyl alcohol) as emulsifier within a phosphate buffer solution (PBS) is determined and compared to drug release profile of PLGA microspheres. PBS was selected as media since buffer anions seemed to regulate drug release, it was prepared using 0,2 M monobasic and 0,2 M dibasic sodium phosphate to achieve pH 8 at 37 °C [1]. PLGA-Ibuprofen and PLA/PLGA-Ibuprofen microspheres were prepared by oil-in-water emulsion solvent evaporation method, the blend of 50 wt.% PLA and 50 wt.% PLGA is formed by physical interactions between them. Once the aqueous solutions of microspheres were prepared, a centrifugation process following by a drying process at 40 °C during 4 h were carried out to obtain microspheres ready for drug release experiments. Figure 1 shows both PLGA-Ibuprofen and PLA/PLGA-Ibuprofen drug release profiles determined by UV-Vis spectroscopy, results indicate that microspheres with blended polymers as shell material exhibit lower release rate, whereas PLGA-Ibuprofen achieve its full release at about 5 min, PLA/PLGA-Ibuprofen does at approximately 10 min from the beginning of experiment, which hints that polymer hydrophobicity is a key factor to explain ibuprofen release rate; the presence of methyl groups in PLA interferes with water penetration into the matrix and consequently, reduces rate of polymer degradation [4]. Thermogravimetric analysis (TGA) was performed from 30 to 700 °C under nitrogen atmosphere on ibuprofen, PLA/PLGA-Ibuprofen, PLA/PLGA-Ibuprofen after drug release experiment in PBS media and PLA/PLGA without ibuprofen, first derivative of TGA (DTG) was applied to obtain curves in Figure 2. Results state that after drug release, signal of degradation stage corresponding to ibuprofen diminishes to unnoticeable, which corroborates that drug release was successfully completed while PLA/PLGA/PVA structure remains and exhibits a signal similar to blank PLA/PLGA microspheres.

References

- [1] Laura J. Waters and Evangelos V. Pavlakis, Journal of Pharmacy & Pharmaceutical Sciences, In vitro controlled drug release form loaded microspheres – dose regulation through formulation (2007) 464-472.
- [2] Cory Berkland, Martin King, Amanda Cox, Kyekyoon (Kevin) Kim, Daniel W. Pack, Journal of Controlled Release, Precise control of PLG microsphere size provides enhanced control of drug release rate (2002) 137-147.
- [3] Aragón, Marcela & Rosas, J.E. and Martínez, Fleming, Latin American applied research Pesquisa aplicada latino americana = Investigación aplicada latinoamericana, Effect of the ibuprofen solubility in acetone and dichloromethane on its release profiles from PLGA microspheres (2014) 87-92.
- [4] Makadia HK and Siegel S.J., Polymers, Poly Lactic-co-Glycolic Acid (PLGA) as Biodegradable Controlled Drug Delivery Carrier. (2011) 1377-1397.

Figures

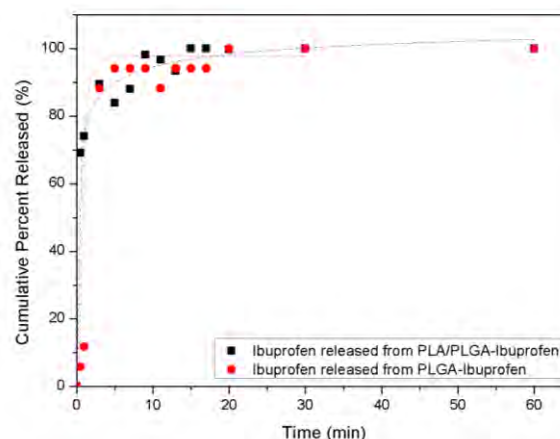


Figure 1. Drug release profiles of PLGA-Ibuprofen and PLA/PLGA-Ibuprofen.

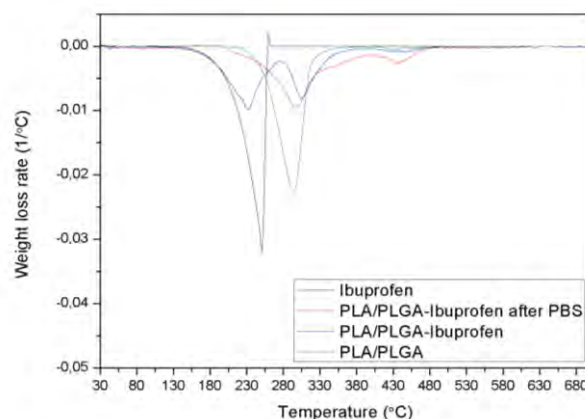


Figure 2. DTG of Ibuprofen, PLA/PLGA-Ibuprofen, PLA/PLGA-Ibuprofen after drug release experiment in PBS media and PLA/PLGA microspheres without active principle.

Training and force adaptability of 3D-bioprinted biological actuators based on skeletal muscle tissue

Rafael Mestre¹

Tania Patiño¹, Xavier Barceló¹, Samuel Sánchez^{1,2}

¹Institute for Bioengineering of Catalonia (IBEC), The Barcelona Institute of Science and Technology, Baldri Reixac 10-12, 08028 Barcelona Spain

²Institució Catalana de Recerca i Estudis Avançats (ICREA), Barcelona, Spain

ssanchez@ibecbarcelona; tpatino@ibecbarcelona; rmestre@ibecbarcelona

Current robotics systems are facing many challenges in a world that requires them to adapt to different environments and interact with humans and other living organisms. For this reason, many recent advances in material science have opened up the possibility of combining biological systems with artificial materials to obtain hybrid bio-robotic devices that can offer complex capabilities, like self-healing, high adaptability and response to different stimuli.¹ Several groups have developed hybrid bio-actuators based on cardiac² and skeletal muscle cells,³ which, in particular, have shown three-dimensional architectures and some of the commented complex behaviours.

In parallel, the 3D bioprinting technique has emerged as a powerful tool for the development of functional three-dimensional tissues and, in particular, skeletal muscle tissue.⁴ Although 3D printing of artificial materials has been used to fabricate scaffolds or molds for hybrid bio-actuators, 3D bioprinting of skeletal muscle tissue, together with soft skeletons, has not been reported in the field of hybrid bio-robotics. Here, we present our recent advances in the fabrication of 3D bioprinted hybrid bio-actuators based on skeletal muscle tissue, taking advantage of the unique versatility, rapid-prototyping and simplicity of the technique.⁵ We report a full characterization and optimization of the printing from the material point of view, but also paying special attention to the biocompatibility, as well as differentiation, maturation and alignment of cells inside the bioprinted hydrogel.

We take advantage of the multi-material printing capabilities of the technique to 3D-bioprint a hybrid biological actuator whose contractions can be completely controlled by external electric fields. We prove the adaptability of the hybrid bio-actuator applying training protocols at different frequencies and with different stiffnesses of the mechanical constraints. By analysing the expression of maturation-related proteins and the evolution of the force with time, we find that these bio-actuators can

adapt to the requirements of the performance according in several ways. In particular, medium frequencies show the greater improvement beyond the natural maturation, while low and high frequencies cannot produce a sufficiently large improvement. These results will help understand the training capabilities of future bio-hybrid actuators and acquire basic knowledge on the behaviour of 3D-engineered skeletal muscle tissue.

References

- [1] T. Patino, R. Mestre, S. Sanchez, *Lab Chip* **2016**, 16, 3626
- [2] Nawroth, J. C., Lee, H., Feinberg, A. W., Ripplinger, C. M., McCain, M. L., Grosberg, A., ... & Parker, K. K., *Nat. biotechnology* **2014**, 30(8), 792.
- [3] R. Raman, C. Cvetkovic, S. G. M. Uzel, R. J. Platt, P. Sengupta, R. D. Kamm, R. Bashir, *Proc. Natl. Acad. Sci.* **2016**, 113, 3497.
- [4] H.-W. Kang, S. J. Lee, I. K. Ko, C. Kengla, J. J. Yoo, A. Atala, *Nat. Biotechnol.* **2016**, 34, 312.
- [5] R. Mestre, T. Patino, X. Barceló, S. Anand, A. Pérez-Jiménez, S. Sánchez. In submission.

Figures

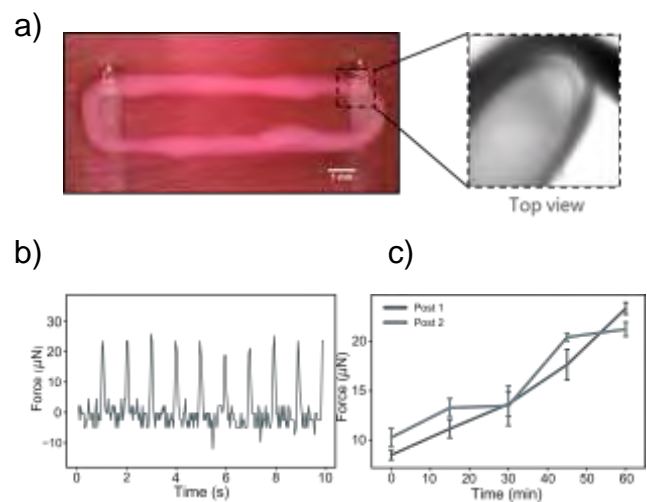


Figure 1. a) Image of a 3D-bioprinted bio-actuator composed of two PDMS posts and a skeletal muscle tissue ring. b) After applying electric pulse stimulation, the force exerted by the tissue can be calculated by measuring the deflection of the posts, c) and its evolution with time can be studied.

Single Cell ICP-MS: The Advantages of Quantifying Metals and Nanoparticulate Number Content in Individual Cells

Chady Stephan¹, Stan Smith¹,
Lauren Amable².

¹PerkinElmer, Shelton, USA

² National Institutes of Health, Bethesda, USA

Chady.Stephan@perkinelmer.com

The ability to rapidly quantify the elemental concentration of individual cells, as well as the distribution in concentration throughout the cell population, has been a limiting factor in life science applications focusing on uptake rates, bioavailability, and bioaccumulation for drug delivery and toxicity assessment. Traditional methods for measuring uptake rates can be a time-consuming process with long instrument analysis and sample preparation time, often leading to qualitative or population-averaged results. We present a new technique, Single Cell ICP-MS (SC-ICP-MS), which is capable of quantifying this offering a unique opportunity to quantitatively measure the metal content in individual cells, unveiling new capabilities to study intrinsic metals and the uptake of dissolved (ionic) and nanoparticulate metals into cells, providing new insights into drug delivery, toxicity assessment, bioavailability, and bioaccumulation mechanisms. Here we provide insights into the uptake of cisplatin into ovarian cancer lines as well as nanoparticles into algae cells to show the power of this technique for the development of targeted drugs and the toxicity of metals to environmental systems, giving fast and in-depth information on the mass and distribution mass of metals in cells that can be linked to biological cellular responses.

References

- [1] Britta Stordal, Mary Davey, "Understanding Cisplatin Resistance Using Cellular Models," International Union of Biochemistry and Molecular Biology Life Journal, 2007, Vol. 59, Issue 11, pp.696–699
- [2] American Cancer Society, "What Is Ovarian Cancer?," About Ovarian Cancer website, February 4, 2016, <https://www.cancer.org/cancer/ovarian-cancer/about/what-is-ovarian-cancer.html>, accessed February 13, 2014
- [3] Cleveland Clinic, "Ovarian Epithelial Cancer," Cleveland Clinic Health Library, February 13, 2017.

Figures

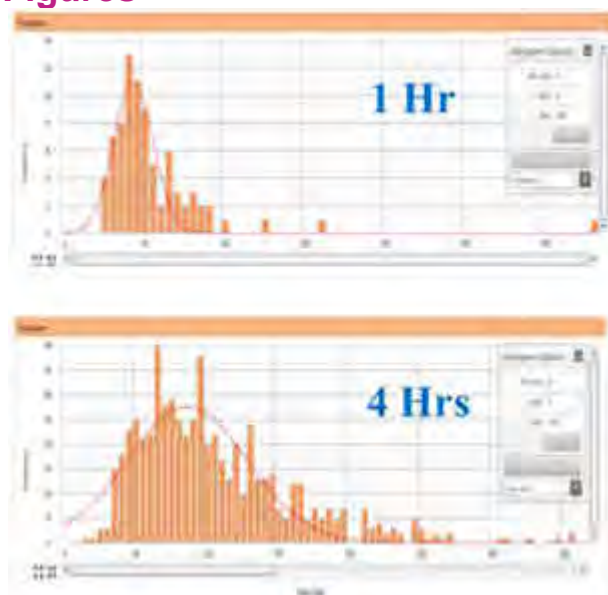


Figure 1. Platinum content distribution in A2780-CP70 ovarian cancer cell line exposed to 1 and 4 hours of Cisplatin.

Nanostructured electrochemical biosensors as fit-for-purpose analytical devices

Beatriz Prieto Simón^{1,2},

Keying Guo, Muamer Dervisevic, Clara Pérez Ràfols, Grace Chin, Katrin Tücking, Roshan Vasani, Nekane Reta, Maria Alba, Nicolas H. Voelcker²

¹ Department of Electronic Engineering, Universitat Rovira i Virgili, Avda. Països Catalans, 26, Tarragona, Spain

² Monash Institute of Pharmaceutical Sciences, Monash University, Melbourne, Australia

Beatriz.prieto-simon@urv.cat

Our research focuses on the development of novel fit-for-purpose electrochemical sensing tools, which exploit the use of chemically and mechanically stable synthetic materials to design nanostructured biosensors [1,2]. Materials that can easily tailor their electrochemical properties and morphological features (Figure 1), are highly desired.

Our recent research has led to the creation of the next generation of highly versatile electrochemical biosensing platforms by harnessing silicon fabrication and modification methods [3,4,5]. These novel structures feature major advantages for electrochemical analysis, such as high surface-to-volume ratio, unique charge transport properties, control over morphological features, even in multilayered configurations, and ease of surface modification and control of the electric properties.

We have produced arrays of nanoneedles intended to be used as wearable sensors, and porous membrane-based electrochemical biosensors that have been successfully used for the label-free detection of DNA, toxins and even whole viruses (Figures 2 & 3).

This new set of porous silicon-based nanostructures is designed to unlock new sensing paradigms and potentially achieve greater sensitivities and shorter analysis times, providing solutions for environmental, biosecurity and healthcare issues.

References

- [1] N. Reta, C.P. Saint, A. Michelmore, B. Prieto-Simón, N.H. Voelcker. ACS Appl. Mater. Interfaces, 10 (2018) 6055
- [2] G. Rajeev, B. Prieto-Simón, L.F. Marsal, N.H. Voelcker. Adv. Health. Mat., 7 (2018) 1700904
- [3] N. Reta, A. Michelmore, C. Saint, B. Prieto-Simón, N.H. Voelcker. Biosens. Bioelectron., 80 (2016) 47
- [4] D. Brodoceanu, R. Elnathan, B. Prieto-Simón, B. Delalat, T. Guinan, E. Kroner, N. Voelcker,

T. Kraus. ACS Appl. Mater. Interfaces, 7 (2015) 1160

- [5] K.-S. Tücking, R.B. Vasani, A.A. Cavallaro, N.H. Voelcker, H. Schönherr, B. Prieto-Simón. Macromol. Rapid Commun., (2018) 1800178

Figures

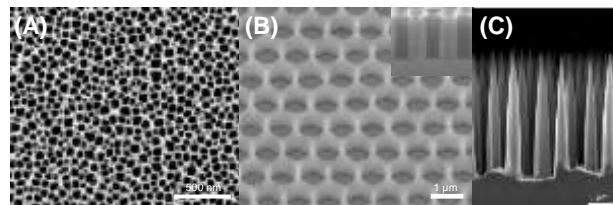


Figure 1. Porous silicon structures prepared by electrochemical anodisation (A), and metal-assisted chemical etching (B) and (C).

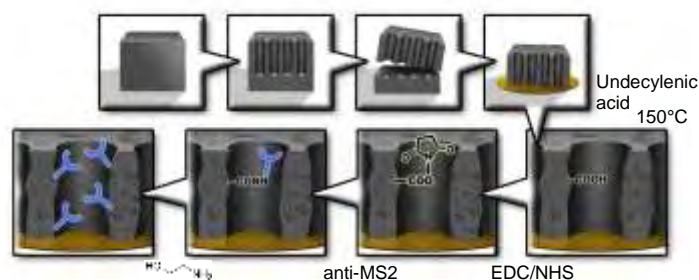


Figure 2. Fabrication and functionalisation of a porous silicon membrane-based immunosensing platform for the electrochemical detection of MS2 bacteriophage, used as model of enteric viruses.

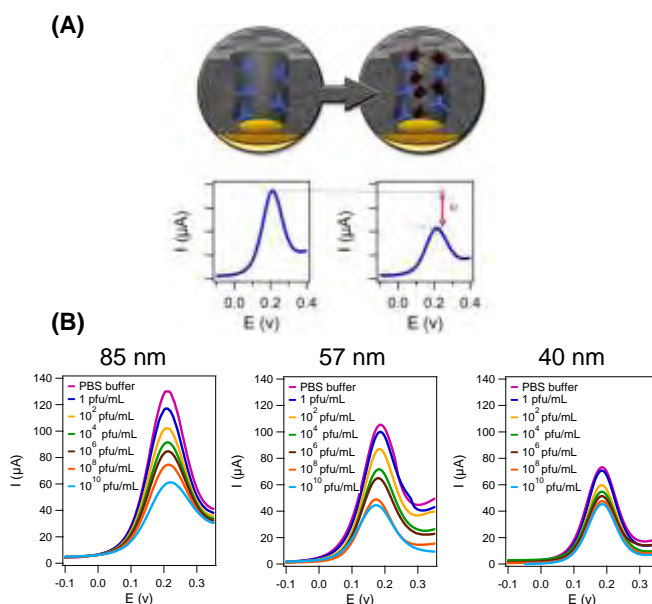


Figure 3. (A) Scheme of the sensing mechanism based on electrochemically measuring the partial nanopore blockage caused upon analyte binding. (B) Effect of the pore size of a porous silicon membrane attached onto a gold electrode, on the differential pulse voltammetry signal measured upon incubation of increasing concentrations of MS2 bacteriophage.

Enhancing anticancer activity of chemotherapeutics with antiangiogenic biodegradable nanoparticles

Claudia Conte¹, Francesca Moret², Diletta Esposito¹, Giovanni Dal Poggetto³, Concetta Avitabile¹, Francesca Ungaro¹, Alessandra Romanelli¹, Paola Laurienzo³, Elena Reddi², **Fabiana Quaglia**¹

¹ Department of Pharmacy, University of Napoli Federico II, Italy;

² Department of Biology, University of Padova, Italy;

³ Institute for Polymers, Composites and Biomaterials, CNR, Pozzuoli (Napoli), Italy
quaglia@unina.it

The formation of new blood vessels is fundamental for the supply of nutrients and oxygen to cancer cells and greatly contributes to tumor progression, invasion and metastasis [1, 2]. "Angiogenic switch" in tumors is strictly related to the secretion of pro-angiogenic factors such as Vascular Endothelial Growth Factor (VEGF). Over-expression of FLT1, a subtype receptor of VEGFR family, has been correlated with severe disease progression and poor prognosis, as well as metastasis and cancer recurrence in humans [3].

In the past thirty years, nanotechnology has been proposed as a valuable tool to target chemotherapeutics to solid tumors with the goal to improve response, to alleviate side effects as well as to overcome multidrug resistance. Polymeric nanoparticles (NPs) are in the limelight in cancer nanotechnology due to the advantages of prompt manipulation of the overall features (size, surface, release rate, biodegradability) through appropriate tailoring of the chemistry of building blocks. Here we combine the concept of limiting angiogenesis to the delivery of a lipophilic chemotherapeutic through multifunctional NPs with the final aim to ameliorate antitumor efficacy. To this purpose biodegradable NPs bearing an antiangiogenic anti-FLT1 hexapeptide on the surface and transporting Docetaxel (DTX) in the core were developed.

Amphiphilic diblock (DBL) poly(ϵ -caprolactone)-polyethyleneglycol (PCL-PEG₁₅₀₀) copolymers conjugated with an anti-FLT1 peptide (GNQWFI-NH₂) at PEG-OH end where synthesized and characterized. This copolymer was mixed in appropriate ratios with unmodified PCL-PEG to give core-shell NPs entrapping DTX by nanoprecipitation (Fig. 1). NPs of PCL-PEG were produced as control. NPs antiangiogenic properties were evaluated by endothelial tube formation assay in endothelial cells (HUVEC). Cytotoxicity was evaluated in a triple negative breast cancer cell line (MDA-MB-231). Finally, activity of NPs was tested in chicken embryo chorioallantoic membranes (CAMs) previously

xenografted with MDA-MB-231 cells. On 9-days old CAMs, MDA-MB-231 cell tumors were treated once a day, for a total of five days, with free DTX or loaded in NPs in the concentration of 1 μ M/day.

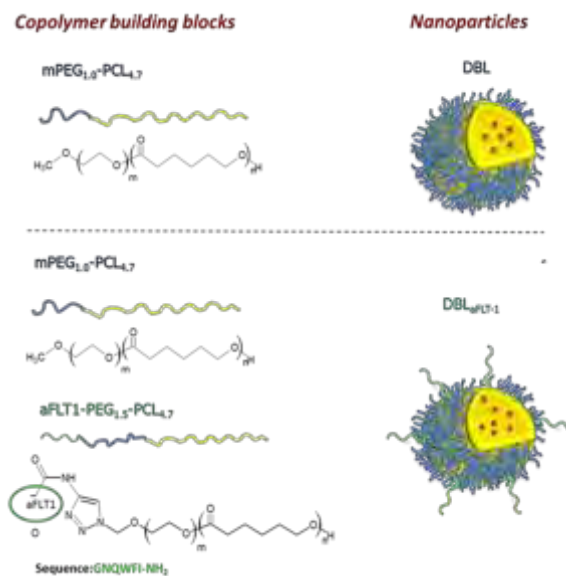


Fig. 1. Composition of NPs employed for the study.

Formulation parameters were selected to give NPs with a size around 100 nm and entrapping DTX with high efficiency, thus sustaining its release along time in simulated biological conditions. anti-FLT1 was partly confined to the surface of NPs and located amid PEG chains. A soft protein corona was formed around NPs in human serum.

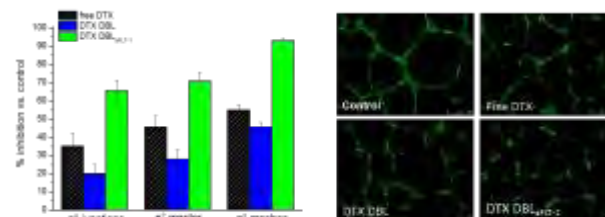


Fig. 2. In vitro tube formation assay in HUVEC cells. Representative images and summary of results on percent inhibition of tube formation after cell incubation for 16 h with 5 μ g/ml of DTX free or delivered in NPs.

anti-FLT1-NPs were internalized in HUVEC through VEGFR1 receptor and found more antiangiogenic than free peptide at equivalent peptide concentrations. Moreover, the loading of the chemodrug potentiated the inhibition of formation of properly conformed tubes in vitro (Fig. 2). Concerning cytotoxicity, DTX delivered by NPs showed a clear dose-dependent cell mortality in both HUVEC and MDA-MB-231, reaching 20% of cell survival after 72 h of treatment. Finally, we tested the formulations in MDA-MB-231 cells xenografted on CAMs. In this model,

antiangiogenic properties of anti-FLT1-NPs were found to be statistically comparable to free DTX, while an anticancer effect higher than that of free DTX and fully PEGylated NPs was found.

Taken together, these results point at anti-FLT1 NPs as a novel platform to potentiate anticancer activity of DTX in highly resistant triple negative breast cancer.

This work was supported by Italian Association for Cancer Research (IG2014 #15764).

References

- [1] Al-Abd AM, Alamoudi AJ, Abdel-Naim AB, Neamatallah TA, Ashour OM, J Adv Res., 8 (2017) 591-605.
- [2] Roudsari LC, West JL, Adv Drug Deliver Rev 97 (2016) 250-259.
- [3] Fischer C, Mazzone M, Jonckx B, Carmeliet P, Nat Rev Cancer, 8 (2008) 942-956.

Reversible monolayer-bilayer transition in supported phospholipid Langmuir-Blodgett films: morphological and nanomechanical behavior

Silvia Ruiz-Rincón^{1,2,5},
Alejandro González-Orive^{1,2}, Jesús M. de la Fuente^{3,4} and Pilar Cea^{1,2,5}

¹Organization, Address, City, Country (Arial 9)

¹Instituto de Nanociencia de Aragón (INA). Campus Río Ebro, Universidad de Zaragoza, C/Mariano Esquillor, s/n, 50018 Zaragoza, Spain.

²Laboratorio de Microscopias Avanzadas (LMA) Campus Río Ebro, Universidad de Zaragoza, C/Mariano Esquillor, s/n, 500018 Zaragoza, Spain.

³Instituto de Ciencia de Materiales de Aragón (ICMA), Universidad de Zaragoza-CSIC, 50009 Zaragoza, Spain

⁴Networking Biomedical Research Center of Bioengineering, Biomaterials and Nanomedicine (CIBER-BBN). Spain.

⁵Departamento de Química Física, Facultad de Ciencias, Universidad de Zaragoza, 50009, Zaragoza, Spain

sruiz@unizar.es

The Langmuir-Blodgett technique (LB) has been used to fabricate biomimetic lipid membranes in order to investigate in an easier way the lipid-lipid interactions and the processes that take place at the membrane level. With this aim, mixed monolayer LB films of 1,2-dipalmitoyl-sn-glycero-3-phosphocholine (DPPC) and cholesterol (Chol) in the 1:1 ratio have been prepared onto solid mica substrates by means of LB. Upon immersion in water or in an aqueous HEPES solution (pH 7.4) the monolayer LB films were spontaneously converted into well-organized bilayers leaving free mica areas in between [1]. The process has been demonstrated to be reversible upon removal of the aqueous solution resulting thus in remarkably free of defects monolayers. The latter process has been summarized in Figure 1. In addition, the nanomechanical properties exhibited by the as-formed bilayers have been determined by means of AFM breakthrough force studies which allow studying the local properties of the mimic membranes in a quantitative way with the possibility of controlling the environmental conditions [2]. The bilayers formed by immersion of the monolayer in an aqueous media exhibit nanomechanical properties and stability under compression analogue to those of DPPC:Chol supported bilayers obtained by other methods previously described in the literature [3]. Consequently, the hydration of a monolayer LB film has been revealed as an easy method to produce well-ordered bilayers that mimic the cell membrane and that could be used then as model cell membranes.

References

- [1] Ruiz-Rincón, S.; González-Orive, A.; de la Fuente, J.M.; Cea, P. *Langmuir* **2017**, *33*, 7538-7547
- [2] Dufrene, Y.F.; Martinez-Martin, D.; Medalsy, I.; Alsteens, D.; Muller, D.J. *Nat Meth* **2013**, *10*, 547-854
- [3] Lima, L.; Gianotti, M.I.; Redondo-Morata, L.; Vale, M.; Marques, E.F.; Sanz, F. *Langmuir* **2013**, *29*, 9352-9361

Figures

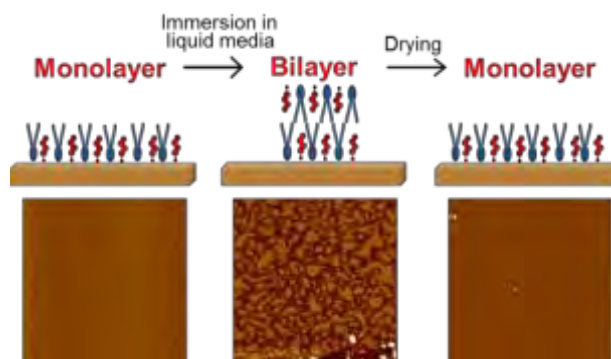


Figure 1. Scheme of the reversible transition from monolayer to bilayer and subsequent transition to monolayer after drying.

I+Med S. Coop. an innovative company in the field of controlled delivery

Virginia Saez-Martinez¹,

Raul Perez, Manu Muñoz, Sergio Cadierno, Iñaki Lopez²

^{1,2}i+Med, Albert Einstein 15, nave15, Parque Tecnológico de Álava, 01510 Miñano, SPAIN

vsaez@imasmed.com

Abstract

I+Med, the Company

i+Med is an innovative and technologically company established in 2014 and structured as a cooperative, in the field of development and commercialization of biomedicine solutions based on nanohydrogels for the controlled release of drugs, vitamins, growth factors and other compounds of interest. Within its business objectives, it also intends to develop new production methods, adapted to new technologies. i+Med has an innovative character and can design, develop and manufacture new products in the field of biomedical engineering, thanks to the research expertise of the team and their experience not just in the development of the product and manufacture but also in the quality assurance and medical device certification.

In i+Med we develop our own products and also we develop drug products and medical devices for third parties in the field of encapsulation, vehiculization and controlled release based on our technologies. The company is the owner of two patents about nanogels for biomedical applications, and manufactures medical devices with CE Mark and following the European regulation 2017/745. We are certified and manufacturers by the Spanish Agency of Drugs and Medical Devices (AEMPS).

Competitive Advantages

Development of different types of polymeric matrices that can integrate many properties in one product:

- Time: less recovery time of the patient
- Usability: Easy to use
- Packaging: ergonomic, safe.
- Morphology/structure/formulation: adaptable polymers depending on final application
- Patient/final user: Better recovery, improvement in quality of life
- Ratio cost/profit: profitable.
- controlled release of drugs over conventional pharmacological treatments: greater control of the dose (quantity and frequency), prevents overdoses, increases the effectiveness of the treatment and minimizes the side effects, the periods of treatment and monitoring of the patient and the pharmaceutical expenditure.

Our R+D projects / research lines

Four selected projects are described herein:

1.- Biomimetic nanohydroxyapatite (nHAp): (Fig.1)
nHAp is a natural mineral produced by the organism. I+Med has applied a synthesis method that mimics the physiologic biosynthesis conditions to get biomimetic nanoparticles avoiding toxic residues. The product will be used as active ingredient with remineralizing and antibacterial properties to be applied in Odontology. The main properties apart from the nanometric size that helps to get better into the inner layers of the enamel, is their spherical shape to increase the biocompatibility.

2.- Long-lasting eye drops: (Fig 2)

I+Med has developed long-lasting eye drops to treat dry eye syndrome. They are made of a viscoelastic hydrogel formulation with highly mucoadhesive properties that extend the treatment up to 12 hours. These drops have humectant and lubricating properties and also release in a controlled way a natural antiinflammatory ingredient, the ectoin. The innovative packaging avoids the use of preservatives that can affect negatively the ocular surface in chronic treatments.

3.- Therapeutic coatings for advanced biomedical products: (Fig.3)

Biodegradable polymeric coatings with controlled load and release properties of antibiotic ingredients in cardiac stimulating devices (CEDs o pacemakers). The risk of post-surgical infections and the need to remove the implanted device is the origin of this project.

It is based in the combination of hydrogels technology combined with anchoring monolayers covalently bonded to the surface of the device, to get a protective physical barrier against bacteria and biofilm formation, with hydrophilic character and controlled release properties to prevent from potential post-surgical infections.

The coatings are characterized by ATR-FTIR, NMR, XPS, electronic microscopy, contact angle, biocompatibility, etc.

4.- Ophthalmic Viscoelastic Device (OVD): (Table 1)

Our own product developed for ophthalmic surgeries, such as cataracts to be used as replacement of aqueous humour. It is made of high molecular weight Hyaluronic acid solution at specific concentrations to get the required viscoelastic properties

Figures

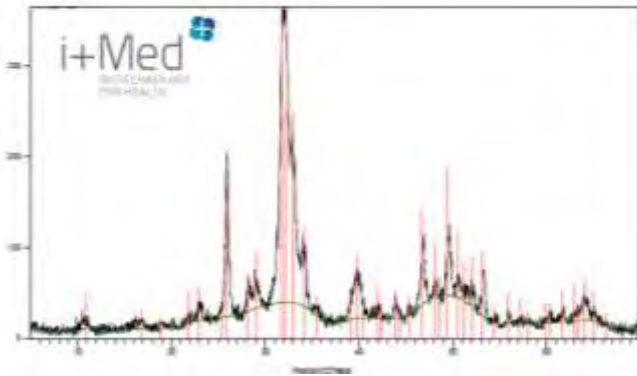


Figure 1. XRD spectra of the obtained nHAP

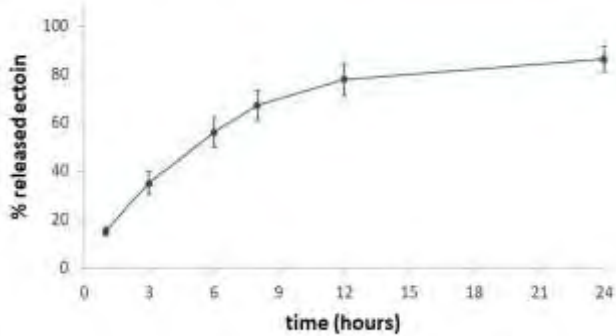


Figure 2. In vitro release profile of the ectoin for 24h. In 6h 50% of the total amount is released, and a 75-80% in the first 12h.



Figure 3. Contact angle measurement of a flat sample coated (left) and uncoated (right): a decrease in contact angle after coating is observed, which means an increase in wettability.

MODEL	OpHLiNE 1.4%	OpHLiNE 2%	OpHLiNE 3%	Method (ref)
VISCOSITY (cP)*	15 000 - 25 000	40 000 - 40 000	180 000 - 220 000	Ph. Eur. method 2.2.10
pH	7.2 - 7.6	7.2 - 7.6	7.2 - 7.6	Ph. Eur. method 2.2.3
CHARGALITY	250-330mOsm/kg	280-400mOsm/kg	280-400mOsm/kg	Ph. Eur. method 2.2.25
VOLUME	1.2 ml	1.2 ml	1.2 ml	
CONTAINER	270 Luer lock Capsula	250 Luer lock Capsula	250 Luer lock Capsula	
STERILIZATION	Heat treat			
STERILITY CONTROL	Sterile product			Ph. Eur. method 2.6.3
BIOBURDEN	Aerobic: <500FC/ml Anaerobic: <500FC/ml Fungi and yeasts: <500FC/ml			Ph. Eur. method 2.6.12
ENDOTOXIN	Less than 0.5EU/ml			Ph. Eur. method 2.6.14
BIOCOMPATIBILITY	Biocompatible product			ISO 10993
SELF LIFE	2 years			
STORAGE	Protect from light and avoid freezing. Store between 5°C and 25°C.			

Table 1. Properties of the different models of OpHLiNE product.

Multicellular spheroids as novel tools for the evaluation of melanoma nano-vaccines and BRAF-MEK-targeted nanomedicines

Anna Scomparin¹,

Sabina Pozzi¹, Eilam Yeni¹, Joao Conniot²,
Shani Koshrovski¹, Evgeni Pisarevsky¹,
Helena F. Florindo², Ronit Satchi-Fainaro¹

¹Department of Physiology and Pharmacology, Tel Aviv University, Israel

²Research Institute for Medicines (iMed.U LISBOA), University of Lisbon, Portugal

Anna.scomparin@gmail.com

The development of BRAF inhibitors (BRAFi) targeting the V600E mutation in the BRAF gene, and their use in combination with MEK inhibitors (MEKi) result in a marked improvement compared to the monotherapy of BRAFi¹. In parallel, immune checkpoint therapy significantly enhanced the clinical outcome of melanoma treatment compared to standard therapy². However, results are far from the initially expected, mainly due to the complex mechanisms behind anti-tumor immunity and cancer resistance. The combination of complementary approaches, such as cancer nano-vaccines, immune checkpoint modulators and BRAF and MEK - targeted nano-sized drugs can improve the clinical outcome. The pre-clinical development of these therapies suffers from the lack of proper metastatic melanoma immunocompetent models to predict their behaviour in clinical settings. Therefore, we developed a spheroid model formed of BRAF-mutated melanoma cells and their microenvironment to evaluate the effect of the developed combinational therapies.

In our study, C57BL/6 mice were immunized with 3 weekly injections of poly(lactic-co-glycolic acid) and poly(lactic acid)-based cancer nano-vaccine bearing antigenic peptides. The splenocytes were isolated following an immunization protocol. Multicellular spheroids were obtained using the hanging-drop method³, with mCherry-labeled D4M.3A murine melanoma, astrocytes and GFP-labelled endothelial cells isolated from C57BL/6 mice. Spheroids were then embedded in reduced matrigel in the presence and in the absence of splenocytes isolated either from healthy naïve, immunized, or D4M.3A subcutaneous tumor-bearing C57BL/6 mice, seeded in a 96-well plate and treated with monotherapy or combination of immune checkpoint modulators, poly(lactic-co-glycolic acid)-based nanoparticles

bearing BRAFi and MEKi or poly(glutamic acid)-based polymer therapeutic bearing BRAFi and MEKi.

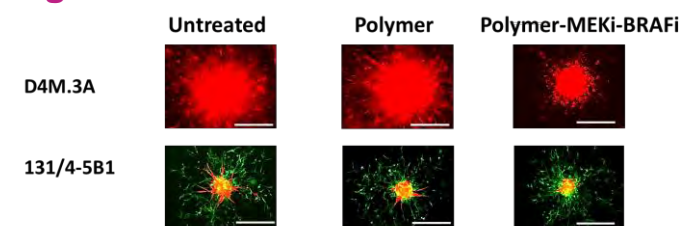
We obtained spheroids mimicking the primary tumors with BRAF-mutated D4M.3A cells and stromal cells and evaluated the inhibition of sprouting and invasion in the presence of different targeted monotherapies and combinations of polymeric nanomedicines. All the different spheroids were embedded in matrigel containing splenocytes isolated from immunized, naïve or melanoma-bearing mice. Endothelial sprouting and cancer cell invasion were inhibited following treatment with immune checkpoint modulators and targeted therapy combinations. Confocal analysis of spheroids 48 hours after treatment allowed for the identification of the morphological and migration properties of the cancer cells, and for the identification of the different subpopulations of T cells, immune checkpoint receptors and their response to treatment.

We developed a method to efficiently evaluate and screen combinational therapies for primary and metastatic melanoma treatment. We hope this method will enable us to accurately predict the response to treatment, while reducing the number of mice required for the preclinical evaluation of polymeric precision nanomedicines.

References

- [1] Spagnolo, F.; Ghiorzo, P.; Orgiano, L.; Pastorino, L.; Picasso, V.; Tornari, E.; Ottaviano, V.; Queirolo, P. *OncoTargets and therapy* 2015, 8, 157-168.
- [2] Alexander, W. *Pharmacy and Therapeutics* 2016, 41, (3), 185-191.
- [3] Ferber, S.; Tiram, G.; Sousa-Herves, A.; Eldar-Boock, A.; Krivitsky, A.; Scomparin, A.; Yeini, E.; Ofek, P.; Ben-Shushan, D.; Vossen, L. I.; Licha, K.; Grossman, R.; Ram, Z.; Henkin, J.; Ruppin, E.; Auslander, N.; Haag, R.; Calderón, M.; Satchi-Fainaro, R. *eLife* 2017, 6, e25281.

Figures



mCherry-cancer cells; Astrocytes; Microglia; GFP-Brain endothelial cells. Scale bar 400 μm

Figure 1. Biodegradable polymer-drug conjugate bearing BRAFi + MEKi inhibits murine and human melanoma cell sprouting

Engineered Combinations of Nitric Oxide Photoreleasers with Doxorubicin as Innovative Strategy to Overcome Multidrug Resistance

Salvatore Sortino¹,

Aurore Fraix,¹ Konstantin Chegaev,² Elena Gazzano,³ Gamal Eldein F. Abd-Ellatef,³ Marco Blangetti,² Chiara Riganti,³ Roberta Fruttero,² Alberto Gasco²

¹Laboratory of Photochemistry, Department of Drug Sciences, University of Catania, I-95125 Catania (Italy).

²Department of Drug Science and Technology, University of Torino, 10125 Torino (Italy).

³Department of Oncology, University of Torino, Via Santena 5/bis, I-10126 Torino (Italy)

ssortino@unict.it

Nitric oxide (NO) is a small, inorganic free radical that plays a multiple role in human physiology and pathophysiology.^[1] NO is involved in a number of biological processes, such as vasodilation, platelet aggregation, neurotransmission, and macrophage-mediated immunity. NO plays also a key role in tumour biology where it displays either stimulatory or inhibitory effects on cancer progression and metastasis. These effects are strictly depending on several factors including concentration and dose.^[2] NO-donors are products that can release NO under physiological conditions, and that can consequently be used as NO-prodrugs. Classical NO-donors, such as *S*-nitrosopenicillamine, and *S*-nitrosoglutathione were able to reduce the efflux of the anticancer drug Doxorubicin (DOX) in human cancer cells.^[3] The mechanism responsible for this effect is the nitration of critical tyrosine residues of P-gp, ABCB1, and MRPs/ABCCs transporters. On these bases, new DOX derivatives have been proposed in which moieties containing NO-releasing groups are covalently linked to DOX. Some of these products can overcome multidrug resistance (MDR) by inhibiting the ABC transporters that extrude the drug. However, these NO donors have different NO release kinetics, and spatiotemporal control is totally lacking. This makes it necessary to use high concentrations of the NO donors and prolong their incubation time to reach an intracellular concentration sufficient for protein nitration. Light is a powerful and minimally invasive “microsyringe” for the injection of NO into biological systems, with excellent spatiotemporal accuracy, using suitable NO photodonors (NOPs).^[4,5] These compounds must satisfy several prerequisites for bio-application, including excitation with visible light, and formation

of non-toxic and non-visible-light-absorbing side photoproducts.

In this contribution, we report engineered combination of NOPs with DOX as such, covalently linked or delivered through polymeric nanoparticles as innovative strategy to overcome the main drawbacks of DOX. We show that photoregulation of NO release at doses not toxic to cells, but able to inhibit several efflux pumps that are mainly responsible for MDR, may be a suitable approach not only to potentiate the anticancer activity of DOX, but also to reduce its toxicity towards healthy cells such as cardiomyocytes and fibroblasts (Figure 1).

References

- [1] Ignarro, L. J. Nitric Oxide: Biology and Pathobiology, 2nd ed.; Elsevier Inc., (2010).
- [2] Fukumura, D.; Kashiwagi, S.; Jain, R. K. Nat. Rev. Cancer, 6 (2006) 521.
- [3] Riganti, C.; Miraglia, E.; Viarisio, D.; Costamagna, C.; Pescarmona, G.; Ghigo, D.; Bosia, A. Cancer Res., 65 (2005) 516.
- [4] Sortino, S. Chem. Soc. Rev., 39 (2010) 2903.
- [5] Sortino, S. J. Mater. Chem., 22 (2012) 301.

Figures

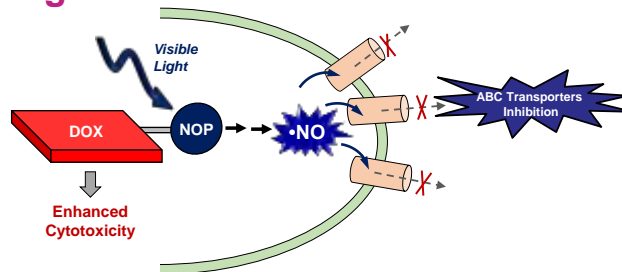


Figure 1. Potentiated anticancer activity of DOX through release of NO from NOP regulated by visible light stimuli.

Development of a non-invasive breath test for early diagnosis of tropical diseases “TROPSENSE”

D.Ulieru¹,

Oana-Maria Ulieru¹, Xavi Vila¹, A.Topor¹, F.Babarada²

¹SITEX 45 SRL, 114, Ghica Tei Blvd, Bl.40, AP.2, Dept.2, Bucharest

² Bucharest Polytechnica University, Splaiul Independenței nr. 313, Sector 6, Bucharest, Romania
ulierud@yahoo.com

Tropical illnesses are frequent infections in tropical and subtropical regions from Africa, Asia and America, that affect specially to low-income persons in developing countries, while in Europe only affect to turist that travel to these zones. The study is focused to investigate hidatidosis, leishmaniosis and dengue, all of them included in the 17 deseases not attended by the World Health Organisation.

The research will be based in analysis of breath samples, easy to obtain and don't represent any discomfort or risk for the patient's health. For this project will be taken samples from pacients already diagnosed with one of these illnesses and from pacients with other tropical diseases to establish the control group. Analysis will be done through chemical analytic processes to identify biomarkers. After this will be developed chemical steam sensors with hight affinity, selecting the most appropriate sensible nanomaterials. Researchers will analyse different techniques (resistive sensors, transistors, sensors to mesure changes in weight, infrared spectroscopy, etc) and finally will be developed one integrated prototype using the best techniques. During the last six months the prototype will be tested in different hospitals from Africa and America. This project aims at demonstrating the feasibility of a non-invasive, safe and patient-friendly methodology for on-site rapid diagnosis of tropical diseases. The proposed approach is based on breath samples analyses, which are easy to obtain and present no discomfort or risk for patients health. In this study will be enrolled patients with three different types of neglected tropical diseases (Hydatidosis, Leishmaniosis and Dengue) from different geographical locations (Europe, South America and Maghreb). Breath sampling will follow a standardised procedure. Analytical chemistry methods will be employed for the identification of the breath volatile biomarkers of these diseases. A pool of potential nanomaterials with high affinity towards the identified VOCs will be selected (e.g., gold nanoparticles, carbon nanotubes and semiconducting nanowires, either pristine or functionalised with selected hydrophobic organic molecules and/or biomolecules).

For maximising the possibility of success of our methodology, we will investigate the synergic effect of

different advanced and complementary chemical sensing techniques: Mid-Infrared Quantum Cascade Laser

spectroscopy and different types of Chemical Gas Sensors devices. These techniques are particularly attractive, since they can be miniaturised and are suitable for building on-site portable systems. Advanced pattern recognition algorithms will be employed for building discriminative models for the identification of the fingerprints of the different tropical diseases studied, and multisensors data fusion will be then applied for obtaining enhanced resulyts. A point of care prototype will be proposed on the basis of the results obtained and validated on-site.

By our deeply involvement as system integrator of TROPSENSE device under Marie-Curie H2020 project have performed successfully also following objectives :

1. To develop a non-invasive and safely methodology for the early and fast diagnosis of tropical deseases
2. The simptoms of these diseases are difficult to identify. The main project's objective is to obtain a fast tool, inexpensive, portable, non-invasive and easy to use for the diagnosis of these deseases.

Figures



Figure 1. Analysis of breath samples composition



Figure 2. Schematic representation of the point-of-care prototype



Posters

Bacterial nanocellulose as a cell culture platform

Irene Anton-Sales

Soledad Roig-Sánchez, Anna Laromaine, Anna Roig

¹Institute of Materials Science of Barcelona
Campus de la UAB, Bellaterra, Spain

Contact: ianton@icmab.es

Nanocelluloses are cellulosic products with at least one dimension in the nanoscale. Nanocellulose can be extracted from natural sources like wood, cotton or algae but it can also be directly produced by microorganisms [1].

Bacterial nanocellulose (BNC) is a biopolymer naturally synthesized and secreted by *Komagataeibacter xylinus* that forms a 3D-network of pure cellulose nanofibres (Image 1) resembling the structure of collagen. BNC exhibits attractive properties for biomedical applications such as high liquid holding capacity, high tensile strength, flexibility and porosity [2]. On the other hand, there are still a limited number of natural biomaterials that meet all the requirements to fit in the regenerative medicine settings. Thus, our goal is to develop versatile and portable supports based on BNC for cell-manipulation, envisioning regenerative medicine applications.

The BNC pellicles were obtained after 3-day static cultures of *Komagataeibacter xylinus*. The BNC films were then thoroughly washed and autoclaved (Image 2b) before being used for culturing human dermal fibroblasts. When appropriate, BNC was functionalized with TiO₂ nanoparticles by a microwave-assisted method [3]. Attachment, morphology, distribution and growth kinetics of cells cultured on these BNC-based supports were studied by cell viability assays and confocal microscope imaging.

Firstly, structural characterization of BNC and BNC functionalized with TiO₂ nanoparticles (BNC/TiO₂) will be presented. Then, we will show in detail that both BNC and BNC/TiO₂ films support the attachment and proliferation of human dermal fibroblasts (Image 2c). Growth kinetics on BNC substrates is very similar to that on culture plates with the advantage of representing a transportable platform for adherent cells. Moreover, cell morphology studies showing that fibroblasts exhibit their expected phenotype on BNC and BNC/TiO₂ substrates (Image 2a) will be presented. Altogether, our data point out that BNC is a promising and versatile biomaterial to be used i.e. as a cell carrier in cell transplantation therapies and that BNC

functionalization with model functional nanoparticles (TiO₂) does not alter its properties.

References

- [1] Klemm D, Cranston ED, Fischer D, Gama M, Kedzior SA, Kralisch D, et al., *Mater Today*, 7 (2018) 720-748
- [2] De Oliveira Barud HG, da Silva RR, da Silva Barud H, Tercjak A, Gutierrez J, Lustrri WR, et al., *Carbohydr Polym*, 153 (2016) 153:406–20
- [3] Zeng M, Laromaine A, Feng WQ, Levkin PA, Roig A., *J Mater Chem C*, 31 (2015) 6312-8

Figures

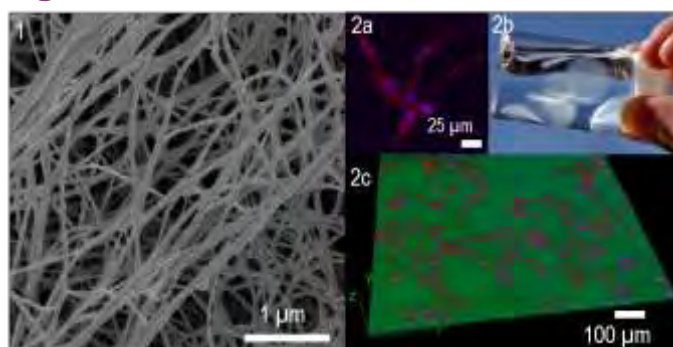


Figure: Image 1 shows a scanning microscope image of the bacterial nanocellulose fibres. Image 2a and 2c depict human dermal fibroblast growing on top of bacterial nanocellulose substrates at different magnifications under confocal microscope. 2b corresponds to a digital picture of the bacterial nanocellulose hydrogels used in our research.

Effect of enzyme type, quantity and distribution on the motion behavior of microswimmers

Xavier Arqué¹,

Tania Patiño¹, Natalia Feiner¹,
Lorenzo Albertazzi^{1,4}, Samuel Sánchez^{1,3}

¹ Insitut de Bioenginyeria de Catalunya (IBEC), Baldiri i Reixac 10-12, Barcelona, Spain

² Department of Biomedical Engineering, Institute for Complex Molecular Systems (ICMS), Eindhoven University of Technology, Eindhoven, The Netherlands

³ Institució Catalana de Recerca i Estudis Avançats (ICREA), Pg. Lluís Companys 23, Barcelona, Spain

xarque@ibecbarcelona.eu
tpatino@ibecbarcelona.eu
ssanchez@ibecbarcelona.eu

Biocatalytic micro- and nanoswimmers are able to navigate due to the enzymatic conversion of substrates into products.¹ Biocatalysis offers a unique combination of properties, such as biocompatibility, bioavailability and versatility, making it greatly appealing for certain biomedical applications.² However, to make these implementations feasible, a deeper understanding on the fundamental aspects that rule self-propulsion is still required. We have focused our research on the role of the enzyme type, quantity and distribution.

In order to achieve active motion, asymmetry has been claimed to be crucial³, yet an enhanced Brownian diffusion (self-propulsion) has been reported for non-Janus nanoparticles.⁴ In this project, the effect of enzyme quantity and distribution was investigated with stochastically optical reconstruction microscopy (STORM) to detect single enzymes on polystyrene microswimmers with and without an outer silica surface.⁵ The binding efficiency was observed to be significantly higher on the rough silica, although both present a non-homogeneous enzyme distribution. This was correlated with the propulsive force measured using optical tweezers and the speeds produced by these forces, which were obtained through optical tracking.

We also tested the capacity of different enzymes to study the versatility of such systems. Acetylcholinesterase (AChE), glucose oxidase (GOx) and aldolase (ALS) were used to propel hollow silica microcapsules and the motion behavior was compared with microswimmers powered by urease (UR). The motion behavior appeared to be strongly dependent on the enzyme type and its intrinsic properties. The different enzymes are studied to elucidate what are the relevant enzymatic parameters ruling self-propulsion. Among these properties, the catalytic rate appeared to be a key factor for the generation of active motion, which was

further confirmed by exposing urease microswimmers to a competitive reversible inhibitor. These results provide new insights on the underlying mechanism of active motion and on the intelligent design of enzymatic micro- and nanoswimmers.

References

- [1] (1) Ma, X.; Hortelão, A. C.; Patiño, T.; Sánchez, S. Enzyme Catalysis To Power Micro/Nanomachines. *ACS Nano* 10 (2016) 9111–9122.
- [2] (2) Hortelão, A. C.; Patiño, T.; Perez-Jiménez, A.; Blanco, À.; Sánchez, S. Enzyme-Powered Nanobots Enhance Anticancer Drug Delivery. *Adv. Funct. Mater.* 28 (2018) 1705086.
- [3] (3) Golestanian, R.; Liverpool, T. B.; Ajdari, A. Propulsion of a Molecular Machine by Asymmetric Distribution of Reaction Products. *Phys. Rev. Lett.* 94 (2005) 1–4.
- [4] (4) Dey, K. K.; Zhao, X.; Tansi, B. M.; Méndez-Ortiz, W. J.; Córdova-Figueroa, U. M.; Golestanian, R.; Sen, A. Micromotors Powered by Enzyme Catalysis. *Nano Lett.* 15 (2015) 8311–8315.
- [5] (5) Patiño, T.; Feiner-Gracia, N.; Arqué, X.; Miguel-López, A.; Jannasch, A.; Stumpp, T.; Schäffer, E.; Albertazzi, L.; Sánchez, S. Influence of Enzyme Quantity and Distribution on the Self-Propulsion of Non-Janus Urease-Powered Micromotors. *J. Am. Chem. Soc.* 140 (2018) 7896–7903.

Figures

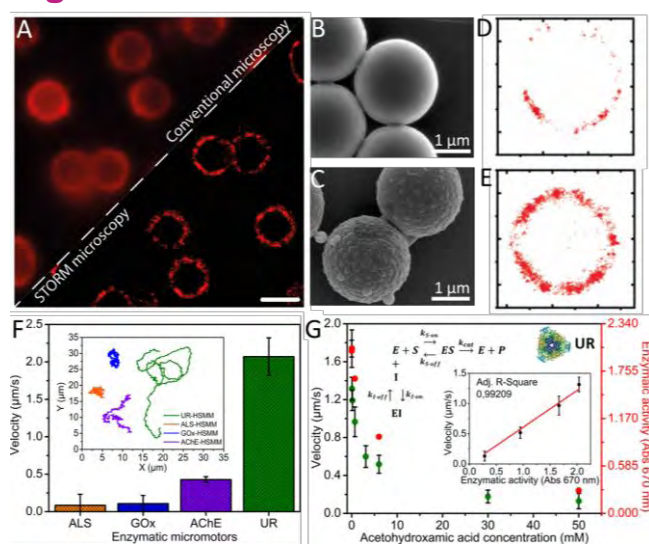


Figure 1. A) Comparison between the conventional fluorescence and STORM images. SEM micrographs of B) PS- and C) PS@SiO₂-microswimmers. STORM single-molecule detection of urease on the D) PS- and E) PS@SiO₂-microswimmers' surface. F) Average velocities of different enzymatic microswimmers. Inset: Representative tracking trajectories of the microswimmers. G) Average velocity of urease microswimmers, extracted from the MSD analysis, for different inhibitor concentrations with substrate (urea) present in excess (500 mM). Inset: Correlation of velocity with enzymatic activity depending on inhibition.

Ultrastructural Imaging of *Salmonella*–Host Interactions Using Super-resolution Correlative Light-Electron Microscopy of Bioorthogonal Pathogens

Thomas Bakkum^{1#},

D.M. van Elsland^{2#}, S. Pujals^{3#}, A.J. Koster², L. Albertazzi³, and S.I. van Kasteren¹

¹Leiden Institute of Chemistry and The Institute for Chemical Immunology, Leiden University Einsteinweg 55, 2333 CC, Leiden, The Netherlands

²Department of Cell and Chemical Biology and the Institute for Chemical Immunology Leiden University Medical Center LUMC Einthovenweg 22, 2333 ZC, Leiden, The Netherlands

³Department of Nanoscopy for Nanomedicine Institute of Bioengineering of Catalonia (IBEC) Barcelona Institute of Science and Technology 08028, Barcelona, Spain

#These authors contributed equally to this work

t.bakkum@lic.leidenuniv.nl

The imaging of intracellular pathogens inside host cells is complicated by the low resolution and sensitivity of fluorescence microscopy and by the lack of ultrastructural information to visualize the pathogens. Herein, we present a new method to visualize these pathogens during infection that circumvents these problems: by using a metabolic hijacking approach to bioorthogonally label the intracellular pathogen *Salmonella typhimurium* and by using these bioorthogonal groups to introduce fluorophores compatible with stochastic optical reconstruction microscopy (STORM) and placing this in a correlative light electron microscopy (CLEM) workflow, the pathogen can be imaged within its host cell context with a resolution of 20 nm. This STORM-CLEM approach thus presents a new approach to understand these pathogens during infection^[1].

References

- [1] D.M. van Elsland, S. Pujals, T. Bakkum, E. Bos, N. Oikomeas-Koppas, I. Berlin, J. Neefjes, A.H. Meijer, A.J. Koster, L. Albertazzi and S.I. van Kasteren, ChemBioChem, 19 (2018) 1766-1770

Figures

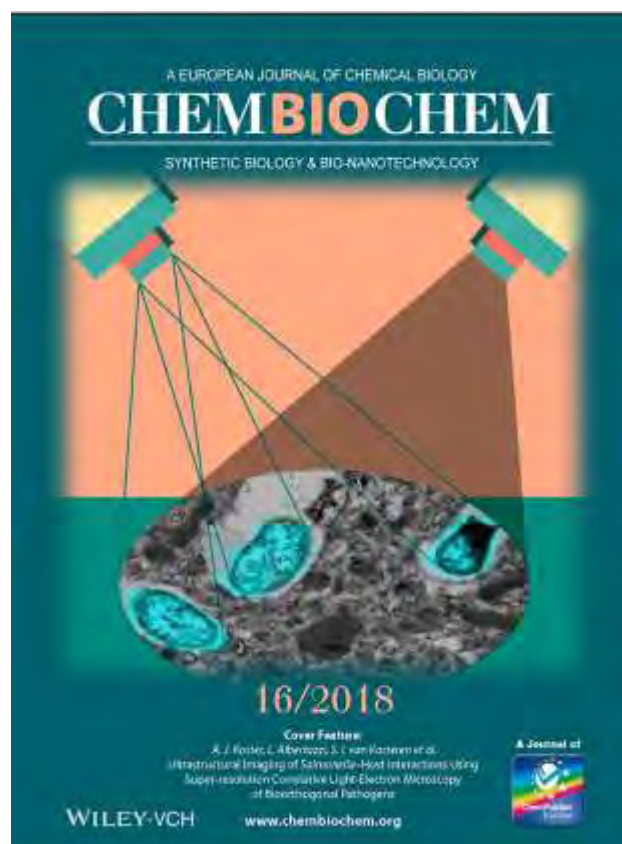


Figure 1. Cover feature of publication.

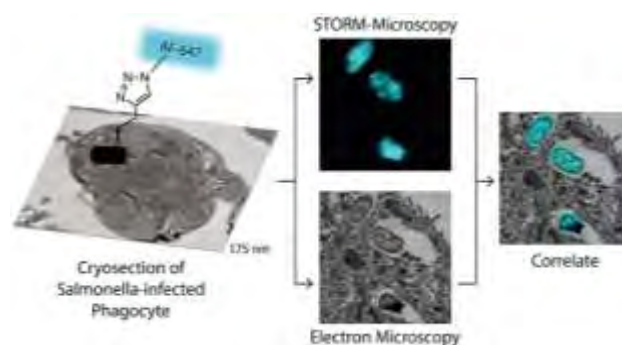


Figure 2. Graphical illustration of the newly developed STORM-CLEM technique on bioorthogonally labeled pathogenic bacteria, inside host immune cells.

MicroRNAs EXPRESSION CHANGES ASSOCIATED TO LONG TERM NANOMATERIALS EXPOSURE

Sandra Ballesteros¹, Ricard Marcos, Alba Hernández²

¹Grup de Mutagènesi, Departament de Genètica i de Microbiologia, Facultat de Biociències, Universitat Autònoma de Barcelona, Bellaterra, Spain
²CIBER Epidemiologia y Salud Pública, ISCIII, Spain

Sandra.ballesteros@uab.cat

Nanotechnology is an emerging field that predicts good perspectives in many biomedical or industrial applications. For this reason, the presence of nanoparticles in the environment is spectacularly rising and thus the human exposure. Therefore, we have to make a deep research on the action of these nanoparticles to achieve a better understanding of their exposure associated risks in regard to human's health.

MicroRNAs (miRs) are small non-coding single-strand RNA molecules of 20-24 nucleotides-long, which main function is posttranscriptional regulation of gene expression. They participate in numerous biological processes, such as cancer, inflammatory processes, etc. Consequently, changes in their expression can serve as biomarkers for early detection of tumoral phenotype.

The main objective of this study is to establish if there are expression changes in a battery of microRNAs related to cancer and other processes that can lead cell stress after an in vitro long-term low-dose exposure to nanomaterials. We choose these methodologies (long-term, low doses) to try to get closer to what happens in reality. In addition, cell transformation caused by the nanomaterials used was proven by previous long-term exposure studies. For that purpose, Human lung epithelial BEAS 2B cells were exposed chronically during different times and doses to different nanomaterials, specifically, titanium dioxide nanoparticles (nano-TiO₂) and multi walled carbon nanotubes (MWCNT). Then, the cells were collected before and after the tumoral-like phenotype acquisition and changes in the microRNAs expression were evaluated by qPCR technique. This study revealed changes in the microRNAs expression during the long term exposure and at the different doses.

In conclusion, some of the microRNAs evaluated are not useful as biomarkers. Nevertheless, some others show different microRNA expression before and after the acquisition of the tumoral-like phenotype. Therefore, we propose that they can be useful biomarkers for the establishment of tumoral-like phenotype or as exposure biomarkers.

References

- [1] Vales, G., Rubio, L. and Marcos, R., Journal of Hazardous Materials, Genotoxic and cell-transformation effects of multi-walled carbon nanotubes (MWCNT) following in vitro sub-chronic exposures (2015) 306: 193-202.
- [2] Vales, G., Rubio, L. and Marcos, R., Nanotoxicology, Long-term exposure to low doses of titanium dioxide nanoparticles induce cell transformation, but not genotoxic damage in BEAS-2B cells (2015) 9(5): 568-578.
- [3] Ha, M., and V. N. Kim., Nat Rev Mol Cell Biol, Regulation of microRNA biogenesis (2014) 15: 509-24
- [4] Castro, D, et al., Oncotarget, MicroRNAs in lung cancer (2017) Vol. 8, (No. 46), pp: 81679-81685

Figures

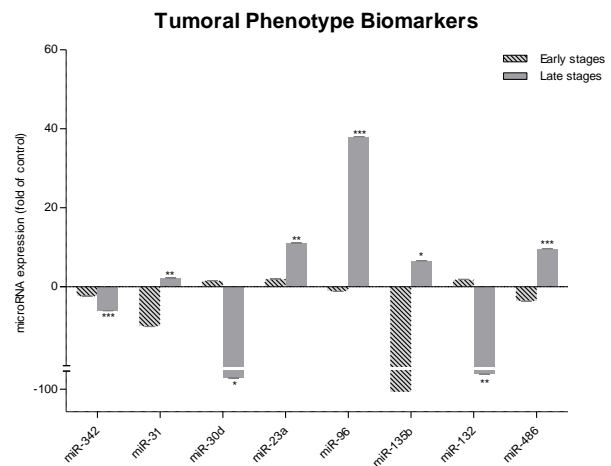


Figure 1. MicroRNA expression changes of cells treated with TiO₂-NPs with significant changes in the late stages, indicating the transformation process. P [0'01,0'05]; **P [0'001,0'01]; *** P [0, 0'001].

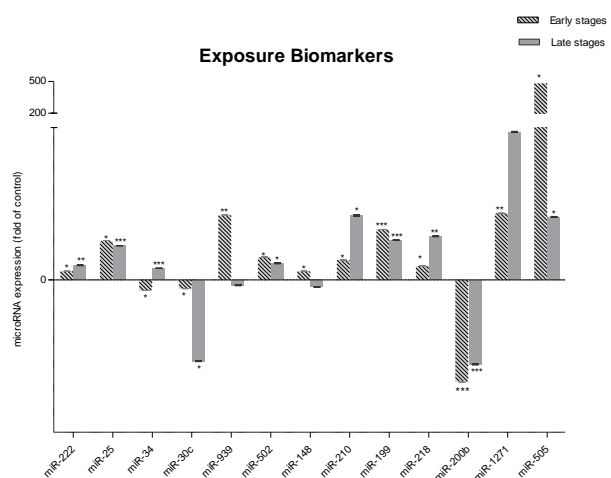


Figure 2. MicroRNA expression changes of cells treated with TiO₂-NPs with significant changes since early stages, indicating being sensitive to the NM exposure. P [0'01,0'05]; **P [0'001,0'01]; *** P [0, 0'001].

Tumoral Phenotype Biomarkers

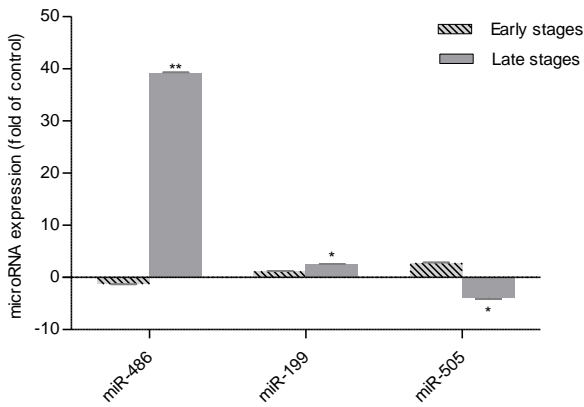


Figure 3. MicroRNA expression changes of cells treated with MWCNT with significant changes in the late stages, indicating the transformation process. P [0'01,0'05]; **P [0'001,0'01]; *** P [0, 0'001].

Exposure Biomarkers

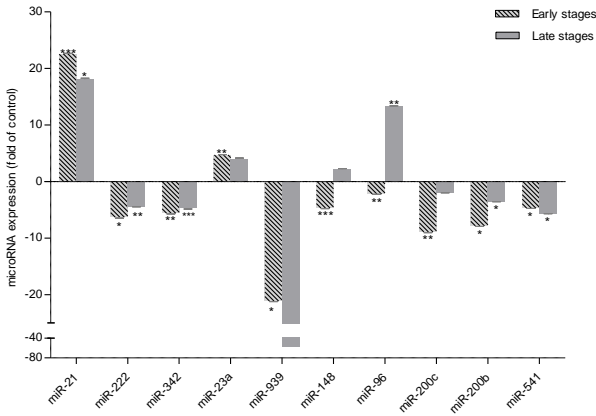


Figure 4. MicroRNA expression changes of cells treated with MWCNT with significant changes in the late stages, indicating the transformation process. P [0'01,0'05]; **P [0'001,0'01]; *** P [0, 0'001].

Formation of protein-based nanoparticles in *Lactobacillus plantarum* as a new source for the isolation of functional protein.

Ricardo Baltà-Foix¹,

Caterina Serrano-Adrover¹, Adrià Lòpez-Cano¹,
Laia Gifre-Renom¹, Alejandro Sanchez-Chardi²,
Elena Garcia-Fruitós¹, Anna Arís¹

¹Department of Ruminant Production, Institut de Recerca i Tecnologia Agroalimentàries (IRTA), 08140 Caldes de Montbui, Spain

²Servei de Microscòpia, Universitat Autònoma de Barcelona (UAB), Bellaterra, Barcelona 08320, Spain

ricardo.balta@irta.cat

The use of Generally Regarded as Safe (GRAS) bacteria as cell factories for the recombinant protein production is taking on increasing importance [1,2]. In contrast with the traditional systems such as *Escherichia coli*, GRAS-derived products show relevant advantages. The absence of endotoxins in these products is one of the main advantages, especially if the recombinant proteins have to be used for therapeutic purposes. In this context, *Lactococcus lactis* have been broadly explored in the last years as a promising microbial cell factory for protein production purposes [3,4]. Aiming to expand the catalogue of GRAS recombinant systems, we have explored the possibilities of *Lactobacillus plantarum* as expression system. Although the production of soluble proteins has already been described in this microorganism [5-7], the formation of protein-based nanoparticles has been never explored in this GRAS microorganism. Thus, the aim of this work has been focused in the study of the production of both soluble and nanoparticulated formats of metalloproteinase 9 (MMP-9), which is a relevant protein in the immune response and in tissue remodeling processes.

The first step accomplished has been the cloning of the gene of interest in *L. plantarum*. Specifically, we have used pSIP plasmid and *L. plantarum* NC8 strain. After that, we have evaluated the production of soluble MMP-9 and MMP-9 nanoparticles, observing an aggregation rate of 99,3%. At this point, we have proven for the first time that it is possible to produce *L. plantarum* nanoparticles and use them for the isolation of pure and functional soluble protein. In addition, we have also seen that these nanoparticles are active and can be used in this appealing format.

Thus, these results prove that *L. plantarum* can be used as a new platform for the production of functional, endotoxin-free protein-based nanoparticles that can be used not only to produce these nanoparticles but also for the isolation of functional soluble proteins.

References

- [1] García-Fruitós E. Microb Cell Fact. 11 (2012):157.
- [2] Song AA, In LLA, Lim SHE, Rahim RA. Microb Cell Fact. 16(2017):55.
- [3] Cano-Garrido O, Sánchez-Chardi A, Parés S, Giró I, Tatkiewicz WI, Ferrer-Miralles N, Ratera I, Natalello A, Cubarsi R, Veciana J, Bach À, Villaverde A, Arís A, Garcia-Fruitós E. Acta Biomater. 43(2016):230-239.
- [4] Boumaiza M, Colarusso A, Parrilli E, Garcia-Fruitós E, Casillo A, Arís A, Corsaro MM, Picone D, Leone S, Tutino ML. Microb Cell Fact.;17(2018):126.
- [5] Karlskås IL, Maudal K, Axelsson L, Rud I, Eijsink VG, Mathiesen. PLoS One. 9(2014):e91125
- [6] Sørvig E, Mathiesen G, Naterstad K, Eijsink VG, Axelsson L. Microbiology. 151(2005):2439-49.
- [7] Sørvig E, Grönqvist S, Naterstad K, Mathiesen G, Eijsink VG, Axelsson L. FEMS Microbiol Lett. 229(2003):119-26.

Figures

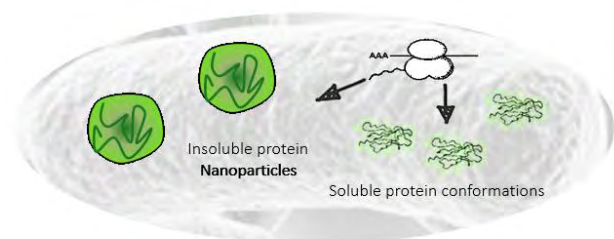


Figure 1. Protein production in *Lactobacillus plantarum*.

Nanocrystal-based magnetic aerogels for hyperthermia and environmental remediation

Taisiia Berestok¹,
Pablo Guardia^{1,2}, Andreu Cabot^{1,3}

¹Catalonia Institute for Energy Research-IREC, 08930
Sant Adrià de Besòs, Barcelona, Spain

²Istituto Italiano di Tecnologia, Via Morego 30 16163,
Genova, Italy

³ICREA, Pg. Lluís Companys 23, 08010 Barcelona, Spain

taisiiia.berestok@gmail.com

Drug targeting and drug delivery together with magnetic recording and storage are among the novel applications developed when nanostructured magnetic materials achieved at the nanoscale. Nanocrystals (NCs) usage allows control of crystallinity; enables facet and morphology engineering that is beneficial for improving of magnetic performance. However, the efficient performance is determined by NC implementation strategy along with the proper surface chemistry that allows maintaining peculiar NCs properties at the nanoscale and results into improved efficiency at macroscale. Assembly of NCs into gels and aerogels provides preserving intrinsic NC properties while obtaining porous nanomaterials with high crystallinity, tuned composition and controlled surface facets at the macroscale resulting in improved performance. At the same time mesoporous gels and aerogels show high accessible surface area that they provide to reactive species and fluids.

Iron oxide NCs are of great importance which mainly attributed to their magnetic behaviour under certain conditions. Nanostructuring and amplified surface area of NC-based aerogel can boost the performance of iron oxide NC building blocks and facilitate their usage for application where interaction with the media is crucial, including biomedical application, sensing, separation, decontamination, catalysis, etc.

We present a novel method to produce crystalline iron oxide aerogels which is based on the cross-linking of preformed colloidal NCs triggered by propylene oxide (PO) [1]. Iron oxide colloidal NCs with tuned sizes were produced in solution from the decomposition of a suitable salt in the presence of oleic acid [2]. The native surface ligands were replaced by amino acids, rendering the NCs colloidally stable in polar solvents [3]. The NC colloidal solution was then gelled by adding PO, which gradually stripped the ligands from the NC surface, triggering NC assembly. Such aerogels displayed both high surface areas and excellent crystallinity associated with the crystalline nature of the constituent building blocks, even without any annealing step. Due to well-defined crystallographic

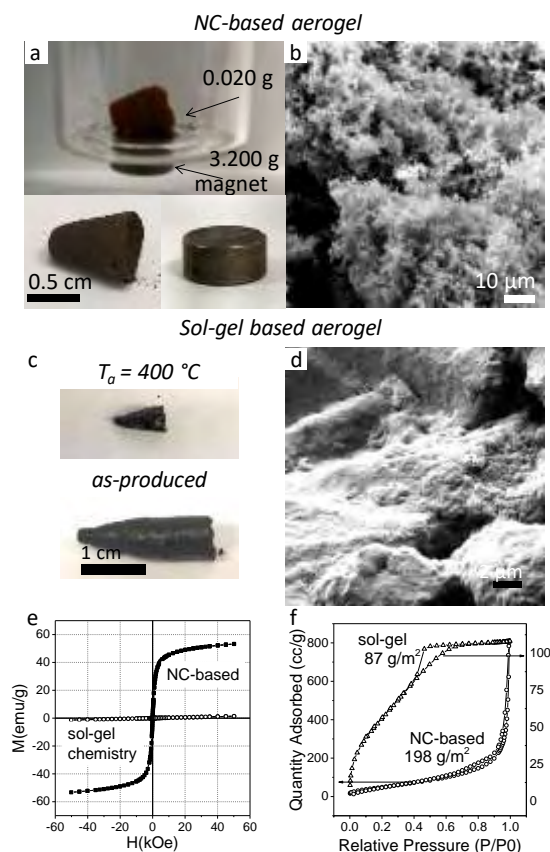


Figure 1. Optical photographs and SEM image of NC-based iron oxide aerogel (a-b). Optical photographs of the aerogels produced using sol-gel approach, showing 50% shrinkage after annealing at 400 °C (c). SEM image of the sol-gel based aerogel (d). Magnetic hysteresis loops at room temperature of as-produced aerogels (e). Adsorption and desorption isotherms of iron oxide aerogels obtained after thermal treatment (f)

structure, such NC-based iron oxide aerogels showed already excellent magnetic behavior without necessity of further heat treatment, required to transform the amorphous into crystalline structure of aerogels produced from ionic precursors using conventional sol-gel chemistry.

Developed procedure, allows to produce aerogels with precise control over the magnetic properties which show appealing properties for hyperthermia applications. Moreover, assembled iron oxide NCs into aerogel being highly magnetic can demonstrate a great promise as reusable electrodes for application related with environmental remediation.

References

- [1] Berestok, T.; Guardia, P.; Du, R.; Blanco, J.; Estradé, S.; Peiró, F.; Brock, S.L.; Cabot, A., *ACS Applied Materials and Interfaces*, 10 (18) (2018) 16041.
- [2] Yu, W. W.; Falkner, J. C.; Yavuz, C. T.; Colvin, V. L., *Chemical Communications*, 20 (2004) 2306.
- [3] De Roo, J.; Coucke, S.; Rijckaert, H.; De Keukeleere, K.; Sinnaeve, D.; Hens, Z.; Martins, J. C.; Van Driessche, I. *Langmuir*, 32 (8) (2016) 1962.

Small particles, big improvement: Fluorescent nanoprobes for singlet oxygen and other reactive oxygen species detection in biological systems

Roger Bresolí-Obach¹,
Santi Nonell¹

¹Institut Químic de Sarrià, Universitat Ramon Llull,
Via Augusta 390, E-08017 Barcelona (Spain)

Rogerbresolio@iqs.url.edu

Production of singlet oxygen is a major component of anticancer and antimicrobial PDT.[1,2] Its facile generation by photosensitisation, together with its high reactivity against a wide variety of cellular and tissue components, make singlet oxygen a highly attractive species for oxidation-based treatment of localised diseases.[3] The amount of singlet oxygen actually produced during PDT depends on several variables and is therefore difficult to control, which detracts from the efficacy and safety of PDT treatments.[4] Developing tools for monitoring singlet oxygen during treatments can contribute to improve the clinical outcome. As part of our efforts towards this end, we report herewith the results in the development of fluorescent nanoprobes and their performance in cells.[5-7]

Under that purpose, a number of nanoprobes for singlet oxygen detection in biological systems have been developed, namely a polyacrylamide-based biocompatible fluorescent nanoprobe (nanoSOSG), the mesoporous silica-bound Anthracene DiPropionic Acid (nanoADPA) and dichloro-dihydro-fluorescein diacetate (nanoDCFH-DA). The reactivity against singlet oxygen has been optimized by choosing appropriate linkers. The nanoparticle scaffolds shield the fluorescent probes from the external medium but not from singlet oxygen, thereby preventing unwanted interactions with proteins and the photosensitizer. Moreover, internalization by HeLa cancer cells or *E. coli* bacteria has been observed and intracellular singlet oxygen and other ROS sensing has been demonstrated as well.

The higher resistance to oxidation by air and to self-sensitized photooxidation, as well as lower affinity for interaction with proteins, make these nanoprobes safer and more reliable fluorescence markers for ROS in cells. The “nano” approach overcomes many of the shortcomings of molecular probes and is a useful strategy to extend their utility to complex biological systems.

This work was supported by the Spanish Ministerio de Economía y Competitividad (grant CTQ2016-78454-C2-1-R). R. B.-O. thanks the European Social Funds and the SUR del DEC de la Generalitat de Catalunya for a predoctoral fellowship (2017 FI_B2 00140).

References

- [1] Agostinis, P., *et al.* Photodynamic therapy of cancer: an update. *CA Cancer J. Clin.*, 61 (2011) 250-281.
- [2] Wainwright, M., *et al.* Photoantimicrobials-are we afraid of the light? *Lancet Infect. Dis.*, 17 (2017) e49-e55.
- [3] Nonell S., Flors. C. (editors). Singlet Oxygen. Applications in Biosciences and Nanosciences, The Royal Society of Chemistry, London, 2016.
- [4] Pogue, B.W., *et al.* Revisiting photodynamic therapy dosimetry: reductionist & surrogate approaches to facilitate clinical success. *Phys. Med. Biol.*, 61 (2016) R57–R89.
- [5] Bresolí-Obach, R., *et al.* Anthracene-based fluorescent nanoprobes for singlet oxygen detection in biological media. *Methods*, 109 (2016) 64-72.
- [6] Ruiz-González, R., Bresolí-Obach, R., *et al.* NanoSOSG: a nanostructured fluorescent probe for the detection of intracellular singlet oxygen. *Angew. Chem. Int. Ed.*, 56 (2017) 2885-2888.
- [7] Bresolí-Obach, R. *et al.* NanoDCFH-DA: a silica-based nanostructured fluorogenic probe for the detection of reactive oxygen species. *Photochem. Photobiol.* (2018) Accepted. Doi: 10.1111/php.13020

Validation of a titration method to determine chondroitin sulfate loaded to solid lipid nanoparticles in an experimental factorial design.

Eduviges Bustos Araya^{1,2},

Anna Nardi-Ricart¹, Pilar Pérez-Lozano^{1,3}, Encarna García-Montoya^{1,3}, JM Suñé-Negre^{1,3}, JR Ticó^{1,3}, Montserrat Miñarro-Carmona^{1,3}.

¹ Department of Pharmacy and Pharmaceutical Technology and Physical Chemistry, Faculty of Pharmacy and Food Sciences, Barcelona University, Spain.

² Ministry of Science, Technology and Telecommunications of Costa Rica (MICITT) and University of Costa Rica (UCR).

³ Pharmacotherapy, Pharmacogenetics and Pharmaceutical Technology Research Group. IDIBELL-UB, Hospitalet de Llobregat, Barcelona, Spain.

Email mbustoar10@alumnes.ub.edu

Abstract

Previous efforts at the Faculty of Pharmacy and Food Sciences of the University of Barcelona, have achieved to obtain cationic solid lipid nanoparticles (cSLN), with an average size of less than 200 nm, by the hot microemulsion method, which have been tested as a vehicle for pDNA and siRNA, in the transfection of cell lines [1,2]. It is of scientific interest to evaluate the capacity of SLN transporting different types of biomolecules with pharmacological potential. Chondroitin sulfate (CHON) is a major component of the extracellular matrix of several connective tissues, including skin, bone, ligaments, tendons and cartilage. For that reason, CHON is a potential therapeutical agent in Osteoarthritis (OA), which is characterized by progressive structural and metabolic changes in joint tissues [3]. Studies recommend topical administration in treating OA as first line therapy, and the development of topical systems with nanotechnology may introduce a new perspective for future treatment of OA [4].

An experimental factorial design, to optimize the production of SLN of CHON, was employed. The variables were defined as Concentration (mg/ml), Stirring rate (rpm) and Reaction time (min). Different properties were tested, including entrapment efficiency of CHON, zeta potential and particle size. A titration method was validated to test entrapment efficiency of CHON. A calibration curve was obtained from 0.10 to 1.20 mg mL⁻¹ ($r > 0.9994$). Within-day % RSD was 0.7 and between-day % RSD was 1.11. Specificity/ selectivity experiments revealed the absence of important interference from excipients, mean recovery from spiked samples for CHON was 93.6 %.

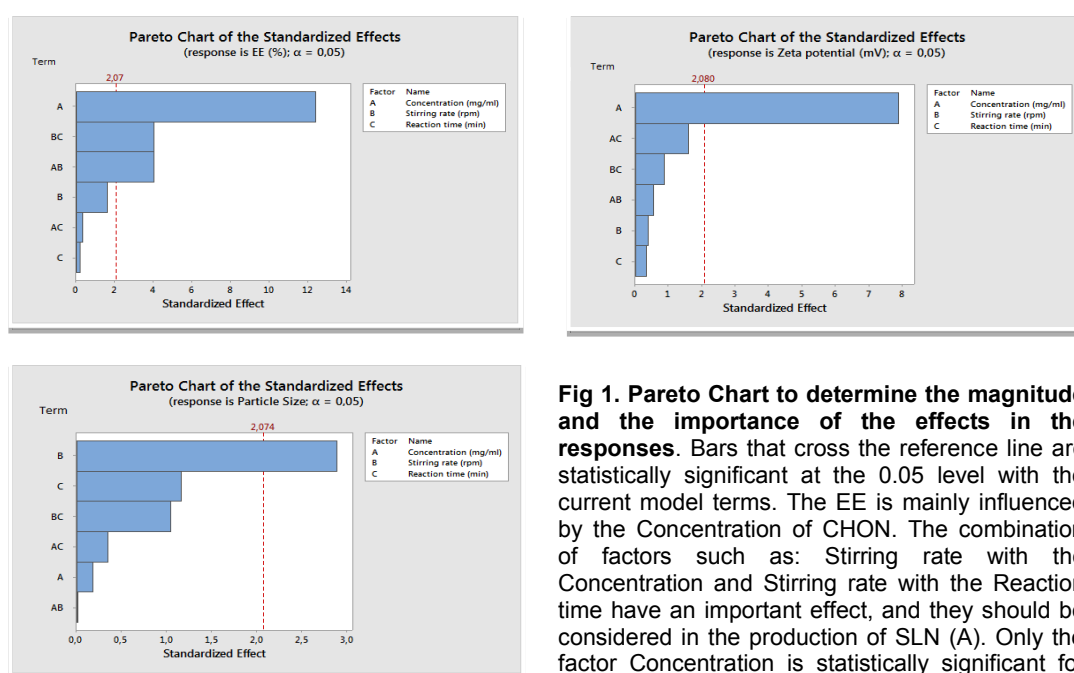


Fig 1. Pareto Chart to determine the magnitude and the importance of the effects in the responses. Bars that cross the reference line are statistically significant at the 0.05 level with the current model terms. The EE is mainly influenced by the Concentration of CHON. The combination of factors such as: Stirring rate with the Concentration and Reaction time have an important effect, and they should be considered in the production of SLN (A). Only the factor Concentration is statistically significant for

The optimal factors were attained by Minitab® program, using design of experiment (DOE) and pareto chart, see Figures 1 and 2.

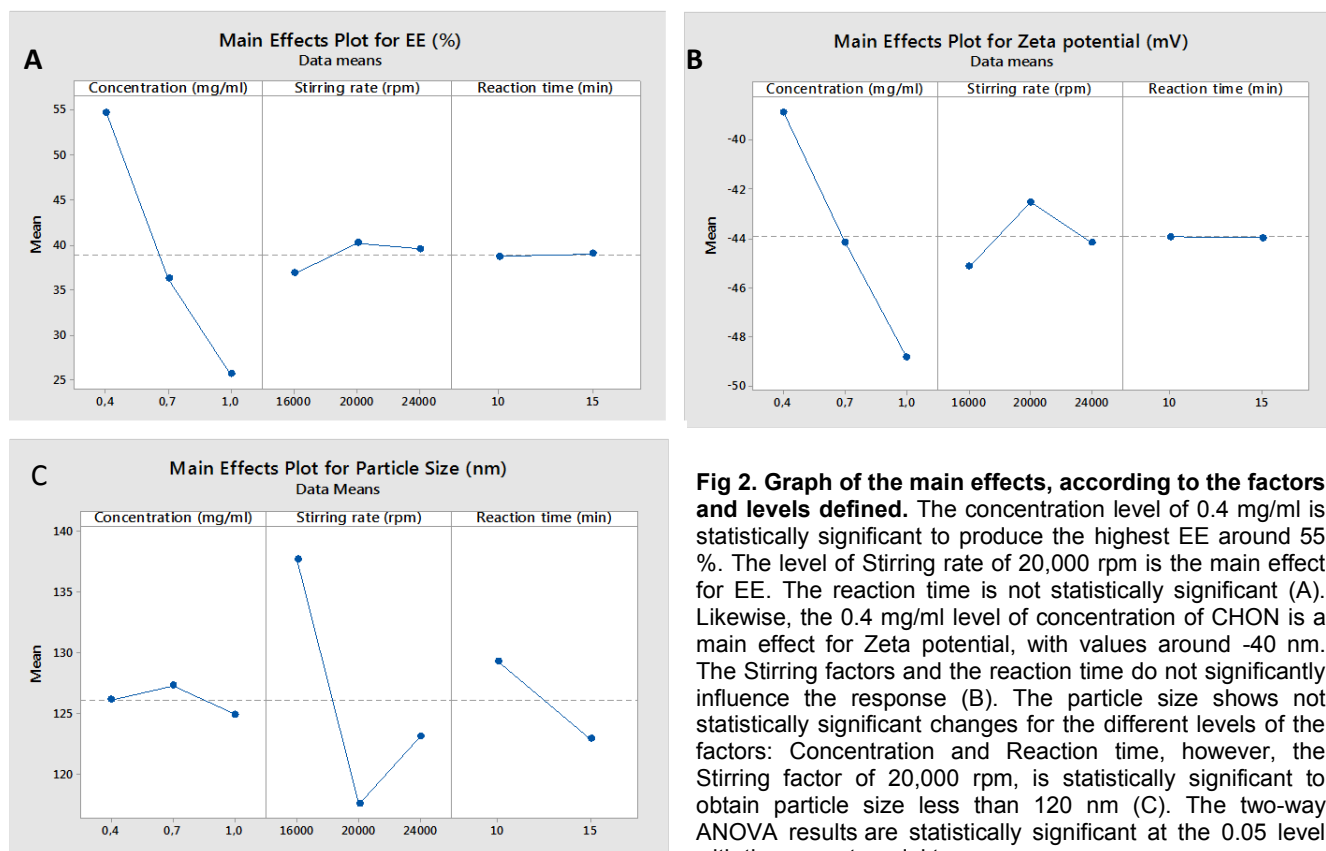


Fig 2. Graph of the main effects, according to the factors and levels defined. The concentration level of 0.4 mg/ml is statistically significant to produce the highest EE around 55 %. The level of Stirring rate of 20,000 rpm is the main effect for EE. The reaction time is not statistically significant (A). Likewise, the 0.4 mg/ml level of concentration of CHON is a main effect for Zeta potential, with values around -40 nm. The Stirring factors and the reaction time do not significantly influence the response (B). The particle size shows not statistically significant changes for the different levels of the factors: Concentration and Reaction time, however, the Stirring factor of 20,000 rpm, is statistically significant to obtain particle size less than 120 nm (C). The two-way ANOVA results are statistically significant at the 0.05 level with the current model term.

In conclusion, the titration method is a simple, rapid and reliable method for the determination of chondroitin sulfate loaded to SLN. The DOE revealed that reaction time does not have a significant impact in the evaluated responses. However, concentration (0.4 mg/ml) and stirring rate (20 000 rpm) were determinant to maximize entrapment efficiency of CHON in SLN and to get the optimum size and zeta potential of SLN.

References

- [1] Fàbregas A, Prieto S, Suñé-Pou M, Boyero-Corral S, Ticó JR, García-Montoya E, et al. Improved formulation of cationic solid lipid nanoparticles displays cellular uptake and biological activity of nucleic acids. *Int J Pharm.* 2017; 516(1–2):39–44.
- [2] Fàbregas A. Nanopartícules lipídiques sòlides catiòniques (cSLN) com a sistema d'elecció per a transfecció cel·lular de DNA/RNA. Universitat de Barcelona; 2015.
- [3] Henrotin Y, Mathy M, Sanchez C, Lambert C. Chondroitin Sulfate in the Treatment of Osteoarthritis: From in Vitro Studies to Clinical Recommendations. *Therapeutic Advances in Musculoskeletal Disease.* 2010; 2(6):335-348.
- [4] Leite, C.B.S., Coelho, J.M., Muehlmann, L.A., de Azevedo, R.B. and Sousa, M.H. Skin Delivery of Glucosamine and Chondroitin Sulphates—A Perspective on the Conservative Treatment for Osteoarthritis of the Knee. *Journal of Biosciences and Medicines,* 2017; 5:11-20.

Polymer Therapeutics for treating neurodegenerative disorders: exploring the intranasal route to bypass the BBB

I. Conejos-Sánchez, F. Rodriguez-Otormin, E. Masiá, I. Dolz-Perez, T. Melnyk, M. Palomino-Schätzlein, M.J. Vicent
Laboratorio Polímeros Terapéuticos, Centro de investigación Príncipe Felipe, Valencia, Spain.

iconejos@cipf.es

The growing incidence and increasing societal costs caused by neurodegenerative disorders in an ageing population, together with the lack of effective treatments, point out the need for novel approaches in order to address their enormous burden. Only in Europe it has been estimated that 35 % of all disease burden is attributable to brain-related disorders.¹ In particular, Alzheimer's Disease (AD) is one of the largest global public health challenges to be faced. Moreover, Central Nervous System (CNS) drug discovery and development is a challenging task due to the presence of the most impenetrable biological barrier in the human body- the Blood Brain Barrier (BBB).² Indeed, only 2 % of small-molecule drugs and almost 0 % of biologic drugs do reach the brain, thus limiting the development of efficient treatments for brain diseases.³

Focus on designing non-invasive strategies for brain targeting and active delivery through nanotechnological approaches, we are developing a polymer-based platform for intranasal delivery using polyglutamates underpinned on previously established findings of our lab (Fig.1).^{4,5} These versatile biodegradable carriers with controlled architecture and self-assembled behavior hold several key features.

First, they are crosslinked with reversible disulfide chemistries, prone to disassemble under reductive media to facilitate chemical adsorption to the mucosa via disulfide interchange with cysteine-rich glycoproteins and also to allow greater diffusion/penetration rates in brain. In parallel, surface modification with targeting motifs has been exploited to improve the ability to cross the mucosal barrier that would synergize with the disulfide cross-linking motifs. Screening studies have been performed through mucodiffusion evaluation by NMR techniques and *ex vivo* permeation assays in a sheep mucosal model.

Second, they can bear a rationally designed combination therapy. In this direction, we have identified adequate neuroprotectant-neurorescuer drug combination therapy for the treatment of AD

and linking chemistry of the resultant combinations is now under development.

If successful, this novel delivery method for intranasal delivery will be of interest for other CNS-related diseases

References

- [1] Olesen, J. Eur J Neurology 2003, 10 (5), 471.
- [2] Obermeier, B. Nature medicine 2013, 19 (12), 1584
- [3] Pardridge, W. Drug Discov Today 2007, 12, 54.
- [4] Duro-Castano, A. et al., Adv Mater 2017, 29:39.
- [5] Vicent, M. J.; Duro Castaño, A; Nebot, V.J. WO2017025298 (A1)

Figure

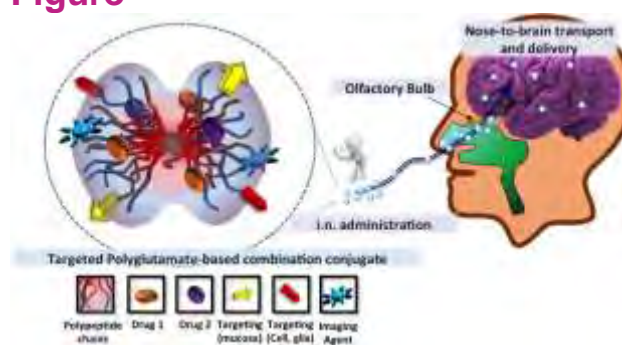


Figure 1. A novel polymer-based combination platform for efficient intranasal delivery.

Effects of differently shaped TiO₂NPs (nanospheres, nanorods and nanowires) on the *in vitro* model (Caco-2/HT29) of the intestinal barrier

Constanza Cortés, PhD¹,

Alba García-Rodríguez¹, Laura Vila¹, Alba Hernández^{1,2} and Ricard Marcos^{1,2}

¹Grup de Mutagènesi, Departament de Genètica i de Microbiologia, Facultat de Biociències, Universitat Autònoma de Barcelona, Edifici Cn, Campus de Bellaterra, 08193 Cerdanyola del Vallès, Barcelona, Spain

²CIBER Epidemiología y Salud Pública, ISCIII, Madrid, Spain

Constanza.cortes@uab.cat

The food industry has used titanium dioxide (TiO₂) since it was approved by the Food and Drug Administration (USA) in 1966 as a food additive [1]. Recent evidence indicates that the use of nanosized titanium dioxide (TiO₂NPs) in consumer and industrial products has exponentially increased due to their refractive, photocatalytic and pigmenting properties [2]. Even though TiO₂ was classified by the International Agency for Research on Cancer (IARC) as a possible human carcinogen on group 2B in 2010, the Nanotechnology Consumer Products Inventory has documented around 100 consumer products containing TiNPs and TiO₂NPs to date [3]. Estimations based on the consumption of TiO₂-containing food lead to the conclusion that, in the US, children and adults may be ingesting around 1–2 and 0.2–0.7 mg/kg bw/day of TiO₂, respectively [4]. This highlights the relevance of ingestion as an important entryway of TiO₂ and TiO₂NPs in humans.

Considering oral exposure as one of the main entry routes to the human body, the lack of conclusive studies reporting the impact of newly engineered TiO₂NPs is striking. Accordingly, our study aims to evaluate the biointeractions, biodistribution, and toxicokinetics of TiO₂NPs in the intestinal barrier by assessing the biological effects of three differently-shaped TiO₂NPs (nanospheres, nanorods and nanowires). For this purpose, we used an *in vitro* model comprised of Caco-2/HT29 cocultures. After 21 days, the coculture acquires a barrier structure that faithfully mimics the human small intestine epithelium at both the morphological and functional level [5]. Derived from a human colon adenocarcinoma, Caco-2 cells, as enterocyte-like cells, are able to express microvilli, tight junctions

(TJ) and present paracellular, transcellular, active and transcytotic transport [6]. On the other hand, the other human colon adenocarcinoma-derived cell line, HT29, is characterized by its ability to produce and secrete mucus [7]. According to this, we chose the Caco-2/HT29 model to determine whether the mucus layer, as well as the barrier structure, could be compromised by the exposure to TiO₂NPs. Moreover, we aimed to assess if the potential adverse effects are shape- and structure-dependent by comparing the most commercialized TiO₂NPs, namely nanospheres (anatase-structure), nanorods (rutile-structure) and nanowires (TiO₂-structure). For this purpose, we analyzed the barrier's integrity and permeability after 24 and 48 h of TiO₂NPs' exposure, detected cellular uptake and intracellular localization by using laser confocal microscopy, and assessed the barrier functionality by gene expression. In addition, genotoxic and oxidative DNA damage were also evaluated by using the comet assay.

References

- [1] Code of Federal Regulations (CFR). Title 21, updated April 1, 2016
- [2] Chen X, Mao SS., Chem Rev. 107 (2007) 2891–959.
- [3] Vance M, Kuiken T, Vejerano E, McGinnis S, Hochella M Jr, Rejeski D, Hull M., Beilstein J Nanotechnol. 6 (2015) 1769–80.
- [4] Weir A, Westerhoff P, Fabricius L, Hristovski K, von Goetz N. Environ. Sci. Technol., 46 (2012) 2242–50.
- [5] Antunes F, Andrade F, Araújo F, Ferreira D, Sarmiento B., Eur J Pharm Biopharm. 83 (2013) 427–35.
- [6] Artursson P, Palm K, Luthman K. Adv Drug Deliv Rev. 46 (2001) 27–43.
- [7] Lesuffleur T, Barbat A, Dussaulx E, Zweibaum A. Cancer Res. 50 (1990) 6334–43.

Figures

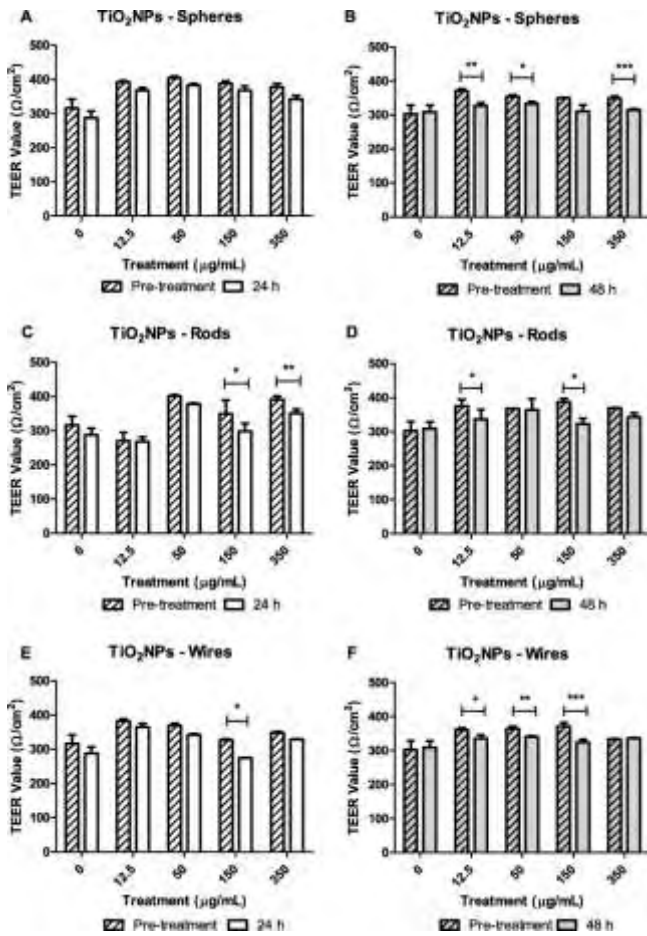


Figure 1. TEER measurements of Caco-2/HT29 co-culture barriers before and after 24 and 48 h of exposure to TiO₂NPs-S (a and b), TiO₂NPs-R (c and d), and TiO₂NPs-W (e and f). Results were analyzed with a paired Student's *t*-test and represented as mean ± SEM. **P*<0.05, ***P*<0.01, ****P*<0.001

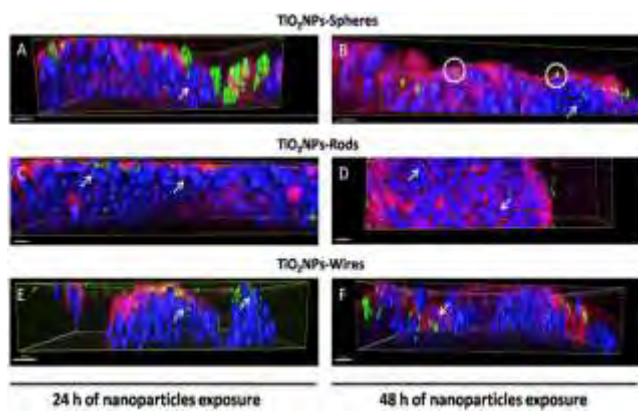


Figure 2. Three-dimensional confocal images of the Caco-2/HT29 co-culture barriers z-scans from Fig. 6. Images were taken after exposures of 24 or 48 h to TiO₂NPs-S (a and b), TiO₂NPs-R (c and d), and TiO₂NPs-W (e and f). Cell nuclei (blue) were stained with Hoechst, and mucus (red) was stained with WGA. NPs were visualized by reflection and

marked with a green mask. White arrows indicate NPs in the cell cytoplasm and NPs-nucleus interactions. Images were processed with the Imaris 7.2.1 software

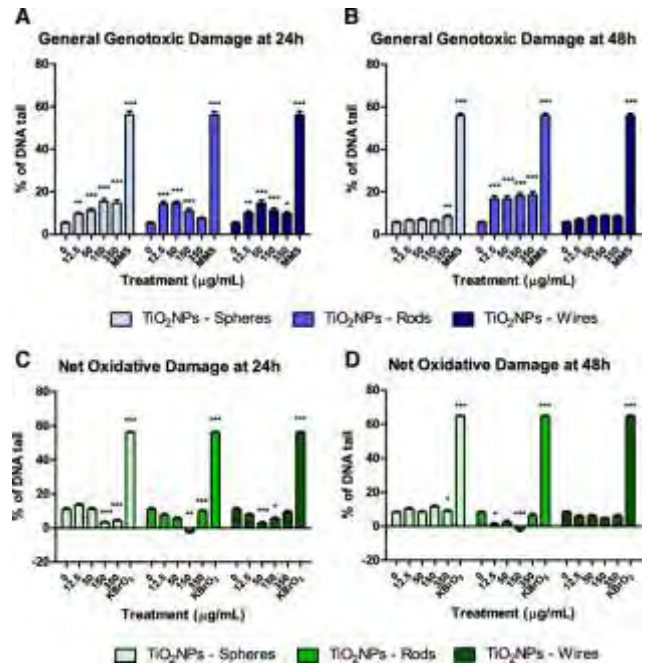


Figure 3. DNA damage studies using the Comet assay complemented with the FPG enzyme. Genotoxic damage observed after 24 (a) or 48 (b) h of exposure to TiO₂NPs (-S, -R and -W). Mean oxidative damage observed after 24 (c), and 48 (d) h of exposure to TiO₂NPs (-S, -R and -W). (*) denotes significant differences according to the one-way ANOVA with Tukey's post-test (**P*<0.05, ***P*<0.01****P*<0.001). Results are represented as mean ± SEM

Effects of GO and GNPs on the *in vitro* model of the intestinal barrier (Caco2/HT29)

Josefa Domenech¹

Constanza Cortés¹, Alba Hernández^{1,2}, Ricard Marcos^{1,2}

¹Grup de Mutagènesi, Departament de Genètica i de Microbiologia, Facultat de Biociències, Universitat Autònoma de Barcelona, Bellaterra, Spain

²CIBER Epidemiología y Salud Pública, ISCIII, Spain
Josefa.Domenech@uab.cat

Nanotechnology has become a booming discipline due to the wide range of applications of new nanomaterials (NMs). Among these, graphene stands out as an attractive carbon-based NM due to its physicochemical properties: its optical and electric properties make it a perfect candidate for applications in a variety of fields such as physics, healthcare, material science and, recently, biomedicine [1, 2].

Nowadays, humans are exposed to a large range of different nanoparticles through occupational and environmental exposure, or through food and healthcare products [3, 4]. Pulmonary, intestinal and skin barriers protect us to face nanoparticles exposure [5]. Accordingly, our study aims to evaluate the biointeractions, biodistribution, and toxicokinetic of graphene nanoparticles in the intestinal barrier by assessing the biological effects induced by graphene oxide (GO) and graphene nanoplatelets (GNPs).

For this purpose, we use a co-culture *in vitro* model composed by differentiated Caco-2 and HT29 cells. Both human colon adenocarcinoma-derived cell lines mimic the small intestine epithelium at morphological and functional level after 21 days of differentiation [5]. While enterocyte-like Caco-2 cells are able to express microvilli, tight junctions (TJ), and present paracellular, transcellular, active and transcytotic transport [6], HT29 cells have the ability to produce and secrete mucus [7].

According to this, we chose the Caco-2/HT29 *in vitro* model to determine the commitment of both the mucus layer and the barrier structure in face of the exposure to graphene nanomaterials. For this purpose, we studied the barrier's integrity and permeability after 24 h of both GO and GNPs exposure and analysed cellular uptake by laser confocal microscopy. Also, genotoxic and oxidative DNA damage was assessed by the comet assay and the evaluation of ROS-related gene expression changes. In addition, expression levels of 36 human cytokines were determined after 24 h of GO and GNPs treatment.

The obtained results showed the barrier's integrity and permeability remain intact after GO and GNPs

treatments. In addition, the amount of NM retained on the mucus layer of the barrier appeared to be dose dependent for both treatments while nanoparticles inside the cells only were found when the barrier was treated with GNPs. However, Caco-2/HT29 barrier cells showed genotoxic damage after the treatment with GO and GNPs, while oxidative damage was not found at any tested concentration. The study of the expression of *HO1*, *SOD2* and *GSTP1* genes supported these results. Ongoing experiments will confirm the barrier oxidation state.

References

- [1] Banerjee A. N., Interface Focus, 3 (2018)
- [2] Madni A., Noreen S., Maqbool I., Rehman F., Batool A., Kashif P. M., Rehman M., Tahir N., Khan M. I., Journal of Drug Targeting, 10 (2018) 858–83
- [3] Gottschalk F., Nowack B., Journal of Environmental Monitoring, 13 (2011) 1145–55
- [4] Piccinno F., Gottschalk F., Seeger S., Nowack, B., Journal of Nanoparticle Research, 9 (2012)
- [5] Vance M. E., Kuiken T., Vejerano E. P., McGinnis S. P., Hochella M. F., Rejeski D., Hull M. S., Beilstein Journal of Nanotechnology, 6 (2015) 1769–80
- [6] Antunes F., Andrade F., Araújo F., Ferreira D., Sarmiento B., Eur J Pharm Biopharm, 83 (2013) 427–35
- [7] Artursson P., Palm K., Luthman K., Adv Drug Deliv Rev, 46 (2001) 27–43
- [8] Lesuffleur T., Barbat A., Dussaulx E., Zweibaum A., Cancer Res, 50 (1990) 6334–43

Figures

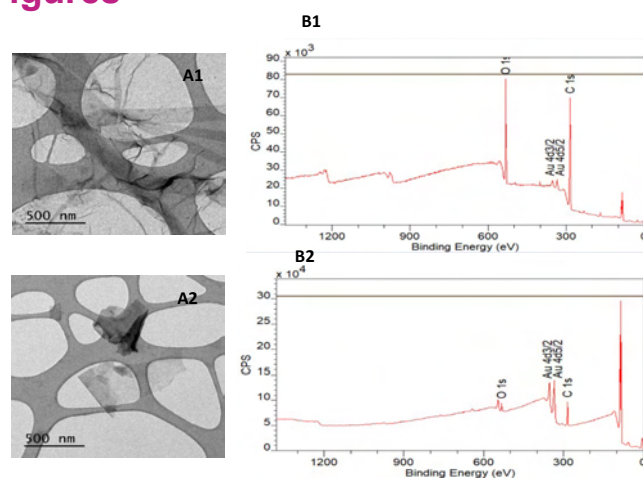


Figure 1. TEM (A) and XPS (B) characterization of GO (A1 and B1) and GNPs (A2 and B2) nanomaterials.

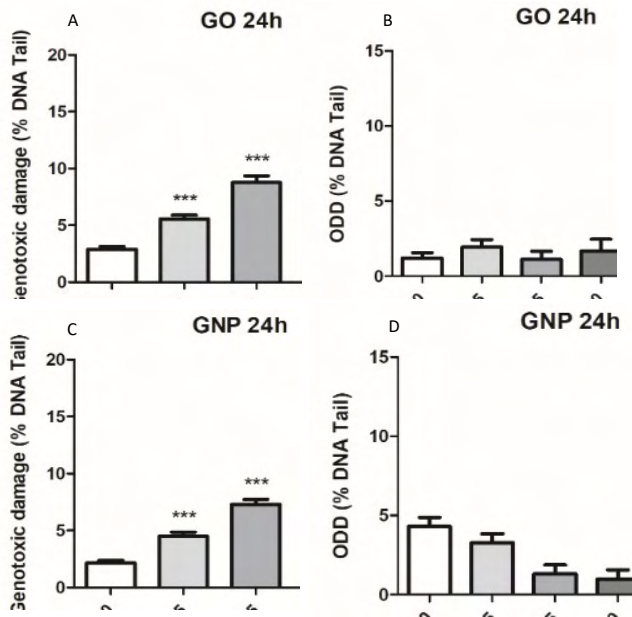


Figure 2. DNA damage studies using the Comet assay complemented with the FPG enzyme. Genotoxic damage observed after 24 h of exposure to GO (A) and GNPs (C). Mean oxidative DNA damage observed after 24 h of exposure to GO (B) and GNPs (D). (*) denotes significant differences according to the one-way ANOVA with Tukey's post-test (* $P < 0.05$, ** $P < 0.01$ **** $P < 0.001$). Results are represented as mean \pm SEM.

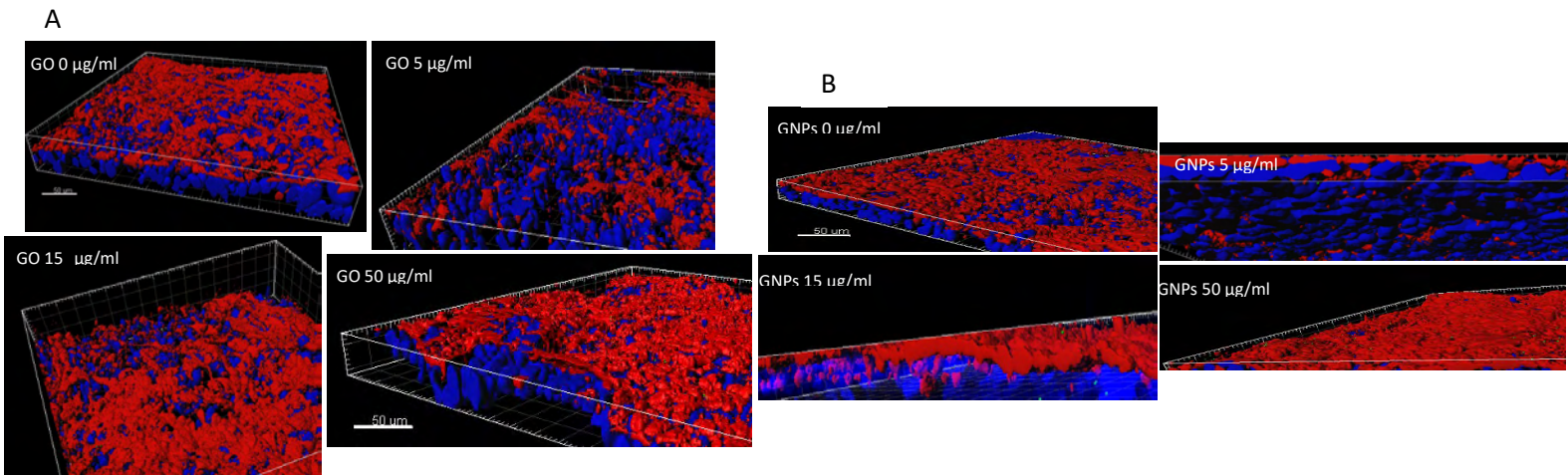


Figure 3. Three-dimensional confocal images of the Caco-2/HT29 co-culture barrier. Images were taken after exposures of 24 h to GO (A) and GNPs (B). Cell nuclei (blue) were stained with Hoechst, and mucus (red) was stained with WGA. NPs were visualized by reflection and marked with a green mask. Images were processed with the software Imaris 8.2.1.

Impairment of colorectal tumor microenvironment with lipid nanocapsules

Fourniols Thibaut¹,

Agueda Martinez², Alessandra Lopes¹, Bernard Ucakar¹, Nicolas Dauguet³, Andrew Scott⁴, Olivier de Wever⁵, Fabienne Danhier¹, Diego Arango²
Véronique Prétat¹

¹Advanced Drug Delivery & Biomaterials, LDRI, UCLouvain, avenue Mounier 73, 1200 Brussels, Belgium

²Biomedical Research in Digestive Tract Tumors Group, CIBBIM-Nanomedicine, VHIR, Vall d'Hebron Barcelona Hospital Campus, 08035 Barcelona, Spain

³De Duve Institute, UCLouvain, avenue Mounier 75, 1200 Brussels, Belgium

⁴Olivia Newton-John Cancer Research Institute and School of Cancer Medicine, La Trobe University, Melbourne, Victoria, Australia

⁵Department of Radiation oncology and experimental cancer research, Universitair Ziekenhuis Ghent, Belgium

thibaut.fourniols@uclouvain.be

Cancer-associated fibroblasts (CAF) are a key population of the tumor microenvironment. Indeed they participate to the setting of the whole tumor microenvironment with neoangiogenesis, extracellular matrix production, and immunosuppressive cells recruitment [1]. They are also part of the metastasis event, and of the chemoresistance of the tumor [1,2].

Following the results of some teams working with pancreatic tumor models [3,4], we hypothesize that some new nanomedicines, specifically targeting and killing CAF population, would lead to an impairment of the tumor microenvironment and an improved sensitivity to further immuno- or chemotherapy. To assess this experimental treatment, we used a colorectal cancer (CRC) model, because stroma-rich CRC are a challenging disease in clinic, with a poor response to classical combination of chemotherapeutical drugs [5].

The nanomedicine is based on a lipid nanocapsule (LNC), constituted of an oily core that can contain the drug, and a membrane with a mix of lecithin and hydroxystearic acid with a Poly(Ethylene-Glycol) arm. To assess the added value of a targeted nanomedicine, we are associating an human antibody, ESC11 [6] or a single chain variable fragment against the extracellular Fibroblast Activation Protein (FAP) with a post-insertion method.

In vitro, we used an immortalized human CAF cell line CT5.3hTERT [7]. Their FAP expression was checked by Flow cytometry with the human monoclonal antibody. We assessed their sensitivity to a set of different drugs including cytotoxics, kinase inhibitors and other drugs. Acriflavine (ACF), an HIF-1 pathway inhibitor, and paclitaxel (PTX), an antimicrotubulin agent, were selected as drug candidates to inhibit CAF with an IC50 below 1µM at

48h of incubation. Both drugs were encapsulated in our LNC with high drug loading of 1.5 mg/mL of formulation (PTX) or up to 2.5mg/mL (ACF), thanks to the use of reverse micelles.

In vivo, the mouse colon carcinoma cell line CT26 was subcutaneously grafted on syngeneic BalbC mice. We tuned the CAF infiltration by treating mice with intraperitoneal injection of oxaliplatin, a chemotherapeutic agent. After 2 weeks of treatment, tumors are extracted for Immunofluorescence quantification of CAF with Smooth Muscle Actin (SMA) staining. Oxaliplatin treatment increases SMA expression in the tumor. Different schedules of treatment were assessed and the combination of the 2 formulations with ACF and PTX administered the same day gave the best effect after a single intratumoral injection.

We compared the CT26 with another syngeneic tumor cell line, MC38, for its microenvironment in term of stromal and immune cell infiltration.

An orthotopic model was geared to get closer to colorectal environment, by injecting cells on the caecal wall. The combination therapy, twice per week intravenously, is administered to evaluate the efficacy of the untargeted nanomedicine alone.

The future objectives are to combine this treatment with classical therapy to assess the microenvironment impairment on tumor sensitivity.

References

- [1] R. Kalluri, Nature Reviews Cancer, 9 (2016), 582
- [2] Z. Liao & al, Cellular Immunology, 2018
- [3] Q. Yang & al, ACS Applied MAT. & Interfaces, 21 (2016), 13251
- [4] T. Miyashita & al, Anticancer research, 1 (2018), 337
- [5] A. Calon, NATURE Genetics, 4 (2015), 320
- [6] E. Fischer & al, Clin Cancer Res., 22 (2012), 6208
- [7] E. De Vlieghere & al, Biomaterials (2015), 148

Optimized lipid nanoparticles decorated with TRAIL exhibit enhanced cytotoxicity against cancer cells

Ana Gallego-Lleyda^{1,2},

Diego De Miguel³, Javier Plou¹, Alberto Anel^{1,2}, Luis Martinez-Lostao^{2,4,5,6}

¹Departamento de Bioquímica, Biología Molecular y Celular, Universidad de Zaragoza, Zaragoza, Spain ²

²Instituto de Investigación Sanitaria de Aragón (ISS), Zaragoza, Spain Organization, Address, City, Country)

³Cell Death, Cancer and Inflammation, University College of London, London, UK

⁴Servicio de Inmunología, Hospital Clínico Universitario Lozano Blesa, Zaragoza, Spain

⁵Departamento de Microbiología, Medicina Preventiva y Salud Pública, Universidad de Zaragoza, Zaragoza, Spain

⁶Instituto de Nanociencia de Aragón, Zaragoza, Spain

annaiss89@hotmail.com

The TNF cytokine family member namely tumour necrosis factor (TNF)-related apoptosis-inducing ligand (TRAIL), was described capable of inducing apoptosis in tumor cells while sparing most normal cells [1, 2]. This fact made that TRAIL was soon considered as potentially useful drug for anti-cancer therapy and a large number of phase II/III clinical trials were carried out using TRAIL-based therapy on a wide variety of human cancers [3]. Unfortunately, although TRAIL therapies was probed as safe molecule, TRAIL-based therapies showed very limited therapeutic activity in clinical trials [4, 5]. In order to overcome TRAIL resistance, better sensitization strategies [6, 7], as well as novel TRAIL formulations with improved bioactivity can be of great usefulness for future clinical use of this death ligand as anti-tumor agent [8, 9].

TRAIL has four membrane-bound receptors in humans: TRAIL-R1/DR4, TRAIL-R2/DR5, TRAIL-R3/DcR1 and TRAIL-R4/DcR2. In addition, TRAIL has been described to be able to bind to the soluble receptor osteoprotegerin (OPG). Among these five receptors, only DR4 and DR5 are able to transduce the apoptotic signal upon TRAIL binding while DcR1 and DcR2 act as decoy receptors and do not transmit apoptotic signal [10].

Our group demonstrated that, in physiological conditions, TRAIL was indeed released by activated human T cells in its transmembrane form, inserted in the membrane of lipid microvesicles called exosomes [11]. On this basis, we have generated artificial lipid nanoparticles containing membrane-bound TRAIL (LUV-TRAIL) resembling those natural exosomes. Preparation of LUV (Large Unilamellar Vesicles)-type lipid nanoparticles with soluble recombinant TRAIL (sTRAIL) anchored on their surface resembling the lipid composition of natural exosomes was carried out as previously described [12]. Briefly, a mixture of phosphatidylcholine (PC),

sphingomyelin (SM), cholesterol (CHOL), and 1,2-dioleoyl-sn-glycero-3-[[N-(5-amino-1-carboxypentyl)-iminodiacetic acid]succinyl](nickel salt) (DOGS-NTA-Ni) in the weight ratio of 55:30:10:5 were firstly dried under a nitrogen and next under vacuum. Lipid mixture was resuspended in PBS buffer. Then, resuspended lipids were freeze-thawed 10 times and extruded 10 times through two polycarbonate membranes with a pore size of 0.2 µm using an extruder. LUV and soluble TRAIL (rTRAIL-His₆, corresponding to amino acids 95–281 cloned into the pET-28c plasmid) kindly provided by Dr. M. MacFarlane [13] were incubated in PBS buffer for 30 minutes at 37°C. Then LUV with soluble TRAIL anchored on their surface (LUV-TRAIL) were ultracentrifugated for 6 hours at 100,000g at 4°C, supernatant was removed, and finally, the pellet containing LUV-TRAIL was resuspended in an equal volume of sterile PBS buffer and stored at 4°C until use.

We already demonstrated that LUV-TRAIL was more effective inducing apoptosis than soluble TRAIL both *in vitro* and *in vivo* when compared to soluble TRAIL against distinct hematologic malignancies as well as epithelial carcinoma cells [14-19]. However, although LUV-TRAIL showed more pro-apoptotic potential than soluble TRAIL all tumor cell lines tested, they only induced a limited cytotoxicity in soluble TRAIL-resistant cells. In this line, optimization of LUV-TRAIL in order to enhance its cytotoxic ability is a plausible experimental approach. Therefore, we have generated a novel version of LUV-TRAIL encapsulating inside them the chemotherapeutic drug doxorubicin (DOX). For that, DOX was loaded inside liposomal lumen by the pH gradient method [20]. First, LUV-AS were prepared by using 300 mM (NH₄)₂SO₄ (ammonium sulphate, AS) at pH=4 instead of PBS to resuspend the dry lipid film. The rest of the LUV-AS generation protocol was similar to that of normal LUV. Once obtained, the LUV-AS were incubated with DOX at a molar drug-to-lipid ratio of 1/3.8. After the incubation, the obtained liposomal DOX formulation (LUVDOX) was incubated with TRAIL to obtain LUVDOX-TRAIL with final concentrations of total lipid, TRAIL and DOX of 2.5 mM, 12 µg/ml and 775 µM, respectively (Figure 1). LUVDOX-TRAIL with a concentration of DOX 10 times less than those previously described (LUVDOX-TRAIL 1/10) was also generated. To assess the encapsulation efficiency of DOX inside the liposomal lumen, the absorbance of DOX at 480 nM was measured and calibration curve using free DOX (concentration range from 0 to 40 µM) was used to finally quantify the amount of encapsulated DOX.

Finally, cytotoxic ability of LUVDOX-TRAIL were analyzed by annexin V staining in a panel of different cancer types. LUVDOX-TRAIL significantly improved LUV-TRAIL cytotoxicity in all cancer cell lines tested when compared to LUV-TRAIL (Figure 2). Moreover, we show that LUVDOX-TRAIL with a particular concentration of DOX (ten times less than initially use), LUVDOX-TRAIL maintained their

greater cytotoxicity against tumor cells while were no toxic againsts normal cells (Figure 3). Our results validate the potential clinical application of LUVDOX-TRAIL as anti-tumor agent.

References

- [1] Pitti RM, Marsters SA, Ruppert S, Donahue CJ, Moore A, Ashkenazi A. *J Biol Chem*; 271:12687-90 (1996).
- [2] Wiley SR, Schooley K, Smolak PJ, Din WS, Huang CP, Nicholl JK, et al. *Immunity*; 3:673-82 (1995).
- [3] von Karstedt S, Montinaro A, Walczak H. *Nat Rev Cancer*; 17:352-66 (2017).
- [4] Lemke J, von Karstedt S, Zinngrebe J, Walczak H. *Cell Death Differ*; 21:1350-64 (2014).
- [5] Micheau O, Shirley S, Dufour F. *Br J Pharmacol*; 169:1723-44 (2013).
- [6] den Hollander MW, Gietema JA, de Jong S, Walenkamp AM, Reyners AK, Oldenhuis CN, et al. *Cancer Lett*; 332:194-201 (2013).
- [7] Dimberg LY, Anderson CK, Camidge R, Behbakht K, Thorburn A, Ford HL. *Oncogene*; 32:1341-50 (2013).
- [8] De Miguel D, Lemke J, Anel A, Walczak H, Martinez-Lostao L. *Cell Death Differ*; 23(5):733-47 (2016).
- [9] Wajant H, Gerspach J, Pfizenmaier K. *Cancer Lett*; 332:163-74 (2013).
- [10] Martinez-Lostao L, Marzo I, Anel A, Naval J. *Biochem Pharmacol*; 83:1475-83 (2012).
- [11] Martinez-Lorenzo MJ, Anel A, Gamen S, Monleon I, Lasierra P, Larrad L, et al. *J Immunol*; 163:1274-81 (1999).
- [12] Martinez-Lostao L, Garcia-Alvarez F, Basanez G, Alegre-Aguaron E, Desportes P, Larrad L, et al. *Arthritis Rheum*; 62:2272-82 (2010).
- [13] MacFarlane M, Ahmad M, Srinivasula SM, Fernandes-Alnemri T, Cohen GM, Alnemri ES. *J Biol Chem*; 272:25417-20 (1997).
- [14] De Miguel D, Basanez G, Sanchez D, Malo PG, Marzo I, Larrad L, et al. *Mol Pharm*; 10:893-904 (2013).
- [15] De Miguel D, Gallego-Lleyda A, Anel A, Martinez-Lostao L. *Leuk Res*; 39:657-66 (2015).
- [16] De Miguel D, Gallego-Lleyda A, Ayuso JM, Erviti-Ardanaz S, Pazo-Cid R, del Agua C, et al. *Nanotechnology*; 27:185101 (2016).
- [17] De Miguel D, Gallego-Lleyda A, Ayuso JM, Pawlak A, Conde B, Ochoa I, et al. *Recent Pat Anticancer Drug Discov*; 11:197-214 (2016).
- [18] De Miguel D, Gallego-Lleyda A, Ayuso JM, Pejenaute-Ochoa D, Jarauta V, Marzo I, et al. *Cancer Lett*; 383:250-60 (2016).
- [19] De Miguel D, Gallego-Lleyda A, Galan-Malo P, Rodriguez-Vigil C, Marzo I, Anel A, *Clin Transl Oncol*; 17:657-67 (2015).
- [20] Haran G, Cohen R, Bar LK, Barenholz Y. *Biochim Biophys Acta*; 1151:201-15 (1993).

Figures

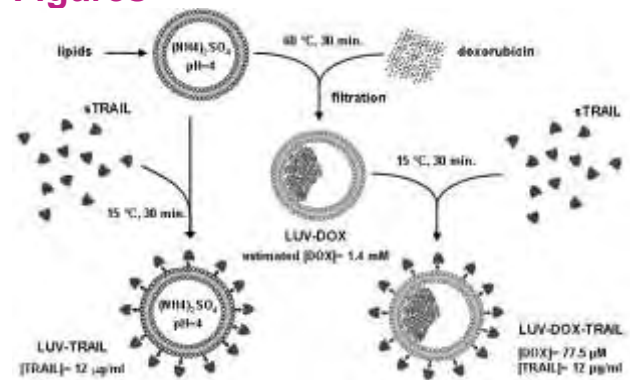


Figure 1. Schematic illustration of the preparation of LUVDOX-TRAIL.

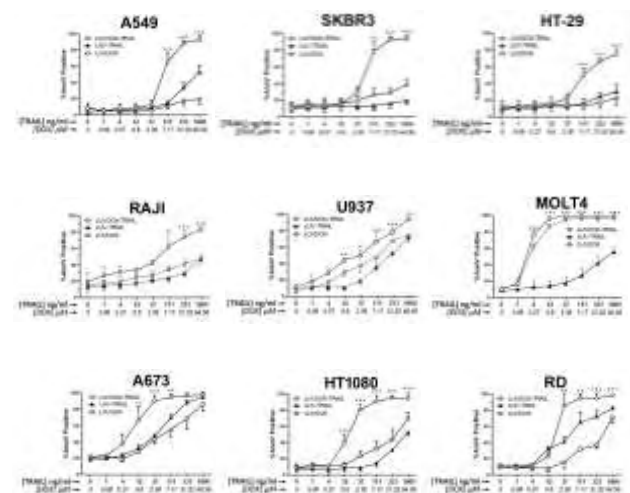


Figure 2. Cytotoxicity assays using LUV-TRAIL, LUVDOX, and LUVDOX-TRAIL in a panel of different cancer types.

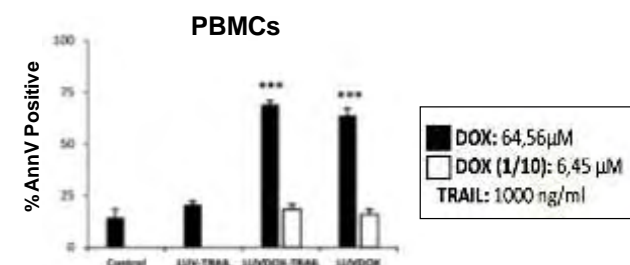


Figure 3. Cytotoxicity assays using LUV-TRAIL, LUDOX, and LUVDOX-TRAIL with two DOX concentrations (64.56 and 6.45 μ M) in normal peripheral blood mononuclear cells (PBMCs).

Enantio-Selective Sensing Using Plasmonic Racemic Arrays

Jose García-Guirado¹,
Mikael Svedendahl^{1,2}, Joaquim Puigdollers³,
Romain Quidant^{1,4}

¹ICFO Institut de Ciències Fotòniques, The Barcelona Institute of Science and Technology, 08860 Castelldefels (Barcelona), Spain

²KTH Royal Institute of Technology, Roslagstullsbacken 21, 10691 Stockholm, Sweden

³UPC Universitat Politècnica de Catalunya, Departament d'Enginyeria Electrònica, 08034 Barcelona, Spain

⁴ICREA Institució Catalana de Recerca i Estudis Avançats, 08010 Barcelona, Spain

romain.quidant@icfo.eu

Abstract

Building blocks of life show well-defined chiral symmetry which has a direct influence on their biochemical properties and role in Nature. Chirality, geometrically understood as the lack of symmetry under specular reflection, is typically exhibited by bio-molecules with a single configuration, i.e. left or right handed. Such molecules are involved in physiological processes like odor, taste, metabolism, neural transmission etc. However, when they are artificially synthesized both enantiomers, the mirrored images, occur. In general, the asymmetric specie does not follow the natural pathways and in the worse scenario one enantiomer acts as a medicine while the other has detrimental effects. Therefore, it is of mayor importance for the pharmaceutical industry to properly synthesize and characterize the artificial chiral compounds [1-3].

On the side of characterizing chiral molecules, several techniques have been developed over the years to differentiate enantiomers. Such techniques include circular dichroism (CD), optical rotatory dispersion (ORD) or Raman optical activity (ROA), where CD is the most widely used. However, the weak chiro-optical activity of the molecules and low sensitivity of the technique makes high concentration and sample volumes a requirement. Additionally, the location of the molecular resonances in the ultraviolet (UV) spectral range makes CD equipment expensive [4,5].

Recent developments in nanotechnologies and photonic sensors come with promising properties that can boost sensitivity in bio-sensing applications [6,7]. In the field of chirality, plasmonic structures have been specially designed to mimic the properties of chiral molecules as well to generate optical fields that better interact with such molecules. These structures can be used as sensors as their optical responses are modified under molecular

interaction. This approach allows translating the CD measurements from the UV to the visible (VIS) spectral range and enables better sensitivity and lower sample volumes than the classical CD technique [8]. However, the best implementation remains unknown and controvert due to low reproducibility of the results presented in the literature over the last years. One of the major drawbacks is to find the optimal sensor, which provides the optimal near and far fields while keeping the experimental implementation feasible. It has been a matter of discussion if sensors producing near-optimal near field configurations and simultaneously high CD signals are the most appropriate for sensing, as their large CD might over-shadow the molecular signatures. At the same time, the theoretical optimization of these parameters has often led unrealizable nanostructures due to nanofabrication limitations. The other major drawback is the reproducibility of the methods and the standards for comparing results. On this side, discussions about the molecular coating of the sensors, solvent compatibility or the significance of the molecular model have been raised [9,10].

In this contribution [11] we present a novel plasmonic sensor configuration that allows the discrimination of chiral molecules. The sensor consists of handed gold nanostructures of gammadion shape, distributed in a racemic (50/50 mixture) matrix with C_4 symmetry. Its optical response enhances the electric field as well as the optical chirality in the near field. Thus, the interaction with molecules is enhanced, while the bare sensors exhibit a flat CD signal, providing background-free CD measurements for molecular detection (Fig. 1a-b). We have used a complete chiral molecular model based on L-, D-, and the racemic mixture of phenylalanine, which allows us to evaluate the opposite chiral effects while having a reference system. Additionally, we have used molecular thermal evaporation (MTE) technique to deposit a dense molecular layer on top of the sensors in a controllable and reproducible way (Fig. 1c-d). Our results show the discrimination of phenylalanine enantiomers through positive or negative peaks while the racemic mixture shows a flat signal (Fig. 2).

As an outlook, we therefore present preliminary results that show that this approach is also suitable for microfluidics systems with much lower density of chiral molecules [12].

References

- [1] Brandt, J. R.; Salerno, F.; Fuchter, M. J.; Nat. Rev. Chem. 2017, 1 (6), 0045.
- [2] Chhabra, N.; Aseri, M.; Padmanabhan, D. A.; Int. J. Appl. Basic Med. Res. 2013, 3 (1), 16.

- [3] Maugh, T. H.; Science (80). 1983, 221 (4608), 351–354.
- [4] Berova, N.; Nakanishi, K.; Woody, R.; John Wiley & Sons, 2000.
- [5] Berova, N.; Polavarapu, P. L.; Nakanishi, K.; Woody, R. W.; Wiley, 2012.
- [6] Aćimović, S. S.; Ortega, M. a.; Sanz, V.; Berthelot, J.; Garcia-Cordero, J. L.; Renger, J.; Maerkl, S. J.; Kreuzer, M. P.; Quidant, R.; Nano Lett. 2014, 14 (5), 2636–2641.
- [7] Yavas, O.; Svedendahl, M.; Dobosz, P.; Sanz, V.; Quidant, R.; Nano Lett. 2017, 17 (7), 4421–4426.
- [8] Hentschel, M.; Schäferling, M.; Duan, X.; Giessen, H.; Liu, N.; Sci. Adv. 2017, 3 (5), e1602735.
- [9] Hendry, E.; Carpy, T.; Johnston, J.; Popland, M.; Mikhaylovskiy, R. V.; Laphorn, a J.; Kelly, S. M.; Barron, L. D.; Gadegaard, N.; Kadodwala, M.; Nat. Nanotech. 2010, 5 (11), 783–787.
- [10] Maoz, B. M.; Chaikin, Y.; Tesler, A. B.; Bar Elli, O.; Fan, Z.; Govorov, A. O.; Markovich, G.; Nano Lett. 2013, 13 (3), 1203–1209.
- [11] García-Guirado, J.; Svedendahl, M.; Puigdollers, J.; Quidant, R.; Nano Lett. 2018, acs.nanolett.8b02433.
- [12] Guirado, J. G.; Quidant, R.; UPC Universitat Politecnica de Catalunya, 2018.

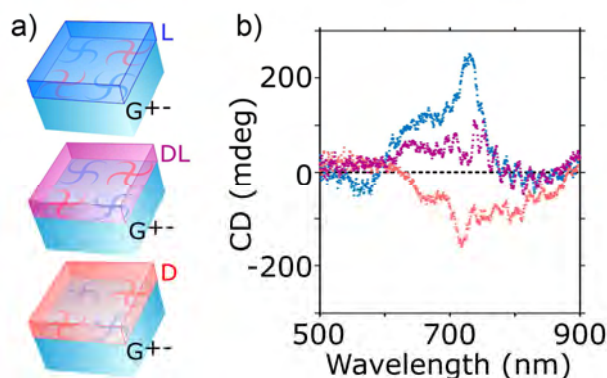


Figure 2. Enantiomer detection in the visible spectral range using racemic gammadian arrays. (a) The molecules were deposited on different sensor arrays, showing the corresponding (b) CD spectrum.

Figures

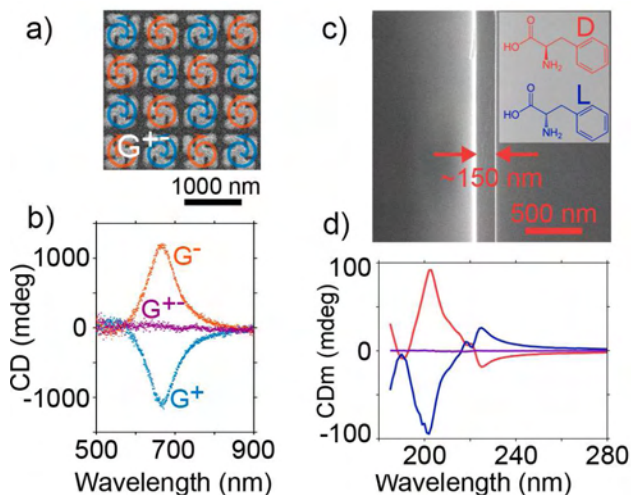


Figure 1. Optical characterization of handed and racemic gammadian arrays and phenylalanine coatings. (a) SEM images of the racemic G⁺ array. (b) CD spectra of the fabricated nanostructures. (c) SEM image of a 150 nm thin layer of DL phenylalanine. (d) CD spectra of the molecular coatings, named CD_m to be distinguished from sensors CD.

Challenging breast cancer brain metastases formation with the plant defensin *PvD₁*

Diana Gaspar¹,
Tiago N. Figueira¹
Filipa D. Oliveira¹
Inês Almeida¹
Érica O. Mello²
Valdirene M. Gomes²
Miguel A. R. B. Castanho¹

¹Instituto de Medicina Molecular, Faculdade de Medicina, Universidade de Lisboa, Av. Prof. Egas Moniz, Lisboa 1649-028, Portugal

²Laboratório de Fisiologia e Bioquímica de Microrganismos do Centro de Biociências e Biotecnologia da Universidade Estadual do Norte Fluminense Darcy Ribeiro, Avenida Alberto Lamego 2000, Campos dos Goytacazes, Rio de Janeiro, 28013-602, Brazil

dianagaspar@medicina.ulisboa.pt

Improvements on breast lesions' treatment are allowing patients to survive to breast cancer disease for longer periods. There is, however, an increase in the incidence of the metastatic disease as the tumor cells have time to settle into different organs, such as the brain.

The management of breast cancer brain lesions requires drugs that efficiently overcome the blood-brain barrier (BBB) but that also recognize cancer cells and accumulate in the intracranial tissues. Breaching the BBB is an important step to consider when designing new therapeutic approaches for the treatment of the metastatic disease.

Our study reveals a potential dual role for a natural antimicrobial plant defensin, *PvD₁*. *PvD₁* is shown to interfere with the integrity of breast tumor cells and with the breast cancer cells' adhesion to human brain endothelial cells [1].

We have used atomic force microscopy (AFM), zeta potential and fluorescence spectroscopy techniques to study the interaction of *PvD₁* with human breast and brain cells. Our data suggests that the plant defensin internalizes in cancer cells while remaining in the membrane of brain cells with no significant changes at the biomechanical level. AFM also revealed *PvD₁* ability in suppressing cell-to-cell adhesion by promoting not only the de-adhesion of breast tumor cells, but also by preventing breast tumor cells' attachment to the BBB cells.

PvD₁ is presented as a potential alternative strategy for managing the formation of brain lesions derived from breast cancer with an innovative therapeutic mechanism of action: manipulation of the biomechanical properties of tumor cells and

suppression of tumor cell adhesion to the BBB surface.

Acknowledgements: This work was supported by a grant from Laço (Portugal). The authors thank Fundação para a Ciência e a Tecnologia (FCT I.P., Portugal) and Marie Skłodowska-Curie Research and Innovation Staff Exchange (RISE) for funding-PTDC/BBB-BQB/1693/2014 and call H2020-MSCA-RISE-2014, Grant agreement 644167, 2015-2019, respectively, and acknowledge the financial support of the Brazilian agencies CNPq, CAPES, FAPERJ (E-26/203.090/2016; E-26/202.132/2015). T. N. Figueira, F. D. Oliveira and Diana Gaspar acknowledge FCT I.P. for fellowships SFRH/BD/5283/2013, PD/BD/135046/2017 and SFRH/BPD/109010/2015.

References

- [1] Figueira, T. N., Oliveira, F. D., Almeida, I., Mello, E. O., Gomes, V. M., Castanho, M. A. R. B., Gaspar, D., *Nanoscale*, 9 (2017) 16887

Characterization and stability of chitosan-based nanoparticles as efficient non-viral gene delivery system

Limeres María José^{1,3}, Prieto-Sánchez S.², Hernández-Munain C.², Suñé C.², Nusblat A.⁴, Cuestas M.L.³, Suñé-Negre J.M.¹, Suñé-Pou M.^{1,2}

¹ Service of Development of Medicines (SDM), Faculty of Pharmacy, University of Barcelona, Barcelona, Spain.

² Institute of Parasitology and Biomedicine "López-Neyra" (IPBLN-CSIC), Granada, Spain.

³ Institute of Research in Microbiology and Medical Parasitology (IMPAM), Faculty of Medicine, University of Buenos Aires, Buenos Aires, Argentina

⁴ Institute of Nanobiotechnology (NANOBIOTEC), Faculty of Pharmacy and Biochemistry, University of Buenos Aires, Buenos Aires, Argentina.

mj.limeres@conicet.gov.ar

Introduction:

Chitosan (CS) is a linear cationic polysaccharide that is obtained commercially by the deacetylation of the chitin which is a biopolymer that is widely distributed in nature. Due to its characteristics of biocompatibility, biodegradability and non-immunogenicity, constitutes a suitable biomaterial for the design of nanoparticles, allowing *in vivo* applications [1]. It is also considered as a GRAS substance by the FDA.

This polysaccharide has in its structure primary amino groups with a pKa of 6.5, therefore, in moderately acidic media these groups are protonated allowing the interaction with multivalent negatively charged molecules such as the polyelectrolyte sodium tripolyphosphate (TPP). Thus, the interaction between them in defined proportions and with the established parameters of a suitable technique leads to the self-assembly and the formation of chitosan-TPP nanoparticles.

The aim of this work is to define and characterize the most suitable formulation of chitosan cationic polymeric nanoparticles with the addition of a diblock copolymer of ethylene oxide and propylene oxide (poloxamer P188), evaluating their potential application as non-viral gene delivery system [2,3].

Materials & Methods:

The CS-based nanoparticles were produced using a modified ionotropic gelation method [4,5] in the presence of the TPP ionic cross-linker molecule. Briefly, a solution of chitosan (low molecular weight) at 0.2% (w/v) was prepared in acetic buffer solution at pH=5 and was stirred overnight to allow the complete dissolution of the polymer. In one part of the chitosan solution, 1% (w/v) and 0.5% (w/v) poloxamer P188 was added to evaluate the stability of nanoparticles in the presence of this surfactant. The solutions were filtered to discard not dissolved chitosan molecules. Then, a solution of 0.84 mg/mL

TPP was added dropwise to the chitosan solution for 5 minutes under constant stirring at room temperature. The final suspension was centrifuged and filtered to obtain de CS-based nanoparticles. The stability of two different ratios of CS-TPP nanoparticles, 6:1 and 3:1, was assessed at 4 °C and 25 °C. The particle size and the zeta potential were measured by the laser diffraction method (Mastersizer) and the laser Doppler microelectrophoresis method (Zetasizer) respectively. The morphology of the nanoparticles of CS-TPP-1%P188 was characterized by transmission electron microscopy (TEM), and finally the loading efficiency with different amounts of plasmidic DNA was performed by agarose gel electrophoresis.

Results:

Stability studies showed the presence of aggregates in the nanoparticles formulation of CS-TPP without P188 at day 7 at 4 °C and at day 3 at 25 °C, while formulations containing the surfactant maintained their size at that time. In addition, we observed that the nanoparticles with the highest amount of P188 were smaller in size, which may explain their higher stability. Regarding the zeta potential, all the formulations maintained the values over the time. However, the initial zeta potential of the ratio 3: 1 nanoparticles was lower, therefore being discarded as non-viral gene delivery system. The TEM images confirm the results obtained with the Mastersizer, showing spherical nanoparticles with a homogenous distribution. Finally, the loading efficiency performed by agarose gel electrophoresis suggested that CS-TPP-1%P188 nanoparticles are capable to complex DNA at the studied proportions, and no free DNA was observed in the gel.

Conclusions:

The characterization of the different chitosan nanoparticles obtained and the stability studies determining particle size and zeta potential over time at different conditions allow the selection of the most stable and suitable formulation. In addition, polyplexes with DNA were obtained with 100% loading efficiency, demonstrating its potential application a non-viral gene delivery system.

References

- [1] Garcia-Fuentes M. *et al.* Journal of Controlled Release, 161 (2012) 496-504.
- [2] Prego C. *et al.* Vaccine, 28 (2010) 2607-2614.
- [3] Carrillo C. *et al.* Biomedicine and Pharmacotherapy, 68 (2014) 775-783.
- [4] Calvo P. *et al.* Journal of Applied Polymer Science, 63 (1997) 125-132.
- [5] Fàbregas A. *et al.* International Journal of Pharmaceutics, 446 (2013) 199-204.

Figures

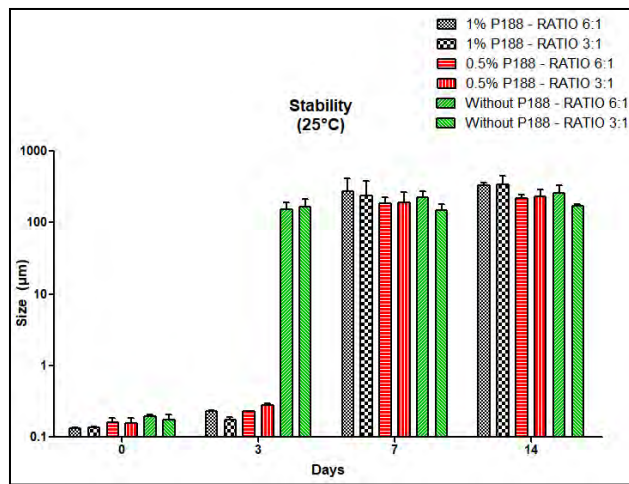
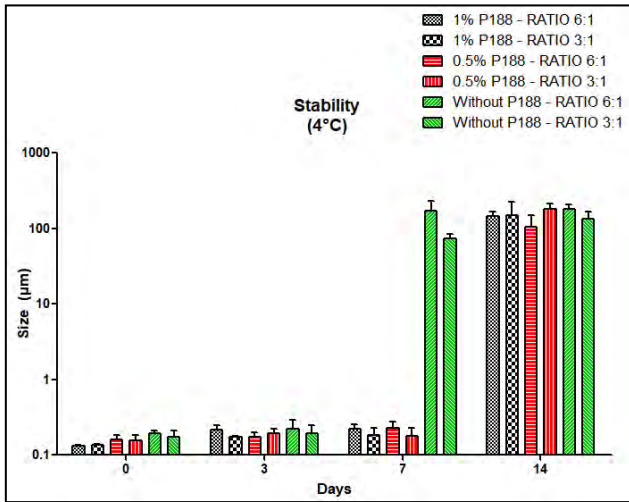


Figure 1 and 2. Variation of the size as a function of time at 4° C and 25 °C respectively of chitosan-TPP nanoparticles with and without poloxamer P188. The ratios of Chitosan-TPP assessed were 6:1 and 3:1.

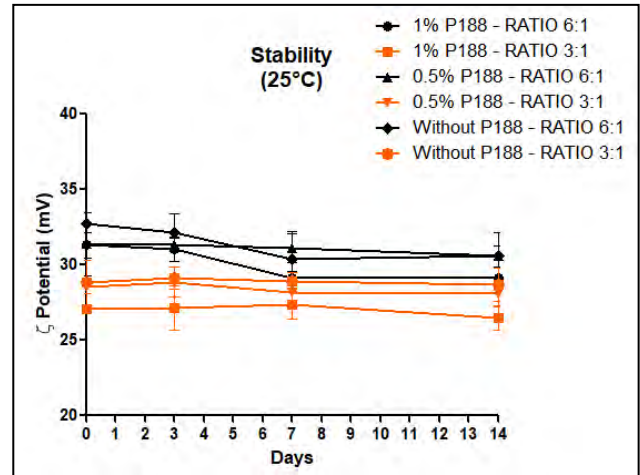
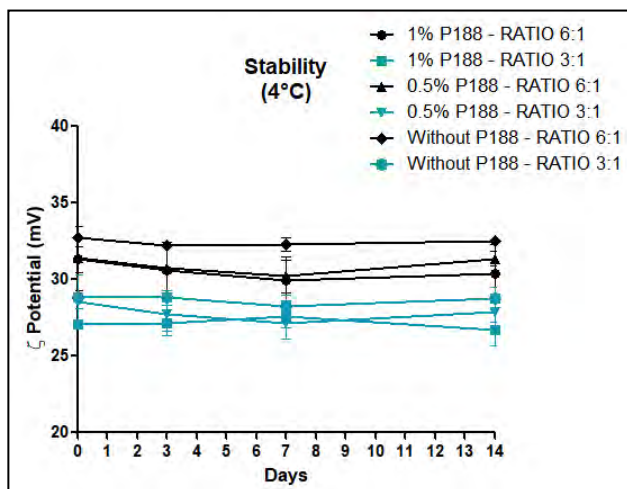
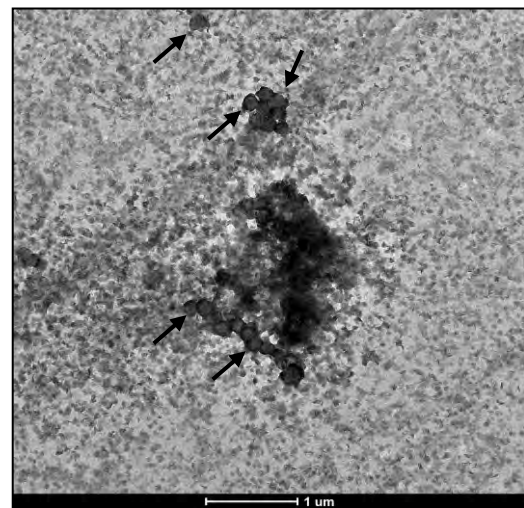


Figure 3 and 4. Variation of the zeta potential as a function of time at 4 °C and 25 °C respectively of chitosan-TPP nanoparticles with and without poloxamer P188. The ratios of Chitosan-TPP assessed were 6:1 and 3:1.



Average size	Shape
(0,131 ± 0,010) µm	Spherical

Figure 5 and table 1. Morphological analysis of CS-TPP-1%P188 nanoparticles by transmission electron microscopy (TEM).

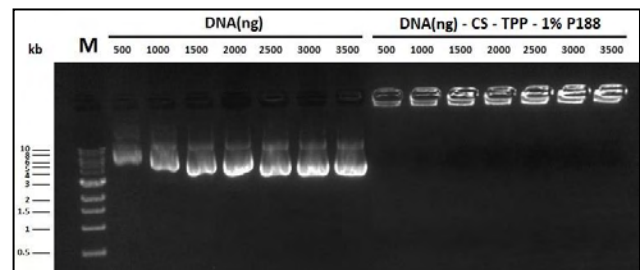


Figure 6. Loading efficiency of CS-TPP-1%P188 nanoparticles to different amounts of plasmidic DNA by agarose gel electrophoresis.

Enzyme-Powered Nanomotors for Biomedical Applications

Ana C. Hortelão¹, Tania Patiño¹, Samuel Sánchez^{1,2}

¹ Institute for Bioengineering of Catalonia (IBEC), The Barcelona Institute of Science and Technology (BIST), Baldiri Reixac 10-12, 08028 Barcelona Spain

² Institució Catalana de Recerca i Estudis Avançats (ICREA), Pg. Lluís Companys 23, 08010, Barcelona, Spain

ahortelao@ibecbarcelona.eu

Catalytic nanomotors are structures able to propel in fluids due to the conversion of a substrate into products.¹ Inspired by nature, bio-hybrid micro- and nanomotors that use enzymes as power sources have recently been developed.^{2,3} These biocatalytic nanomotors have unique properties, such as biocompatibility, bioavailability and versatility, which make them excellent candidates for biomedical applications. Herein, we present the potential of enzymatic nanorobotic devices for cancer therapy. In this regard, we explored the effect of active motion on the doxorubicin anti-cancer drug release and intracellular delivery, using urease-powered nanomotors. We observed a four-fold increase on drug release from active nanomotors in the presence of fuel compared to passive nanoparticles, leading to an improved anti-cancer efficiency towards HeLa cells. This arises from a synergistic effect of the boosted drug release and the ammonia produced by urea breakdown.⁴ The potential of urease-powered nanomotors as anti-cancer agents was further explored by modifying their surface to target cancer cells in 3D cell cultures (spheroids). A 14-fold increase of the penetration of targeted nanomotors into 3D spheroids was observed, when compared to passive non-targeted nanoparticles. These results could pave the way towards the implementation of enzyme-powered nanomachines as smart drug delivery vehicles to address current challenges in nanomedicine.

References

- [1] Katuri, J.; Ma, X.; Stanton, M. M.; Sanchez, S., *Acc. Chem. Res.*, 50 (2016) 2-11
- [2] Ma, X.; Hortelão, A. C.; Patiño, T.; Sánchez, S., *ACS Nano*, 10 (2016) 9111–9122
- [3] Patiño, T.; Feiner-Gracia, N.; Arqué, X.; Miguel-López, A.; Jannasch, A.; Stumpp, T.; Schäffer, E.; Albertazzi, L.; Sánchez, S. *J. Am. Chem. Soc.*, 140 (2018) 7896–7903
- [4] Hortelão, A. C.; Patiño, T.; Perez-Jiménez, A.; Blanco, À.; Sánchez, S. *Adv. Funct. Mater.*, 28 (2018) 1705086

Figures

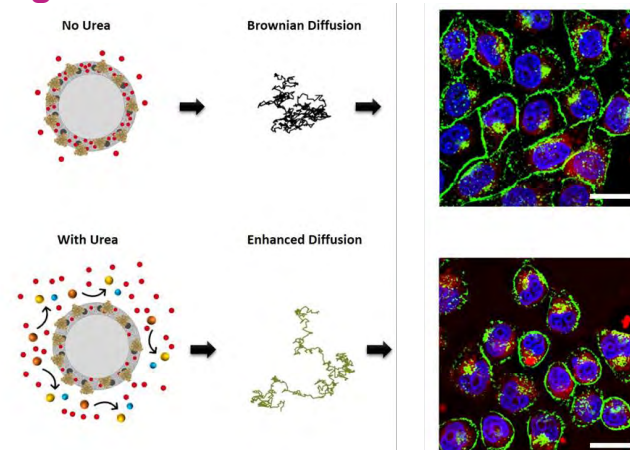


Figure 1. Enhanced anti-cancer drug release and delivery efficiency to HeLa cells by actively moving urease-powered nanomotors.

IL15 vehiculized Iron Oxide nanoparticles as a tool to enhance NK cell mediated-activity

I. Mikelez-Alonso^{1,2},

Juan C. Mareque-Rivas³, F. Borrego^{2,4}, Aitziber L. Cortajarena^{1,4}

¹CIC biomaGUNE, Parque Científico y Tecnológico de Gipuzkoa. Paseo Miramón 182, 20014 Donostia / San Sebastián, Spain

²Biocruces Bizkaia Health Research Institute, Cruces Plaza, 48903 Barakaldo, Spain
³Swansea University Singleton Park Swansea SA2 8PP Wales, UK

⁴Ikerbasque, Basque Foundation for Science 48011 Bilbao, Spain

francisco.borregorabasco@osakidetza.eus
alcortajarena@cicbiomagune.es

Nanoparticles (NPs) have a clinical interest because of their usefulness for non-invasive imaging, diagnosis and therapy. Using NPs in cancer immunotherapy is a promising therapeutic strategy. Important challenges are targeting the therapy to specific locations [1], [2] and the induction of specific cytotoxic activity against cancer cells. Natural killer (NK) cells are one type of immune cell that is currently used in cancer immunotherapy with very promising results [3].

It is known that the activation of NK cells with cytokines such as interleukin (IL)15 enhance their effector functions [4], [5]. NPs coated with activating molecules could be an effective new approach to generate robust and potent immune responses against cancer through the innate immune response. In this study we show a nanoformulation, based on biocompatible, biodegradable and traceable materials, which is able to selectively enhance NK cell function.

Spherical hydrophobic Iron Oxide NPs (IONPs) coated with PEG-phospholipid were used. Recombinant human his-tagged IL15 (hIL15HIS) was expressed and purified for a his-tag based bioconjugation strategy (Figure 1).

Activation of human NK cells from Peripheral Blood Mononuclear Cells (PBMCs) was explored by incubating the cells with the activation molecule.

We are able to demonstrate *in vitro* that his-tagged human IL15 (hIL15HIS) is able to enhance NK cell mediated-activity in a similar way, or even slightly stronger, compared with the commercial hIL15 administered in solution.

We expect that in on going and future experiments, that the transpresentation of IL15 using the

hIL15HIS-IONP nanoformulation, compared with soluble IL15, will significantly enhance NK cell mediated-activity against cancer cells.

References

- [1] A. Ruiz-De-Angulo, A. Zabaleta, V. Gómez-Vallejo, J. Llop, and J. C. Mareque-Rivas, "Microdosed lipid-coated 67Ga-magnetite enhances antigen-specific immunity by image tracked delivery of antigen and cpg to lymph nodes," *ACS Nano*, vol. 10, no. 1, pp. 1602–1618, 2016.
- [2] A. Aires, J. F. Cadenas, R. Guantes, and A. L. Cortajarena, "An experimental and computational framework for engineering multifunctional nanoparticles: Designing selective anticancer therapies," *Nanoscale*, vol. 9, no. 36, pp. 13760–13771, 2017.
- [3] R. Romee *et al.*, "Cytokine-induced memory-like natural killer cells exhibit enhanced responses against myeloid leukemia," *Sci. Transl. Med.*, vol. 8, no. 357, p. 357ra123-357ra123, 2016.
- [4] H. Kobayashi *et al.*, "Role of trans -cellular IL-15 presentation in the activation of NK cell – mediated killing , which leads to enhanced tumor immunosurveillance," *Blood*, vol. 105, no. 2, pp. 721–727, 2005.
- [5] I. Terrén *et al.*, "Implication of interleukin-12/15/18 and ruxolitinib in the phenotype, proliferation, and polyfunctionality of human cytokine-preactivated natural killer cells," *Front. Immunol.*, vol. 9, no. APR, 2018.

Figures

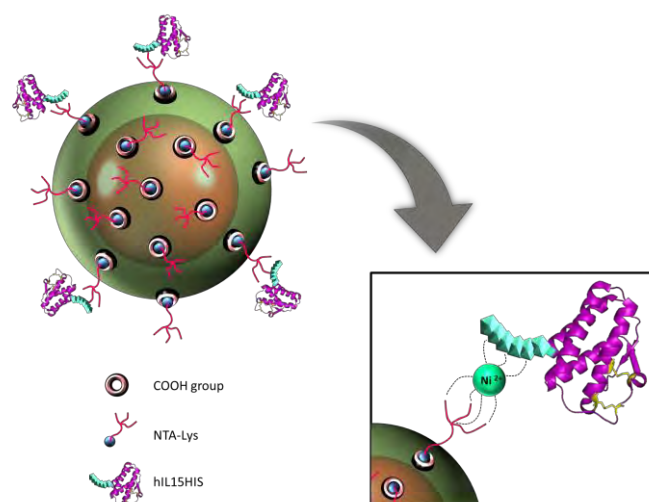


Figure 1. Schematic representation of the strategy used for the preparation of hIL15HIS-IONP.

Monitoring cancer cell treatment by Nanoparticle-assisted lab-on-a-chip (LoC)

Marta Monge^{1,2,3,4},

John González-Murillo^{4,5}, María José García-Celma^{1,3,4}, Mauricio Moreno^{4,5}, Albert Romano-Rodríguez^{4,5},
Josep Samitier^{3,4,5,6}, Winnie E Svendsen⁷ and Romen Rodríguez-Trujillo^{4,5,6}

¹Department of Pharmacy and Pharmaceutical Technology and Physical Chemistry, Universitat de Barcelona, Barcelona, 08028, Spain

²Institute for Advanced Chemistry of Catalonia (IQAC-CSIC), Spain

³Networking Centre on Bioengineering, Biomaterials and Nanomedicine (CIBER-BBN), Spain

⁴Institute of Nanoscience and Nanotechnology (IN2UB), Universitat de Barcelona, 08028 Barcelona, Spain

⁵Department of Electronics and Biomedical Engineering, Universitat de Barcelona, Barcelona, 08028, Spain

⁶Institute for Bioengineering of Catalonia (IBEC-BIST), 08028 Barcelona, Spain

⁷Department of Micro & Nanotechnology, Technical University of Denmark (DTU-Nanotech), 2800 Kgs. Lyngby, Denmark

marta.monge@iqac.csic.es

In the field of nanomedicine, the design of biocompatible nanocarriers to achieve a selective and efficient targeting either to treat or tag specific tumour or diseased cells is a challenge. Among the numerous developed colloidal systems, nanoparticles have demonstrated to be excellent carriers for drug delivery (1). Nanoparticles are advantageous for biomedical applications for different reasons. They can be designed using non-toxic, biocompatible and biodegradable compounds, employing low-energy methods at low temperature to maintain the material properties (2). Nanoparticles can be designed with the required characteristics, such as shape, size, surface charge, conformation and hydrophilicity, which have been described in the literature to play an important role for the nanoparticle fate in the body (3)

When new drugs are developed for their use in cancer research, it is very important to evaluate their performance in a fast and accurate way. In this direction, the ability of monitoring the viability of cancer cells that have been treated with a specific drug can determinably influence the applied therapy and have a strong effect on the associated morbidity rates. Cell viability and cytotoxicity assays are used for drug screening and cytotoxicity tests of chemicals. In particular, the MTT assay is a colorimetric assay for assessing cell metabolic activity. This method is a well-used standard because it is easy-to-use and safe. However some considerations must be taken into account to improve the reproducibility of the MTT assay (4). In addition, MTT assay is a not automated process that needs large technical operation and the viability rates are obtained after 3 days. A faster and more reliable method to address cell viability during nanoparticle-assisted cancer treatment assays in vitro would then be highly desirable.

The study of cell electrical response at different frequencies provides one with information concerning not only geometrical aspects of the cells (size, shape, etc...) but also information about cell internal structure and composition (5). It has already

been demonstrated, for example (6), that cells have unique electrical properties that can be used to identify cell populations. Of particular interest results to determine whether the cell is alive or dead using purely electrical methods.

In this context, the aim of this work is to develop a fast and easy protocol to monitor experimentally nanoparticle-based cancer drug treatment, which can be further extended to other cancer-treatment methodologies. The device presented is a combination of a therapeutic nanosystem based on polymeric drug-carrier nanoparticles, and a microfluidic device to test an on-set viability assessment monitoring technology based on Single-cell electrical impedance spectroscopy analysis (7). This type of label-free technique has many advantages, the most important being the possibility to detect the cancer cell viability based on their intrinsic electrical properties (8), overcoming the limitations of the existing methods as sensitivity, reproducibility and, especially, long test waiting times. This permits the detection and identification of cells without the need of any kind of pre-treatment steps, like fluorescence labelling, used typically in commercial flow cytometers or colorimetric assays (7).

In this work, a sc-EIS microcytometer (8) has been used in order to address the viability test. The chip is made in a glass wafer by means of standard UV photolithography and metal evaporation. It is composed by 100nm thick gold coplanar electrodes, a 30 μ m thick layer of SU8 to make a microfluidic channel and a flat PDMS gasket used to seal the channel (Figure 1). The Poly(lactic-co-glycolic acid) (PLGA) nanoparticles have been produced from nano-emulsions by the PIC method using the PBS 0.16 M (W)/polysorbate 80 (S)/[4 wt% PLGA in ethyl acetate] (O) system (Figure 2). A HeLa cells suspension, previously treated with PLGA nanoparticles drug-loaded with Paclitaxel, was injected into the microcytometer. Impedance signals acquired were processed to make the cell viability assessment by comparing the amplitude of the high

(HF) and low frequency (LF) components. The viability results obtained from the MTT assay and the microfluidic device were then compared.

References

- [1] Couvreur P. *Adv Drug Deliv Rev*, 65 (1), (2013), 21-23.
- [2] Anton N, Benoit JP, Saulnier P. *J Control Release*, 128(3), (2008) 185-99
- [3] Duchene D, Gref R., *Int J Pharmaceutics* 502, (2016) 219-231
- [4] Wan H, Williams R, Doherty P, Williams DF. *J Mater Sci: Mater Med*, 5 (3), (1994) 154-159.
- [5] Marx GH, Davey CL. *Enzyme Microb Tech*, 25, (1999) 161-171.
- [6] Yang J, Huang Y, Wang XB, Becker FF, Gascoyne PRC. *Anal Chem*, 71, (1999) 911-918.
- [7] T. Sun and H. Morgan, "Single-cell microfluidic impedance cytometry: a review," *Microfluid. Nanofluidics*, 8(4), (2010) 423–443
- [8] J Kirkegaard, C.H. Clausen, R. Rodriguez-Trujillo, W.E. Svendsen, *Biosensors*, 4(3) (2014) 257-272..

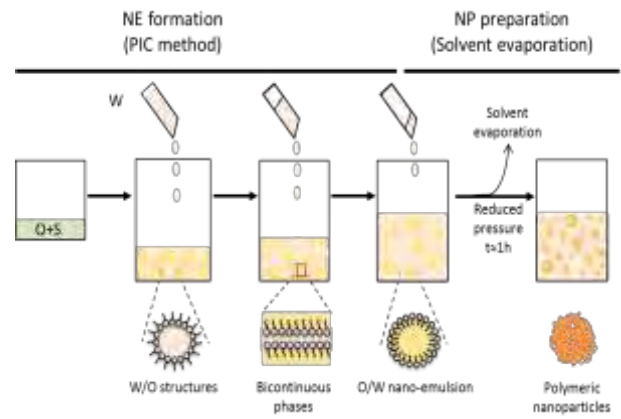


Figure 2. Schematic of the PLGA nanoparticle synthesis

Figures

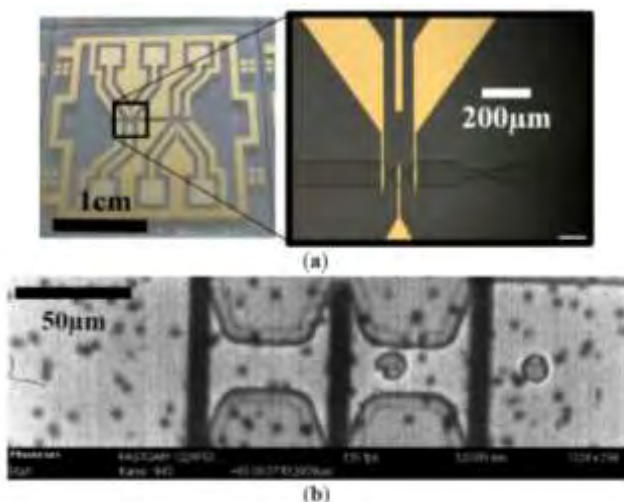


Figure 1. (a) Picture of the microfabricated impedance cytometer showing the zoom of the sensing area. (b) HeLa cells crossing the constricted channel sensing area with gold electrodes

A Portable System for Measuring the Tactile Temporal Discrimination Threshold in Cervical Dystonia

Yaiza Montes-Cebrián^{1,2},

Albert Álvarez-Carulla¹, Jordi Colomer-Farrarons¹, Eugene O'Rourke², Ihedinachi Ndukwe³, Sean O'Riordan³, Michael Hutchinson³, Pere LL. Miribel-Català¹, Richard B. Reilly².

¹ Discrete-2-Integrated Research Group (D2In), Department of Electronics and Biomedical Engineering Faculty of Physics, University of Barcelona Barcelona, Spain

² Trinity Centre for Bioengineering, Trinity College Institute of Neuroscience, School of Engineering, Trinity College, The University of Dublin, Ireland

³ Department of Neurology, St Vincent's University Hospital, Dublin, Ireland

ymontes@ub.edu

Background

This multidisciplinary study combined both bioelectronics and neuroscience, with the aim of developing a tool to probe the underlying neuropathology of the movement disorder Dystonia.

Dystonia is the third most common neurological movement disorder - after Parkinson's disease and Essential Tremor [1] *Fahn*. It is characterized by sustained or intermittent muscle contractions causing abnormal, often repetitive, movements or postures. The hypothesis of the pathomechanisms of dystonia is based on disordered inhibition affecting brainstem mechanisms of covert attentional orienting. Temporal discrimination is the shortest time interval at which an observer can discriminate two sequential stimuli as being asynchronous. Temporal discrimination provides a mechanism for probing covert attentional orienting [2]. Visually assessed temporal discrimination thresholds (V-TDT) have demonstrated that covert attention is abnormal in cervical dystonia patients [3]. A portable system for V-TDT testing has been previously developed [4] , [5].

In this study, we developed a portable biosensor platform for measuring digit based tactile based temporal discrimination threshold (T-TDT). By combining tactile with visual temporal discrimination thresholds, it is hypothesised that one can increase the discrimination ability to probe covert attentional orienting in dystonia. The new portable instrument for T-TDT testing was validated against the gold standard methods described in the literature.

Methods

A hardware and software system were developed to produce two vibro-tactile stimuli of 5msec duration with precise inter-stimulus intervals (ISI). In the 'staircase' mode of the TDT experiment the ISI is varied from 0msec in increasing steps of 5ms. At each ISI the participant is asked to state if they perceive a single stimulus, i.e. synchronous, or two stimuli separated in time as asynchronous. The test ends when the participant responds "asynchronous" for three consecutive increasing ISIs. The experiment is then ended by the Experimenter pressing a stop button. The TDT is then reported as the first of these ISIs.

In another mode of the experiment a random method of ISI presentation can be selected. Here the ISI is randomized between 0 to 100 ms. The experiment ends after a set duration with the Experimenter pressing a stop button.

The system realised has small dimension. The device was designed and built in-house at the Trinity Centre for Bioengineering, Trinity College Dublin.

The system is divided into three main blocks: the control unit, the vibrotactile stimulation unit and the Experimenter's user interface. See Figure 1.

The control unit is based on an Arduino ATmega328 microcontroller and includes a USB port to provide power and data communications. The microcontroller controls the vibrotactile stimulation unit that produces square pulses that generates the stimuli presented to the participant's fingers.

To generate the tactile stimuli, two vibration motors were employed. Vibrotactile stimulation generation is more power efficient than electrotactile stimulation systems [6]. Microcontrollers can only provide a small amount of current from their output as these are intended to send control signals, not to act as power sources. In order to control a high-current DC load, such as a DC motor it is necessary to use a motor driver. In this device a Metal-oxide-semiconductor Field-effect transistor (MOSFET) was employed as a switch for high-current loads.

The microcontroller also controls the user interface consisting of a 2.4" touch Thin Film Transistor-Liquid Crystal Display (TFT-LCD) screen. This screen provides the experimenter with a means for entering data relevant to the TDT experiment (experimental mode). The interface also allows data (experimental mode, ISI interval when stimulus asynchrony detected etc.) to be sent and saved to a computer via serial port avoiding errors in data collection.

Results

To validate the system, two TDT test were performed to two healthy control participants (2 females of 22 and 26 years old) with a mean TDT raw score of 30 msec and 32.5 msec respectively.

These values compare to the those in the literature [7], [8].

Discussion

The portable platform developed is a reliable and accurate method for tactile temporal discrimination testing in outpatient clinic environments. Furthermore, as it is a portable and easy-to-use system it increases the opportunity to gather more TDT data in the target population. Further development will focus on integrating both visual and tactile temporal discrimination threshold testing in one multimodal portable system.

References

- [1] S. Fahn, 'Concept and classification of dystonia.', *Fahn S, Marsden CD, Calne DB, Ed. Dystonia 2. Adv. Neurol. New York Raven Press*, vol. 50, pp. 1–8, 1988.
- [2] M. Hutchinson *et al.*, 'Cervical dystonia: a disorder of the midbrain network for covert attentional orienting.', *Front. Neurol.*, vol. 5, p. 54, 2014.
- [3] D. Bradley *et al.*, 'Temporal discrimination thresholds in adult-onset primary torsion dystonia: an analysis by task type and by dystonia phenotype', *J. Neurol.*, vol. 259, no. 1, pp. 77–82, Jan. 2012.
- [4] A. Molloy *et al.*, 'A headset method for measuring the visual temporal discrimination threshold in cervical dystonia.', *Tremor Other Hyperkinet. Mov. (N. Y.)*, vol. 4, p. 249, 2014.
- [5] R. B. Beck *et al.*, 'Measurement & Analysis of the Temporal Discrimination Threshold Applied to Cervical Dystonia', *J. Vis. Exp.*, no. 131, pp. e56310–e56310, Jan. 2018.
- [6] V. Yem and H. Kajimoto, 'Comparative Evaluation of Tactile Sensation by Electrical and Mechanical Stimulation', *IEEE Trans. Haptics*, vol. 10, no. 1, pp. 130–134, Jan. 2017.
- [7] G. Kägi *et al.*, 'Endophenotyping in idiopathic adult onset cervical dystonia', *Clin. Neurophysiol.*, vol. 128, no. 7, pp. 1142–1147, Jul. 2017.
- [8] A. Conte *et al.*, 'Does the Somatosensory Temporal Discrimination Threshold Change over Time in Focal Dystonia?', *Neural Plast.*, vol. 2017, pp. 1–6, Sep. 2017.

Figures

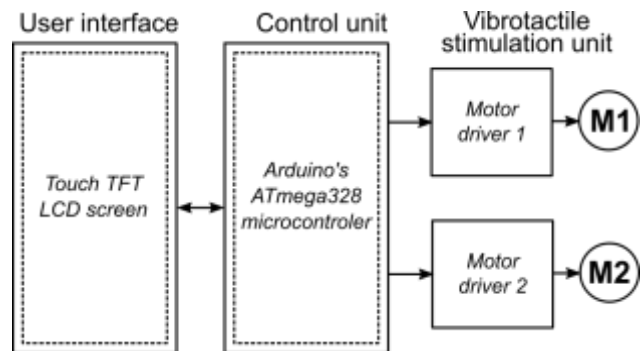


Figure 1. Block diagram of the system.



Figure 2. Picture of the device.

Acknowledgment

This project has been developed within the framework of an international predoctoral stay that has established a collaboration between the University of Barcelona and Trinity College, The University of Dublin.

Yaiza Montes-Cebrián would like to thank the University of Barcelona for the international fellowship granted to carry out predoctoral stay in Dublin (Ireland). Also, the authors would like to acknowledge the support of the MINAUTO Project (TEC2016-78284-C3-3-R), Ministerio de Economía, Industria y Competitividad – Agencia Estatal de Investigación, and Fondo Europeo de Desarrollo Regional (AEI/FEDER, UE).

Purification, characterization and drug loading of extracellular vesicles derived from *Plasmodium*-infected and non-infected red blood cells

Livia Neves Borgheti-Cardoso^{1,2}, Lucía Gutiérrez Chamorro^{1,2}, Irene Fernández³, Xavier Fernández-Busquets^{1,2,4}

¹Nanomalaria Group, Institute for Bioengineering of Catalonia (IBEC), Barcelona, Spain

²Barcelona Institute for Global Health (ISGlobal), Barcelona, Spain

³Unitat d'Espectrometria de Masses de Caracterització Molecular CCiTUB, Universitat de Barcelona (UB), Barcelona, Spain

⁴Nanoscience and Nanotechnology Institute (IN2UB, UB), Barcelona, Spain

lborgheti@ibecbarcelona.eu

Extracellular vesicles (EVs) are membranous vesicles released by almost all cell types and can be classified into microvesicles and exosomes based on their size and the origin of their formation. EVs have been recently gaining considerable scientific interest due to their confirmed involvement in numerous essential cellular processes [1] and their established participation in the pathology of numerous parasitic diseases [2]. Malaria is a life-threatening disease caused by the parasite *Plasmodium* that is transmitted to people through the bites of infected female *Anopheles* mosquitoes during a blood meal. According to the World Health Organization, in 2016, there were an estimated 216 million cases of malaria in 91 countries, leading to 445,000 deaths [3]. EVs containing parasite proteins and nucleic acids are released from both early and late *Plasmodium* stages. It has been demonstrated that EVs mediate cell–cell communication and are internalized by *Plasmodium*-infected red blood cells (pRBCs) [4,5]. Moreover, host-derived vesicles from endothelial cells, erythrocytes and platelets have been also found to increase their quantity during infection and have been related to enhanced disease pathogenesis [6], promoting the pRBC adhesion to brain capillaries characteristic of severe malaria [7,8]. The potential use of EVs as drug delivery vehicles has been recently gaining increased attention due to intrinsic cell targeting properties imparted by their surface ligand and adhesion molecules, their natural ability to deliver cargo into cells, and their protection from degradation in the circulation. In addition, they are able to cross biological filters such as the blood–brain barrier and, they are nearly non-immunogenic when used autologously [9]. In this way, we are proposing EVs derived from pRBCs or non-infected red blood cells (RBCs) as a targeted drug delivery

system for the treatment of malaria. The supernatants of pRBC and RBC cultures have been used to isolate EVs, which were purified combining sequential rounds of centrifugation at increasing speed, high molecular weight cut-off filters and size exclusion chromatography (SEC). Purified EVs derived from pRBCs and RBCs were characterized by dynamic light scattering, cryogenic transmission electron microscopy, and proteomic and lipidomic analyses. The antimalarial drug chloroquine (CQ) has been loaded in RBCs before EV isolation and the capacity of the resulting CQ-loaded EVs to inhibit the growth of *Plasmodium falciparum* parasites was evaluated. EVs derived from RBCs were used as control in this study. EVs from both pRBCs and RBCs exhibited vesicular shape and size around 200 nm with low polydispersity (Figure 1). EVs had different protein composition as a function of their origin, whereas no significant differences in lipid composition have been detected between EVs derived from RBCs and pRBCs. Both EVs and CQ-loaded EVs interfere with parasite growth (Figure 2 and 3). Further experiments will be performed to improve the efficiency of CQ-loaded EVs to inhibit the growth of parasites and to understand the effect of EVs without drugs on parasite growth. Funding: grant BIO2014-52872-R (MINECO, Spain), and European Commission under Horizon 2020's Marie Skłodowska-Curie Actions COFUND scheme (Grant Agreement no. 712754), Severo Ochoa programme (Grant SEV-2014-0425 (2015-2019)).

References

- [1] S. El Andaloussi, I. Mäger, X.O. Breakefield, & M.J.A. Wood., Nat. Rev. Drug Discov., 12 (2013) 347–57.
- [2] A. Marcilla, L. Martin-Jaular, M. Trelis, A. de Menezes-Neto, A. Osuna, D. Bernal, C. Fernandez-Becerra, I.C. Almeida, & H.A. del Portillo., J. Extracell. Vesicles, 3 (2014) 25040.
- [3] "World Health Organization", (2018), <http://www.who.int/news-room/fact-sheets/detail/malaria>.
- [4] P.Y. Mantel, A.N. Hoang, I. Goldowitz, D. Potashnikova, B. Hamza, I. Vorobjev, I. Ghiran, M. Toner, D. Irimia, A.R. Ivanov, N. Barteneva, & M. Marti, Cell Host Microbe, 13 (2013) 521–534.
- [5] N. Regev-Rudzki, D.W. Wilson, T.G. Carvalho, X. Sisquella, B.M. Coleman, M. Rug, D. Bursac, F. Angrisano, M. Gee, A.F. Hill, J. Baum, & A.F. Cowman., Cell, 153 (2013) 1120–1133.
- [6] N.G. Sampaio, L. Cheng, & E.M. Eriksson. Malar. J., 16 (2017) 1–11.
- [7] L.B. Pankoui Mfonkeu, I. Gouado, H. Fotso Kuate, O. Zambou, P.H. Amvam Zollo, G.E.R. Grau, & V. Combes, PLoS One, 5 (2010) e13415.

- [8] F.M.F. Campos, B.S. Franklin, A. Teixeira-Carvalho, A.L.S. Filho, S.C.O. de Paula, C.J. Fontes, C.F. Brito, & L.H. Carvalho. , *Malar. J.*, 9 (2010) 327.
- [9] P. Vader, E.A.Mol, G. Pasterkamp, R.M. Schiffelers, *Adv. Drug Deliv. Rev.*, 106 (2016) 148–156.

Figures

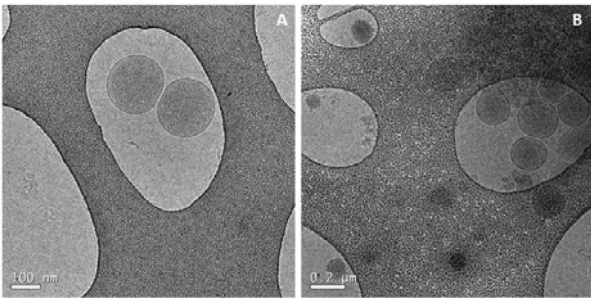


Figure 1. Cryogenic transmission electron microscopy (cryo-TEM) images of extracellular vesicles derived from non-infected RBCs (A) and *Plasmodium*-infected RBCs (B).

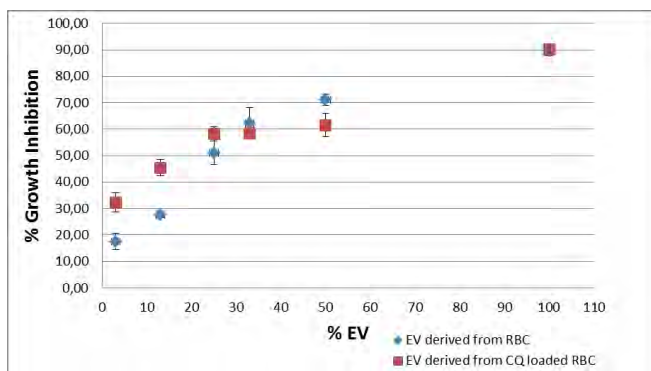


Figure 2. Growth inhibition of *Plasmodium falciparum* at ring stage treated for 48 h with EVs derived from RBC and RBC pre-loaded with chloroquine.

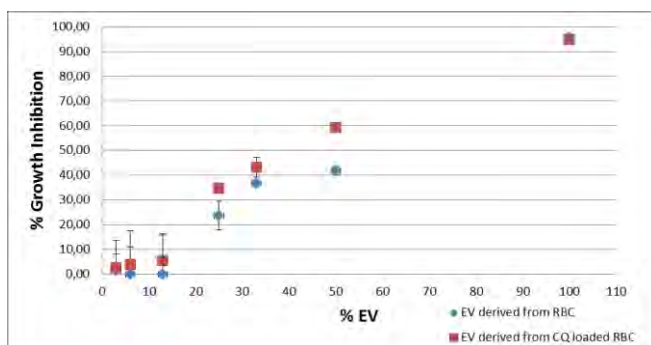


Figure 3. Growth inhibition of *Plasmodium falciparum* at late stage treated for 48 h with EVs derived from RBC and RBC pre-loaded with chloroquine.

Poly(pseudorotaxane) / Graphene Oxide supramolecular hydrogels for controlled drug release

Felipe Olate-Moya¹,
Humberto Palza¹

¹Departamento Ingeniería Química, Biotecnología y Materiales, Universidad de Chile, Beaucheff 851, Santiago, Chile.

felipe.olate@ing.uchile.cl

Supramolecular hydrogels are very attractive biomaterial for drug delivery system due to versatile properties as biocompatibility, easy synthesis, reversible sol-gel transition and processability. [1] Particularly, poly(pseudorotaxane) supramolecular hydrogels (PSH) based on cyclodextrin (CD) rings threaded by self-assembling into poly(ethylenglycol) (PEG) chains have been used as matrix for injectable drug delivery systems. [2] With the aim of enhance the drug release control, nanomaterials based on carbon such as graphene oxide (GO) have been added in nanocomposite hydrogels for improve the response to external stimuli like variations of temperature and pH environment. [3] Drug delivery systems with pH-responsive drug release are focus of interest due to the micro-environment of tumors have an acidic pH. [4] This work shows a low-cost GO/PSH nanocomposite for controlled pH-responsive doxorubicin hydrochloride (DOX) release.

Table 1. Supramolecular hydrogels composition.

PSH	α -CD (mg/mL)	PEG (mg/mL)	DOX (mg/mL)	GO (mg/mL)
PEG/ α -CD	64	200	0.1	0
GO/PEG/ α -CD	64	200	0.1	1

GO was synthesized from graphite according to modified Hummers method. The synthesis of GO/PSH were formulated by mixing of precursors solution of α -CD, PEG, GO and DOX to obtain the final concentrations showed in Table 1. The nanocomposite hydrogel and GO were characterized by means of XRD, TEM, FTIR and UV-VIS spectroscopy. The cumulative release of DOX was quantified by absorptiometry at 488 nm. The experiments were performed using PBS at pH values of 7.4 and 5.5 at 37 °C for study the pH-dependence of releasing.

Our results show that GO and GO/PSH nanocomposite were successfully synthesized. The FTIR spectra of GO confirm the presence of oxygen rich functional groups, with bands at 3200 cm^{-1} , 1712 cm^{-1} and 1040 cm^{-1} associated to stretching of O-H, C=O and C-O bonds respectively. UV-Visible spectra of a GO suspension in water showed a main

peak around 230 nm corresponding to $\pi \rightarrow \pi^*$ electronic transitions in the aromatic basal plane and a shoulder around 300 nm consistent with $n \rightarrow \pi^*$ transitions due to oxygen atoms present in the functional groups.

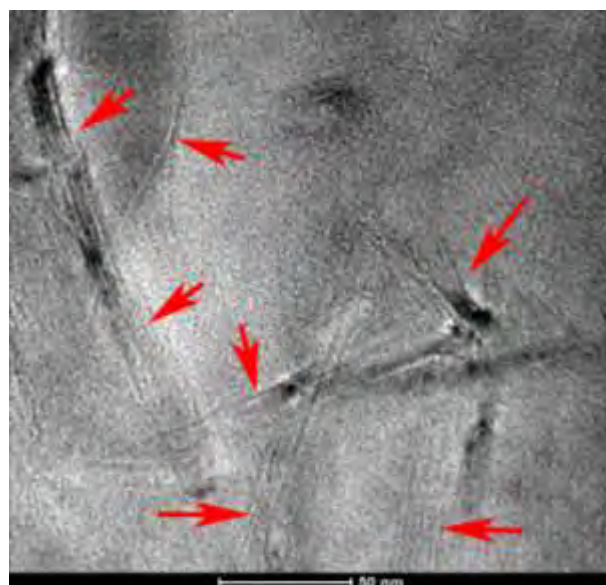
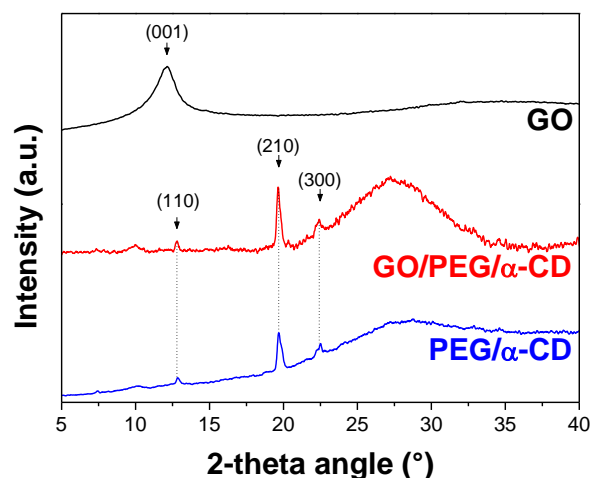


Figure 1. Microstructural analysis of GO and PSHs. a) XRD patterns of GO and PSH nanocomposites measured in powder and hydrogel state respectively. b) TEM microphotography of polypseudorotaxane aggregates (indicated by arrows) on a GO sheet in GO/PEG/ α -CD xerogel.

Figure 1a display the XRD patterns of GO (powder) and GO/PEG/ α -CD (hydrogel state). The XRD pattern of GO exhibited a peak at 12.37° ($d = 0.71$ nm) corresponding to 001 planes reflections of few-layer GO. On the other hand, the XRD pattern of the supramolecular hydrogel matrix (PEG/ α -CD) showed the characteristic peaks of columnar hexagonal structures with an intense reflection at 19.6°. This structure is associated to the channel type crystal where α -CD rings are threading with the PEG through "head-to-head/tail-to-tail" sequences. [5] The diffractogram of GO/PEG/ α -CD confirm that incorporation of GO does not affect the formation and microstructure of the PSH. The Figure 1b show a TEM microphotography of poly(pseudorotaxane)

aggregates with channel type assembly over a GO sheet surface. The columnar supramolecular structures interact with the basal plane of GO probably through hydrogen bonding between their functional groups (epoxy, hydroxyl groups) and external hydroxyl groups from poly(pseudorotaxanes).

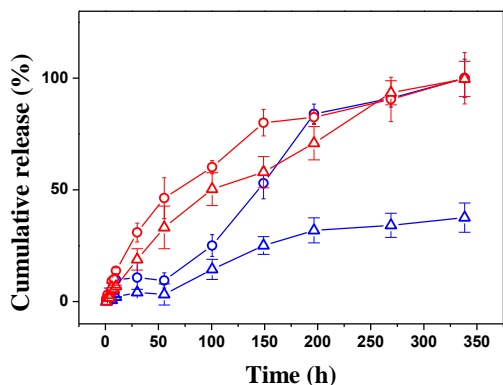


Figure 2. *In vitro* DOX cumulative release from PEG/α-CD (circles) and GO/PEG/α-CD (triangles) at 37 °C and pH= 7.4 (blue lines) or pH= 5.5 (red lines).

In Figure 2 is shown the cumulative release of DOX from synthesized PSHs in physiological and acidic pH conditions at 37 ° C. During the first 200 hours is possible observe a slight pH-dependence on DOX release from PEG/α-CD, however, after 340 hours 100% release of DOX was reached out from this PSH under both pH conditions. When GO was incorporated (GO/PEG/α-CD), a significant pH-dependence of DOX release was observed. While 100% of DOX was released from PEG/α-CD at 340 hours, only 37% of the drug was released at same time from GO/PEG/α-CD meaning a pH-responsive controlled release. This behavior could be explained because an attractive ionic interaction is produced between carboxylate groups on GO and ammonium groups in DOX. [6] In acidic environment (pH = 5.5) this carboxylate groups are protonated and the ionic union with DOX is disrupted releasing the drug.

In conclusion, a novel PSH nanocomposite was developed as platform for controlled DOX release system. Poly(pseudorotaxane) aggregates of PEG/α-CD can interact with GO probably by means of hydrogen bonding. The GO/PEG/α-CD nanocomposite shows a pH-responsive release of DOX due to attractive and pH-dependent ionic interaction between GO and the anticancer drug. This work displays a DOX-loaded GO/PEG/α-CD nanocomposite as low-cost and facile synthesis biomaterial with potential use in localized and pH responsive drug delivery systems to improve the drug accumulation inside tumor sites.

Acknowledgements

The authors thank the financial support of CONICYT under FONDECYT Project 1150130. F. O.-M. thanks to Beca de Doctorado Nacional CONICYT 21150039.

References

- [1] M. J. Webber, E. A. Appel, E. W. Meijer, R. Langer, *Nature Materials*, 15 (2016) 13.
- [2] J. Li, *Adv. Polym. Sci.*, 222 (2009) 79.
- [3] P. Zhu, Y. Deng, C. Wang, *Carbohydr. Polym.*, 174 (2017) 804.
- [4] S. Peppicelli, F. Bianchini, L. Calorini, *Cancer Metastasis Rev.*, 33(2-3) (2014) 823.
- [5] I. N. Topchieva, A. E. Tonelli, I. G. Panova, E. V. Matuchina, F. A. Kalashnikov, V. I. Gerasimov, C. C. Rusa, M. Rusa, M. A. Hunt, *Langmuir*, 20 (2004) 9036.
- [6] Y. Chen, W. Cheng, L. Teng, M. Jin, B. Lu, L. Ren, Y. Wang, *Macromol. Mater. Eng.*, (2018) 1700660.

Antigen-loaded chitosan nanoparticles and their interaction with immune cells

Maruthi Prasanna¹, Emilie Camberlein², Cristina Calviño³, Ruben Varela³, Daphnée Soulard⁴, François Trottein⁴, Marcos Garcia-Fuentes¹, Cyrille Grandjean², Noemi Csaba¹

¹Center for Research in Molecular Medicine and Chronic Diseases, University of Santiago de Compostela, Spain;

²Unit Function & Protein Engineering, UMR CNRS 6286, University of Nantes, France;

³Department of Biochemistry and Molecular Biology, University of Santiago de Compostela, Spain;

⁴Centre d'Infection et d'Immunité de Lille, Université de Lille, CHU Lille- Institut Pasteur de Lille, France

maruthi.prasanna@usc.es

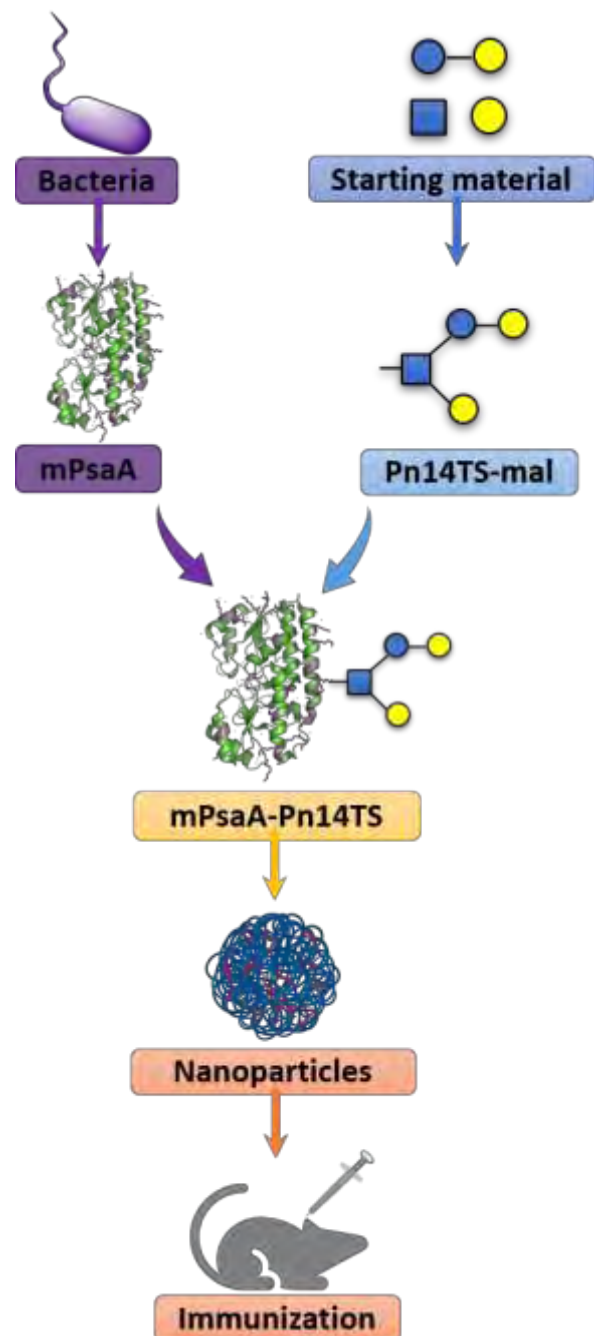
Abstract

Introduction

Historically, vaccination represent greatest medical advancements and successful strategies employed in the prevention of infectious diseases. First-generation vaccines contain attenuated or inactivated microbes, such as viruses or bacteria but they have shortcomings related to their safety (i.e. virulence). More recent, second-generation vaccines such as subunit vaccines or conjugate vaccines such as Pneumococcal conjugate vaccines have proved to be more efficient and non-virulent. The conjugate vaccines are very effective in generating strong and long-lasting antigen-specific T cell responses and can induce strong immune response in young children despite of their immature immune system. Although the pneumococcal vaccines have reduced the burden of epidemics, they still have the limitation of serotype replacement. To overcome this, we have developed a glycoconjugate based on the universal pneumococcal surface adhesin-A (mPsaA) as a carrier protein and a synthetic mimic of pneumococcal serotype 14 tetrasaccharide (Pn14TS). The presence of mPsaA in all pneumococcal serotypes and effectiveness as immunogen has made it a preferred choice as a carrier protein.

Methods and Results

Initially, the Pn14PS was synthesized chemically and the mPsaA was expressed in *E. coli* BL21 (DE3) strain, then purified using affinity chromatography. The obtained mPsaA and Pn14PS were successfully conjugated by thiol-maleimide coupling chemistry to obtain protein/sugar conjugates at ratio 1/5.4 as confirmed by MALDI-TOF. The secondary structure of the mPsaA was evaluated by circular dichroism (CD) after the conjugation and lyophilization. The CD spectra revealed that the secondary structure of mPsaA was stable throughout the process of conjugation and conservation. The mPsaA-Pn14TS loaded chitosan nanoparticles (CNPs) were prepared by ionic gelation method. The Dynamic light scattering (DLS) measurement showed that the obtained CNPs had a size of 118 ± 3 nm and zeta potential of 31 ± 1 mV.



Scheme 1: Graphical Abstract

The encapsulation efficiency of mPsaA-Pn14TS in the CNPs was found to be 70 ± 3 %.

The evaluation of the nanoparticles by nanoparticle tracking analysis (NTA) revealed that the average particle size of CNPs was 101 ± 33 nm, and particle count of 1.69×10^{10} per 1 mg of CNPs (fig 1A). The surface characterization of the CNPs by scanning electron microscopy (FEG-SEM) revealed the morphology of the CNPs that were spherical in shape and had smooth surface (fig 1B). The CNPs lyophilized in the presence of 5% trehalose (w/v) could be easily resuspended without variation in their size. In addition, antigen-loaded nanoparticles were stable over a period of 24 h in simulated nasal fluid.

Recognition and uptake by the antigen presenting cells (APC) is the prerequisite for the activation of the immune system. In order to confirm the interaction of CNPs with APCs the studies were performed with human monocyte-derived dendritic cells (MoDCs). The internalization of the mPsaA-Pn14TS loaded CNPs by the APCs was confirmed by confocal microscopy and flow cytometry by fluorescently labelling the CNPs. The flow cytometry results showed the maximum uptake of nanoparticles was observed in less than 2 hours.

Finally, preliminary immunization studies performed in the mice revealed that the groups immunized with mPsaA-Pn14TS produced a robust IgG response against the Pn14TS, when compared to the mice treated with mPsaA alone or BSA-Pn14TS conjugate.

Conclusion

The stable semi-synthetic glycoconjugate was synthesized and was successfully encapsulated into CNPs. The results obtained from preliminary immunization studies in mice are encouraging. Further studies are ongoing to evaluate the potential of the nanoparticulate systems when coupled with mPsaA-Pn14TS.

References

- [1] Safari D et al., *Nanomedicine (Lond)* (2012) 7:651–662.
 [2] Larentis AL, et al., *Protein Expr Purif* (2011) 78:38–47.

- [3] Calvo P et al., *Pharm Res* (1997) 14:1431–1436.

Figures

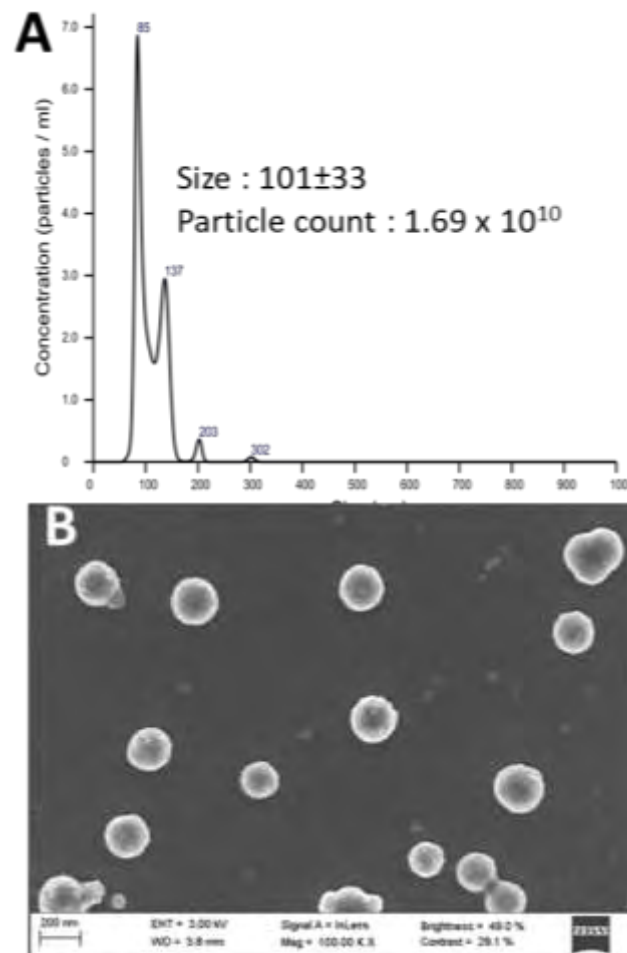


Figure 1: Characterization of Antigen loaded Chitosan nanoparticles A) Nanoparticle tracking analysis; B) FEG-SEM

Acknowledgements

The project has received funding from NanoFar, Erasmus Mundus Joint Doctorate in Nanomedicine and Pharmaceutical Innovation under European Union's Horizon 2020 and RETOS-Spanish Ministry of Economy and Competitiveness (SAF2016-79230-R).

Reversible monolayer-bilayer transition in supported phospholipid Langmuir-Blodgett films: morphological and nanomechanical behavior

Silvia Ruiz-Rincón^{1,2,5},
Alejandro González-Orive^{1,2}, Jesús M. de la Fuente^{3,4} and Pilar Cea^{1,2,5}

¹Organization, Address, City, Country (Arial 9)

¹Instituto de Nanociencia de Aragón (INA). Campus Río Ebro, Universidad de Zaragoza, C/Mariano Esquillor, s/n, 50018 Zaragoza, Spain.

²Laboratorio de Microscopias Avanzadas (LMA) Campus Río Ebro, Universidad de Zaragoza, C/Mariano Esquillor, s/n, 500018 Zaragoza, Spain.

³Instituto de Ciencia de Materiales de Aragón (ICMA), Universidad de Zaragoza-CSIC, 50009 Zaragoza, Spain

⁴Networking Biomedical Research Center of Bioengineering, Biomaterials and Nanomedicine (CIBER-BBN). Spain.

⁵Departamento de Química Física, Facultad de Ciencias, Universidad de Zaragoza, 50009, Zaragoza, Spain

sruiz@unizar.es

The Langmuir-Blodgett technique (LB) has been used to fabricate biomimetic lipid membranes in order to investigate in an easier way the lipid-lipid interactions and the processes that take place at the membrane level. With this aim, mixed monolayer LB films of 1,2-dipalmitoyl-sn-glycero-3-phosphocholine (DPPC) and cholesterol (Chol) in the 1:1 ratio have been prepared onto solid mica substrates by means of LB. Upon immersion in water or in an aqueous HEPES solution (pH 7.4) the monolayer LB films were spontaneously converted into well-organized bilayers leaving free mica areas in between [1]. The process has been demonstrated to be reversible upon removal of the aqueous solution resulting thus in remarkably free of defects monolayers. The latter process has been summarized in Figure 1. In addition, the nanomechanical properties exhibited by the as-formed bilayers have been determined by means of AFM breakthrough force studies which allow studying the local properties of the mimic membranes in a quantitative way with the possibility of controlling the environmental conditions [2]. The bilayers formed by immersion of the monolayer in an aqueous media exhibit nanomechanical properties and stability under compression analogue to those of DPPC:Chol supported bilayers obtained by other methods previously described in the literature [3]. Consequently, the hydration of a monolayer LB film has been revealed as an easy method to produce well-ordered bilayers that mimic the cell membrane and that could be used then as model cell membranes.

References

- [1] Ruiz-Rincón, S.; González-Orive, A.; de la Fuente, J.M.; Cea, P. *Langmuir* **2017**, *33*, 7538-7547
- [2] Dufrene, Y.F.; Martinez-Martin, D.; Medalsy, I.; Alsteens, D.; Muller, D.J. *Nat Meth* **2013**, *10*, 547-854
- [3] Lima, L.; Gianotti, M.I.; Redondo-Morata, L.; Vale, M.; Marques, E.F.; Sanz, F. *Langmuir* **2013**, *29*, 9352-9361

Figures

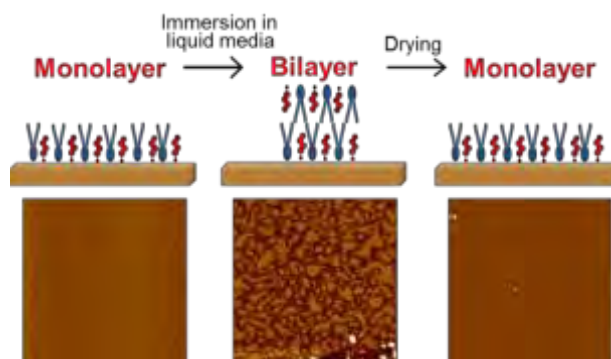


Figure 1. Scheme of the reversible transition from monolayer to bilayer and subsequent transition to monolayer after drying.

Multifunctional (Mg,Fe)₃O₄ nanoparticles: Test for possible magnetic hyperthermia and radionuclide carriers applications

V. Spasojevic¹,

I. Spasojevic², M. Ognjanovic¹, M. Mirkovic¹, M. Radovic¹, S. Vranjes Djuric¹, T. Stanojkovic³, Z. Prijovic¹ and B. Antic¹

¹"Vinca" Institute of Nuclear Sciences, University of Belgrade PO Box 522, 11000 Belgrade, Serbia

²Catalan Institute of Nanoscience and Nanotechnology (ICN2), CSIC and The Barcelona Institute of Science and Technology, Campus UAB, Bellaterra, 08193 Barcelona, Spain

³ Institute of Oncology and Radiology of Serbia , Pasterova 14, RS-11000 Belgrade

vojas@vinca.rs

Mg_xFe_{3-x}O₄ magnetic nanoparticles (0≤x≤0.6) coated with oleic acid (OA), citric acid (CA), and polyethylene glycol (PEG), were synthesized in the form of ferrofluids. Some of these magnetic nanoparticles (MNPs) were additionally radiolabeled by β-emitter yttrium-90 (⁹⁰Y). The main objective was to test the MNPs and optimize their characteristics for magnetic hyperthermia and regional radiotherapy, which can be used either individually or simultaneously in cancer treatment. A complete characterization was made for all samples from which information about external morphology of MNPs, their size distribution and magnetic characteristics was obtained.

The cytotoxicity of the coated MNPs was tested in vitro on four cell lines: HeLa (human cervical adenocarcinoma cells), LC174 (human colon cancer cells), A549 (lung cancer cells) and MRC5 (healthy fetal lung fibroblast cells). The obtained results show that the examined cancer lines demonstrate different sensitivity to MNPs and that cytotoxicity depends on the type of nanoparticle coating. It was found that HeLa cells exhibit the highest sensitivity, regardless of the type of coating while at the same time healthy cells are almost insensitive to MNPs.

The labeling yield for all MNPs is very high and for PEG coated nanoparticles is almost 100%. Stability of ⁹⁰Y-labeled MNPs was investigated in both saline and human serum at 37°C up to 72h. It was found that MNPs/PEG/⁹⁰Y stability is almost 100% while citric acid nanoparticles (MNPs/CA/⁹⁰Y) demonstrate lower stability of 65%.

Magnetic hyperthermia measurements show that all samples have good heating ability. SPA values of MNPs doped with Mg are increasing with concentration x and applied frequency, showing

improvement of heating efficiency comparing to pure magnetite. Measured SPA values are comparable or higher with so far known commercial ferrofluids.

MOLECULAR DYNAMICS STUDY ON SUBSTITUENT AND SOLVENT EFFECTS FOR NANOCUBE FORMED WITH GEAR-SHAPED AMPHIPHILE MOLECULES

Masanori Tachikawa¹,
Takako Mashiko¹, Shuichi Hiraoka²,
and Umpei Nagashima³

¹Yokohama City University, 22-2 Seto, Kanazawa-ku,
Yokohama-shi, Kanagawa 236-0027, Japan

²The University of Tokyo, 3-8-1 Komaba, Meguro-ku,
Tokyo 153-8902, Japan

³FOCUS, 7-1-28 Minatojiminamimachi, Chuo-ku,
Kobe-shi, Hyogo 650-0047, Japan

tachi@yokohama-cu.ac.jp

Recently, Hiraoka *et al.* have synthesized a gear-shaped amphiphile molecule **1**, shown in Figure 1. **1s** are self-assembled into a cubic-shaped hexameric structure, nanocube (**1₆**), in 25% aqueous methanol [1, 2]. Another gear-shaped molecule (**2**), in which three methyl groups of **1** are replaced with hydrogen atoms, does not form the nanocube (**2₆**). Hiraoka *et al.* further found that **1** is not assembled in pure methanol. Previously, the static molecular orbital of density functional theory studies have already reported [3]. The purpose of this work is to elucidate the stability of these hexameric capsules **1₆** and **2₆** in water [4], in methanol [5], and in 25% aqueous methanol with the aid of molecular dynamics simulation.

In all solvents, the nanocube **1₆** structure for all trajectories are maintained. On the other hand, the **2₆** structure in water for one trajectory and seven trajectories in 25% aqueous methanol are collapsed. In methanol solvent, the **2₆** for all trajectories are collapsed. The number of collapsed trajectories of **2₆** is raised, as the number of methanol solvent molecules is increased. We focus on the nanocube structure of the π - π stacking between pyridines and CH- π interactions between the methyl group and pyridine. The CH- π network among pyridyl groups and CH₃ groups can be constructed on the **1₆** as shown in Figure 2 because the nanocube structure can be stable by van der Waals force.

References

- [1] S. Hiraoka, K. Harano, M. Shiro, and M. Shionoya, *J. Am. Chem. Soc.*, 130, 14368 (2008).
- [2] S. Hiraoka, K. Harano, and T. Nakamura, *et al.*, *Angew. Chem., Int. Ed.*, 48, 7006 (2009).
- [3] J. Koseki, Y. Kita, S. Hiraoka, U. Nagashima, M. Tachikawa, *Theor. Chem. Acc.*, 2011, 130, 1055-1059.
- [4] T. Mashiko, K. Yamada, T. Kojima, S. Hiraoka, U. Nagashima, M. Tachikawa, *Chem. Lett.*, 2014, 43, 366-368.
- [5] T. Mashiko, K. Yamada, S. Hiraoka, U. Nagashima, M. Tachikawa, *Mol. Simul.*, 2015, 41, 10-12.
- [6] T. Mashiko, S. Hiraoka, U. Nagashima, M. Tachikawa, *Phys. Chem. Chem. Phys.*, 2017, 19, 1627-1631.

Figures

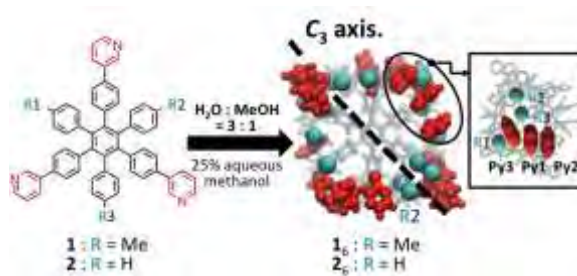


Figure 1. Chemical formulae of gear-shaped amphiphile molecules, **1** (R = CH₃) and **2** (R = H).

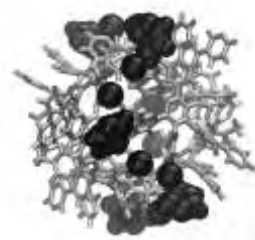


Figure 2. Black atoms are the CH- π network in nanocube **1₆**.

Colorimetric tests for food safety and genetic traceability based on DNA-functionalized gold nanoparticles

Giuseppina Tatulli^{1,2},

Davide Maggioni³, Andrea Galimberti³, Valeria Terzi⁴, and Pier Paolo Pompa²

¹University of Salento, Piazza Tancredi 7, 73100 Lecce, Italy

²Nanobiointeractions & Nanodiagnostics, Istituto Italiano di Tecnologia (IIT), Via Morego 30, 16163 Genoa, Italy

³Department of Biotechnology and Biosciences, University of Milano-Bicocca, P.za Della Scienza 2, 20126 Milan, Italy

⁴Genomics Research Centre (CREA-GPG), Council for Agricultural Research and Economics, Via San Protaso 302, 29017 Fiorenzuola d'Arda (PC), Italy

Giuseppina.tatulli@iit.it

In recent years, food trade globalization has brought several benefits for consumers such as lower prices, supplies available all year and a greater variety of foods. Nevertheless, it has raised growing concern for food safety and genetic traceability, driving a need for technological innovations. In particular, such technologies have to be compliant with the food distribution and market requests for accuracy, rapidity, and low costs. Traditional methods (real-time PCR, sequencing (DNA barcoding [1]), or microbiological assays) have important drawbacks, as they require expensive instrumentation, qualified personnel, long times, and high-quality DNA extraction. We developed a universal approach that combines an asymmetric PCR [2] to a fast and colorimetric read-out based on DNA-functionalized gold nanoparticles [3, 4]. In the presence of the target, the gold nanoparticles aggregate and a red-to-purple color change is visible at room temperature within 5 minutes. This technique is useful for applications in several fields, due to its specificity, sensitivity, versatility, and cost-effectiveness. This approach has been applied to two cases of study. The first application, in the food-safety field, deals with the detection of *Fusarium langsethiae* in cereal crops. It is a toxigenic fungus and the main producer of two toxins (T-2 and HT-2), which are damaging both for human health and crop yields. Our colorimetric technology can specifically detect the presence of this fungus in the genomics extracted from real plants, distinguishing it from other similar species that belong to the genus *Fusarium* (such as *Fusarium culmorum*, *graminearum*, and *sporotrichioides*). When the sample is contaminated with *F. langsethiae*, the aggregation of the gold nanoparticles causes a color-shift visible by naked-eye (Figure 1). The second application, related to food authentication, aims the discrimination of *Sepia officinalis*, usually substituted with other two species (*Sepia hierredda* and *pharaonis*) that look similar

and are genetically analogous. When an unknown sample contains the *S. officinalis*, a color change of the gold nanoparticles occurs (Figure 2).

References

- [1] Hebert, P.D., Cywinska, A., Ball, S.L., deWaard, J.L., Proc. R. Soc. Lond. B, 270 (2003);
- [2] Wooddell, C.I., Burgess, R.R., Genome Res., 6 (1996) 886;
- [3] Valentini, P., Pompa, P.P., Angew. Chem. Int. Ed. Engl., 55 (2016) 2157;
- [4] Valentini, P., Galimberti, A., Mezzasalma, V., De Mattia, F., Casiraghi, M., Labra, M., Pompa, P.P., Angew. Chem. Int. Ed., 56 (2017) 8094;

Figures



Figure 1. Specificity test for the colorimetric detection of *F. langsethiae*. Sample 1: *F. langsethiae*, 2: *F. culmorum*, 3: *F. graminearum*, 4: *F. sporotrichioides*, NC: mQH₂O.



Figure 2. Colorimetric discrimination of *S. officinalis*. Sample 1: *S. officinalis*, 2: *S. hierredda*, 3: *S. pharaonis*, NC: mQH₂O.

Novel nanoparticles made of polyester-peptide copolymers

Ernesto Tinajero-Diaz¹

Antxon Martínez-de Ilarduya¹,

Sebastián Muñoz-Guerra¹, Andreas Heise².

¹ Universitat Politècnica de Catalunya, Departament d'Enginyeria Química ETSEIB, Diagonal 647, 08028, Barcelona, Spain.

²Department of Pharmaceutical and Medicinal Chemistry, Royal College of Surgeons in Ireland, 123 St. Stephens Green, Dublin 2, Ireland.

Contact: sebastian.munoz@upc.edu

Abstract:

New chemistries are being devised to generate polymers from non-food stock sources, or by novel fermentation and bioengineering techniques. Polymers obtained from renewable resources are already under investigation for drug delivery, and presently there are many examples using carbohydrates and polypeptides [1].

Polymeric materials based on synthetic polymers bearing amino acids in the main-chain or in the side-chain are very interesting biomimetic materials. Apart from being biodegradable and/or biocompatible, these materials exhibit properties that combine those from both the amino acid sequences and the synthetic counterpart. The application of certain stimuli provokes conformational, physical or chemical changes that can be utilized in biomedicine as well as in bio- and nano-technology [2].

Globalide (GI), a macrolactone derived from a non-toxic hydroxy fatty acid, is particularly interesting because it contains one unsaturation that can be used for functionalization *via* thiol-ene chemistry [3]. Graft copolymers were prepared following the synthetic route depicted in Figure 1.

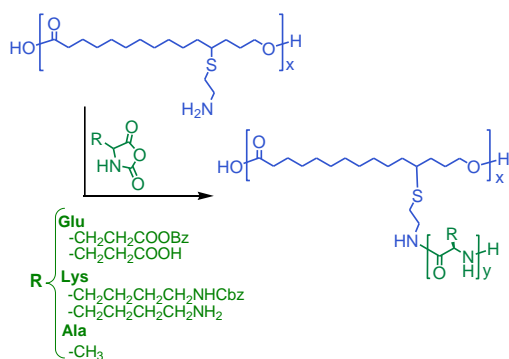


Figure 1. Synthetic route to poly(globalide)-*g*-poly(α -amino acid)s graft copolymers.

GI was polymerized by enzymatic ROP to render polyglobalide (PGI) with M_n around 15,000 g mol⁻¹. Amine functionalization of PGI was performed by thiol-ene click reaction with 2-*boc*-aminoethanethiol and removal of the protecting group with trifluoroacetic acid (TFA). Grafting was made by ROP of duly protected amino acids *N*-carboxyanhydrides (NCA) initiated by the amino side groups of modified PGI. By treatment with TFA-HBr, the Bc or Cbz protecting groups were fully removed from the PBLG or PZLLys side chains, respectively, to render polypeptidic chains with the carboxylic or amine groups in the free form. All copolymers were characterized by ¹H and ¹³C-NMR, FT-IR, GPC, TGA and DSC techniques. After removal of the Bc or Cbz protecting group, water-soluble copolymers PGI_{*x*}-*g*-PLGA_{*y*} and PGI_{*x*}-*g*-PLLys_{*y*} were obtained.

Nanoparticles (NPs) with diameters in the ~80-170 nm range were prepared from the PGI_{*x*}-*g*-PBLG_{*y*} and PGI_{*x*}-*g*-PZLLys_{*y*}. Figure 2 displays the size distribution and TEM micrograph of NPs made of PGI₂₀-*g*-PBLG₅₀.

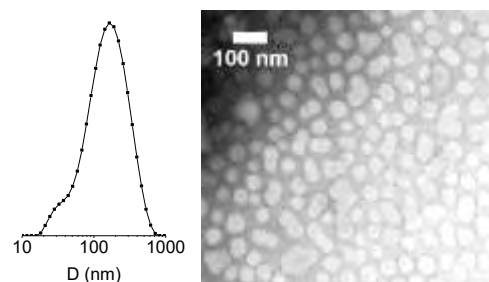


Figure 2. DLS profile and TEM image of NPs made of PGI₂₀-*g*-PBLG₅₀.

Water-soluble copolymers PGI_{*x*}-*g*-PLGA_{*y*} and PGI_{*x*}-*g*-PLLys_{*y*} were obtained after deprotection of PGI_{*x*}-*g*-PBLG_{*y*} and PGI_{*x*}-*g*-PZLLys. Aqueous polymer solutions of these compounds were prepared, and the NPs size distribution was directly measured by DLS. NPs with diameters in the ~30-150 nm range were formed as it is shown in Figure 3.

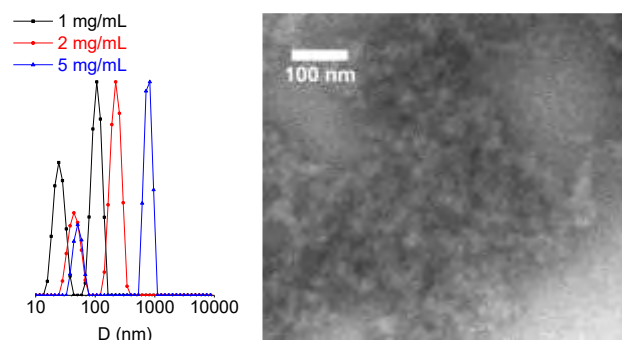


Figure 3. DLS profile and TEM image of NPs made of PGI₂₀-*g*-PLGA₅₀.

By using the emulsion/evaporation technique, the PGI₂₀-g-PLGA₅₀ and PGI₂₀-g-PLLys₅₀ copolymers provided NPs with diameters in the ~300-500 range. These NPs exhibited good stability when incubated in water for several days as it is displayed in Figure 4.

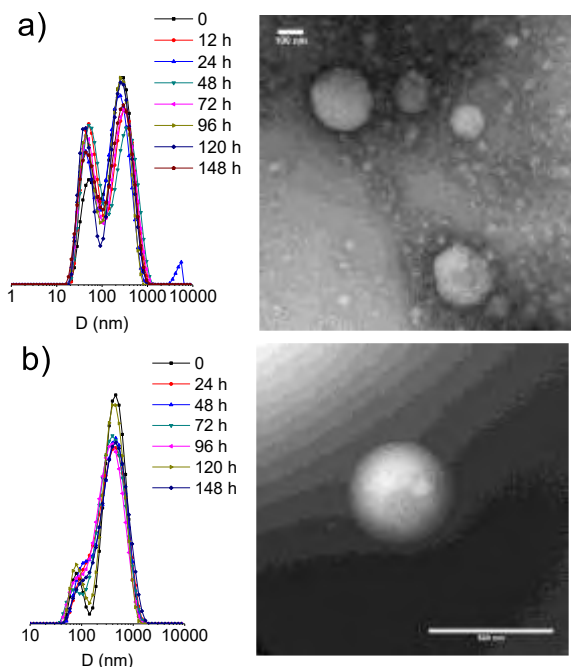


Figure 4. DLS and TEM measurements of NPs made after one week of incubation in water: a) PGI₂₀-g-PLGA₅₀ and b) PGI₂₀-g-PLLys₁₅₀.

These results give support to the potential of these copolymers to be used as carrier and delivery systems for active biomedical agents.

Acknowledgements

Financial support for this research was afforded by MINECO (Spain) with grant MAT-2016-77345-CO3-01. E. Tinajero-Díaz thanks CONACYT (México) for the Ph.D. grant and to l'Obra Social la Caixa (Spain) for the Beca de Mobilitat Internacional awarded in 2016.

References

- [1] ^aSaraiva, C., Praça, C., Ferreira, R., Santos, T., Ferreira, L., Bernardino, L., *J. Control. Release.*, 235 (2016) 34-47. ^bK.K. Bansal, D. Kakde, L. Purdie, D.J. Irvine, S.M. Howdle, G. Mantovani, C. Alexander, *Polym. Chem.*, 6, (2015) 7196–7210.
- [2] Bauri, K., Nandi, M., De, P., *Polym. Chem.*, 9, (2018), 1257-1287.
- [3] Ates, Z., Thorthon, P.D., Heise, A., (2011), *Polym. Chem.*, 2, 309-312.

Encapsulation of docetaxel with Elastin Like Recombinamers by supercritical CO₂ for advanced anticancer applications in biomedicine

Reinaldo Vallejo Vicente^{1,2},
Soraya Rodríguez Rojo¹
Mercedes Santos García²
Francisco Javier Arias Vallejo²
María José Cocero Alonso¹

¹ High Pressure Processes Group, Universidad de Valladolid, Escuela de Ingenierías Industriales, Sede Dr. Mergelina, Doctor Mergelina s/n, 47011 Valladolid, Spain
² BIOFORGE Research Group, Universidad de Valladolid, Edificio LUCIA, Paseo Belén 19, 47011 Valladolid, Spain

reinal.vv@gmail.com

INTRODUCTION

The controlled release of drugs from biodegradable polymer nanoparticles (NPs) is having a great medical impact in a wide range of therapeutic areas [1]. Elastin-like Recombinamers (ELRs) are an interesting option to achieve this goal because of their ability to perceive their environment and respond to changes in it. The ELR biopolymers are polypeptides whose sequence is formed by repeats of the sequence (VPGXG)_n, or their permutations, which gives the elastin its unique mechanical properties, i.e. extraordinary elasticity, self-assembly capability and excellent resistance to stress. Moreover, ELRs are a new class of biomaterials with an extraordinary biocompatibility and an interesting bioactivity [2]. Thus, new NPs production processes have been developed to protect the functionality of this type of polymers. Carbon dioxide, CO₂, in supercritical state (scCO₂) becomes a very powerful solvent [3] and serves as a completely clean separation agent since it uses mild temperatures in the process that do not harm the product, it is a non-flammable, non-corrosive, non-toxic, non-carcinogenic element, has a large selective capacity and does not generate waste.

MATERIALS & METHODS

Materials

Dimethyl sulfoxide (DMSO) was purchased from Sigma Aldrich with a purity $\geq 99.7\%$. Carbon dioxide was supplied by Carburros Metálicos S.A. with a purity of 99.95%. The selected ELRs are amphiphilic polymers which contain 1107 amino acids [4] with Glutamic acid and Isoleucine as guest residues (ELR1). The same biopolymer with a block which contains peptide loop presented in the human fibronectin protein with the well-known RGD (ELR2) [5] sequence for cell adhesion was used for future cell assays. These ELRs have been designed and

bioproduced by BIOFORGE. Docetaxel (DTX) was provided by Apollo Scientific with a purity of 99%. Deuterium oxide was purchased from Sigma Aldrich with a purity of 99.9 atom % D.

Methods

Supercritical-Antisolvent (SAS) pilot plant is equipped with diaphragm pump (Dosapro, France) to reach the scCO₂ conditions. When the mass flow is constant and the working pressure and temperature remain stable, a defined amount of ELR and DTX dissolved in DMSO is pumped by a chromatographic pump (Gilson 305 pump) into the precipitator at the desired flow rate through a coaxial nozzle. This process uses the capacity of scCO₂ to be dissolved in the solvent [6], so an instantaneous supersaturation of the solution takes place in the tip of the nozzle and the solute precipitates in particles. Particles formed by DTX and ELR were recovered out of the precipitator vessel in a porous metal filter with a screen size of 1 μ m.

The proportions of each material in the particles were determined by NMR spectroscopy (Agilent Technologies) by comparison of methyl groups integral value belonging specifically to the ELR and the integral of the aromatic protons belonging to the DTX. Surface charge of the particles (ζ -Potential) and micelles was measured by Dynamic light scattering (DLS) using a Zetasizer Nano ZS (Malvern Instruments Ltd.). Samples analysed by DLS were dissolved at 1 mg/mL in ultrapure deionized water and three measurements were taken per sample at 37°C and neutral pH. Furthermore, the nanoparticle agglomerate morphology was studied by Scanning Electron Microscopy (SEM) (ESEM QUANTA 200 FEG).

In vitro drug delivery experiment was performed in triplicate using dialysis method at 37 °C. 1 mg of ELR1+DTX was dispersed in 1mL of 7:3 (v/v) water/ethanol release medium comprising 0.6 mg of DTX encapsulated (Table 1). Previously activated dialysis bags (MWCO 12000 kD) were filled, sealed in both ends and then immersed in 30 mL glass vials filled with 20 mL of release medium. Vials were stirred at 80 rpm and 37 °C in an incubator during all the experiment. Samples of 2 mL were withdrawn at predetermined time intervals from the release medium and the same volume was replaced with fresh medium to maintain sink conditions. A triplicate of the same amount of DTX dissolved in 1 mL of release medium was used as control. The released DTX was measured by UV-vis spectrometer (UV-Vis NanoDrop 2000, Thermo scientific) following the Lambert and Beer's law with a quartz cuvette at 234 nm wavelength.

RESULTS & DISCUSSION

Preliminary precipitation experiments with pure ELR were performed to determine the best operating conditions that proved to be 110 bar, 308.15 K and 30 mg/mL in ELR weight.

Entry	Experiment	%ELR	%DTX	%DMSO
1	ELR1 control	96.40	-	3.40
2	ELR2 control	96.90	-	3.10
3	ELR1+DTX	38.62	57.93	3.45
4	ELR2+DTX	38.57	57.85	3.58

Table 1, experiments carried out with ELR1, ELR2 and DTX. Initial ratio 1:1 w/w (ELR:DTX) was not kept in the particles after processing (entry 2 and 3, table 1). A small amount of ELR was lost during the experiment and the final ratio was 1:1.5 w/w, respectively. This might be caused because the drug precipitates first and some amount of ELR is washed down with the scCO₂. This new rate must be taken in consideration for future cell assays. SEM images of the samples (Figure 1) clearly show that the particles produced during the SAS experiments did not present aggregation and had a smooth surface with a range size between 3-10 μm (n=1035). The stability of the micelles of ELR containing DTX were measured by DSL during 5 days after its preparation as previously described. The differences in size, which vary between 35±11 and 45±14 nm, are not statistically remarkable; and polydispersity index below 0.2 found, indicates a monodisperse behaviour. This feature was confirmed measuring the ζ-Potential, where the NPs show values around -30 mV, which indicates that they had charge enough to repel between each other avoiding aggregation.

Figure 2 represents the % of drug release loaded in the ELR1-DTX and the control samples versus time during 96 h. As it can be observed, 55 ± 11% of the drug is released in the first 10 h of experiment, and then, the release velocity started to decrease until the total release at 96 h. However, in the control sample 53 ± 2% is released in the first 2 h reaching the total release at 24 h of experiment. These results show a clear delay in the delivery of the drug.

Mathematical model	Parameters	COD R ²
Ritger-Peppas	k ₁ = 0.2100±0.0040 k ₂ = -0.0118±0.0005	0.9969
Lindner-Lippold	k ₁ = 0.2988±0.0480 n = 0.2812±0.3054 b = -0.0660±0.0445	0.9787
Peppas-Shalin	k ₁ = 0.2230±0.0070 k ₂ = -0.0134±0.0008 n = 0.4731±0.01260	0.9979

Table 2, parameters and COD R² of the equations fitted from the drug delivery profile.

Release profile from Figure 2 was then fitted with the well-known semiempirical equation of Ritger-Peppas, which describes the kinetic release of active compounds, with Lindner and Lippold equation, which is a modification of the generalized equation of Higuchi to describe the burst effect, and with biexponential equation of Peppas-shalin, which is a generalization of Ritger-Peppas equation to determine the contribution of the Fick diffusion process and the relaxation of the polymer chains regardless of the geometry of the release system. Lindner-Lippold fitting shows that it is not statistically able to describe well the releasing because of its lower value of coefficient of determination (COD R²) (Table 2). On the other hand, Ritger-Peppas and Peppas-Shalin equations have similar COD R², so both of them are enough accurate to describe the

process of diffusion of the drug to the release medium.

CONCLUSIONS

In this work, micro-particles of a highly hydrophobic drug coated with Elastin like Recombinamers were produced successfully with scCO₂ by SAS, making a drug delivery system with amount of solvent residues well below the legal limits. Thanks to the amphiphilic behaviour of the biopolymer, the drug delivery system keeps stable in time and the drug delivery profiles show a controlled release, compared with the control samples, following Fick diffusion processes as it is shown with the mathematical models proposed.

References

- [1] Effrey J. Lochhead, Robert G. Thorne, *Advanced Drug Delivery Reviews*, 64 (2012) 614.
- [2] F.J. Arias, M. Santos, A. Fernández-Colino, G. Pinedo, A. Girotti, *Current Topics in Medicinal Chemistry*. 14 (2016) 819.
- [3] M.J. Cocero, A. Martín, F. Mattea, S. Varona, *The Journal of Supercritical Fluids*, 47 (2009) 546.
- [4] L. Martín, F. J. Arias, M. Alonso, C. García-Arévalo and J. C. Rodríguez-Cabello. *Soft Matter*, 6 (2010) 1121.
- [5] 2504C. Garcia-Arevalo, M. Pierna, A. Girotti, F. J. Arias and J. C. Rodríguez-Cabello, *SoftMatter*, 8 (2012) 3239.
- [6] A. Martín, K. Scholle, F. Mattea, D. Meterc, M.J. Cocero, *Crystal Growth & Desing*, 9 (2009) 2504.

Figures

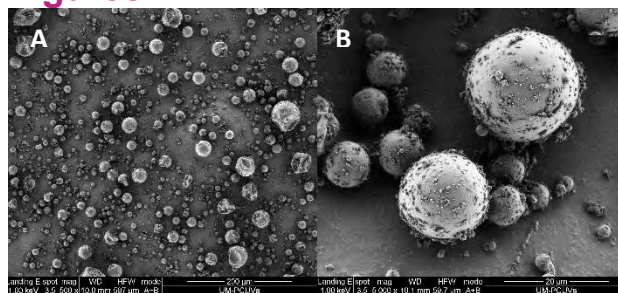


Figure 1. SEM photomicrographs from ELR1+DTX. (A) size bar 200 μm, (B) size bar 20 μm.

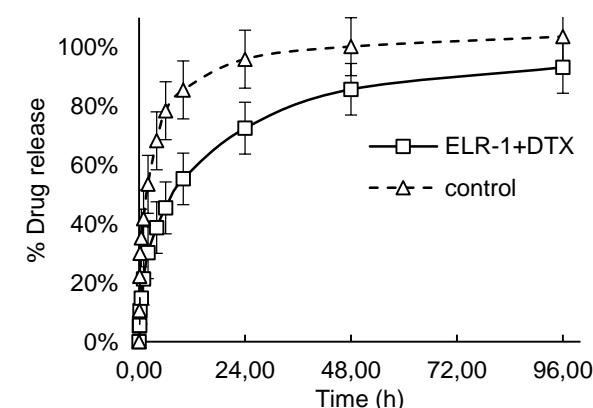


Figure 2. % drug release of ELR1-DTX and control sample vs. time (h).

Medical Imaging for the Tracking of Micromotors

D. Vilela¹, U. Cossío², J. Parmar¹, A. M. Martínez-Villacorta², V. Gómez-Vallejo², J. Llop², and S. Sánchez^{1,3}

¹Institute for Bioengineering of Catalonia (IBEC), The Barcelona Institute of Science and Technology, Baldori Reixac 10-12, 08028 Barcelona, Spain.

²Radiochemistry and Nuclear Imaging Group, CIC biomaGUNE, Paseo Miramón 182, 20014 San Sebastián, Spain.

³Institució Catalana de Recerca i Estudis Avancats (ICREA), Pg. Lluís Companys 23, 08010 Barcelona, Spain
dvilela@ibecbarcelona.eu

Scientists have dreamt for long of miniature robots that can be controlled and navigated inside human body, to help the medical doctors to diagnose and treat the diseases.¹ Recently, these micro/nanorobots have demonstrated to be useful tools for several biomedical applications, including drug carriers and delivery vehicles, biological sensing, cell transport as well as cell and tissue penetration, highlighting their great potential for developing smart drug delivery systems along with their efficacy in sensing and microsurgical applications.² However, in order to facilitate the biomedical applications of the micro/nanorobots, in particular for *in vivo* applications, imaging and real-time tracking of these tiny agents are crucial before they can be safely applied on a living body.³ The use of current optical microscope-based 2D and 3D techniques for whole-body *in vivo* imaging is limited to superficial areas, just below the skin or the surface of internal organs and cavities, because visible light has an inherently low capacity for penetrating biological tissue.

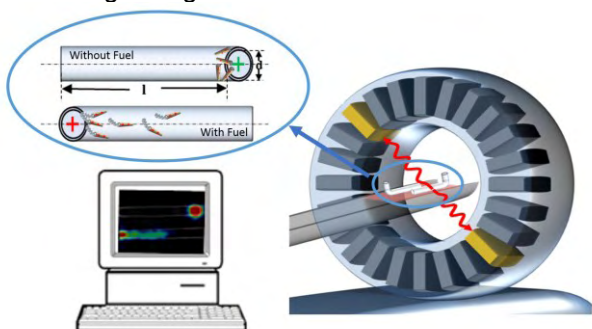


Figure 1. Schematic approach of PET-CT for the tracking of micromotors.

Here, we show that positron emission tomography (PET), a molecular imaging technique widely used in medical imaging, can also be used to track a large population of tubular Au/PEDOT/Pt micromotors (see **Figure 1**).

We used catalytic self-propelled micromotors containing a surface layer of gold as a model of an active system. The gold layer allows for radiolabeling using the positron emitting isotope ¹²⁴I (half-life: 4.2 days) due to the high affinity binding between gold and iodine. Two identical longitudinal tubular phantoms were prepared to examine the suitability of PET-CT for tracking the location of

micromotors (both self-propelled and inert) at a macroscopic level. We observed that PET-CT could track the location of swarming micromotors (see **Figure 2A**) over 15 min, providing quantitative information on the temporal evolution of their spatial distribution within the phantoms. Afterwards, for validation purposes, we repeated the previous experiment using similar phantoms to those used in PET-CT and we acquired optical images of the bubbles released from the micromotors (**Figure 2B**) and micromotor trajectories while swimming. The PET-CT results were in good agreement with tracking observations obtained using optical microscopy, demonstrating that PET is a suitable technique for the imaging of large populations of active micromotors in opaque environments.⁴

Finally, we have used the same type of micromotors for their tracking using PET-CT in a rat being able to observe the distribution of the tubular structures *in vivo*. As **Figure 2C** displays, after 48 hours, the micromotors accumulated in the thyroids, lungs and liver.

This work demonstrated the use of this mature imaging technology for the *in vivo* localization of artificial swimmers and open new opportunities for the medical tracking and better control of micro/nanomotors for biomedical applications.

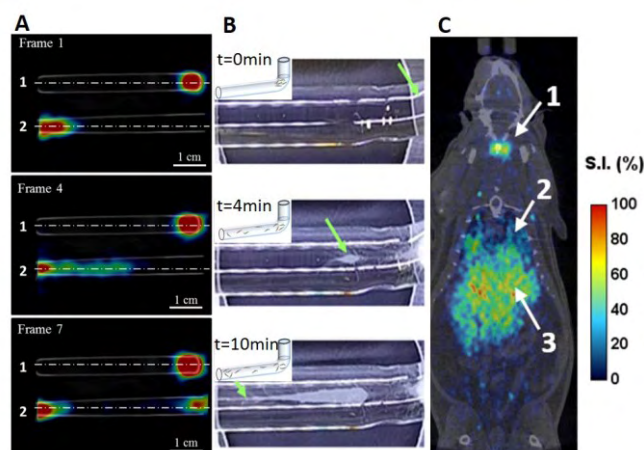


Figure 2. Imaging of micromotors: (A) PET-CT images corresponding to different times (up to 15 min) of analysis for two *in vitro* Phantoms: micromotors without (1) and with (2) fuel. (B) Optical imaging of self-propelled catalytic Au-micromotors inside the phantom tubes (d = 4 mm). (C) PET-CT images of microtubular structures without fuel *in vivo* after 48h of analysis to demonstrate traceability (1: thyroid; 2: lung; 3: liver)

References

- [1] B. Wang, Y. Zhang, L. Zhang. *Quant Imaging Med. Surg.* 8 (2018) 461-479.
- [2] J. Katuri, M. Stanton, X. Ma, S. Sanchez. *Accounts of chemical research* 50 (2016) 2-11.
- [3] M. Medina-Sánchez and O. G. Schmidt. *Nature* 54 (2017) 407-408.
- [4] D. Vilela, U. Cossío, J. Parmar, A. M. Martínez-Villacorta, V. Gómez-Vallejo, J. Llop, and S. Sánchez. *ACS Nano* 12 (2018) 1220-1227.



**Calle Alfonso Gomez 17
Planta 2 - Loft 16
28037 Madrid (Spain)**

**info@phantomsnet.net
www.phantomsnet.net**